# Statistical Mechanics

## Principles of Chemical Equilibrium

Based on lectures notes by Prof. David Chandler

(UC Berkeley 1991)

Jürg Hutter
Physikalisch-Chemisches Institut
Universität Zürich
Winterthurerstrasse 190
8057 Zürich
hutter@pci.uzh.ch

May 14, 2012

# Contents

# Part I

# Lectures

# Chapter 1

# Principles of Macroscopic Systems

## 1.1 Introduction

Let's start with a simple experiment

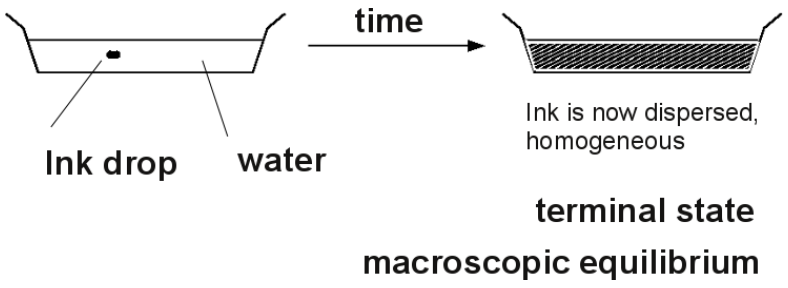


scheme 001

We can do this experiment with system totally *isolated*, i.e. insulated, at constant energy.

What is the driving force?
– It has to do with fluctuations, statistics, and chaos.

Consider an enlargement of the experiment, and for the purpose of keeping track of things, mark the system with a grid.

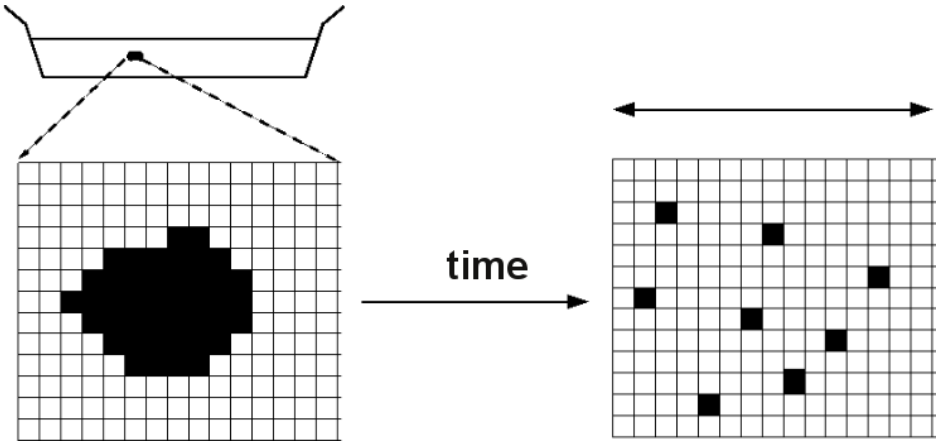


scheme 002

Each cell of volume $\Delta\nu$; black cells are those containing dye molecules.
$\Delta\nu$ is very little – so small that no more than one dye molecule can fit in it.

With light (through scattering or absorption) we can observe or measure

$\rho$ = concentration of dye molecules in observed region of volume $\nu$
= number of molecules/$\nu$

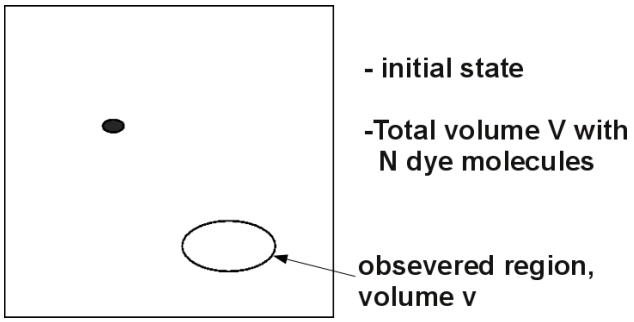

scheme 003

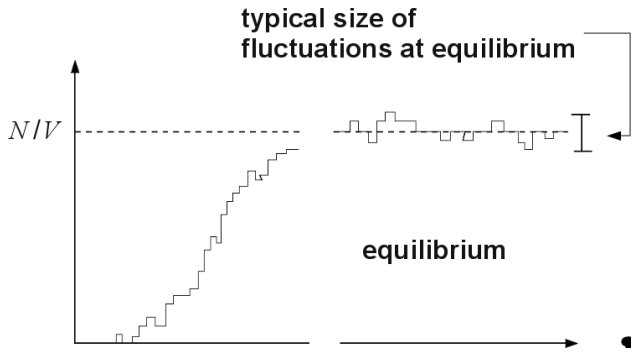


scheme 004

Even at equlibrium, fluctuations never stop.
These microscopic fluctuations are a consequence of molecular motions. The relative size of the fluctuations in $\rho$ depends on the size of the observed system – the size of $\nu$.

For $\nu = \Delta\nu =$ microscopic volume $\approx$ size of a molecule, $\rho$ looks like this when the total system is at equilibrium:

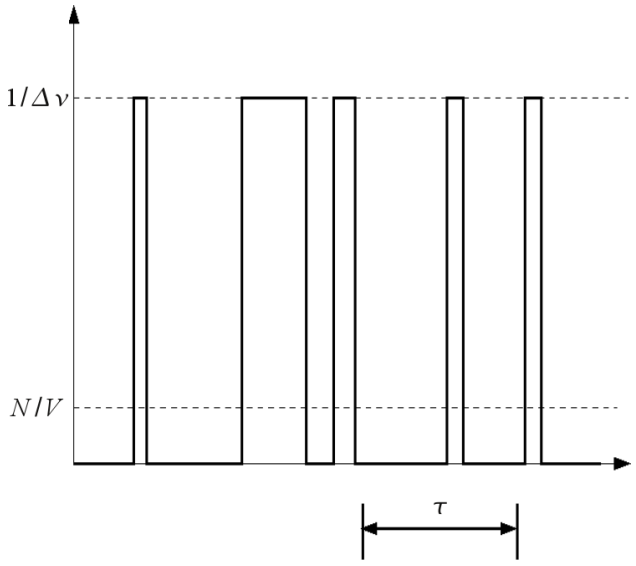

($\rho$ axis is schematic, not drawn to scale.)

If observations are made over short periods of time and over short distance scales, the system will always look chaotic. On the other hand, observations over long times or over long length scales will be easy to characterize (at macroscopic equilibrium) – ordinary, self evident, boring.

How long is "long" – long enough so that in effect, one observation corresponds to many statistically independent measurements.

• Observation over a long time $T$:

$$\begin{aligned}
\langle\rho\rangle &= \frac{1}{T}\int_0^T \rho(t)\ \mathrm{d}t && \leftarrow \text{This is a time average} \\
&= \frac{1}{K}\sum_{n=1}^{K}\frac{1}{\tau}\int_{(n-1)\tau}^{n\tau}\rho(t)\ \mathrm{d}t\ ; && T = K\tau \\
&= \frac{1}{K}\sum_{n=1}^{K}[\rho]_{\text{nth observation}}
\end{aligned}$$

If $T$ is long enough and if the system is at equlibrium, $\langle\rho\rangle$ will be a "constant", i.e., we will get the same value every time we do the experiment.

• Observation over a large region of volume $\nu$.

$$\begin{aligned}
\langle\rho\rangle &= \frac{1}{\nu}\sum_{j=1}^{m}[\text{molecules in cell } j]/\Delta\nu && \nu = m\Delta\nu \\
&= \frac{1}{m}\sum_{j=1}^{m}[\rho]_{\text{jth cell}}
\end{aligned}$$

If m is large enough and if system is at macroscopic equilibrium, this $\langle\rho\rangle$ is also a constant, and should have the same value as $\langle\rho\rangle$ corresponding to a time average.

## 1.2 Range or length of correlations

Correlation: Distance over which a disturbance of fluctuation has an effect. Usually, this distance is very short (microscopic).

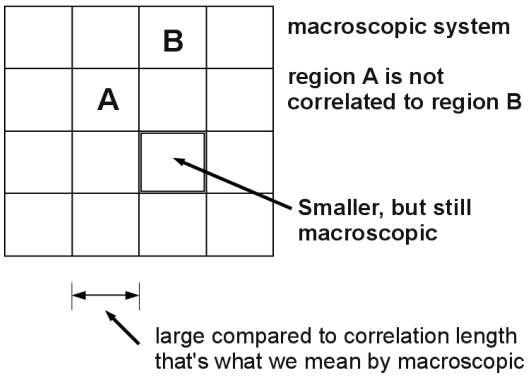


scheme 006

A very big system can be divided into an enormous number of smaller, but still big systems.

The very big system is an *ensemble* of subsystems. Observation of whole system corresponds to an *ensemble average*.

What does it mean to be correlated?

Example:

$P(\rho_A, \rho_B)$ *joint* probability that subsystem $A$ has density $\rho_A$ and that subsystem $B$ has density $\rho_B$. It is a normalized histogram built up from many measurements.

Clearly,

$$\langle \rho_A \rho_B \rangle = \sum_{\rho_A} \sum_{\rho_B} P(\rho_A, \rho_B) \rho_A \rho_B$$

But if subsystems are uncorrelated,

$$P(\rho_A, \rho_B) = P(\rho_A) \cdot P(\rho_B)$$

where $P(\rho_B)$ is a histogramm from observations of $B$ ignoring $A$.
Thus,

$$\begin{aligned}\langle \rho_A \rho_B \rangle_{\text{uncorrelated}} &= \sum_{\rho_A} \sum_{\rho_B} P(\rho_A) P(\rho_B) \rho_A \rho_B \\ &= \left( \sum_{\rho_A} P(\rho_A) \rho_A \right) \left( \sum_{\rho_B} P(\rho_B) \rho_B \right) \\ &= \langle \rho_A \rangle \, \langle \rho_B \rangle\end{aligned}$$

Therefore,

$$\langle \rho_A \rho_B \rangle - \langle \rho_A \rangle \, \langle \rho_B \rangle = \langle (\rho_A - \langle \rho_A \rangle)(\rho_B - \langle \rho_B \rangle) \rangle$$

is a measure of correlations.

When

$$\langle (\rho_A - \langle \rho_A \rangle)(\rho_B - \langle \rho_B \rangle) \rangle \neq 0$$

the two subsystems are correlated.

**Relaxation time** Time for a system to forget a particular fluctuation or disturbance.

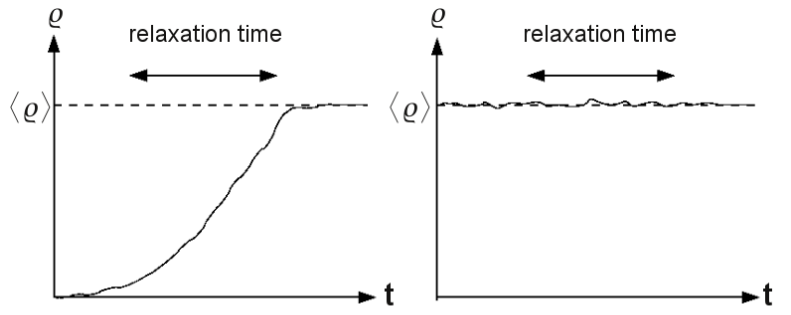


ρ relaxing to equilibrium ρ fluctuating at equilibrium

Macroscopic systems are at equilibrium, if they have been prepared and controlled over times long compared to relaxation time.

$$\langle\rho\rangle = \text{observed } \rho = \begin{cases} \text{either time average of } \rho \\ \text{or ensemble average of } \rho \end{cases}$$

The assumed equivalence of the two averages is called the *ergodic* assumption – if you believe it, it means you believe in relaxation (loss of memory and chaos) and finite correlation lengths; and you are thinking about experiments performed over long times and/or large spatial scales.

What does it mean to be uncorrelated at different times?
(Time correlations, a sophisticated concept!)

Consider the "time line" for $\rho$ in an equilibrium system.

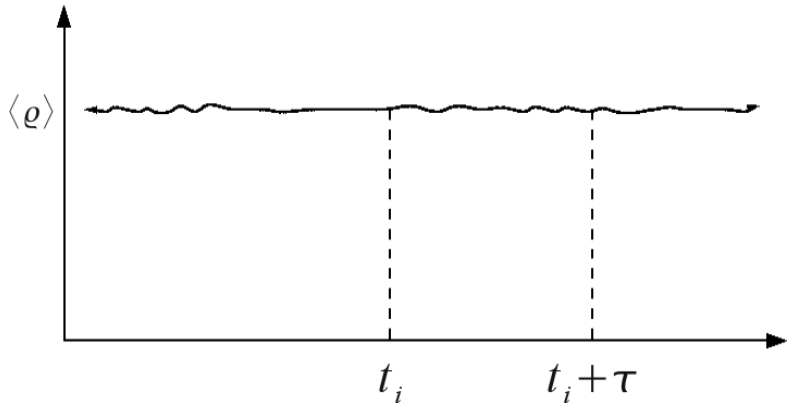




For every time $t_i$, look also at $t_i + \tau$ and calculate $\rho(t_i)\rho(t_i + \tau)$. Average this quantity over many $t_i$'s. The average gives a function of $\tau$.

$$\begin{aligned} C(\tau) &= \frac{1}{K}\sum_{i=1}^{K}\rho(t_i)\rho(t_i+\tau) \\ &= \langle\rho(0)\rho(\tau)\rangle \end{aligned}$$

Zero time refers to the initial time that is averaged over.
If $\tau$ is larger than the relaxation time

$$C(\tau) \longrightarrow \langle\rho(0)\rangle\langle\rho(\tau)\rangle = \langle\rho\rangle\langle\rho\rangle$$

## 1.3 Fluctuations, large numbers, extensive and intensive

**Question**: How many particles (e.g. dye molecules in a solution, or air molecules in air) will we find in an observed volume $V = M\Delta\nu$ ?

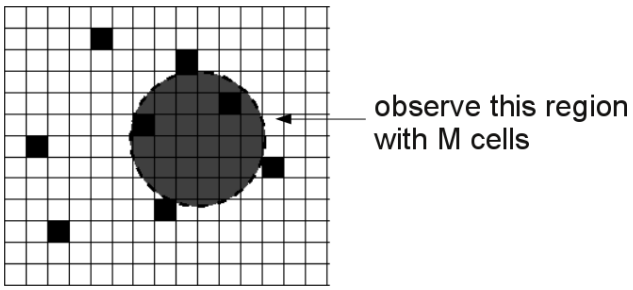


scheme 009

Let

$$n_i = 1, \quad \text{if a molecules is in cell i}$$
$$n_i = 0, \quad \text{if no molecule is in cell i} \ .$$

We will be assuming low concentrations and very small $\Delta\nu$, so $n_i > 1$ is "impossible".

Total number of particles in system at a particular instant is

$$N = \sum_{i=1}^{M} n_i$$

Thus,

$$\langle N \rangle = \sum_{i=1}^{M} \langle n_i \rangle = M \langle n \rangle$$

The last step makes use of the fact, that at equilibrium, on the average, each cell is the same.

Here,

$$\begin{aligned} \langle n \rangle &= \text{average of } n_i \text{ for any one cell} \\ &= \text{probability that one particular cell is occupied} \end{aligned}$$

At low concentrations (i.e. $\frac{\langle N \rangle}{V} \Delta\nu$ is small)

$$\langle n \rangle \ll 1$$

Notice that $\langle N \rangle$ scales linearly with $M$, the size of the system. Thus $\langle N \rangle$ is called an **extensive** property.

On the other hand, $\langle n \rangle$ appears to be independent of the system size. As such, $\langle n \rangle$ is called an **intensive** property.

Examples of **intensive** properties:
pressure, average concentrations, ...

Examples of **extensive** properties:
volume, total average energy, ...

**Question**: Is $\langle N \rangle$ a meaningful estimate of an instantaniously observed $N$?

To see, let us estimate the size of typical fluctuations

$$\delta N = N - \langle N \rangle$$

We test for the average of $\delta N^2$ as $\langle \delta N \rangle = 0$.

$$\begin{aligned}
\langle (\delta N)^2 \rangle &= \langle (N - \langle N \rangle)^2 \rangle \\
&= \langle N^2 - 2N\langle N \rangle + \langle N \rangle^2 \rangle \\
&= \langle N^2 \rangle - 2\langle N \rangle \langle N \rangle + \langle N \rangle^2 \\
&= \langle N^2 \rangle - \langle N \rangle^2
\end{aligned}$$

Now write both $\langle N^2 \rangle$ and $\langle N \rangle^2$ in term of averages involving the "occupation" numbers, the $n_i$'s:

$$\begin{aligned}
\langle (\delta N)^2 \rangle &= \left\langle \sum_{i=1}^{M} \sum_{j=1}^{M} n_i n_j \right\rangle - \left\langle \sum_{i=1}^{M} n_i \right\rangle \left\langle \sum_{j=1}^{M} n_j \right\rangle \\
&= \sum_{i=1}^{M} \sum_{j=1}^{M} [\underbrace{\langle n_i n_j \rangle - \langle n_i \rangle \langle n_j \rangle}_{\substack{\text{this is only nonzero,} \\ \text{if } n_i \text{ is correlated to } n_j}}]
\end{aligned}$$

At low concentrations, $n_i$'s of different cells are uncorrelated, only the $i = j$ terms are nonzero. So,

$$\begin{aligned}
\langle (\delta N)^2 \rangle &= \sum_{i=1}^{M} [\langle n_i^2 \rangle - \langle n_i \rangle^2] \\
&\text{(make use of } n_i^2 = n_i \text{ !)} \\
\langle (\delta N)^2 \rangle &= M[\langle n \rangle - \langle n \rangle^2] = M\langle n \rangle \underbrace{(1 - \langle n \rangle)}_{\approx 1} \\
&\approx M\langle n \rangle = \langle N \rangle
\end{aligned}$$

Thus, particle fluctuations for a gas or solution of *uncrorrelated* particles obeys

$$\boxed{\langle (\delta N)^2 \rangle = \langle N \rangle}$$

Things to notice

1. $\langle (\delta N)^2 \rangle$ is extensive

2. Relative size of fluctuations

$$\frac{\sqrt{\langle(\delta N)^2\rangle}}{\langle N\rangle} = \frac{\sqrt{\langle N\rangle}}{\langle N\rangle} = \frac{1}{\sqrt{\langle N\rangle}} = \frac{1}{\sqrt{M\langle n\rangle}}$$

are small for big systems and large for little systems.

Equivalentely, if we observe concentrations or densities, $\rho = N/V$, then

$$\langle\rho\rangle = \langle n\rangle/\Delta\nu$$

and

$$\langle(\delta\rho)^2\rangle = \frac{\langle N^2\rangle - \langle N\rangle^2}{V^2} = \frac{\langle N\rangle}{V^2} = \langle\rho\rangle\frac{1}{M\Delta\nu}$$

For M large, fluctuations in the intensive property $\rho$ become negligible.

$P(\rho)$ = probability distribution for $\rho$

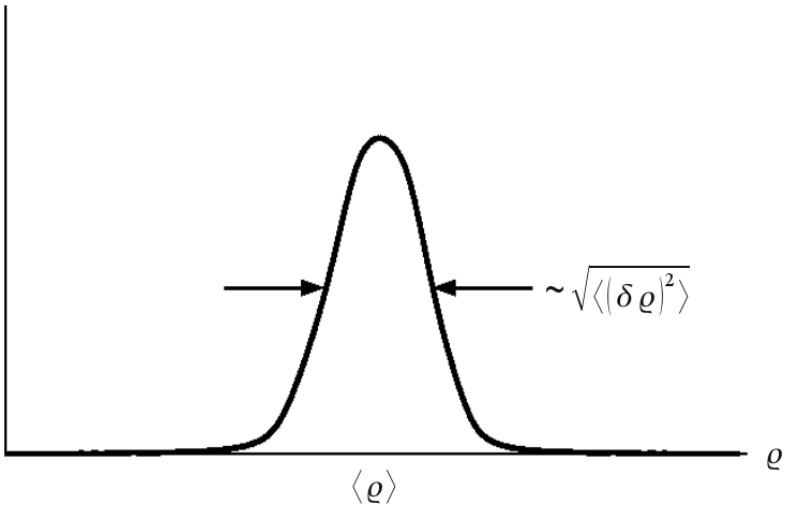


scheme 010

The density distribution function for a large system exhibits little dispersion.

## 1.4 Principle of equal weight

Statistical characterization of macroscopic equilibrium.

Think about the ink dye experiment. It seems to illustrate that terminal stationary states are most random or chaotic macroscopic states, i.e. all possible microscopic states are equally likely.

In other words, all fluctuations consistent with the constraints that define the system occur with the same probability.

As we will see shortly, the Second Law of thermodynamics follows from this principle.

For example, consider an isolated system of fixed size

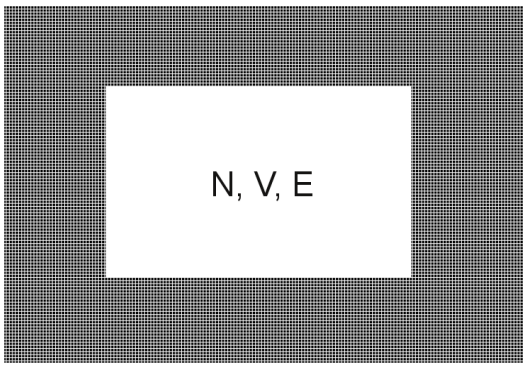


scheme 011

System is totally insulated from its surroundings. No particlescan come in or get out, no energy can be transmitted through the boundaries.

$N$ and $V$ are fixed, and from conservation of total energ $E$, the energy is fixed too. These are the constraints defining this system – fixed $N$, $V$, and $E$.

Let $\Omega(N, V, E) =$ total number of states, microscopic states that is, constraint with fixed $N$, $V$, and $E$.

That is like the degeneracy of the macroscopic system.

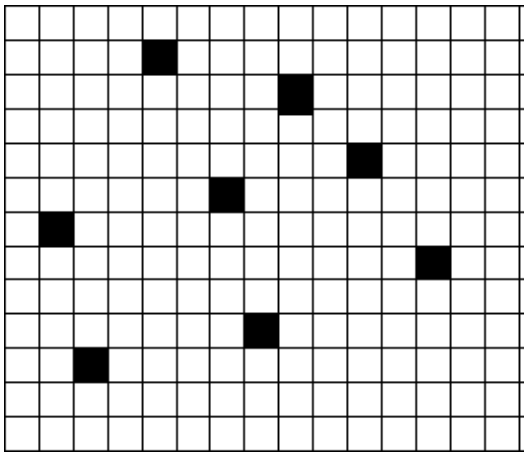

scheme 012

How many ways can you put $N = 5$ particles in the available boxes?

At macroscopic equilibrium, the principle of equal weights implies that for each of these microscopic states the probability is

$$P = \frac{1}{\Omega(N, V, E)}$$

A related quantity is the **entropy**, S, which we *define* as

$$\boxed{S(N, V, E) \equiv \mathrm{k_B} \ln \Omega(N, V, E)}$$

$\mathrm{k_B}$ is, at this point, an arbitrary constant. It will be Boltzmann's constant.

We expect that S is extensive.

**Example 1** N identical particles, each on can exist in one of two degenerate states ( both having the same energy)

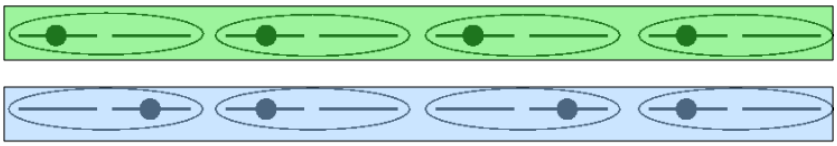

Two different microscopic states of the total N particle system

scheme 013

In this case, there area total of $2^N$ states, i.e.,

$$\Omega = 2^N \Rightarrow S = \mathrm{k_B} \ln \Omega = N \mathrm{k_B} \ln 2 \leftarrow \text{it is extensive!}$$

**Example 2** $N$ uncorrelated and indistinguishable particles in a volume composed of $M$ cells.

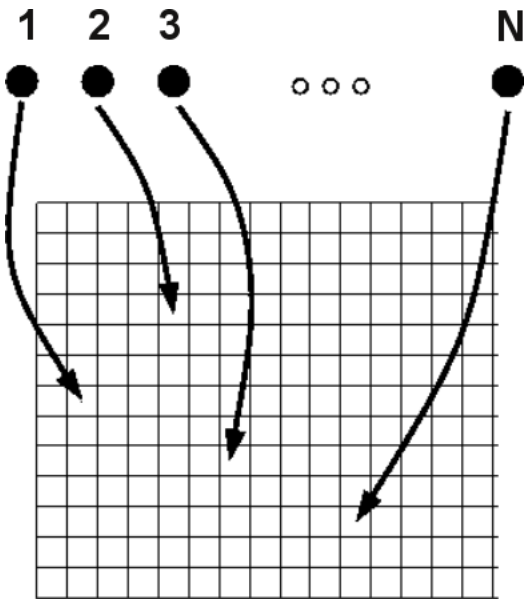


scheme 014

particle 1 has $M$ places to go
particle 2 has $M$ places to go
$\vdots$
particle 1 has $M$ places to go

This seems to suggest $\Omega = M^N$.
This is based on $M \gg N$ and one particle per cell. For smaller $M$ we would have $\Omega = M(M-1)(M-2)\cdots(M-N)$.

But due to indistinguishability

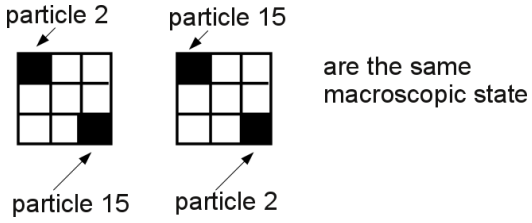


scheme 015

The number of equivalent configurations is the number of ways to relabel the indistinguishable particles, and that number is $N!$ = number of permutations of $N$ things.

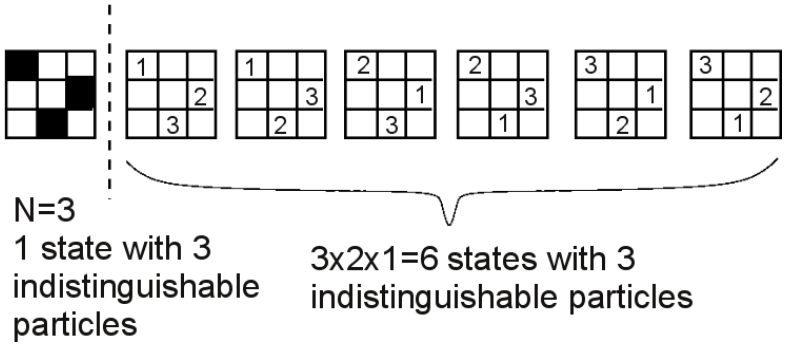


scheme 016

Thus, $\Omega = M^N$ over counts the number of different states by a facor of $N!$. Hence,

$$\Omega = \frac{1}{N!} M^N \ .$$

As a result, in this case

$$S/\mathrm{k_B} = N \ln M - \ln N! \ .$$

For N large, Stirling's formula is

$$\ln N! \approx N \ln N - N \ .$$

Thus, finally,

$$\begin{aligned} S/\mathrm{k_B} &= N \ln M - N \ln N + N \\ &= N \left[ \ln \frac{M}{N} + 1 \right] \\ &= N \left[ \ln \frac{1}{\langle n \rangle} + 1 \right] \\ &= N \left[ 1 - \ln \langle n \rangle \right] \end{aligned}$$

which is extensive.

# Chapter 2

# The Second Law and the Meaning of Temperature

## 2.1 The Second Law of thermodynamics

**Partitionfunction**

$$\Omega(N, V, E) = \begin{array}{l}\text{number of } \textit{all} \text{ possible microscopic} \\ \text{states (i.e., instantaneous fluctuations)} \\ \text{with } N,\ V,\ E \text{ fixed.}\end{array}$$

Consider a subset of all these fluctuations which can be realized through *internal* constraints.

**Example**

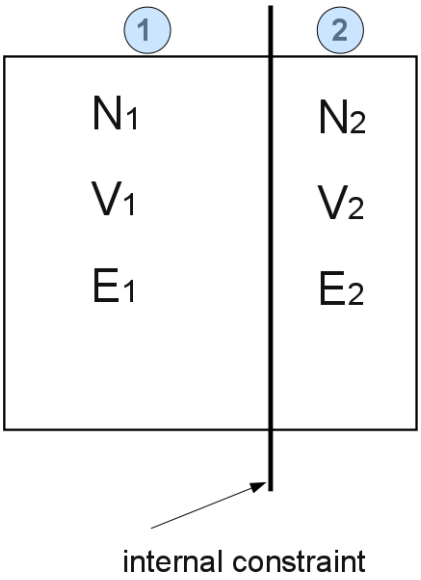


scheme 017

Divide the system into two subsystems, such that

$$N = N_1 + N_2$$
$$V = V_1 + V_2$$
$$E = E_1 + E_2$$

If "internal constraint" was impermeable, then it could be used to enforce an inhomogenious distribution of particles in the system. If it was insulating and rigid, it could enforce a partitioning of energy that was inconsistent with the partitioning at equilibrium without the constraint.

Let $\Omega'(N, V, E) =$ total number of microscopic states with internal constraints applied

Since the constraint reduces the total number of possible fluctuations

$$\Omega'(N, V, E) < \Omega'(N, V, E)$$

or

$$S'(N, V, E) < S'(N, V, E) \ .$$

But macroscopic states accessed through the application of internal constraints correspond to nonequilibrium macroscopic states without those constraints.
Thus

$\boxed{S \text{ is max. at equilibrium}}$

This idea is the essence of the Second Law of thermodynamics.

To see what this law can predict, consider the following question.

How is the total energy of a system partitioned at equilibrium?

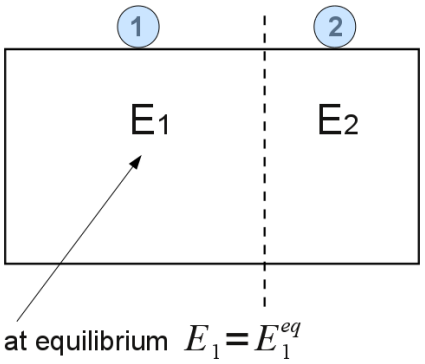


scheme 018

$$E = E_1 + E_2 \qquad \text{since energy is extensive}$$
$$E_1 = E_1^{\text{eq}} + \Delta E$$
$$E_2 = E_2^{\text{eq}} + \Delta E$$

$\Delta E$ is the fluctuation in energy.

Entropy as a function of $N$, $V$, $E$.

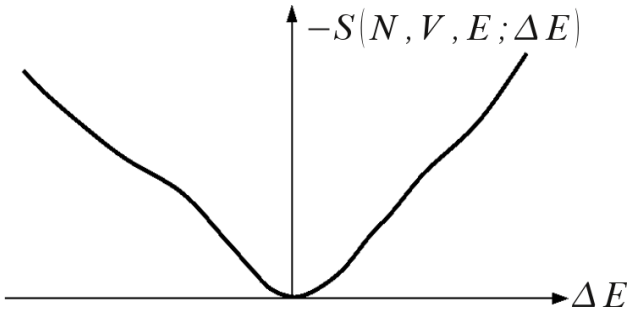


scheme 019

Since $S$ is extensive $S = S_1 + S_2$ and

$$\frac{\partial(-S)}{\partial \Delta E} = \frac{\partial(-S_1)}{\partial \Delta E} + \frac{\partial(-S_2)}{\partial \Delta E}$$

Define **temperature**, $T$, by

$$\frac{1}{T} \equiv \left(\frac{\partial(S)}{\partial E}\right)_{N,V} ,$$

since both $E$ and $S$ are extensive, $T$ must be *intensive*.

Thus,

$$\frac{\partial(-S)}{\partial \Delta E} = -\frac{1}{T_1} + \frac{1}{T_2}$$

$\Rightarrow T_1 = T_2$ at thermal equilibrium, and
$\Delta E$ flows from *hot* (high $T$)
to *cold* (low $T$).

## 2.2 Does entropy increase for all natural processes?

**Hahn's echo experiment** (see Brewer and Hahn, Scientific American **251**, pp 50–57, (1984))

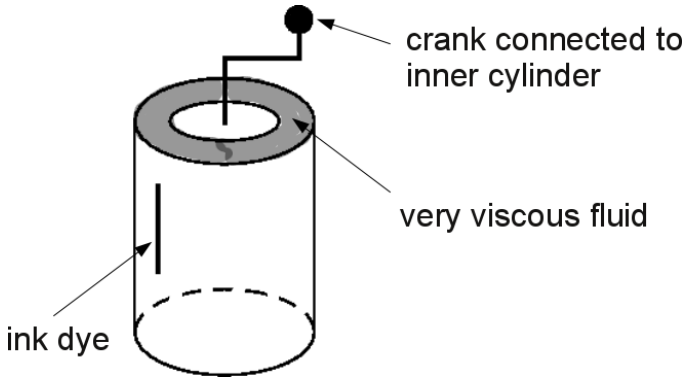


scheme 020

After several turns of crank, dye appears dispense. Is this the Second Law at work? – No, we can return to the initial configuration by simply reversing the turns of the crank.

Evidentally, relaxation times in the viscous fluid are much longer than the times of the experiment.

Are you sure $\Omega(N, V, E)$ must increase with increase of $E$? If not, temperature $T = \left(\frac{\partial S}{\partial E}\right)^{-1}_{N,V}$ will not be positive!

**Example 1**

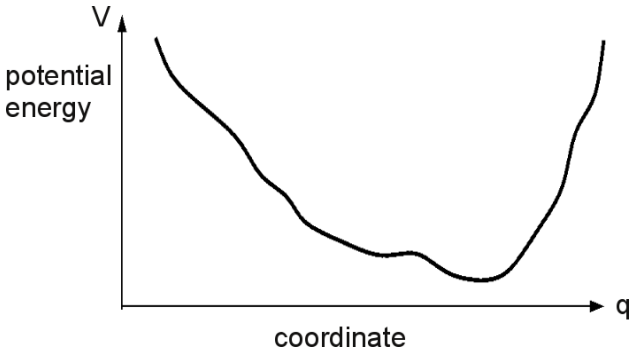


scheme 021

Increase in energy (larger V) leads to increase in possible states

$$\frac{\mathrm{d}\Omega}{\mathrm{d}E} > 0$$

**Example 2** Spin in a magnetic field

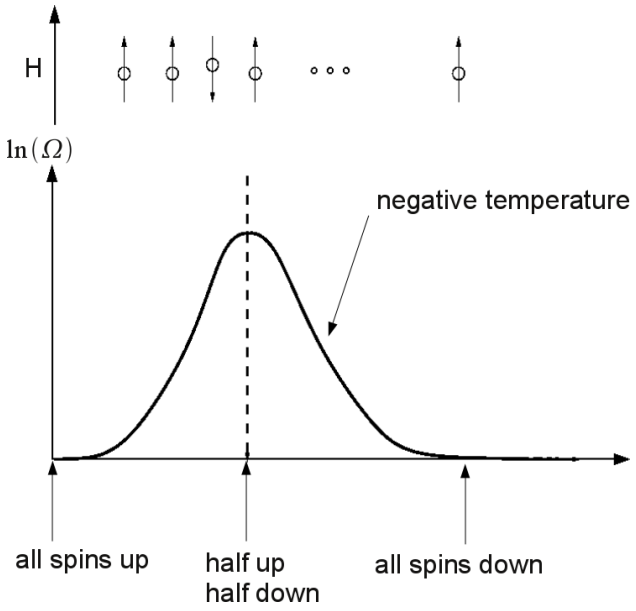


scheme 022

**Example 3**

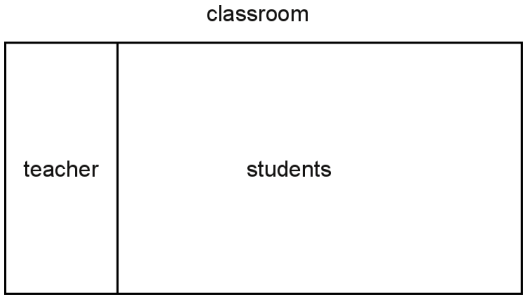

scheme 023

What is the chance no air will be where the teacher is?

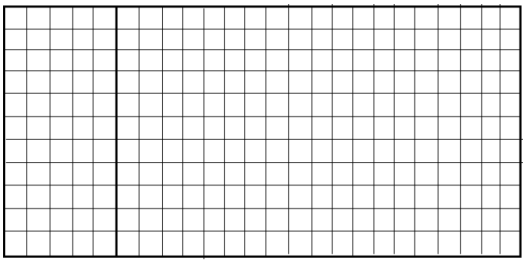


scheme 024

Teacher region with no particles has $\alpha M$ cells, $\alpha \ll 1$, but $\alpha N \gg 1$.

We can use Poisson's formula

$$P_m \approx \frac{(np)^m}{m!} \mathrm{e}^{-np}$$

with $p = \alpha$; $n = N$; $m = 0$, to get

$$P \approx \mathrm{e}^{-\alpha N} \quad \rightarrow \quad \text{very small number!}$$

## 2.3 Entropy as a function of $E$, $N$ and $V$

$$S = \mathrm{k_B} \ln \Omega = S(E, V, N)$$

Specify $E$, $V$, and $N$, and this will give you S for an equilibrium system.

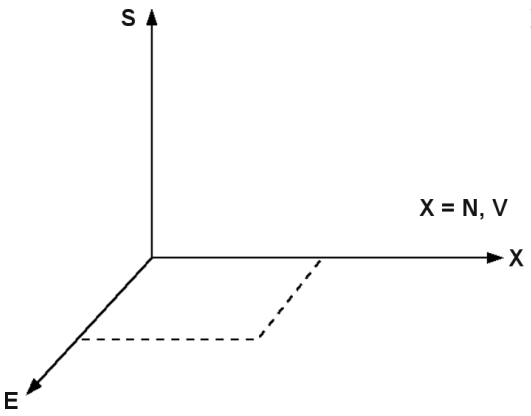


scheme 025

**Note:** The equilibrium manifold of macroscopic states is only a small fraction of allpossible states.

Consider small displacements among the equilibrium states: (total differential)

$$\mathrm{d}S = \left(\frac{\partial S}{\partial E}\right)_{N,V} \mathrm{d}E + \left(\frac{\partial S}{\partial V}\right)_{E,N} \mathrm{d}V + \left(\frac{\partial S}{\partial N}\right)_{V,E} \mathrm{d}N$$

Partial differentiation $\left(\frac{\partial S}{\partial E}\right)_{N,V}$ meaning: We are thinking about $S$ as a function of $E$, $N$ and $V$, and we are considering its rate of change due to changing $E$ in the direction orthogonal to $N$ and $V$.

We have already defined $\frac{1}{T} = \left(\frac{\partial S}{\partial E}\right)_{N,V}$.
Let us now define

$$\frac{p}{T} = \left(\frac{\partial S}{\partial V}\right)_{E,N} \text{, and} \qquad -\frac{\mu}{T} = \left(\frac{\partial S}{\partial N}\right)_{V,E} ,$$

so that

$$\mathrm{d}S = \frac{1}{T}\mathrm{d}E + \frac{p}{T}\mathrm{d}V - \frac{\mu}{T}\mathrm{d}N$$

Notice that as we have defined them, $p$ and $\mu$ are *intensive* functions of $E$, $V$ and $N$.

In analogy with our analysis of thermal equilibrium

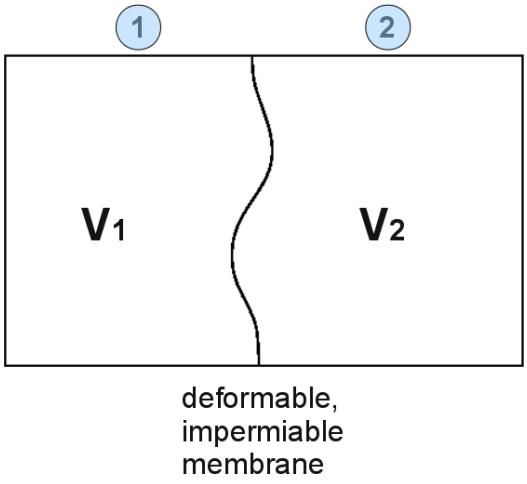


scheme 026

$$V_1 = V_1^{\mathrm{eq}} + \Delta V$$
$$V_2 = V_2^{\mathrm{eq}} - \Delta V$$

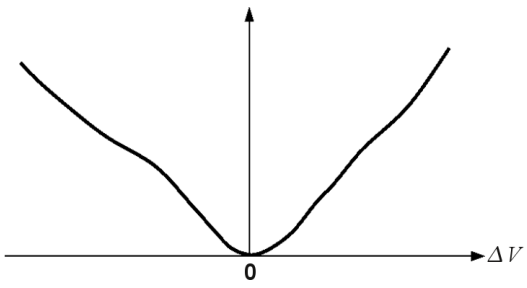


scheme 027

$$\frac{\mathrm{d}S}{\mathrm{d}\Delta V} = 0 \quad \text{at equilibrium}$$
$$\Rightarrow \quad (p/T)_1 = (p/T)_2$$
$$\Rightarrow \quad p_1 = p_2 \quad \text{at equilibrium}$$

and $p_1 > p_2$ causes membrane to deform with $\Delta V > 0$.

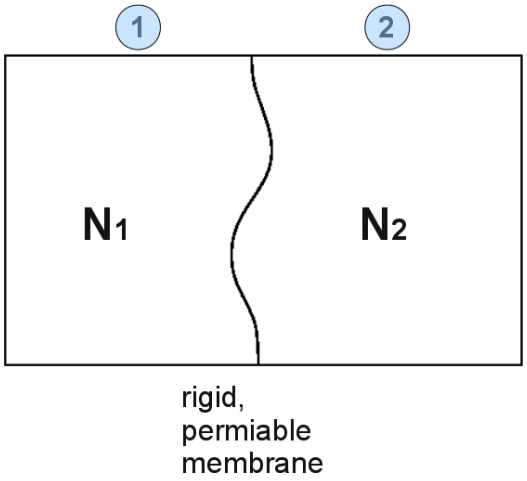


scheme 028

$$N_1 = N_1^{\mathrm{eq}} + \Delta N$$
$$N_2 = N_2^{\mathrm{eq}} - \Delta N$$

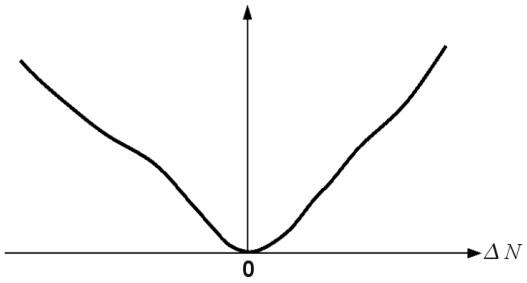

$$\frac{\mathrm{d}S}{\mathrm{d}\Delta N} = 0 \quad \text{at equilibrium}$$
$$\Rightarrow \quad (\mu/T)_1 = (\mu/T)_2$$
$$\Rightarrow \quad \mu_1 = \mu_2 \quad \text{at equilibrium}$$

and $\mu_1 > \mu_2$ causes particles to flow with $\Delta N > 0$.

- quantity $T$ controls energy equilibrium (Temperature).
- quantity $p$ controls volume equilibrium (Pressure).
- quantity $\mu$ controls mass equilibrium (Chemical Potential).

To help further identify the physical meaning of $p$ and $\mu$, rearrange the formula for $\mathrm{d}S$

$$T\mathrm{d}S = \mathrm{d}E + p\mathrm{d}V - \mu\mathrm{d}N$$
$$\boxed{\mathrm{d}E = T\mathrm{d}S - p\mathrm{d}V + \mu\mathrm{d}N}$$

So, here we are thinking about $E$ as a function of $S$, $V$ and $N$ ($E(S, V, N)$).

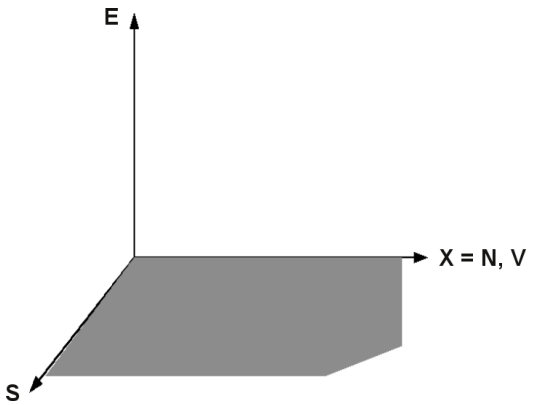

scheme 030

Specify $S$, $V$, $N$ and that will determine $E$ for an *equilibrium* system.

$E$ is the total energy of the system, so called, the *internal energy*. Since energy is conserved, (First Law), $E$ will change only if we do something to the system.

We can do *work*, squeeze or stretch the system, heat or cool it, or add particles.

For example:

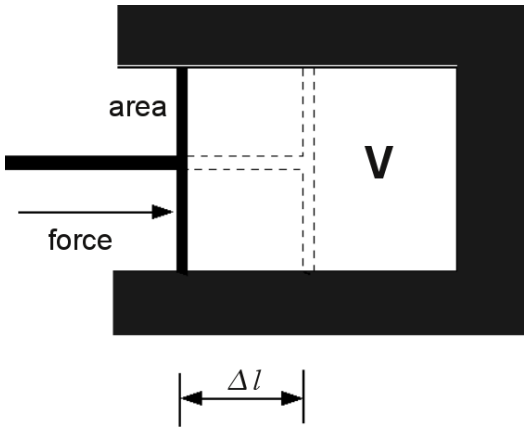


scheme 031

$$\begin{aligned}\text{work done on system} &= (\text{force}) \cdot \Delta l \\ &= - \underbrace{(\text{force}/\text{area})}_{\text{externally applied pressure}} \cdot \Delta V \\ &= -P_{\text{ext}} \cdot \Delta V\end{aligned}$$

Positive work done *on* system decreases system volume.

At equilibrium, Newton tells us that $P_{\text{ext}}$ = pressure of system. Therefore, if work is done *reversibly*, the work differential for changing $V$ is

$$(\mathrm{d}W)_{\text{rev}} = -(\text{pressure of system}) \cdot \Delta V$$

Compare with $\mathrm{d}E = T\mathrm{d}S - p\mathrm{d}V + \mu\mathrm{d}N$,
$\Rightarrow p$ = pressure of system.

*Reversible process* is one that is done slowly enough to move through equilibrium states only.

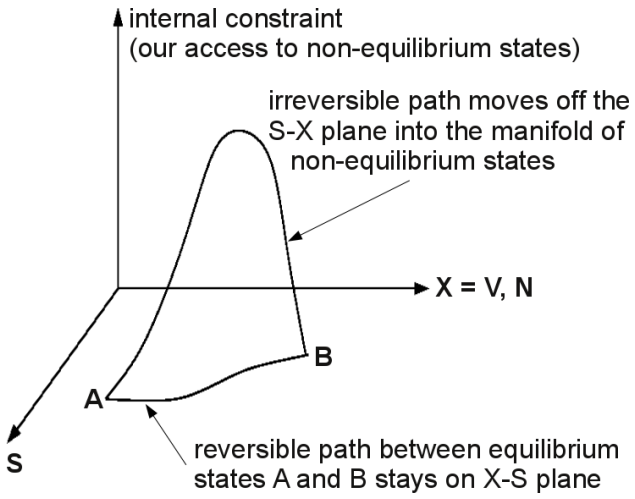


scheme 032

Equlibrium states are relatively simple to characterize (only $S$, $V$ and $N$ need to be specified). So reversing a path through such states is conceivable. Non equilibrium states are , in principle, infinitely more complex, and it is inconceivable that we could retrace on uncontrolled path through such states – thue irreversible.

## 2.4 Ideal gas law

We have established that

$$\left(\frac{\partial S}{\partial V}\right)_{N,E} = \frac{p}{T} \ .$$

Earlier we showed that *uncorrelated* structurless identical particles leads to

$$\Omega(N,V) = M^N/N!$$

or

$$S = \mathrm{k_B}\left[\ln\left(\frac{M}{N}\right) + 1\right] N \ , \qquad M\Delta\nu = V$$

If we also consider the possible energies of such particles

$$\Omega(N,V,E) = \frac{M^N f^N(E)}{N!}$$

$f^N(E)$ = number of ways of distributing energy $E$ among $N$ particles.

Therefore

$$S = \mathrm{k_B}\ln\Omega = \mathrm{k_B}N\left[\ln\left(\frac{M}{N}\right) + 1 + \ln f(E)\right]$$

Thus

$$\frac{1}{T} = \left(\frac{\partial S}{\partial V}\right)_{N,E} = \mathrm{k_B}\frac{N}{f(E)}\frac{\mathrm{d}f(E)}{\mathrm{d}E}$$

$\Rightarrow T = T(E/N)$ or $E/N$ = function of $T$ independent of $V$ or density.

Further

$$\begin{aligned}\frac{p}{T} = \left(\frac{\partial S}{\partial V}\right)_{N,E} &= \mathrm{k_B}N\frac{1}{\Delta\nu}\frac{\partial}{\partial M}\ln\left(\frac{M}{N}\right) \\ &= \mathrm{k_B}\frac{N}{\Delta\nu M} = \mathrm{k_B}\frac{N}{V} = \mathrm{k_B}\rho\end{aligned}$$

Thus, $\frac{p}{\mathrm{k_B}T\rho} = 1$ – compare to $pV = NRT$ (the ideal gas law)

$$R = N_0\mathrm{k_B}$$

$$N_0 = \text{Avogadro's number}$$

Now we know the *essential* physics behind $pV = nRT$ – uncorrelated density fluctuations.

Reversible and isothermal compression of an ideal gas

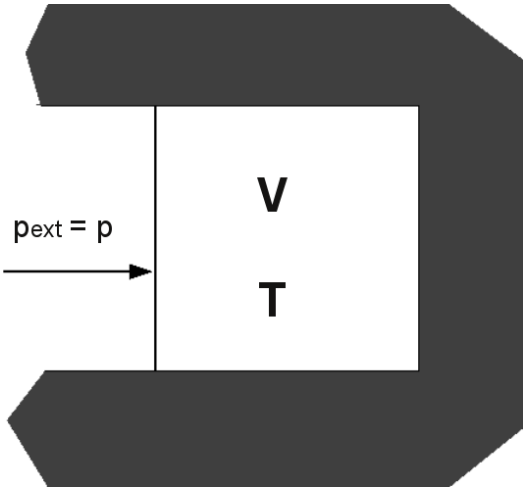


scheme 033

Surrounding is an infinite source of energy which keeps the temperature fixed – it is called a *heat bath*.

The work done in changing $V$ from $V_1$ to $V_2$ is

$$\begin{aligned} W &= \int_{V_1}^{V_2} [-p(T,V,N)]\mathrm{d}V \\ &= -nRT \int_{V_1}^{V_2} \frac{\mathrm{d}V}{V} = -nRT \ln\left(\frac{V_2}{V_1}\right) \\ &= nRT \ln\left(\frac{V_1}{V_2}\right) \end{aligned}$$

But the temperature is constant, so the total change in energy at the ideal gas is zero. – We did work, but there is no change in energy (remeber $E/N$ = function of $T$ alone!)
What is going on?

*HEAT FLOW !*

## 2.5 Temperature and energy fluctuations

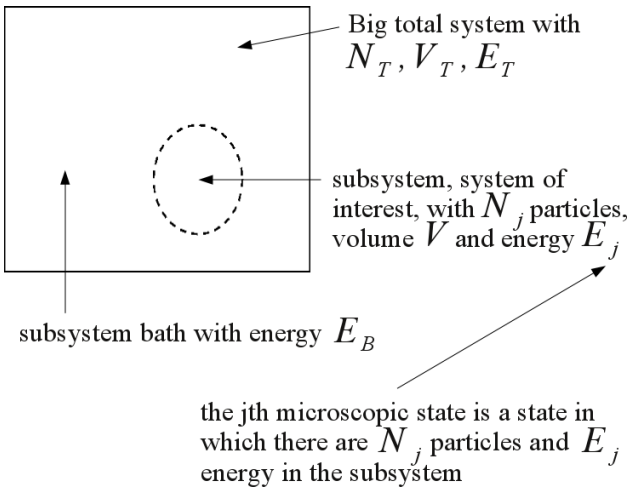


scheme 034

Cosider case where $N_j = N$ is fixed, and fluctuations are those in which $E_j$ changes. (The bath is then a heat bath in equilibrium with the closed – but not isolated – system of interest.)

A given $E_j$ corresbonds to (we are going to assume that the bath is truly enormous.)

$$E_B = E_T - E_j$$

$E_B$ fluctuates as $E_j$ fluctuates, and $E_T$ is fixed. The probability for observing this partitioning of energy is

$$\frac{\Omega(E_T - E_j, N_B, V_B)\ \Omega(E_j, V, N)}{\Omega(E_T, N_T, V_T)} = \frac{(\text{ number of bath states})(\text{number of subsystem states})}{(\text{ number of states of total system })}$$

that is, the probability that the subsystem has energy $E$ is

$$P(E) \propto \Omega(E_T - E_j, N_B, V_B)\ \Omega(E, V, N)$$

(replace $E_j$ by $E$ and omit the normalization factor).

Since the bath is huge, $E_T \gg E$, hence we can truncate the following Taylor series

$$\ln \Omega(E_T - E_j, N_B, V_B) = \ln \Omega(E_T, N_B, V_B) + (-E) \left( \frac{\partial \ln \Omega}{\partial E_T} \right)_{N_B, V_B} + \cdots$$

after the linear term.

Recall ($T$ = bath temperature)

$$\frac{1}{\mathrm{k_B} T} = \left( \frac{\partial \ln \Omega}{\partial E_T} \right)_{N_B, V_B} = \beta$$

Hence, for a very big bath in thermal equilibrium with the system of interest

$$\begin{aligned} P(E) &\propto \Omega(E, V, N) \mathrm{e}^{\ln \Omega(E_T - E, N_B, V_B)} \\ &= \Omega(E, V, N) \underbrace{\Omega(E_T, N_B, V_B)}_{\text{a constant}} \mathrm{e}^{-\beta E} \\ &\propto \Omega(E, V, N) \mathrm{e}^{-\beta E} \end{aligned}$$

$\Omega(E, V, N)$ accounts for the degeneracy of energy levels, and $\mathrm{e}^{-\beta E}$ is the thermal *Boltzmann* factor.

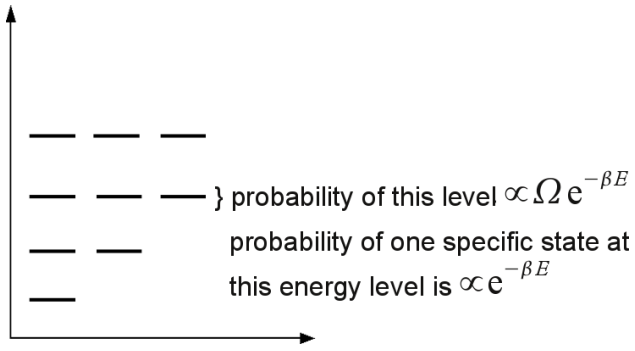


scheme 035

Thus,

$$P(E_j, V, N) = \mathrm{e}^{-\beta E_j} \underbrace{\left[ \frac{1}{\sum_l \mathrm{e}^{-\beta E_l}} \right]}_{\text{normalization constant}}$$

is the probability of observing state $j$ of a closed system of size $N \propto V$ at thermal equilibrium with temperature $T = (\mathrm{k_B}\beta)^{-1}$.

The assembly of all microscopic states of this closed system in contact with a heat bath is called the *canonical ensemble*.

The assembly of all states of the isolated system when $E$ vannot change is called the *micorcanonical ensemble*.

The quantity

$$Q(\beta, V, N) = \sum_j \mathrm{e}^{-\beta E_j} = \sum_E \Omega(N, V, E)\mathrm{e}^{-\beta E}$$

is called the *canonical partition function*.

Let us use the canonical distribution law to study energy fluctuations.

$$\langle E \rangle = \sum_j P_j E_j = \mathrm{e}^{-\beta E_j}/Q \ ,$$

where $P_j$ is probability of $j$th state.

For a large system

$$\begin{aligned}
\langle E \rangle &= \text{mean or average macroscopic energy of} \\
&\qquad \text{observed system} \\
&= \text{thermodynamic } \textit{internal energy} \\
&= \sum_j \mathrm{e}^{-\beta E_j} E_j / \sum_l \mathrm{e}^{-\beta E_l} \\
&= \left( \frac{\partial \ln Q}{\partial(-\beta)} \right)_{N,V} \qquad \text{remember} \quad \frac{\partial \ln f(x)}{\partial x} = \frac{1}{f(x)} \frac{\partial f}{\partial x}
\end{aligned}$$

Similarly,

$$\begin{aligned}
\langle (E-\langle E\rangle)^2\rangle \equiv \langle (\delta E)^2\rangle &= \langle E^2\rangle - \langle E\rangle^2 \\
&= \sum_j P_j E_j^2 - \left(\sum_j P_j E_j\right)^2 \\
&= \sum_j P_j E_j^2 - \sum_j P_j E_j \sum_l P_l E_l \\
&= \underbrace{\sum_j E_j^2 \mathrm{e}^{-\beta E_j}/Q}_{\frac{1}{Q}\frac{\partial \sum_j E_j \mathrm{e}^{-\beta E_j}}{\partial(-\beta)}} - \underbrace{\sum_j E_j \mathrm{e}^{-\beta E_j}/Q \sum_l E_l \mathrm{e}^{-\beta E_l}/Q}_{\frac{1}{Q^2}\underbrace{\sum_{jl} E_j E_l \mathrm{e}^{-\beta E_j}\mathrm{e}^{-\beta E_l}}_{\sum_j E_j \mathrm{e}^{-\beta E_j}\frac{\partial Q}{\partial(-\beta)}}}
\end{aligned}$$

Making use of the identity

$$\frac{1}{Q^2}\frac{\partial Q}{\partial(-\beta)} = -\frac{\partial 1/Q}{\partial(-\beta)}$$

we get

$$\begin{aligned}
\langle (E-\langle E\rangle)^2\rangle &= \frac{1}{Q}\frac{\partial \sum_j E_j \mathrm{e}^{-\beta E_j}}{\partial(-\beta)} - \frac{1}{Q^2}\sum_j E_j \mathrm{e}^{-\beta E_j}\frac{\partial Q}{\partial(-\beta)} \\
&= \frac{1}{Q}\frac{\partial \sum_j E_j \mathrm{e}^{-\beta E_j}}{\partial(-\beta)} + \sum_j E_j \mathrm{e}^{-\beta E_j}\frac{\partial 1/Q}{\partial(-\beta)} \\
&= \frac{\partial}{\partial(-\beta)}\underbrace{\left[\frac{1}{Q}\sum_j E_j \mathrm{e}^{-\beta E_j}\right]}_{\langle E\rangle} \\
&= \left(\frac{\partial\langle E\rangle}{\partial(-\beta)}\right)_{N,V} = \left(\frac{\partial\langle E\rangle}{\partial T}\frac{\partial T}{\partial(-\beta)}\right)_{N,V}
\end{aligned}$$

The last term can be easily calculated

$$\begin{aligned}
\frac{\partial T}{\partial(-\beta)} &= \frac{\partial}{\partial(-\beta)}\frac{-1}{-\beta \mathrm{k_B}} = \frac{-1}{\mathrm{k_B}}\frac{-1}{\beta^2} \\
&= \frac{1}{\mathrm{k_B}}(\mathrm{k_B}T)^2 = \mathrm{k_B}T^2 \ .
\end{aligned}$$

Therefore, we get

$$\langle (\delta E)^2 \rangle = \mathrm{k_B} T^2 \underbrace{\left( \frac{\partial \langle E \rangle}{\partial T} \right)_{N,V}}_{C_V: \text{heat capacity}}$$
$$= \mathrm{k_B} T^2 C_V$$

Remarkable for several reasons:

- $\langle$ (Spontaneous fluctuations in $E)^2 \rangle \propto$ ease of changing $\langle E \rangle$ by altering $T$.
- $C_V$ is extensive. Hence,

$$\sqrt{\frac{\langle (\delta E)^2 \rangle}{\langle E \rangle}} \approx \frac{1}{\sqrt{N}}$$

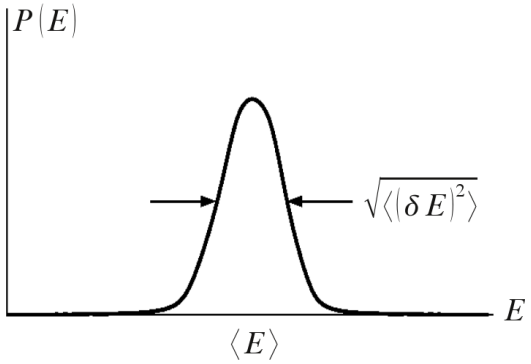


scheme 036

  Hence thermodynamic energy is meaningful.

- Existance of heat capacity is manifestation of microscopic fluctuations.
- $C_V$ is positive! ($\propto \langle (\delta E)^2 \rangle$)

Positivity of $C_V$ also follows from the Second Law.
On the way to equilibrium, heat goes from hot to cold. If $C_V$ were negative, this would cause the system to go even further from equilibrium.
Thus *stability* requires $C_V \geq 0$.

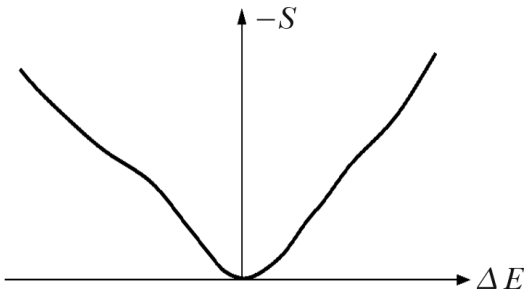


scheme 037

$$-\left(\frac{\partial^2 S}{\partial E^2}\right)_{\text{eq}} > 0 \quad \rightarrow \quad C_V > 0$$

**Using the Boltzmann distribution:** Example

At $300K$, what is the chance of seeing a gaseous $O_2$ molecule inits first vibronically excited state?

$$\begin{array}{c}\text{use ideal gas} \\ \text{approximation}\end{array} \Leftrightarrow \begin{array}{c}\text{independent molecule} \\ \text{approximation}\end{array}$$

We treat each molecule as a system in its own heat bath. Hence, for any one molecule

$$P_j \qquad \propto \mathrm{e}^{-\beta E_j} \ , j \qquad = \text{quantum numbers for}$$

–translation

–rotation

–vibration

–...

Roughly, vibrations are uncoupled from these other motions, and

$$E_{\text{vib}} \approx (n + 1/2)\hbar\omega \ , \quad n = 0, 1, \ldots \ ; \omega = \sqrt{\frac{f}{\mu}}$$

where $f$ is the force constant and $\mu$ the reduced mass.
Thus (assuming no degeneracies)

$$P_{\text{vib}} = p(n) = 1 \cdot \mathrm{e}^{-\beta(1/2+n)\hbar\omega} / \sum_{m=0}^{\infty} \mathrm{e}^{-\beta(1/2+m)\hbar\omega}$$

For $O_2$ we have $\hbar\omega/\mathrm{k_B} = 2230K$ and notice $\mathrm{e}^{-\beta\hbar\omega} = \mathrm{e}^{-2230/300} \approx 6 \cdot 10^{-4} \ll 1$.
Thus,

$$p(1) = \frac{\mathrm{e}^{-3/2\beta\hbar\omega}}{\mathrm{e}^{-1/2\beta\hbar\omega} + \mathrm{e}^{-3/2\beta\hbar\omega} + \cdots} \approx \mathrm{e}^{-\beta\hbar\omega} \approx 6 \cdot 10^{-4}$$

So, probability that one particular molecule is excited is $6 \cdot 10^{-4}$ (meaning small)!.
In one mole, how many molecules are excted? The number is

$$\langle N_{\text{1st excited state}} \rangle = N_0 \cdot p(1) \approx 10^{23} \cdot 10^{-3} \approx 10^{20} \ .$$

## 2.6 Low temperature and the Third Law

Consider the relative probability of two different energy levels ($\beta = 1/\mathrm{k_B}T$)

$$\frac{P(E')}{P(E)} = \frac{\Omega(E')}{\Omega(E)} \mathrm{e}^{-\beta(E'-E)}$$
$$\stackrel{T\to 0}{\longrightarrow} 0 \quad \text{for} \quad E' > E$$

This means that at zero temperature, only the ground state is accessible.

In virtually all circumstances, the lowest energy level is nondegenerate; that is why we say "ground state", not "ground level".

Hence,

$$S|_{T=0} - \mathrm{k_B} \ln \Omega_{\text{ground state}} = \mathrm{k_B} \ln 1 = 0 \ .$$

That is,

$$\boxed{\lim_{T\to 0} S = 0 \qquad \text{The Third Law!}}$$

Thta is not all! Consider the heat capacity

$$C_V = \left[\frac{\partial}{\partial T}\langle E\rangle\right]_{N,V} \quad .$$

Now

$$\langle E\rangle = \left[\frac{\partial}{\partial(-\beta)}\ln Q\right]_{N,V} \quad , \qquad Q = \sum_j \mathrm{e}^{-\beta E_j}$$

and ($E_1$ first excited state)

$$Q = \sum_j \mathrm{e}^{-\beta E_{\text{ground}}}\left(1 + \Omega_1 \mathrm{e}^{-\beta(E_1 - E_{\text{ground}})} + \cdots\right) \quad .$$

For large enough $\beta$ (i.e., low enough $T$),

$$Q \overset{T\to 0}{\longrightarrow} \mathrm{e}^{-\beta E_{\text{ground}}} \quad \text{or} \qquad \ln Q = -\beta E_{\text{ground}}$$

$$\langle E\rangle = \frac{\partial}{\partial(-\beta)}(-\beta E_{\text{ground}}) = E_{\text{ground}}$$

Thus, since $E_{\text{ground}}$ is independent of temperature

$$\boxed{C_V \longrightarrow 0 \quad \text{as} \quad T \longrightarrow 0}$$

No thermal excitations of fluctuations in $E$ at $T = 0$.

Alternative derivation

$$\begin{aligned}
\langle E\rangle &= \sum_j P_j E_j = \frac{1}{\sum_l \mathrm{e}^{-\beta E_l}} \sum_j E_j \mathrm{e}^{-\beta E_j} \\
&= \frac{\mathrm{e}^{-\beta E_{\text{ground}}} \sum_j E_j \mathrm{e}^{-\beta(E_j - E_{\text{ground}})}}{\mathrm{e}^{-\beta E_{\text{ground}}} \sum_j \mathrm{e}^{-\beta(E_l - E_{\text{ground}})}} \\
&= \frac{E_{\text{ground}} + E_1 \mathrm{e}^{-\beta(E_1 - E_{\text{ground}})} + \cdots}{1 + \mathrm{e}^{-\beta(E_1 - E_{\text{ground}})} + \cdots} \\
&= E_{\text{ground}} + (\text{terms involving} \underbrace{\mathrm{e}^{-\beta(E_l - E_{\text{ground}})}}_{\to 0 \text{ for } T\to 0})
\end{aligned}$$

Zero $T$ is the ultimate low temperature and perfectly ordered state. There are no fluctuations (except quantal zero point motions).

Could you ever reach $T = 0$?
No. You would need a 'heat' bath already at $T = 0$ to transfer energy (heat) out of your system as it approaches $T = 0$.

With the Third Law, we know that entropy is, at least in principle, a measurable quantity.

$$S(T, V, N) = \underbrace{S(0, V, N)}_{=0} + \int_0^T \mathrm{d}T' \left(\frac{\partial S}{\partial T'}\right)_{V,N}$$

Since $(\mathrm{d}Q)_{\mathrm{rev}} = T\mathrm{d}S$

$$C_V = \left[\frac{(\mathrm{d}Q)_{\mathrm{rev}}}{\mathrm{d}T}\right]_{N,V const.} = T\left(\frac{\mathrm{d}S}{\mathrm{d}T}\right)_{N,V const.} = T\left(\frac{\partial S}{\partial T}\right)_{N,V}$$

Thus

$$S(T, V, N) = \int_0^T \mathrm{d}T' \frac{C_V(T', N, V)}{T'}$$

Heat capacivities $C_V$ are measurable, and so is $S(T, V, N)$.

## 2.7 Partition function of molecular gases

### 2.7.1 Ideal monoatomic gas

We are considering a

- one component dilute gas with
  - no intermolecular for forces (neglected)
  - no correlation
- particles are treated as mass points with three degrees of freedom (translation)

- independent, indistinguishable particles

$$Q = \frac{1}{N!} q^N$$

assuming the number of available quantum states is large compared to N.

The molecular partition function $q$

$$q = \sum_j \mathrm{e}^{-e_j/\mathrm{k_B}T}$$

Model for the energy levels: quantum particles in a cubic box of length $L$.

$$e_{nlm} = \frac{h^2(n^2+l^2+m^2)}{8ML^2} \qquad n,l,m = 1,2,\ldots$$

with $h$: Planck constant and $M$: particle mass.

Number of states with energy smaller than $\epsilon$ : $\Phi(\epsilon)$.

We define a sphere with radius $R$ in the tree-dimensional space of quantum numbers $n$, $l$, $m$.

$$R^2 = n^2 + l^2 + m^2 = \frac{8MV^{2/3}\epsilon}{h^2}$$

We have used that $L^2 = V^{2/3}$. The number of unique and allowed points inside the sphere (= Volume of octant with $n$, $l$, $m$ positive).

$$\Phi(\epsilon) = \frac{\pi R^3}{6} = \frac{\pi}{6}\left(\frac{8M\epsilon}{h^2}\right)^{3/2} V$$

We need $\Phi(\epsilon) \gg N$ for $\epsilon \approx \mathrm{k_B}T$ as states with $\epsilon \gg \mathrm{k_B}T$ will not be occupied.

$$\Phi(\epsilon) \approx \left(\frac{2\pi M\mathrm{k_B}T}{h^2}\right)^{3/2} V \gg N$$

This is favoured for

- low density $N/V$.

- large mass.
- high temperature.

and can be summarized with

$$\frac{\Lambda^3 N}{V} \ll 1 \quad \text{with} \quad \Lambda = \frac{h}{\sqrt{2\pi M \mathrm{k_B} T}}$$

**Test** : use experimental density of *liquid* at boiling point.

| | $T$[K] | $\Lambda^3 N/V$ |
|---|---|---|
| He | 4.2 | 1.5 |
| $H_2$ | 20.4 | 0.44 |
| Ne | 27.2 | 0.015 |
| Ar | 87.4 | 0.0054 |

Gas phase reduces $\Lambda^3 N/V$ by about a factor of 100. $\Phi(\epsilon) \gg N$ is OK, except for light molecules at high density and very low temperatures.

Molecular partition function

$$q = \sum_{nlm} \mathrm{e}^{-\epsilon(nlm)/\mathrm{k_B}T} \quad .$$

Replace sum by integration, valid if $\Delta\epsilon \ll \mathrm{k_B}T$.

$$\Delta\epsilon \approx \frac{h^2}{MV^{2/3}} \quad \text{and} \quad \frac{\Delta\epsilon}{\mathrm{k_B}T} \approx \frac{\Lambda^2}{V^{2/3}} \ll \frac{1}{N^{2/3}} \approx 10^{-14}$$

Number os states between $\epsilon$ and $\epsilon + \Delta\epsilon$ is

$$\omega(\epsilon)\mathrm{d}\epsilon = \frac{\mathrm{d}\Phi}{\mathrm{d}\epsilon}\mathrm{d}\epsilon = \frac{\pi}{4}\left(\frac{8M}{h^2}\right)^{3/2} V\sqrt{\epsilon}\mathrm{d}\epsilon$$

For the molecular partition function $q$ we get

$$\begin{aligned} q(V,T) &= \int_0^\infty \omega(\epsilon) \mathrm{e}^{-\epsilon/\mathrm{k_B}T} \mathrm{d}\epsilon \\ &= \frac{\pi}{4} \left( \frac{8M\mathrm{k_B}T}{h^2} \right)^{3/2} V \int_0^\infty u^{1/2} \mathrm{e}^{-u} \mathrm{d}u \; ; \qquad u = \frac{\epsilon}{\mathrm{k_B}T} \\ &= \left( \frac{2\pi M\mathrm{k_B}T}{h^2} \right)^{3/2} V = \frac{V}{\Lambda^3} \end{aligned}$$

We see that $q$ is proportional to the volume $V$ and dimensionless.

The fraction of molecules with energies between $\epsilon$ and $\epsilon + \Delta\epsilon$ is

$$P(\epsilon)\mathrm{d}\epsilon = \frac{\omega(\epsilon)\mathrm{e}^{-\epsilon/\mathrm{k_B}T}\mathrm{d}\epsilon}{q} \quad .$$

The state density $\omega(\epsilon)$ is propotional to $\epsilon^{1/2}$, this is the Maxwell-Boltzmann distribution. In classical physics, we have

$$\epsilon = \frac{M}{2}v^2 \quad \longrightarrow \quad P(v) = \left( \frac{M}{2\pi\mathrm{k_B}T} \right)^{3/2} v^2 \mathrm{e}^{-\frac{Mv^2}{2\mathrm{k_B}T}} \quad .$$

**Canonical partition function**

$$Q = \frac{1}{N!} q^N = \frac{1}{N!} \left( \frac{V}{\Lambda^3} \right)^N$$

or

$$\begin{aligned} \ln Q &= -N \ln N + N + N \ln q \\ &= N \ln \left[ \left( \frac{2\pi M\mathrm{k_B}T}{h^2} \right)^{3/2} \frac{Ve}{N} \right] \end{aligned}$$

The canonical partition function is needed to calculate thermodynamic properties of gases.

### 2.7.2 Internal degrees of freedom

The translational Hamiltonian is rigorously separable, electronic and nuclear Hamiltonians are to a high degree seperable.

$$E = \epsilon_{\mathrm{t}} + \epsilon_{\mathrm{e}} + \epsilon_{\mathrm{N}}$$
$$Q = \frac{1}{N!}(q_{\mathrm{t}} q_{\mathrm{e}} q_{\mathrm{N}})^N$$

Nuclear excited states are at very high energy ($\approx 1$ MeV $\approx 10^{10}$ K) and not important for our energy scales. We can replace the nuclear energy partition function by its ground state degeneracy $\omega_{\mathrm{N}}$.

$$q_{\mathrm{N}} = \omega_{\mathrm{N}}$$

Energy differences between electronic states can vary considerably

$$q_{\mathrm{e}} = \sum_j \omega_{\mathrm{e}}^j \mathrm{e}^{-\frac{\epsilon_j^{\mathrm{e}}}{\mathrm{k_B} T}}$$

where $\omega_{\mathrm{e}}^j$ is the degeneracy of electronic states, e.g. hydrogen atom ground states $\omega_{\mathrm{e}} = 2$ (spin).

Zero of energy (arbitrary)

$$E_0 = e_{\mathrm{t}}^0 + e_{\mathrm{e}}^{\mathrm{g}} + e_{\mathrm{N}}^{\mathrm{g}} = 0$$
$$q_{\mathrm{e}}(T) = \omega_{\mathrm{e}}^0 + \omega_{\mathrm{e}}^1 \mathrm{e}^{-\frac{\epsilon_1}{\mathrm{k_B} T}} + \omega_{\mathrm{e}}^2 \mathrm{e}^{-\frac{\epsilon_2}{\mathrm{k_B} T}} + \cdots$$

For halogen atoms at $T = 1000$K contributions of the second term are $0.22, 0.12, 0.0024, 10^{-5}$ for F, Cl, Br, and I.

### 2.7.3 Ideal diatomic gas

We have to include in addition vibrationand rotation. We will assume a further separation of energies

$$\begin{aligned}
\epsilon &= \epsilon_{\mathrm{t}} + \epsilon_{\mathrm{r}} + \epsilon_{\mathrm{v}} + \epsilon_{\mathrm{e}} \\
Q &= \frac{1}{N!} q^N \\
q(V,T) &= q_{\mathrm{t}}(V,T) \quad \underbrace{q_{\mathrm{r}}(T) q_{\mathrm{v}}(T) q_{\mathrm{e}}(T)}_{\text{only depends on T}} \\
q_{\mathrm{t}}(V,T) &= \left[\frac{2\pi M \mathrm{k_B} T}{h^2}\right]^{3/2} V \qquad M\text{: total mass} \\
q_{\mathrm{e}}(T) &= \omega_{\mathrm{e}} \mathrm{e}^{-\frac{\epsilon_1}{\mathrm{k_B} T}} \qquad \text{beware zero of energy!}
\end{aligned}$$

If more than the ground state has to be included, separation becomes difficult, as e.g. vibrations are different in different electronic states.

**Vibration** Harmonic approximation

$$\epsilon_n = (n + \frac{1}{2}) h\nu \qquad \nu = \frac{1}{2\pi}\sqrt{\frac{f}{\mu}}$$

$n = 0, 1, 2, \ldots$ f: force constant $\mu$: reduced mass

$$\begin{aligned}
q_{\mathrm{v}} &= \sum_{n=0}^{\infty} \mathrm{e}^{-\epsilon_n/\mathrm{k_B}T} = \mathrm{e}^{-h\nu/2\mathrm{k_B}T} \underbrace{\sum_{n=0}^{\infty} \left(\mathrm{e}^{-h\nu/\mathrm{k_B}T}\right)^n}_{\frac{1}{1-\mathrm{e}^{-h\nu/\mathrm{k_B}T}}} \\
&= \frac{\mathrm{e}^{-h\nu/2\mathrm{k_B}T}}{1-\mathrm{e}^{-h\nu/\mathrm{k_B}T}} = \frac{\mathrm{e}^{h\nu/2\mathrm{k_B}T}}{\mathrm{e}^{-h\nu/\mathrm{k_B}T}-1}
\end{aligned}$$

**Rotation** There arise difficulties for symmetric ( or highly symmetric in case of polyatomic) molecules because of degeneracies.

Example: rigid linear rotator

$$\epsilon_j = \frac{j(j+1)h^2}{8\pi^2 I} \qquad j = 0, 1, 2, \ldots$$

$$\omega_j = 2j + 1 \qquad \text{degeneracy}$$

I: moment of inertia

$$q_\mathrm{r}(T) = \sum_j \omega_j \mathrm{e}^{-\frac{\epsilon_j}{\mathrm{k_B}T}} = \sum_{j=0}^{\infty} (2j+1)\mathrm{e}^{-j(j+1)\Theta_\mathrm{r}/T}$$

$$\Theta_\mathrm{r} = \frac{h^2}{8\pi^2 I \mathrm{k_B}}$$

At high temperatures we get the classical limit

$$\begin{aligned} q_\mathrm{r} &\longrightarrow \int_0^\infty (2J+1)\mathrm{e}^{-j(j+1)\Theta_\mathrm{r}/T}\mathrm{d}j \\ &= \frac{T}{\Theta_\mathrm{r}} = \frac{8\pi^2 I \mathrm{k_B} T}{h^2} \\ q_\mathrm{r} &\approx \frac{T}{\Theta_\mathrm{r}}\left(1 + \frac{\Theta_\mathrm{r}}{3T} + \cdots\right) \qquad \text{for smaller temperatures} \end{aligned}$$

### 2.7.4 Polyatomic molecules

**Vibration** ($3N - 6$ harmonic oscillators)

'normal modes' decoupling

$$q_\mathrm{v}(T) = \prod_{i=1}^{n'} \frac{\mathrm{e}^{-\Theta_i/2T}}{1 - \mathrm{e}^{-\Theta_i/T}} \qquad \Theta_i = \frac{h\nu_i}{\mathrm{k_B}}$$

**Rotation**

$$q_\mathrm{r}(T) = \frac{\sqrt{\pi}}{\sigma}\left(\frac{8\pi^2 I_A \mathrm{k_B} T}{h^2}\right)^{1/2}\left(\frac{8\pi^2 I_B \mathrm{k_B} T}{h^2}\right)^{1/2}\left(\frac{8\pi^2 I_C \mathrm{k_B} T}{h^2}\right)^{1/2}$$

$I_A$, $I_B$, $I_C$: principle moments of inertia

$\sigma$ symmetry number

specific for special cases, e.g. $\sigma = 12$ for $CH_4$ (tetrahedral symmetry)

High temperature limit

$$q_{\mathrm{r}} = \frac{\sqrt{\pi}}{\sigma} \left( \frac{T^3}{\Theta_A \Theta_B \Theta_C} \right)^{1/2}$$

## 2.8 Partition function and free energy

We have established that

$$\langle E \rangle = \left( \frac{\partial \ln Q}{\partial(-\beta)} \right)_{N,V} \quad .$$

What does that tell us about $Q$?

Consider the Helmholtz free energy, $A$, defined as

$$A \equiv E - TS \; ; \qquad A(E, T, S)$$
$$E : \text{This is the termodynamic } E, \text{i.e. } \langle E \rangle$$

As soon as you see things like "$T$" and "$S$" in an equation you know it is refering to equilibrium because that is the only place where $T$ and $S$ are defined.

Clearly,

$$\mathrm{d}A = \mathrm{d}E - T\mathrm{d}S - S\mathrm{d}T \qquad \text{total differential}$$

Recall that

$$\mathrm{d}E = \underbrace{(\mathrm{d}Q)_{\mathrm{rev}}}_{\text{Heat}} + \underbrace{(\mathrm{d}W)_{\mathrm{rev}}}_{\text{Work}} = T\mathrm{d}S - p\mathrm{d}V + \mu\mathrm{d}N$$

So,

$$\begin{aligned} \mathrm{d}A &= T\mathrm{d}S - p\mathrm{d}V + \mu\mathrm{d}N - T\mathrm{d}S - S\mathrm{d}T \\ &= -S\mathrm{d}T - p\mathrm{d}V + \mu\mathrm{d}N \end{aligned}$$

So, this quantity $A$ is a natural function of $T$, $V$, and $V$.

Equivalently,

$$-\frac{A}{\mathrm{k_B}T} = -\beta A = -\beta A + \frac{S}{\mathrm{k_B}}$$

Differential

$$\mathrm{d}(-\beta A) = \mathrm{d}\left(\frac{S}{\mathrm{k_B}}\right) - \mathrm{d}(\beta E)$$

The first term is

$$\mathrm{d}\left(\frac{S}{\mathrm{k_B}}\right) = \frac{T\mathrm{d}S}{\mathrm{k_B}T} = \beta T\mathrm{d}S$$

and with

$$T\mathrm{d}S = \mathrm{d}E + p\mathrm{d}V - \mu\mathrm{d}N$$

we get

$$\begin{aligned}\mathrm{d}(-\beta A) &= [\beta\mathrm{d}E + \beta p\mathrm{d}V - \beta\mu\mathrm{d}N] - \beta\mathrm{d}E - E\mathrm{d}\beta \\ &= -E\mathrm{d}\beta + \beta p\mathrm{d}V - \beta\mu\mathrm{d}N\end{aligned}$$

From this we get

$$\left(\frac{\partial(-\beta A)}{\partial(-\beta)}\right)_{N,V} = E = \left(\frac{\partial \ln Q}{\partial(-\beta)}\right)_{N,V}$$

and therefore

$$\ln Q = -\beta A + \text{"constant of integration"} = -\beta A$$

The constant of integration we get from (assuming $\Omega_{\text{ground}} = 1$)

$$= \begin{cases} \ln Q = \ln \sum_i \mathrm{e}^{-\beta E_i} \overset{\beta\to\infty}{\longrightarrow} -\beta E_{\text{ground}} \\ -\beta A \overset{\beta\to\infty}{\longrightarrow} -\beta E_{\text{ground}} + S(T=0)/\mathrm{k_B} = -\beta E_{\text{ground}} \end{cases}$$

Thus

$$\boxed{Q = \mathrm{e}^{-\beta A} = \sum_i \mathrm{e}^{-\beta E_i}}$$

Boltzmann weighted sum over all fluctuations with $N$ and $V$ fixed.

$$\boxed{A = -\mathrm{k_B}T \ln Q}$$

We will have many applications of this result.

Other identities derived from

$$\mathrm{d}A = -S\mathrm{d}T - p\mathrm{d}V + \mu\mathrm{d}N \ .$$

Dived by $\mathrm{d}t$ to get

$$\frac{\mathrm{d}A}{\mathrm{d}T} = -S - p\frac{\mathrm{d}V}{\mathrm{d}T} + \mu\frac{\mathrm{d}N}{\mathrm{d}T} \ .$$

keep $N$, $V$ fixed

$$\left(\frac{\partial A}{\partial T}\right)_{N,V} = -S - p\underbrace{\left(\frac{\partial V}{\partial T}\right)_{N,V}}_{=0} + \mu\underbrace{\left(\frac{\partial N}{\partial T}\right)_{N,V}}_{=0}$$

$$S = -\left(\frac{\partial A}{\partial T}\right)_{N,V} = \left(\frac{\partial(\mathrm{k_B}T\ln Q)}{\partial T}\right)_{N,V} = \mathrm{k_B}T\left(\frac{\partial \ln Q}{\partial T}\right)_{N,V} + \mathrm{k_B}\ln Q$$

Similarly, from $\mathrm{d}A/\mathrm{d}V$ and $N$, $T$ fixed we get

$$p = -\left(\frac{\partial A}{\partial V}\right)_{N,T} = \mathrm{k_B}T\left(\frac{\partial \ln Q}{\partial V}\right)_{N,T}$$

and from $\mathrm{d}A/\mathrm{d}N$ and $V$, $T$ fixed we get

$$\mu = \left(\frac{\partial A}{\partial N}\right)_{V,T} = -\mathrm{k_B}T\left(\frac{\partial \ln Q}{\partial N}\right)_{V,T}$$

Another transformation starts with

$$-\beta = \frac{-1}{\mathrm{k_B}T}$$

$$\mathrm{d}(-\beta) = \frac{-1}{\mathrm{k_B}}\left(\frac{\partial 1/T}{\partial T}\right)\mathrm{d}T = \frac{1}{\mathrm{k_B}T^2}\mathrm{d}T$$

and gets

$$E = \left(\frac{\partial \ln Q}{\mathrm{d}(-\beta)}\right)_{N,V} = \mathrm{k_B}T^2\left(\frac{\partial \ln Q}{\mathrm{d}T}\right)_{N,V} \quad .$$

With $\ln Q = -\frac{A}{\mathrm{k_B}T}$ we finally get

$$E = \mathrm{k_B}T^2\left(\frac{\partial\left(-\frac{A}{\mathrm{k_B}T}\right)}{\partial T}\right)_{N,V} = -T^2\left(\frac{\partial A/T}{\partial T}\right)_{N,V}$$

### 2.8.1 Thermodynamic functions of the monoatomic ideal gas

We recall the canonical partition function for an ideal gas

$$Q = \frac{1}{N!}\left(\frac{V}{\Lambda^3}\right)^N \qquad \Lambda = \frac{h}{\sqrt{2\pi M \mathrm{k_B} T}}$$
$$\ln Q = N \ln\left[\left(\frac{2\pi M \mathrm{k_B} T}{h^2}\right)^{3/2} \frac{Ve}{N}\right]$$

The Helmholtz free energy for this system is

$$A(N,V,T) = -\mathrm{k_B} T \ln Q = -N\mathrm{k_B} T \ln\left[\left(\frac{2\pi M \mathrm{k_B} T}{h^2}\right)^{3/2} \frac{Ve}{N}\right] .$$

From the formula for the pressure $p$

$$\begin{aligned} p &= \mathrm{k_B} T \left(\frac{\partial \ln Q}{\partial V}\right)_{T,N} \\ &= N\mathrm{k_B} T \left(\frac{\partial \ln uV}{\partial V}\right)_{T,N} \qquad Q \propto V \\ &= N\mathrm{k_B} T \frac{1}{uV} u = \frac{N\mathrm{k_B} T}{V} \end{aligned}$$

we get the ideal gas law

$$pV = N\mathrm{k_B} T \qquad N\mathrm{k_B} = nR$$

The thermodynamic energy of the system is

$$\begin{aligned} E &= \mathrm{k_B} T^2 \left(\frac{\partial \ln Q}{\partial T}\right)_{V,N} = N\mathrm{k_B} T^2 \left(\frac{\partial \ln uT^{3/2}}{\partial T}\right)_{V,N} \\ &= N\mathrm{k_B} T^2 \frac{1}{uT^{3/2}} \frac{3}{2} u T^{1/2} = \frac{3}{2} N\mathrm{k_B} T \\ &= \frac{3}{2} nRT \end{aligned}$$

The Heat capacity is

$$\begin{aligned} C_V &= \left(\frac{\partial E}{\partial T}\right)_{V,N} = \frac{3}{2}\mathrm{k_B}\left(\frac{\partial NT}{\partial T}\right)_{V,N} = \frac{3}{2}\mathrm{k_B} N \\ &= \frac{3}{2} nR \end{aligned}$$

### 2.8.2 Einstein's model of a crystal

Einstein imagined each atom in a crystal as vibrating in the fixed self consistent field of its neighbors.

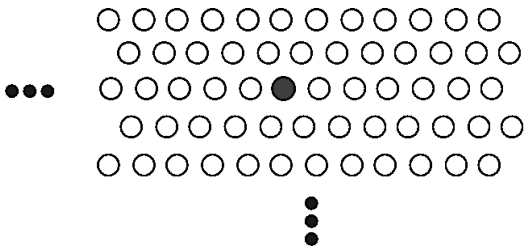

scheme 038

We are considering one single atom. It is vibrating in the potential field created by the surrounding atoms. It is at $\vec{r}_i = \vec{r}_i^{\,0} + \Delta\vec{r}_i$.

Einstein's approximation of the Hamiltonian of a crystal consists of the kinetic energy and a harmonic potential part

$$\mathcal{H} \approx \sum_{i=1}^{N} \left[ \frac{p_i^2}{2m} + \frac{1}{2} k |\Delta\vec{r}_i|^2 \right]$$

The force constant $k$ should be a function of $\rho = N/V$.

Energy levels of an assembly of one-dimensional harmonic oscillators with

$$E = (\frac{1}{2} + n)\hbar\omega \qquad \text{with} \quad \hbar\omega = \hbar\sqrt{\frac{k}{m}}$$

The energy expression for the full system is

$$E(n_{1x}, n_{1y}, n_{1z}, n_{2x}, \ldots, n_{Nz}) = \sum_{i=1}^{N} \sum_{\alpha=x,y,z} (\frac{1}{2} + n_{i\alpha})\hbar\omega$$

The quantum numbers $n_{i\alpha} = 0, 1, 2, \ldots$ specify the quantum state of a 1-dimensional harmonic oszillator associated with the Cartesian coordinate $\alpha$ of the $i$th atom.

Hence, the partition function of the crystal is

$$
\begin{aligned}
Q_{\mathrm{AE}} &= \underbrace{\sum_{n_{1x}=0}^{\infty}\sum_{n_{1y}=0}^{\infty}\cdots\sum_{n_{Nz}=0}^{\infty}}_{3N\text{ sums}} \mathrm{e}^{-\beta(1/2+n_{1x})\hbar\omega}\mathrm{e}^{-\beta(1/2+n_{1y})\hbar\omega}\cdots\mathrm{e}^{-\beta(1/2+n_{Nz})\hbar\omega} \\
&= \left[\sum_{n=0}^{\infty}\mathrm{e}^{-\beta(1/2+n)\hbar\omega}\right]^{3N} \\
&= \left[\mathrm{e}^{-\frac{\beta}{2}\hbar\omega}\left(1+\sum_{n=1}^{\infty}\left(\mathrm{e}^{-\beta\hbar\omega}\right)^{n}\right)\right]^{3N}
\end{aligned}
$$

Making use of

$$
1+\sum_{n=1}^{\infty}\left(\underbrace{\mathrm{e}^{-\beta\hbar\omega}}_{=x<1}\right)^{n} = 1+x+x^2+x^3+\cdots = \frac{1}{1-x}
$$

we get

$$
Q_{\mathrm{AE}} = \left[\frac{\mathrm{e}^{-\frac{\beta}{2}\hbar\omega}}{1-\mathrm{e}^{-\beta\hbar\omega}}\right]^{3N}
$$

Thus, Einstein's theory for the energy $A$, is

$$
\begin{aligned}
-\beta A = \ln Q &= 3N\left[\ln \mathrm{e}^{-\frac{\beta}{2}\hbar\omega} - \ln\left(1-\mathrm{e}^{-\beta\hbar\omega}\right)\right] \\
&= \underbrace{3N}_{\text{extensive}}\ [\ \underbrace{-\beta\hbar\omega/2}_{\substack{\text{ground state}\\ \text{energy of one}\\ \text{oscillator}}}\ -\ \underbrace{\ln\left(1-\mathrm{e}^{-\beta\hbar\omega}\right)}_{\substack{\text{contributions from}\\ \text{finite temperature}\\ \text{thermal fluctuations}}}\ ]
\end{aligned}
$$

The corresponding internal energy is

$$
\langle E\rangle = \left(\frac{\partial \ln Q}{\partial(-\beta)}\right)_{N,V} = 3N\left[\frac{\hbar\omega}{2}+\hbar\omega\frac{\mathrm{e}^{-\beta\hbar\omega}}{1-\mathrm{e}^{-\beta\hbar\omega}}\right]
$$

where

$\dfrac{\hbar\omega}{2}$ is the zero point energy

$\dfrac{\mathrm{e}^{-\beta\hbar\omega}}{1-\mathrm{e}^{-\beta\hbar\omega}}$ is the average number of excitations per oscillator

Thus, heat capacity according to Einstein

$$C_V = \left(\frac{\partial\langle E\rangle}{\partial T}\right)_{N,V} = 3N\hbar\omega\frac{\mathrm{d}}{\mathrm{d}T}\left(\frac{1}{\mathrm{e}^{-\beta\hbar\omega}-1}\right)$$

or

$$\left(\frac{C_V}{N}\right) \approx 3\frac{\hbar\omega}{\mathrm{k_B}T^2}\frac{\mathrm{e}^{-\beta\hbar\omega}}{\left(\mathrm{e}^{-\beta\hbar\omega}-1\right)^2} \overset{T\to 0;\beta\to\infty}{\longrightarrow} 3\frac{\hbar\omega}{\mathrm{k_B}T^2}\mathrm{e}^{-\frac{\hbar\omega}{\mathrm{k_B}T}}$$

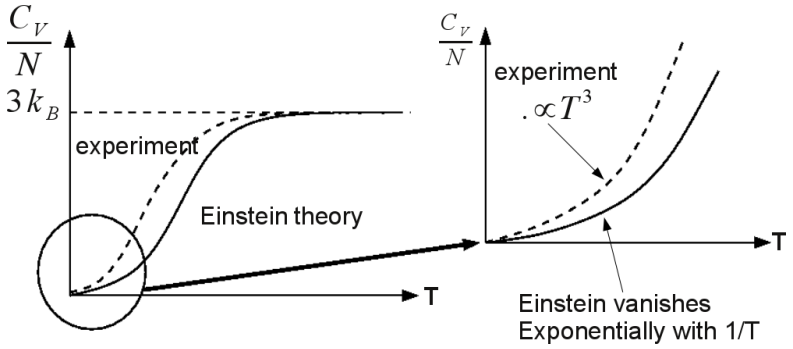


scheme 039

Notice that Einstein's theory says

$$T\left(\frac{C_V}{N}\right) = 3\beta\hbar\omega\mathrm{e}^{-\beta\hbar\omega}/(\mathrm{e}^{-\beta\hbar\omega}-1)^2$$
$$= \text{function of } (\beta\hbar\omega)$$

Changing the crystal changes $\omega$; but with $\omega$ fixed, Einstein predicts that $TC_V/N$ is a universal function of $T$ or $\beta = 1/\mathrm{k_B}T$. That is, Einstein's theory predicts a *Principle of Corresponding States* (see e.g. van der Waals gases).

- High $T$ limit

$$C_V \longrightarrow 3N\mathrm{k_B} \quad \text{(Dulong–Petit)}$$

- Low $T$ limit (experiment: $C_V \propto T^3$)

$$C_V \longrightarrow 3N\mathrm{k_B}\mathrm{e}^{-\Theta/T}$$

Einstein's theory fails for low temperatures. What is the problem?

Einstein's model only involves local, rather high frequency motions. Collective motions at low frequency are ignored. At low temperature these motions will be more important.

Phonon (vibrations in crystals) dispersion, frequency distribution $g(\nu)$.

$$\int_0^\infty g(\nu)\mathrm{d}\nu = 3N$$

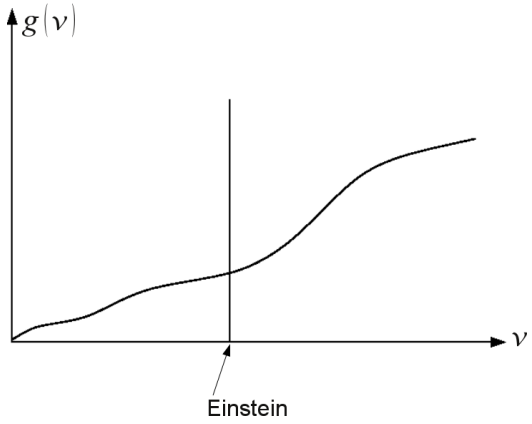


scheme 040

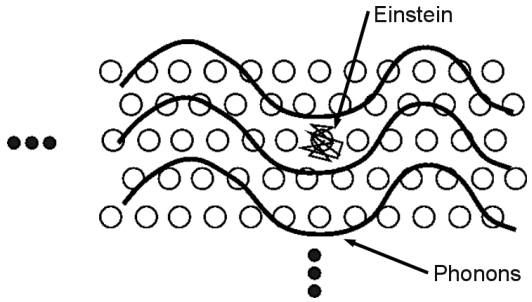


scheme 041

With the general phonon dispersion function one gets

$$-\ln Q = \int_0^\infty \left[\ln\left[1-\mathrm{e}^{-\beta h\nu}\right] + \frac{h\nu}{2\mathrm{k_B}T}\right] g(\nu)\mathrm{d}\nu$$

**Debye approximation** $g(\nu) \propto \nu^2$ (from continuum theory)

Normalization

$$\int_0^{\nu_m} g(\nu)\mathrm{d}\nu = 3N = \frac{\alpha\nu_m^3}{3}$$

where $\alpha$ is a proportionality constant and the cutoff frequency $\nu_m$ is needed to have a finite integral. The normalization fixes the constant alpha for a given cutoff.

$$g(\nu) = \begin{cases} \frac{9N\nu^2}{\nu_m^3} & 0 \le \nu \le \nu_m \\ 0 & \nu > \nu_m \end{cases}$$

For the energy we get

$$\begin{aligned} E &= \mathrm{k_B}T^2 \left(\frac{\partial \ln Q}{\partial T}\right)_{N,V} \\ &= \frac{9N\mathrm{k_B}T}{\nu_m^3} \int_0^{\nu_m} \left(\frac{h\nu}{2\mathrm{k_B}T} + \frac{h\nu/\mathrm{k_B}T}{\mathrm{e}^{h\nu/\mathrm{k_B}T}-1}\right)\nu^2\mathrm{d}\nu \\ &= \frac{9N\mathrm{k_B}T}{u^3} \int_0^{u} \left(\frac{x}{2} + \frac{x}{\mathrm{e}^x - 1}\right)x^2\mathrm{d}x \qquad \text{where} \quad x = h\nu/\mathrm{k_B}T \ ; \ u = h\nu_m \\ kbT. &= \frac{9Nh\nu_m}{8} + 3N\mathrm{k_B}TD(u) \qquad \text{where} \quad D(u) = \frac{3}{u^3}\int_0^u \frac{x^3}{\mathrm{e}^x-1}\mathrm{d}x \end{aligned}$$

Asymptotic values for $D(u)$

$$\begin{aligned} D(u) &= \frac{3}{u^3}\int_0^u \frac{x^3}{\mathrm{e}^x-1}\mathrm{d}x \longrightarrow \frac{\pi^4}{5u^3} && \text{for } T \to 0,\ u \to \infty \\ D(u) &= \frac{3}{u^3}\int_0^u \frac{x^3}{\mathrm{e}^x-1}\mathrm{d}x \longrightarrow 1 && \text{for } T \to \infty,\ u \to 0 \end{aligned}$$

Therefore

$$\begin{aligned} E &\longrightarrow \frac{9Nh\nu_m}{2} + \frac{3N\pi^4 h\nu_m}{5}\left(\frac{\mathrm{k_B}T}{h\nu_m}\right) && T \to 0 \\ E &\longrightarrow 3N\mathrm{k_B}T && T \to \infty \quad \text{(same as Einstein)} \end{aligned}$$

and for the heat capacity

$$\begin{aligned} C_V = \left(\frac{\partial E}{\partial T}\right)_{N,V} &= 3N\mathrm{k_B}\frac{\partial}{\partial T}[TD(u)] \\ &= 3N\mathrm{k_B}\left[4D(u) - \frac{3u}{\mathrm{e}^u - 1}\right] \end{aligned}$$

Introducing the Debye Temperature, $\Theta_{\rm D} = \frac{h\nu_m}{{\rm k_B}}$, $u = \frac{h\nu_m}{{\rm k_B}T} = \frac{\Theta_{\rm D}}{T}$ the low temperature limit of the heat capacity gets

$$C_V \longrightarrow \frac{12N{\rm k_B}\pi^4}{5}\left(\frac{T}{\Theta_{\rm D}}\right)^3 \propto T^3 \quad \text{for} \qquad T \to 0 \ .$$

# Chapter 3

# Summary and Mathematical Properties

## 3.1 Microcanonical ensemble

$$S = \mathrm{k_B} \ln \Omega(E, N, V)$$

Boltzmann's legacy, principle of equal weights; equilibrium states characterized by $E$, $N$, $V$.

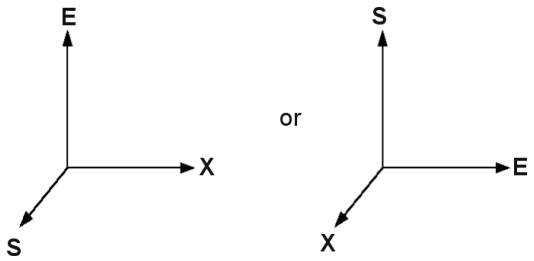


scheme 042

$$S(E, N, V; \text{no extra constraints}) > S(E, N, V; \text{internal constraints})$$

The Second Law. Equilibrium maximizes $S$

$$\left.\begin{array}{l} \mathrm{d}E = T\mathrm{d}S - p\mathrm{d}V + \mu\mathrm{d}N \end{array}\right\} \begin{array}{l} \text{Moving among} \\ \text{equilibrium states} \end{array}$$

$$\left.\begin{array}{l} \mathrm{d}E = \mathrm{d}Q + \mathrm{d}W \\ \\ T\mathrm{d}S = (\mathrm{d}Q)_{\mathrm{rev}} \end{array}\right\} \begin{array}{l} \text{The First Law; conservation of} \\ \text{energy; heat and work are} \\ \text{the two forms of energy transfer} \end{array}$$

$E$ and $S$ are state functions.

Since $C_V = \left(\frac{\partial E}{\partial T}\right)_{N,V}$ is always positive, $T^{-1} \equiv \left(\frac{\partial S}{\partial E}\right)_{N,V} = T^{-1}(E,N,V)$ can be inverted to give $E = E(T,V,N)$. Equilibrium states can therefore be characterized by $T$, $V$, $N$.

## 3.2 Canonical ensemble

**Equilibrium with $T$, $V$, and $N$**

$$P_j = \mathrm{e}^{-\beta E_j}/Q \ , \quad \beta = 1/\mathrm{k_B}T$$

$$Q(T,V,N) = \sum_j \mathrm{e}^{-\beta E_j} = \mathrm{e}^{-\beta A} \ ; \quad \text{partition function}$$

$$A = E - TS \ , \quad \mathrm{d}A = -S\mathrm{d}T - p\mathrm{d}V + \mu\mathrm{d}N \ ; \quad \text{Helmholtz free energy}$$

$$E(T,V,N) = \langle E \rangle = \left(\frac{\partial \ln Q}{\partial(-\beta)}\right)_{N,V}$$

**Repeat what we already know:**

$$S = S(E, V, N) \qquad \text{Entropy as a function of } E,\ V,\ N$$

$$\downarrow \text{its differential}$$

$$\mathrm{d}S = \underbrace{\left(\frac{\partial S}{\partial E}\right)_{N,V}}_{1/T} \mathrm{d}E + \underbrace{\left(\frac{\partial S}{\partial V}\right)_{N,E}}_{p/T} \mathrm{d}V + \underbrace{\left(\frac{\partial S}{\partial N}\right)_{V,E}}_{-\mu/T} \mathrm{d}N$$

$$T\mathrm{d}S = \mathrm{d}E + p\mathrm{d}V - \mu\mathrm{d}N$$

1. $\mathrm{d}E = T\mathrm{d}S - p\mathrm{d}V + \mu\mathrm{d}N$; $E = E(S, V, N)$
   We assume the energy is conserved.
   We know empirically that the energy of a system can be changed by

   - doing work on the system ($W$)
   - allowing heat to flow into the system ($Q$)

   in mathematical notation

2. $\mathrm{d}E = (\mathrm{d}Q)_{\mathrm{rev}} + (\mathrm{d}W)_{\mathrm{rev}}$

   - $(\mathrm{d}Q)_{\mathrm{rev}}$: differential heat flow into the system
   - $(\mathrm{d}W)_{\mathrm{rev}}$: differential work done on the system

   Keep in mind that work and heat are forms of energy transfer!
   You also already know that the mechanical definition of work is the product of the external force on a body times the distance through which the force acts:

   $$(\mathrm{d}W)_{\mathrm{rev}} = (\text{force})x\Delta l = -\left(\frac{\text{force}}{\text{area}}\right) \cdot \Delta V$$

   Remember: positive work done on the system decreases system volume.

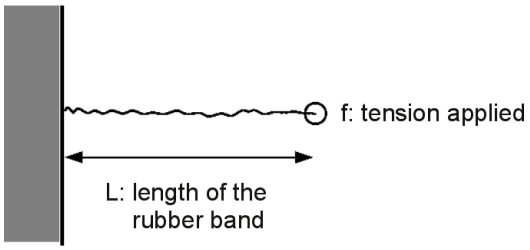

3. $(\mathrm{d}W)_{\mathrm{rev}} = -p_{\mathrm{ext}} \cdot \Delta V$
   external pressure $\times$ change of volume of bulk system

By comparing equations 1), 2), and 3)

$$(\mathrm{d}W)_{\mathrm{rev}} = \underbrace{-p\mathrm{d}V}_{\substack{\text{one form of}\\ \text{mecanical work}}} + \underbrace{\mu\mathrm{d}N}_{\text{chemical work}} + \cdots \begin{matrix}\text{any other}\\ \text{kind of work}\end{matrix}$$

$$(\mathrm{d}Q)_{\mathrm{rev}} = T\mathrm{d}S$$

Recall the example of reversible and isothermal ($T$= const.) compression of an ideal gas:
The energy of an ideal gas depends only on $T$, so when $T$ is fixed, so is the energy.

$$\Delta E_{\text{id. gas}} = 0 = (Q)_{\mathrm{rev}} + (W)_{\mathrm{rev}}$$
$$(W)_{\mathrm{rev}} = nRT \ln \frac{V_{\text{initial}}}{V_{\text{final}}}$$

Consider now the same two states, but connected by an irreversible path with constant $p_{\mathrm{ext}} > p_2 = \frac{nRT}{V_{\text{final}}}$.

$$(W)\text{irrev} = -\int_{V_{\mathrm{I}}}^{V_{\mathrm{F}}} p_{\mathrm{ext}}\ \mathrm{d}V = -p_{\mathrm{ext}}(V_{\mathrm{F}} - V_{\mathrm{I}}) \neq nRT \ln \frac{V_{\mathrm{I}}}{V_{\mathrm{F}}}$$

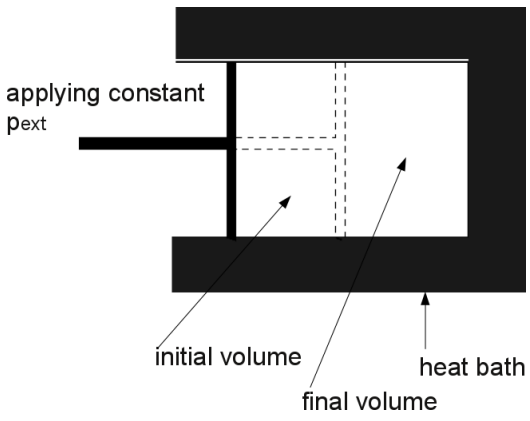

scheme 044

Example of 3 different paths between final and initial states.

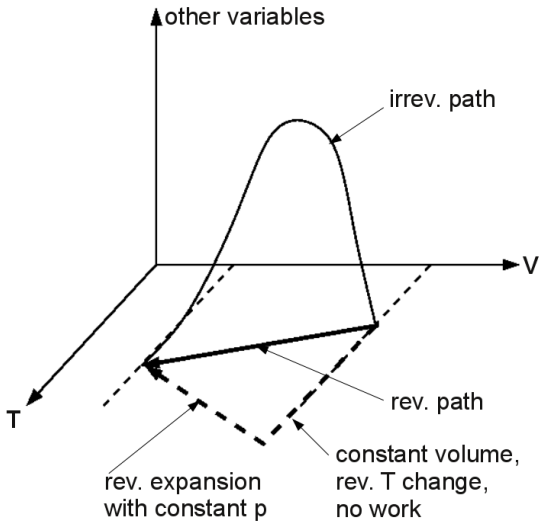


$$(W)_{irrev} \neq (W)_{rev}$$

and

$$(W)_{rev} \neq (W)_{rev'}$$

scheme 045

Another example:

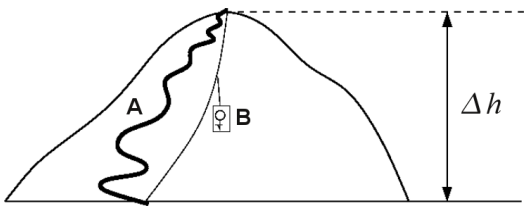


scheme 046

$(W)_A \gg (W)_B$, however the altitude increase for both is the same (= gain in potential energy)!

Lesson:

- work is a function of the path

$$(W)_{\text{path}} = \int_{\text{path}} f(x)\mathrm{d}x$$

- the altitude increase $\Delta h$ during the trip is not a function of the path

If the change in a property of a system is independent of a path, the property is called a State Function. The change in any state function is independent of path.

The altitude increase $\Delta h$ is a state function of the journey and does not depend on the history of any one particular trip.

Recall that the energy $E$ is a function of the variables defining the equilibrium state

$$E = E(S, \underbrace{N, V}_{=X}) = E(S, X) \quad \text{and} \quad (\Delta E)_{\text{cycle}} = 0$$

Consider the energy change in a cyclic process

$$\Delta E = \oint \mathrm{d}E = \int_A^B \mathrm{d}E + \int_B^A \mathrm{d}E = 0$$

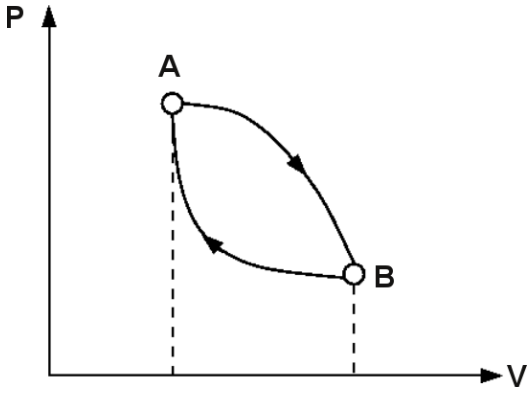


scheme 047

In a cyclic process $(\Delta E)_{\text{cycle}} = 0$ and the work done by the gas or its surrounding must be compensated for by an absorption of heat.

Hence, consider the change in internal energy between two states $A$ and $B$:

$$\Delta E = E_B - E_A = \int_{S_A}^{S_B} \mathrm{d}S \left(\frac{\partial E}{\partial S}\right)_X + \int_{X_A}^{X_B} \mathrm{d}X \left(\frac{\partial E}{\partial X}\right)_S$$

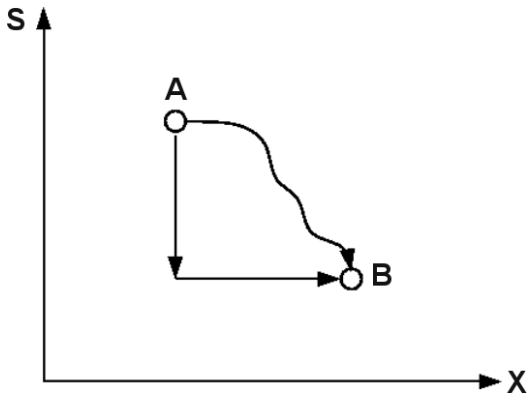


scheme 048

Change in energy on this arbitrary path must equal that of the two step path since $(\Delta E)_{\text{cycle}} = 0$.

$E(S, X) = E(S, V, N)$ is called a *state function*, i.e. it is a real function! By counter example, however, the fact that $W$ depends on path implies there is no unique function $W$!

## 3.3 Mathematical Properties of state functions

- if a function $f(x, y, \ldots)$ exists, its total differential $\mathrm{d}f$ is called *exact*

$$\mathrm{d}f = \left(\frac{\partial f}{\partial x}\right)_{y,\ldots} + \left(\frac{\partial f}{\partial y}\right)_{x,\ldots} + \cdots$$

- if a function $f(x, y, \ldots)$ does not exist, the differential is called *inexact*, and we denote it by the stroke over d: đ

- if $f(x, y)$ does exist (as well as the partial derivatives) the order of differentiation is irrelevant

$$\frac{\partial^2 f}{\partial x \partial y} = \frac{\partial^2 f}{\partial y \partial x}$$

  Thus if $\mathrm{d}f = a(x, y)\mathrm{d}x + b(x, y)\mathrm{d}y$, then (Euler reciprocity theorem)

$$\left(\frac{\partial a}{\partial y}\right)_x = \left(\frac{\partial b}{\partial x}\right)_y$$

  It is satisfied if and only if $f(x, y)$ exists.

**Examples**

- $E$ is a state function and $\mathrm{d}E$ is an exact differential

$$\int_A^B \mathrm{d}E = E_B - E_A$$

  We do not need to know the particular process that leads from $A$ to $B$ to perform integration.

- Work is not a state function and $đW$ is an inexact differential.

$$\int_A^B đW = -\int_A^B p(V)\mathrm{d}V$$

  Cannot be integrated without knowing the dependence of the pressure on volume.

With this notion we can write the First Law of thermodynamics

$$\boxed{\mathrm{d}E = đQ + đW}$$

| | |
|---|---|
| $\mathrm{d}E$ : | exact differential since $E$ is a function of state |
| $đQ$,$đW$: | inexact differentials, they depend upon path |
| | $Q$ and $W$ are the forms of energy transfer, not functions of state. |

## 3.4 Heat capacity

Since heat flow and temperature changes are intimately related, it is useful to quantify their connection by introducing Heat Capacity. It quantifies the amount of heat added to a system in terms of the resulting increase in temperature.

If the system is constrained to have $V$ = const. at constant number of particles, we define

$$C_V = \left(\frac{đQ_{\mathrm{rev}}}{\mathrm{d}T}\right)_{V,N}$$

whilst at $p$ = const.

$$C_p = \left(\frac{đQ_{\mathrm{rev}}}{\mathrm{d}T}\right)_{p,N} .$$

However, one can relate the derivative $\left(\frac{đQ_{\mathrm{rev}}}{\mathrm{d}T}\right)_{V,N}$ to a derivative of the internal energy in the following manner: at constant volume no work is done on the system and $đW = 0 \rightarrow \mathrm{d}E = đQ$

$$C_V = \left(\frac{\partial E}{\partial T}\right)_{V,N}$$

To define $C_p$ in this way, we have to introduce another state function called Enthalpy.

$$(\mathrm{d}E)_{p,N} = (đQ)_{p,N} - (p\mathrm{d}V)_{p,N} = (đQ)_{p,N} - \mathrm{d}(pV)_{p,N}$$
$$\mathrm{d}(E+pV)_{p,N} = (đQ)_{p,N}$$
$$H(\text{enthaply}) \equiv E + pV$$

$E$, $p$, $V$ are state functions and so is $H$.

$$C_p = \left(\frac{\partial H}{\partial T}\right)_{p,N}$$

## 3.5 Free energies

**Tricks to make life easy.** Recall

$$\mathrm{d}E = T\mathrm{d}S - p\mathrm{d}V + \mu\mathrm{d}N \quad \Rightarrow \; E = E(S,V,N)$$

We have also encountered

$$\mathrm{d}A = \mathrm{d}(E - TS) = -S\mathrm{d}T - p\mathrm{d}V + \mu\mathrm{d}N \quad \Rightarrow \; A = A(T,V,N)$$

Look carefully at what has happend here. $E$ is a natural function of $S$, $V$, $N$; $T$ is the intensive variable that is *conjugate* to $S$ (and $-p$ is conjugate to $V$, and $\mu$ is conjugate to $N$).

By subtracting $TS$ from $E$, we get $A$, a natural function of $T$, $V$, $N$.

Can we switch back and forth between any pairs of conjugate variables?

For example, the natural function of $T$, $P$, $N$ is $E - TS + pV$, which is called $G$ the *Gibbs free energy.*

$$\begin{aligned} G &= E - TS + pV \\ \mathrm{d}G &= \mathrm{d}E - T\mathrm{d}S - S\mathrm{d}T + p\mathrm{d}V + V\mathrm{d}p \\ &= (T\mathrm{d}S - p\mathrm{d}V + \mu\mathrm{d}N) - T\mathrm{d}S - S\mathrm{d}T + p\mathrm{d}V + V\mathrm{d}p \\ &= -S\mathrm{d}T + V\mathrm{d}p + \mu\mathrm{d}N \quad \Rightarrow \; G = G(T,p,N) \end{aligned}$$

Notice that you cannot do this switching with non-conjugate variables. Further, the new functions formed by switching conjugate pairs contain the same information as the original function. For example, using $E(S,V,N)$, we get $T(E,V,N) = \left(\frac{\partial E}{\partial S}\right)_{V,N}$ from which, in principle, inversion gives us $E(T,V,N)$. But from $A$ we also get

$$E(T,V,N) = A = TS = A - T\left(\frac{\partial A}{\partial T}\right)_{N,V} = \left(\frac{\partial A/T}{\partial 1/T}\right)_{N,V} .$$

We get the same thing, but without having to carry out the inversion explicitely. It is this saving of effort – not having to do an inversion – that makes it helpful to introduce *auxiliary functions* like $A$ and $G$.

How did we know that the inversion between $E$ and $T$ was possible?
Because

$$C_V = \left(\frac{\partial E}{\partial T}\right)_{N,V} > 0$$

i.e. $E$ is a monotonically increasing function of $T$.

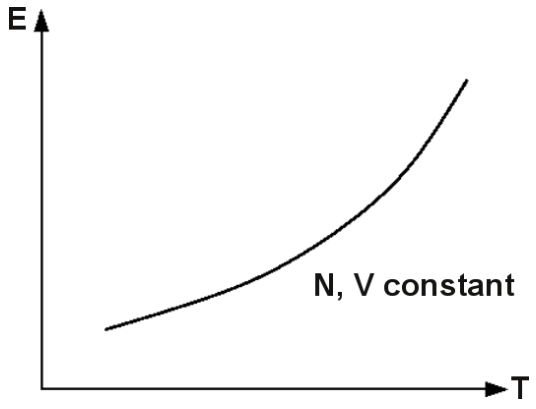


scheme 049

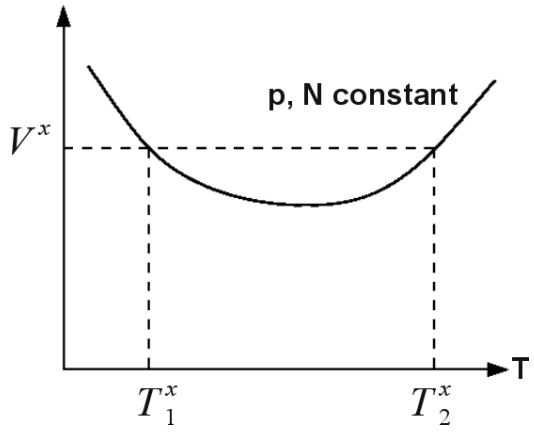


scheme 050

It was the Second Law that implied the stability criterion, $\left(\frac{\partial E}{\partial T}\right)_{N,V} > 0$. Similarly, look back at the derivation and you could also derive

| condition of equilibrium | stability |
|---|---|
| $T$ constant | $(\partial E/\partial T)_{N,V} > 0$ |
| $p$ constant | $-(\partial V/\partial p)_{S,N} > 0$ |
| | $-(\partial V/\partial p)_{T,N} > 0$ |
| $\mu$ constant | $-(\partial N/\partial \mu)_{S,V} > 0$ |
| | $-(\partial N/\partial \mu)_{T,V} > 0$ |

The chart of auxiliary functions

| variables | function | differential | name |
|---|---|---|---|
| $S, V, N$ | $E$ | $\mathrm{d}E = T\mathrm{d}S - p\mathrm{d}V + \mu\mathrm{d}N$ | energy |
| $T, V, N$ | $A = E - TS$ | $\mathrm{d}A = -S\mathrm{d}T - p\mathrm{d}V + \mu\mathrm{d}N$ | Helmholtz free energy |
| $T, p, N$ | $G = E - TS + pV$ | $\mathrm{d}G = -S\mathrm{d}T + V\mathrm{d}p + \mu\mathrm{d}N$ | Gibbs free energy |
| $S, p, N$ | $H = E + pV$ | $\mathrm{d}H = T\mathrm{d}S + V\mathrm{d}p + \mu\mathrm{d}N$ | enthalpy |

To exploit what the auxiliary functions can do for us, we need to review some more mathematics.

Suppose

$$\begin{aligned} f &= f(x,y) \\ \mathrm{d}f &= \left(\frac{\partial f}{\partial x}\right)_y \mathrm{d}x + \left(\frac{\partial f}{\partial y}\right)_x \mathrm{d}y \\ &\equiv a(x,y)\mathrm{d}x + b(x,y)\mathrm{d}y \end{aligned}$$

Since order of differentiation is irrelevant

$$\left(\frac{\partial a}{\partial y}\right)_x = \left(\frac{\partial b}{\partial x}\right)_y$$

Expoliting this will give us *Maxwell relations*.

Also from $\mathrm{d}f$, we see (chain rule)

$$\begin{aligned} 1 &= \left(\frac{\partial f}{\partial x}\right)_y \frac{\mathrm{d}x}{\mathrm{d}f} + \left(\frac{\partial f}{\partial y}\right)_x \frac{\mathrm{d}y}{\mathrm{d}f} \\ \Rightarrow \quad 1 &= \left(\frac{\partial f}{\partial x}\right)_y \left(\frac{\partial x}{\partial f}\right)_y \qquad y \text{ constant!} \end{aligned}$$

in addition, from $\mathrm{d}f$, we see

$$\begin{aligned} \frac{\mathrm{d}f}{\mathrm{d}y} &= \left(\frac{\partial f}{\partial x}\right)_y \frac{\mathrm{d}x}{\mathrm{d}y} + \left(\frac{\partial f}{\partial y}\right)_x \\ \Rightarrow \quad \left(\frac{\partial f}{\partial y}\right)_x &= -\left(\frac{\partial f}{\partial x}\right)_y \left(\frac{\partial x}{\partial y}\right)_f \end{aligned}$$

To illustrate the use of these things, consider the following:
Given $v = v(T,p)$ the *equation of state* of some gas with $v = V/N = 1/\rho$.

How does the entropy change if the gas is compressed isothermally from pressure $p_1$ to pressure $p_2$?

Answer:

$$\Delta S = S(T,p_2,N) - S(T,p_1,N) = \int_{p_1}^{p_2} \mathrm{d}p \left(\frac{\partial S}{\partial p}\right)_{T,N}$$

We think of $S$ as a function of $p$, $T$, and $N$. $p$, $T$, $N$ are a reasonable set of variables, since $p$ is conjugate to $V$ and $T$ is conjugate to $S$. So we have got one entree from each of the $p--V$, $S--T$, and $\mu--N$ families.

To examine the derivative, look to the natural function of $p$, $T$, $N$:

$$\mathrm{d}(\underbrace{E - TS + pV}_{G} = -S\mathrm{d}T + V\mathrm{d}p + \mu\mathrm{d}N$$

Thus (we have a total differential),

$$-\left(\frac{\partial S}{\partial p}\right)_{T,N} = \left(\frac{\partial V}{\partial T}\right)_{p,N}$$

This is one of the Maxwell relations.

Since $N$ is fixed in the derivatives, we can also note

$$\left(\frac{\partial V}{\partial T}\right)_{p,N} = N\left(\frac{\partial V/N}{\partial T}\right)_{p,N} = N\left(\frac{\partial v}{\partial T}\right)_{p}$$

So, the problem is now solved

$$\Delta S = -N\int_{p_1}^{p_2}\mathrm{d}p\left(\frac{\partial v}{\partial T}\right)_{p}$$

since $(\partial v/\partial T)_p$ can be calculated from the equation of state.

**Example:** an ideal gas is compressed $v = \mathrm{k_B}T/p$.

$$\Delta S = -N\int_{p_1}^{p_2}\mathrm{d}p\frac{\mathrm{k_B}}{p} = N\mathrm{k_B}\ln\frac{p_1}{p_2}$$

Similarly, $\Delta S$ for changing the volume of an ideal gas isothermally is

$$\Delta S = N\mathrm{k_B}\ln\frac{V_2}{V_1}$$

You can show this from the preceeding one by computing

$$\Delta S = \int_{V_1}^{V_2}\left(\frac{\partial S}{\partial V}\right)_{T,N}\mathrm{d}V$$

through a Maxwell relation for $\left(\frac{\partial S}{\partial V}\right)_{T,N}$. That Maxwell relation is obtained from the natural function of $V$, $T$, $N$, namely $A$.

We are beginning to see how thermodynamics provides inter-relationships between different macroscopic experiments. For example, heat flow or $\Delta S$ of a process is related to $p--v--T$ measurements.

Here is some more: Consider

$$\mathrm{d}S = \left(\frac{\partial S}{\partial T}\right)_{V,N} \mathrm{d}T + \left(\frac{\partial S}{\partial V}\right)_{T,N} \mathrm{d}V + \left(\frac{\partial S}{\partial N}\right)_{V,T} \mathrm{d}N$$

Now, divide through by $\mathrm{d}T$ and make use of $A = E - TS$

$$\begin{aligned}\left(\frac{\partial S}{\partial T}\right)_{V,N} &= \left(\frac{\partial}{\partial T}\left[\frac{E-A}{T}\right]\right)_{V,N} = \left(\frac{\partial E/T}{\partial T}\right)_{V,N} \underbrace{-\left(\frac{\partial A/T}{\partial T}\right)_{V,N}}_{E/T^2} \\ &= -\frac{E}{T^2} + \frac{1}{T}\underbrace{\left(\frac{\partial E}{\partial T}\right)_{V,N}}_{C_V} + \frac{E}{T^2} \\ &= \frac{C_V}{T}\end{aligned}$$

to get

$$\frac{\mathrm{d}S}{\mathrm{d}T} = \frac{1}{T}C_V + \left(\frac{\partial S}{\partial V}\right)_{T,N} \frac{\mathrm{d}V}{\mathrm{d}T} + \left(\frac{\partial S}{\partial N}\right)_{V,T} \frac{\mathrm{d}N}{\mathrm{d}T}$$

Now hold $p$ and $N$ fixed

$$\left(\frac{\partial S}{\partial T}\right)_{p,N} = \frac{C_p}{T} = \frac{1}{T}C_V + \left(\frac{\partial S}{\partial V}\right)_{T,N} \left(\frac{\partial V}{\partial T}\right)_{p,N}$$

From $\mathrm{d}A = -S\mathrm{d}T - p\mathrm{d}V + \mu\mathrm{d}N$ we get (Maxwell relation)

$$\left(\frac{\partial S}{\partial V}\right)_{T,N} = \left(\frac{\partial p}{\partial T}\right)_{V,N}$$

So,

$$\frac{(C_p - C_V)}{T} = \left(\frac{\partial p}{\partial T}\right)_{V,N} \left(\frac{\partial V}{\partial T}\right)_{p,N} = N \underbrace{\left(\frac{\partial p}{\partial T}\right)_v}_{-\left(\frac{\partial p}{\partial v}\right)_T \left(\frac{\partial v}{\partial T}\right)_p} \left(\frac{\partial v}{\partial T}\right)_p = \underbrace{-N\left(\frac{\partial p}{\partial v}\right)_T}_{\text{stability}>0} \left(\frac{\partial v}{\partial T}\right)_p^2 > 0$$

and we get

$$\boxed{C_p \geq C_V}$$

Thus, we have suceeded at relating $C_p - C_V$ to the *isothermal compressibility*

$$\kappa_T \equiv -\frac{1}{v}\left(\frac{\partial v}{\partial p}\right)_T$$

and the coefficient of thermal expansion $(\partial v/\partial T)_p$.

Here is something else you can show: Let

$$\kappa_S = -\frac{1}{V}\left(\frac{\partial V}{\partial p}\right)_{S,N}, \qquad \text{adiabatic compressibility}$$

The ratio

$$\frac{\kappa_T}{\kappa_S} = \left(\frac{\partial v}{\partial p}\right)_T \Big/ \left(\frac{\partial V}{\partial p}\right)_S = \frac{(\partial v/\partial p)_T}{-\left(\frac{\partial v}{\partial S}\right)_p \left(\frac{\partial S}{\partial p}\right)_v}$$

$$= \frac{(\partial v/\partial p)_T}{-\left(\frac{\partial v}{\partial T}\right)_p \left(\frac{\partial T}{\partial S}\right)_p \left(\frac{\partial S}{\partial T}\right)_v \left(\frac{\partial T}{\partial p}\right)_v} = \frac{(\partial v/\partial p)_T}{-\left(\frac{\partial v}{\partial T}\right)_p \left(\frac{\partial T}{\partial p}\right)_v} \frac{C$$

Thus

$$\boxed{\frac{\kappa_T}{\kappa_S} = \frac{C_p}{C_V}}$$

and since $C_p \geq C_V$ folows $\kappa_T \geq \kappa_S$, another connection between different experiments.

## 3.6 Thermodynamics of rubber bands

We need not confine our thoughts to gases. For example, consider a rubber band

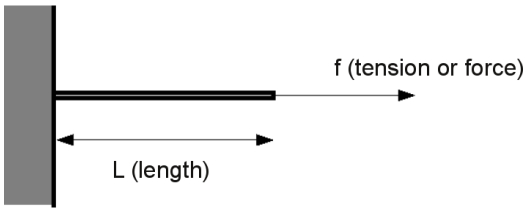

In this case

$$đW = +f\mathrm{d}L$$

We will consider only those processes where the mass of the rubber band remains fixed; so, we have no counter part to $\mu \mathrm{d}N$ in the differential for $E$.

Hence, the First and Second Laws at equilibrium give

$$\mathrm{d}E = T\mathrm{d}S + f\mathrm{d}L \quad \Rightarrow \quad E = E(S, L)$$

As with gases, $T$ constant and $f$ constant throughout material are conditions for equilibrium. Stability criteria are conditions like

$$\left(\frac{\partial S}{\partial T}\right)_f = \frac{C_f}{T} > 0$$

and (note sign!)

$$\left(\frac{\partial L}{\partial f}\right)_S > 0 \quad \text{and} \quad \left(\frac{\partial L}{\partial f}\right)_T > 0$$

Note also that

$$\left(\frac{\partial L}{\partial f}\right)_S > 0 \quad \text{implies that} \quad \left(\frac{\partial L}{\partial f}\right)_T > 0$$

Here, is how:

$$\mathrm{d}L = \left(\frac{\partial L}{\partial f}\right)_S \mathrm{d}f + \left(\frac{\partial L}{\partial S}\right)_f \mathrm{d}S$$

So,

$$\left(\frac{\partial L}{\partial f}\right)_T = \left(\frac{\partial L}{\partial f}\right)_S + \left(\frac{\partial L}{\partial S}\right)_f \left(\frac{\partial S}{\partial f}\right)_T$$

From

$$\mathrm{d}(E - TS - fL) = -S\mathrm{d}T - L\mathrm{d}f$$

follows

$$\left(\frac{\partial S}{\partial f}\right)_T = \left(\frac{\partial L}{\partial T}\right)_f$$

Hence,

$$\left(\frac{\partial L}{\partial f}\right)_T = \left(\frac{\partial L}{\partial f}\right)_S + \left(\frac{\partial L}{\partial S}\right)_f \left(\frac{\partial L}{\partial T}\right)_f$$
$$= \left(\frac{\partial L}{\partial f}\right)_S + \left(\frac{\partial L}{\partial T}\right)_f \left(\frac{\partial T}{\partial S}\right)_f \left(\frac{\partial L}{\partial T}\right)_f$$
$$= \left(\frac{\partial L}{\partial f}\right)_S + \left(\frac{\partial L}{\partial T}\right)_f^2 \frac{T}{C_f}$$

$\frac{T}{C_f}$ positive due to stability

$$\left(\frac{\partial L}{\partial f}\right)_T > \left(\frac{\partial L}{\partial f}\right)_S > 0$$

An auxiliary function in this case is

$$\mathrm{d}(E - TS) = -S\mathrm{d}T + f\mathrm{d}L$$

from which we see, for example that

$$\underbrace{\left(\frac{\partial S}{\partial L}\right)_T}_{\text{related to heat measurements}} = \underbrace{-\left(\frac{\partial f}{\partial T}\right)_L}_{\substack{\text{related to equation of state} \\ f = f(T, L)}}$$

We can thus interrelate different macroscopic measurements, and by applying stability criteria, make some predictions.

What might you expect from the molecular nature of rubber bands?

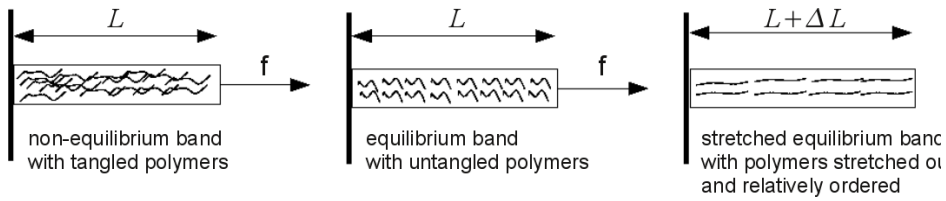

scheme 052

e.g. Polyethylene

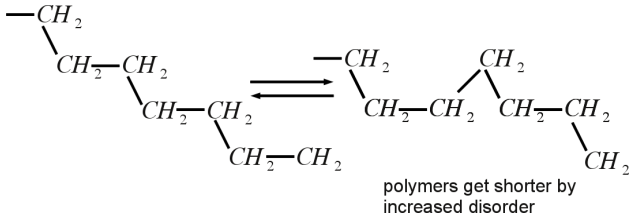


scheme 053

The *expanded* rubber band is more ordered than the contracted rubber band.

One thing you can verify is that if you pull on a rubber band adiabatically, its temperature goes up. That is

$$\left(\frac{\partial T}{\partial L}\right)_S > 0 \quad \text{or} \quad \left(\frac{\partial T}{\partial f}\right)_S > 0$$

Either one, they are equivalent. To see why, use the chain rule

$$\left(\frac{\partial T}{\partial L}\right)_S = \left(\frac{\partial T}{\partial f}\right)_S \left(\frac{\partial f}{\partial L}\right)_S$$

$(\partial f/\partial L)_S$ is positive due to stability, thus $\left(\frac{\partial T}{\partial L}\right)_S > 0$ holds only if $\left(\frac{\partial T}{\partial f}\right)_S > 0$ too.

The experimental fact is certainly reasonable in light of the molecular picture of the polymers. Specifically, stretching polymers removes gauche conformers, the trans conformers have lower energy. The energy therefore released (into vibrations, for example) causes temperature to rise.

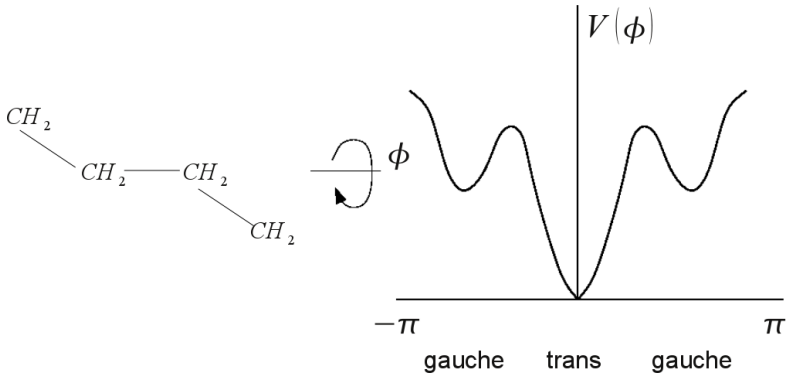


scheme 054

Quite generally, however, without recourse to molecular models, we can use the experimental fact, $(\partial T/\partial L)_S > 0$, to make a prediction about the sign of

$\left(\frac{\partial L}{\partial T}\right)_f$ Does a rubber band under constant tension expand or contract when heated?

Here is what we can do: (use chain rule and definition of heat capacity)

$$\left(\frac{\partial L}{\partial T}\right)_f = \left(\frac{\partial L}{\partial S}\right)_f \left(\frac{\partial S}{\partial T}\right)_f = \left(\frac{\partial L}{\partial S}\right)_f \frac{C_f}{T}$$

Next, to analyse $L(S, f)$, think about

$$\mathrm{d}(E - Lf) = T\mathrm{d}S - L\mathrm{d}f$$

where we have made use of $\mathrm{d}E = T\mathrm{d}S + f\mathrm{d}L$. We can derive a Maxwell relation

$$\left(\frac{\partial T}{\partial f}\right)_S = -\left(\frac{\partial L}{\partial S}\right)_f$$

So,

$$\left(\frac{\partial L}{\partial T}\right)_f = -\left(\frac{\partial T}{\partial f}\right)_S \frac{C_f}{T}$$

With $-\left(\frac{\partial T}{\partial f}\right)_S$ negative according to experiment / positive according to stability $\frac{C_f}{T}$ we predict

$$\left(\frac{\partial L}{\partial T}\right)_f < 0$$

i.e., heat a rubber band and it should shrink (could be checked by experiment).

# Chapter 4

# Chemical Potential and Mass Equilibrium

## 4.1 Conditions for equilibrium


scheme 060

Regions (1) and (2) could have a hypothetical boundary or a real physical boundary. Examples of the latter: interface between two phases (e.g. liquid–vapor) or a membrane separating two different fluids.

At equilibrium, there are $N_{\rm eq}^{(1)}$ molecules in region (1), and $N_{\rm eq}^{(2)}$ molecules in region (2). Now repartition:

$$N^{(1)} = N_{\rm eq}^{(1)} + \Delta N \ , \qquad N^{(2)} = N_{\rm eq}^{(2)} - \Delta N \ .$$

Nonzero $\Delta N$, will make $S$ go down or $E$ go up. Either picture leads to the condition for equilibrium

$$\boxed{\mu^{(1)} = \mu^{(2)}}$$

Similarly, for two components, $\Delta E$ for repartitioning $N_i$'s is

$$0 \leq \Delta E = \left(\mu_1^{(1)} - \mu_1^{(2)}\right) \Delta N_1 + \left(\mu_2^{(1)} - \mu_2^{(2)}\right) \Delta N_2 + \mathcal{O}((\Delta N_i)^2)$$

and from this follows

$$\boxed{\mu_i^{(1)} = \mu_i^{(2)} \ , \quad i = 1, 2}$$

**Example** : Phase equilibria

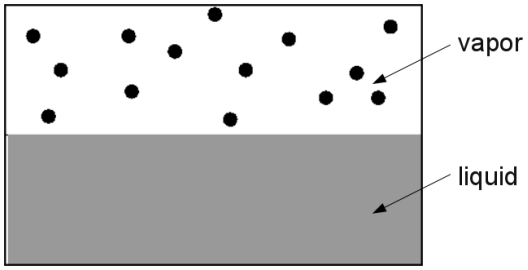


$$\mu^{(liquid)} = \mu^{(gas)}$$

scheme 061

The chemical potential of a one component system can be expressed in terms of $T$, $P$; i.e. $\mu = \mu(T, p)$. Thus, $\mu^{(\rm liquid)}(T, p) = \mu^{(\rm gas)}(T, p)$.

$T$ and $P$ of two phases in equilibria must satisfy conditions of thermal and mechanical equilibrium

$$T^{(1)} = T^{(2)} = T \ ; \qquad p^{(1)} = p^{(2)} = p$$

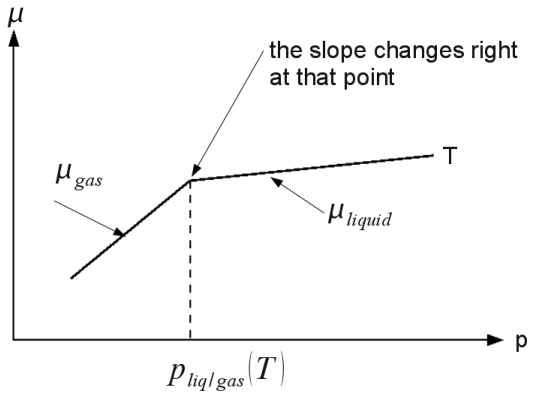


scheme 062

**Example** : Trans–gauche equilibrium

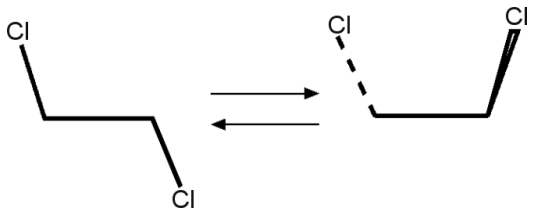


scheme 063

Here, thinking about $mu$ as a function of $T$ and $\rho$.

$$\mu^{(\text{gauche})}(T, \rho_{\text{g}}) = \mu^{(\text{trans})}(T, \rho_{\text{t}})$$

But we have already figured out conformational equilibrium in terms of the Boltzmann distribution. Somehow, the conditions of equilibrium involving $\mu$'s must be equivalent to the Boltzmann distribution.

**Example** : Chemical equilibria

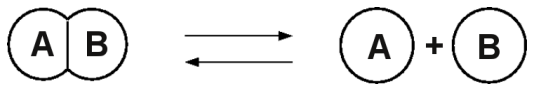

scheme 064

Need to do stoichiometry

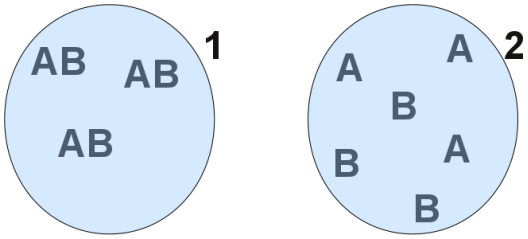


scheme 065

$$N_{AB} + \Delta N \quad \Leftrightarrow \quad N_A - \Delta N \ , \quad N_B - \Delta N$$

Due to stoichiometric constraints on how we can change $N_{AB}$ and $N_A$, $N_B$

$$\begin{aligned} 0 \leq \Delta E &= \mu_{AB}\Delta N_{AB} + \mu_A \Delta N_A + \mu_B \Delta N_B \\ &= (\mu_{AB} - \mu_A \mu_B)\, \Delta N \end{aligned}$$

Therefore, the condition of equilibrium is

$$\boxed{0 = \mu_{AB} - \mu_A - \mu_B}$$

Generalization

$$a\mathrm{A} + b\mathrm{B} + \cdots \leftrightarrow c\mathrm{C} + d\mathrm{D} + \cdots$$

has the condition of equilibrium

$$\boxed{a\mu_A + b\mu_B + \cdots = c\mu_C + d\mu_D + \cdots}$$

To exploit these conditions of equilibrium, we need some thermodynamic relations, and a molecular model.

## 4.2 Gibbs–Duhem equation

Recall,

$$G = E - TS + pV$$

is extensive and satisfies (we consider two components)

$$\mathrm{d}G = -S\mathrm{d}T + V\mathrm{d}p + \mu_1\mathrm{d}N_1 + \mu_2\mathrm{d}N_2 \ .$$

So, $G = G(T, p, N_1, N_2)$.

Consider changing system size. Since $G$, $N_1$ and $N_2$ are extensive, but $T$ and $p$ are intensive,

$$\lambda G = G(T, p, \lambda N_1, \lambda N_2) \ .$$

Hence

$$\begin{aligned} G &= \frac{\mathrm{d}}{\mathrm{d}\lambda}(\lambda G) = \frac{\mathrm{d}}{\mathrm{d}\lambda} G(T, p, \lambda N_1, \lambda N_2) \\ &= \mu_1 N_1 + \mu_2 N_2 \end{aligned}$$

Thus, for any $\lambda$, and thus $\lambda = 1$

$$G(T, p, N_1, N_2) = \mu_1 N_1 + \mu_2 N_2$$

Thinking about $\mu_i$'s as functions of $T$, $p$ and what else?

Now take total differentials

$$\begin{gathered} \mathrm{d}G(T, p, N_1, N_2) = \mathrm{d}G(\mu_1, \mu_2, N_1, N_2) \\ -S\mathrm{d}T + V\mathrm{d}p + \mu_1\mathrm{d}N_1 + \mu_2\mathrm{d}N_2 = \mu_1\mathrm{d}N_1 + \mu_2\mathrm{d}N_2 + N_1\mathrm{d}\mu_1 + N_2\mathrm{d}\mu_2 \end{gathered}$$

**Gibbs–Duhem equation**

$$\boxed{S\mathrm{d}T - V\mathrm{d}p + N_1\mathrm{d}\mu_1 + N_2\mathrm{d}\mu_2 = 0}$$

For a one component system

$$\begin{aligned} N\mathrm{d}\mu &= -S\mathrm{d}T + V\mathrm{d}p \\ \mathrm{d}\mu &= -\frac{S}{N}\mathrm{d}T + \frac{V}{N}\mathrm{d}p \\ \left(\frac{\partial\mu}{\partial p}\right)_T &= \frac{V}{N} = \frac{1}{\rho} \end{aligned}$$

So, the discontinuity of slope at phase equilibrium tells us the discontinuity of density.

## 4.3 Partial molar quantities

For an arbitrary extensive quantity $Y$, we define a partial molar quantity

$$Y_i \equiv \left(\frac{\partial Y}{\partial N_i}\right)_{T,p,N_{j\neq i}} .$$

Example: partial molar volume

$$V_i(T,p,N_{j\neq i}) = \left(\frac{\partial V}{\partial N_i}\right)_{T,p,N_{j\neq i}} .$$

Therefore, the partial molar volume of component $i$ of a system is the differential change of volume per added number of particles. The process is performed at constant temperature, presure, and amount of particles of other types.

$Y$ is a function of $T$, $p$, $N_i$. Hence,

$$\begin{aligned} \mathrm{d}Y &= \left(\frac{\partial Y}{\partial T}\right)_{p,N_i}\mathrm{d}T + \left(\frac{\partial Y}{\partial p}\right)_{T,N_i}\mathrm{d}p + \sum_i \left(\frac{\partial Y}{\partial N_i}\right)_{T,N_{j\neq i}}\mathrm{d}N_i \\ &= \left(\frac{\partial Y}{\partial T}\right)_{p,N_i}\mathrm{d}T + \left(\frac{\partial Y}{\partial p}\right)_{T,N_i}\mathrm{d}p + \sum_i Y_i\mathrm{d}N_i \ . \end{aligned}$$

Reuse arguments of extending system by factor $\lambda$ ...
(Recall result for $G$: $G(T,p,N_i) = \sum_i \mu_i N_i$)

to get in general

$$Y = \sum_i Y_i N_i \ .$$

We also see that the partial molar Gibbs free energy is the chemical potential

$$G_i = \mu_i \ .$$

**Molfraction as independent variable in a homogenous binary phase.**

$$\text{mol fraction} \qquad x = \frac{N_1}{N_1 + N_2} \qquad (1 - x) = \frac{N_2}{N_1 + N_2}$$

Gibbs–Duhem equation

$$S\mathrm{d}T - V\mathrm{d}p + N_1\mathrm{d}\mu_1 + N_2\mathrm{d}\mu_2 = 0$$

Think of the chemical potentials as functions of $T$, $p$, and the mol fraction $x$

$$S\mathrm{d}T - V\mathrm{d}p + N_1\left(\frac{\partial\mu_1}{\partial T}\mathrm{d}T + \frac{\partial\mu_1}{\partial p}\mathrm{d}p + \frac{\partial\mu_1}{\partial x}\mathrm{d}x\right) + N_1\left(\frac{\partial\mu_2}{\partial T}\mathrm{d}T + \frac{\partial\mu_2}{\partial p}\mathrm{d}p + \frac{\partial\mu_2}{\partial x}\mathrm{d}x\right) = 0$$

With

$$\left(\frac{\partial\mu}{\partial p}\right)_T = \frac{V}{N} \quad \text{and} \quad \left(\frac{\partial\mu}{\partial T}\right)_p = -\frac{S}{N}$$

we get

$$S\mathrm{d}T - V\mathrm{d}p - \underbrace{(S_1 + S_2)}_{S}\mathrm{d}T + \underbrace{(V_1 + V_2)}_{V}\mathrm{d}p + \left(N_1\frac{\partial\mu_1}{x} + N_2\frac{\partial\mu_2}{x}\right)\mathrm{d}x = 0 \ .$$

Therefore,

$$N_1\frac{\partial\mu_1}{x} + N_2\frac{\partial\mu_2}{x} = 0$$

$$x\left(\frac{\partial\mu_1}{\partial x}\right)_{T,p} + (1 - x)\left(\frac{\partial\mu_2}{\partial x}\right)_{T,p} = 0$$

## 4.4 Ideal solution chemical potential

### A molecular picture

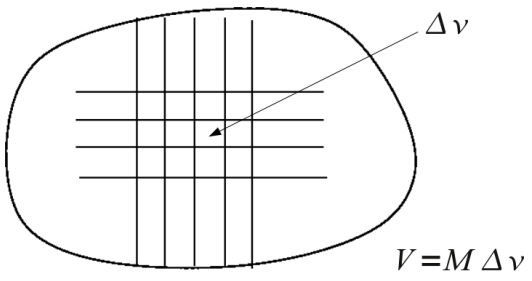


scheme 066

How many ways can we arrange $N$ solute molecules in the above volume?

$$\text{ideal} \;=\; \text{no correlation between solute molecules}$$

$$\Omega = \frac{M^N}{N!}$$

The corresponding entropy is

$$S = \mathrm{k_B} \ln \Omega = N \mathrm{k_B} \left( \ln \frac{M}{N} + 1 \right) = \mathrm{k_B} N \left( \ln \left( \frac{1}{\rho \Delta v} \right) + 1 \right)$$

Consider the solution at $E = \text{const.}$ and $V = \text{const.}$

$$\mathrm{d}S = -\frac{\mu}{T} \mathrm{d}N \quad \Rightarrow \quad \left( \frac{\partial S}{\partial N} \right)_{V,E} = -\frac{\mu}{T} = \mathrm{k_B} \ln \rho \Delta v$$

So, the configurational contribution to the chemical potential:

$$\beta \mu = \ln \rho \Delta v$$

Let's consider now what happens if we *reversibly* create a particle (solute) in the solvent. The chemical potential is related to the Helmholtz free energy

$$\mu = \left( \frac{\partial A}{\partial N} \right)_{T,V} \;,$$

or for $\Delta N = 1$

$$\mu = A(T, V, N+1) - A(T, V, N) \ .$$

We know that $A = \mathrm{k_B} T \ln Q$ and therefore

$$\Delta\mu = -\frac{1}{\beta} \ln Q_{\text{solute}} + \frac{1}{\beta} \ln Q_{\text{solvent}}$$

Using the Boltzmann formula for the partition functions, we get

$$\mathrm{e}^{-\beta\Delta\mu} = \frac{\sum_j \mathrm{e}^{-\beta \hat{E}_j}}{\sum_j \mathrm{e}^{-\beta E_j}} \ ,$$

where the sums run over all solvent states with solute fixed. The energy $\hat{E}_j$ is from the system with the solute fixed in one cell, and the energy $E_j$ is for the same configuration but no solute present.

$\mathrm{e}^{-\beta\Delta\mu}$ is a measure of the solvation energy, and $\Delta\mu$ is independent of $\rho_{\text{solute}}$, depends on $T$ and $\rho_{\text{solvent}}$. Finally, we can define a chemical potential for an ideal solution, namely

$$\boxed{\beta\mu = \beta\Delta\mu + \ln \rho\Delta v}$$

We are not done yet!

**Standard states** Can only measure differences in chemical potentials. We cannot measure absolute chemical potentials.

For example, we can measure $\mu$ at a particular volume (pressure)

$$\beta\mu = \beta\Delta\mu + \ln \rho V + \ln \Delta v/V$$

Remember that the density $\rho$ has units of 1/volume.

In general

$$\beta\mu = \beta\Delta\mu + \ln \rho\Delta v + \text{constant}$$

Consider

$$\beta\mu = \beta\Delta\mu + \ln \rho/\rho_{\text{solvent}} + \ln \rho_{\text{solvent}}\Delta v$$

Absorb the last term into $\beta\Delta\mu$ and define

$$\frac{\rho}{\rho_{\text{solvent}}} = \frac{N_{\text{solute}}}{N_{\text{solvent}}} \approx \frac{N_{\text{solute}}}{N_{\text{solvent}} + N_{\text{solute}}} = X_{\text{sol}}$$

Thus, the more familiar equation (usually found in textbooks) *Raoult's Law*

$$\boxed{\beta\mu = \beta\mu^\star + \ln X_{\text{sol}}}$$

## 4.5 Chemical potential and reversible work

For an ideal solution

$$\beta\mu = \beta\Delta\mu + \ln\rho + \text{constant}$$

| | | |
|---|---|---|
| | $\Delta\mu$ | free energy of one fixed solute. It includes the *solvation energy* – the free energy change of the solvent to accomodate one solute. |
| where | $\rho$ | concentration or density of solutes – always with respect to a standard state (units!) |
| | constant | physically irrelevant constant; its value establishes convention of standard state (see $\rho$). |

An ideal solution is one in which concentration of solutes is very low – low enough that different solute molecules are *uncorrelated*. Thus, $\rho^{-1}$ must be much larger than any relevant (molecular length scale)$^3$.

An ideal solution at the molecular scale

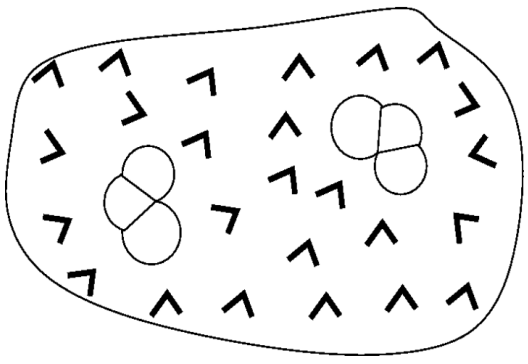

scheme 067

Interested just in a few molecules! Then call those specific few molecules the solutes, and the whole system is an ideal solution.

**Example** Isomerization of 1,2 dichloroethane.

First in vacuum

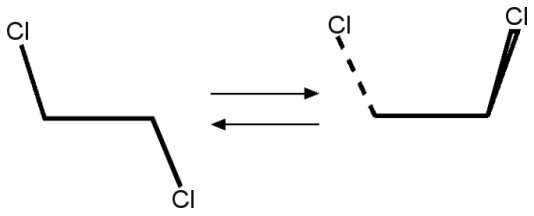


scheme 063

Let

$$\Delta E = \text{ energy of gauche state - energy of trans state}$$

Condition of chemical equilibrium

$$\mu_{\mathrm{g}} = \mu_{\mathrm{t}}$$

or

$$\beta\Delta\mu_{\mathrm{g}} + \ln\rho_{\mathrm{g}} + \text{constant} = \beta\Delta\mu_{\mathrm{t}} + \ln\rho_{\mathrm{t}} + \text{constant}$$

We use the same standard state, so the constant drops out.

So,

$$\rho_{\mathrm{g}}/\rho_{\mathrm{t}} = \mathrm{e}^{-\beta(\Delta\mu_{\mathrm{g}} - \Delta\mu_{\mathrm{t}})}$$

This is also true in solution!

Next consider the gas phase $\Delta\mu$.

$$
\begin{aligned}
\mathrm{e}^{-\beta\Delta\mu_{\mathrm{g}}} &= \sum_{\text{all gauche//states } j} \mathrm{e}^{-\beta E_j} = 2\cdot\mathrm{e}^{-\beta(\Delta E+E_{\mathrm{t}})} \\
\mathrm{e}^{-\beta\Delta\mu_{\mathrm{t}}} &= \sum_{\text{all trans//states } j} \mathrm{e}^{-\beta E_j} = 1\cdot\mathrm{e}^{-\beta E_{\mathrm{t}}} \\
\rho_{\mathrm{g}}/\rho_{\mathrm{t}} &= 2\cdot\mathrm{e}^{-\beta\Delta E} = \mathrm{e}^{-\beta(\Delta E-\mathrm{k_B}T\ln 2)}
\end{aligned}
$$

The common energy $E_{\mathrm{t}}$ drops out and in the final equation we have an energy ($\Delta E$) and an entropy ($\mathrm{k_B}T\ln 2$) contribution to equilibrium.

Chemical equilibrium in solution requires an analysis of $\Delta\mu$ more general than that given above. We consider that now.

In the next few remarks, we will work with the canonical distribution law – energy fluctuates but $N$ is fixed. The remarks are general, however, and apply equally well when $N$ fluctuates too. Convince yourself that this is true.

Grab onto a few degrees of freedom. We will call them *special* or *tagged* degrees of freedom. Perhaps they are the positions of a few atoms. Held them fixed, and allow all other degrees of freedom to fluctuate.

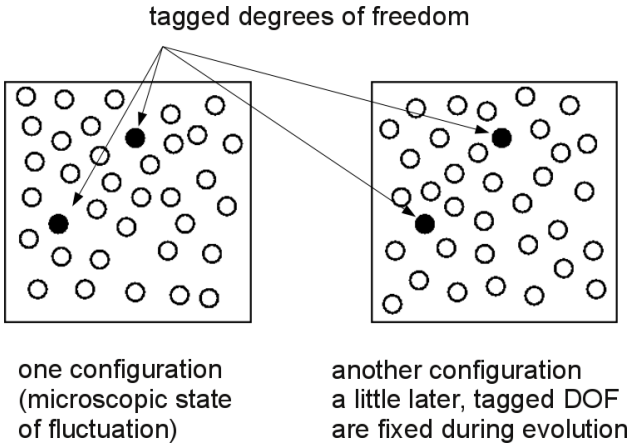


scheme 068

The resulting partition function (the Boltzmann weighted sum over all fluctuations) is

$$\tilde{Q}(\underbrace{x_1,\ldots,x_n}_{\text{fixed coordinates}};\beta,N,V)=\sum_{\substack{i,\text{with}\\ x_1,\ldots,x_n\text{fixed}}}\mathrm{e}^{-\beta E_i}$$

Consider the variation of $\tilde{Q}$ w.r.t. the fixed coordinates

$$\frac{\partial\ln\tilde{Q}}{\partial x_1}=\frac{1}{\tilde{Q}}\sum_{\substack{i\\ (x_1,\ldots,x_n\text{fixed})}}\mathrm{e}^{-\beta E_i}\left(-\beta\frac{\partial E_i}{\partial x_1}\right)$$

Note,

$$(-\partial E_i/\partial x_1)=\begin{array}{l}\textit{force}\text{ on degree of freedom 1 when system is in}\\ \text{the }i\text{th microscopic state (instantaneous fluctuation)}\end{array}$$

which allows us to write

$$\frac{\partial\ln\tilde{Q}}{\partial x_1}=\beta\left(\begin{array}{l}\text{average force on degree of freedom 1}\\ \text{given that } x_1,\ldots,x_n \text{ are fixed}\end{array}\right)$$

similar results hold for $\partial\ln\tilde{Q}/\partial x_i$, $i=2,3,\ldots,n$.

The integration of the average force yields a work, a *reversible* work since for each configuration of the tagged degrees of freedom, all fluctuations are Boltzmann averaged. Thus the quantity $W(x_1\ldots x_n)$ defined by

$$\ln\tilde{Q}(x_1\ldots x_n;\beta,N,V)=-\beta W(x_1\ldots x_n;\beta,N,V)$$

has the interpretation of a reversible work surface, sometimes called a *potential of mean force* or a *free energy surface.*

Suppose you observe some property,$f$, which depends explicitely upon the special coordinates only, i.e., $f=f(x_1\ldots x_n)$. Its observed or averaged value

is

$$\begin{aligned}\langle f\rangle &= \sum_i f_i \mathrm{e}^{-\beta E_i} / \sum_i \mathrm{e}^{-\beta E_i} \\ &= \sum_{x_1 \ldots x_n} \sum_{i//x_1 \ldots x_n \text{fixed}} f_i \mathrm{e}^{-\beta E_i} / \sum_j \mathrm{e}^{-\beta E_j} \\ &= \sum_{x_1 \ldots x_n} f(x_1 \ldots x_n) \mathrm{e}^{-\beta W(x_1 \ldots x_n)} \cdot \frac{1}{\sum_{x_1 \ldots x_n} \mathrm{e}^{-\beta W(x_1 \ldots x_n)}}\end{aligned}$$

Alternatively, we could write

$$\langle f\rangle = \sum_{x_1 \ldots x_n} f(x_1 \ldots x_n) P(x_1 \ldots x_n)$$

where $P(x_1 \ldots x_n)$ = probability of oberving the system with the special coordinates of $x_1 \ldots x_n$.

If the $x_i$'s are truly coordinates, we should use an integral rather than a sum

$$\langle f\rangle = \int \mathrm{d}x_1 \cdots \int \mathrm{d}x_n f(x_1 \ldots x_n) P(x_1 \ldots x_n)$$

in which case $P(x_1 \ldots x_n)$ is then the probability distribution (or density) for $x_1 \ldots x_n$.

Comparision of the two results for $\langle f\rangle$ implies

$$P(x_1 \ldots x_n) \propto \mathrm{e}^{-\beta W(x_1 \ldots x_n)}$$

where the constant of proportionality is the normalization constant.

**In summary** (This is important = The basis of everything)

$$\begin{aligned}&\exp\left[-\beta(\text{reversible work surface for} x_1 \ldots x_n)\right] \\ &\quad = \text{Boltzmann weighted sum over all fluctuations with } x_1 \ldots x_n \text{ fixed} \\ &\qquad \propto \quad \begin{array}{l}\text{probability for observing system with the special} \\ \text{(tagged) degrees of freedom at } x_1 \ldots x_n\end{array}\end{aligned}$$

Note, that $\mathrm{e}^{-\beta A} = Q = \sum_i \mathrm{e}^{-\beta E_i}$ is a special case of the above principle.

## 4.6 Free energy calculations

### 4.6.1 Helmholtz free energy from computer simulations

$$A = \mathrm{k_B}T \ln Q(N,V,T) = -\mathrm{k_B}T \ln \left( \frac{\int \cdots \int \mathrm{d}\boldsymbol{p}\mathrm{d}\boldsymbol{r} \mathrm{e}^{-\beta \mathcal{H}(\boldsymbol{p},\boldsymbol{r})}}{\mathcal{N}} \right)$$

| | | |
|---|---|---|
| $\boldsymbol{p}, \boldsymbol{r}$ | position and momentum of all particles | |
| $\int \cdots \int \mathrm{d}\boldsymbol{p}\mathrm{d}\boldsymbol{r}$ | integral over all phase space | |
| | = all possible realisations of the system | Including |
| $\mathcal{H}(\boldsymbol{p},\boldsymbol{r}) = T(\boldsymbol{p}) + V(\boldsymbol{r})$ | total energy function of the system | |
| $\mathcal{N}$ | normalization constant | |

the following integral in the formula for the free energy

$$\int \cdots \int \mathrm{d}\boldsymbol{p}\mathrm{d}\boldsymbol{r} \mathrm{e}^{-\beta \mathcal{H}(\boldsymbol{p},\boldsymbol{r})} \mathrm{e}^{\beta \mathcal{H}(\boldsymbol{p},\boldsymbol{r})} = \mathcal{N}$$

we get

$$A = \mathrm{k_B}T \ln \left( \frac{\int \cdots \int \mathrm{d}\boldsymbol{p}\mathrm{d}\boldsymbol{r} \mathrm{e}^{-\beta \mathcal{H}(\boldsymbol{p},\boldsymbol{r})} \mathrm{e}^{\beta \mathcal{H}(\boldsymbol{p},\boldsymbol{r})}}{\int \cdots \int \mathrm{d}\boldsymbol{p}\mathrm{d}\boldsymbol{r} \mathrm{e}^{-\beta \mathcal{H}(\boldsymbol{p},\boldsymbol{r})}} \right)$$

The probability density is

$$P(\boldsymbol{p},\boldsymbol{r}) = \frac{\mathrm{e}^{-\beta \mathcal{H}(\boldsymbol{p},\boldsymbol{r})}}{\int \cdots \int \mathrm{d}\boldsymbol{p}\mathrm{d}\boldsymbol{r} \mathrm{e}^{-\beta \mathcal{H}(\boldsymbol{p},\boldsymbol{r})}}$$

and we have

$$A = \mathrm{k_B}T \ln \left( \int \cdots \int \mathrm{d}\boldsymbol{p}\mathrm{d}\boldsymbol{r} \mathrm{e}^{\beta \mathcal{H}(\boldsymbol{p},\boldsymbol{r})} \right)$$

This quantity is difficult to sample because of

| | |
|---|---|
| $\mathcal{H}(\boldsymbol{p},\boldsymbol{r}) =$ large | $\rightarrow \mathrm{e}^{\beta \mathcal{H}(\boldsymbol{p},\boldsymbol{r})}$very large |
| | $\rightarrow P(\boldsymbol{p},\boldsymbol{r})$very small |
| $\mathcal{H}(\boldsymbol{p},\boldsymbol{r}) =$ small | $\rightarrow \mathrm{e}^{\beta \mathcal{H}(\boldsymbol{p},\boldsymbol{r})}$small |
| | $\rightarrow P(\boldsymbol{p},\boldsymbol{r})$large |

Numerical methods (molecular dynamics, Monte Carlo) will sample mostly states with $\mathcal{H}$ small $\rightarrow$ very bad convergence. It is therefore very difficult to determine $A$ accurately.

The same is true in experiment. We measure usually $\Delta A$ or derivatives of $A$

$$\left(\frac{\partial A}{\partial V}\right)_{N,T} = -p \quad \text{or} \quad \left(\frac{\partial A/T}{\partial 1/T}\right)_{V,N} = E$$

### 4.6.2 Thermodynamic perturbation

R.W. Zwanzig, J. Chem. Phys. **22** 1420–1426 (1954)

We consider two systems $X$ and $Y$, e.g. ethanol in water and ethanthiol in water. The energy functions of the systems are $\mathcal{H}_X$ and $\mathcal{H}_Y$.

The free energy difference between the two systems is

$$\Delta A = A_Y - A_X = -\mathrm{k_B}T \ln \frac{Q_Y}{Q_X}$$

This can be computed from

$$\begin{aligned}
\Delta A &= -\mathrm{k_B}T \ln \left( \frac{\int \cdots \int \mathrm{d}\boldsymbol{p}\mathrm{d}\boldsymbol{r} \mathrm{e}^{-\beta \mathcal{H}_Y(\boldsymbol{p},\boldsymbol{r})}}{\int \cdots \int \mathrm{d}\boldsymbol{p}\mathrm{d}\boldsymbol{r} \mathrm{e}^{-\beta \mathcal{H}_X(\boldsymbol{p},\boldsymbol{r})}} \right) \\
&= -\mathrm{k_B}T \ln \left( \frac{\int \cdots \int \mathrm{d}\boldsymbol{p}\mathrm{d}\boldsymbol{r} \mathrm{e}^{-\beta \mathcal{H}_Y(\boldsymbol{p},\boldsymbol{r})} \mathrm{e}^{\beta \mathcal{H}_X(\boldsymbol{p},\boldsymbol{r})} \mathrm{e}^{-\beta \mathcal{H}_X(\boldsymbol{p},\boldsymbol{r})}}{\int \cdots \int \mathrm{d}\boldsymbol{p}\mathrm{d}\boldsymbol{r} \mathrm{e}^{-\beta \mathcal{H}_X(\boldsymbol{p},\boldsymbol{r})}} \right) \\
&= -\mathrm{k_B}T \ln \left\langle \mathrm{e}^{-\beta(\mathcal{H}_Y(\boldsymbol{p},\boldsymbol{r}) - \mathcal{H}_X(\boldsymbol{p},\boldsymbol{r}))} \right\rangle_X
\end{aligned}$$

where $\langle \cdot \rangle_X$ stands for a canonical sampling over distribution of system $X$.

A completely analogous derivation also leads to

$$\Delta A = \mathrm{k_B}T \ln \left\langle \mathrm{e}^{-\beta(\mathcal{H}_X(\boldsymbol{p},\boldsymbol{r}) - \mathcal{H}_Y(\boldsymbol{p},\boldsymbol{r}))} \right\rangle_Y$$

with a sampling over the distribution of system $Y$.

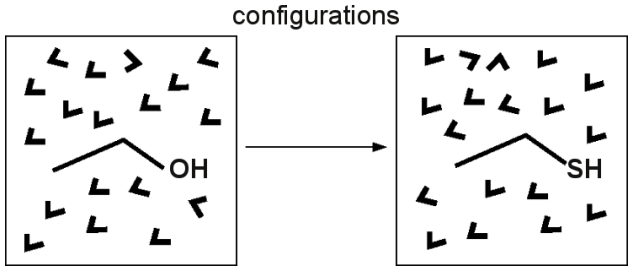


scheme 069

A problem arises if the phase spaces sampled for systems $X$ and $Y$ do not sufficiently overlap: $\|(\mathcal{H}_Y(\boldsymbol{p},\boldsymbol{r}) - \mathcal{H}_X(\boldsymbol{p},\boldsymbol{r}))\| \gg \mathrm{k_B}T$

Solution: intermediate systems

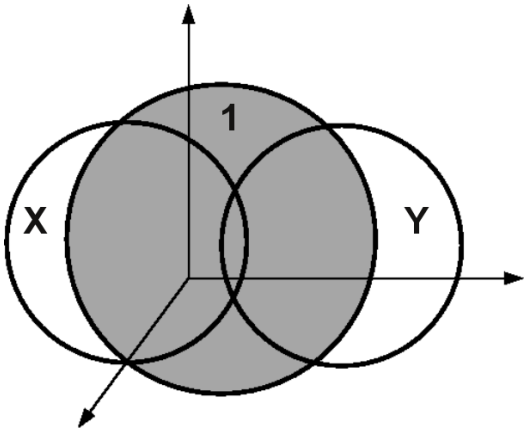


scheme 070

$$\begin{aligned}
\Delta A &= A_Y - A_X \\
&= (A_Y - A_1) + (A_1 - A_X) \\
&= -\mathrm{k_B}T \ln\left(\frac{Q_Y}{Q_1}\frac{Q_1}{Q_X}\right) \\
&= -\mathrm{k_B}T \ln\left\langle \mathrm{e}^{-\beta(\mathcal{H}_Y(\boldsymbol{p},\boldsymbol{r})-\mathcal{H}_1(\boldsymbol{p},\boldsymbol{r}))}\right\rangle_1 - \mathrm{k_B}T \ln\left\langle \mathrm{e}^{-\beta(\mathcal{H}_1(\boldsymbol{p},\boldsymbol{r})-\mathcal{H}_X(\boldsymbol{p},\boldsymbol{r}))}\right\rangle_X
\end{aligned}$$

Generalization to $N$ systems

$$\begin{aligned}\Delta A &= A_Y - A_X \\ &= (A_Y - A_N) + (A_N - A_{N-1}) + \cdots + (A_1 - A_X)\end{aligned}$$

Implementation: Parametrization of system energy

$$\mathcal{H}(\lambda) \quad \text{with} \quad \begin{matrix}\mathcal{H}(\lambda = 0) = \mathcal{H}_X \\ \mathcal{H}(\lambda = 1) = \mathcal{H}_Y\end{matrix}$$

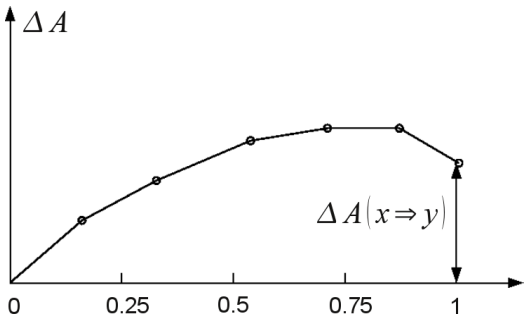


scheme 071

### 4.6.3 Thermodynamic integration

We make the assupmtion that the Helmholtz free energy is a continuous function of a parameter $\lambda$.

$$\begin{aligned}A(\lambda) &= -\mathrm{k_B}T \ln Q(\lambda) \\ \Delta A &= A(\lambda = 1) - A(\lambda = 0) \\ \Delta A &= \int_0^1 \frac{\partial A(\lambda)}{\partial \lambda} \mathrm{d}\lambda\end{aligned}$$

We get

$$\Delta A = -\mathrm{k_B}T \int_0^1 \left[\frac{\partial \ln Q(\lambda)}{\partial \lambda}\right] \mathrm{d}\lambda = \int_0^1 \frac{-\mathrm{k_B}T}{Q(\lambda)} \frac{\partial Q(\lambda)}{\partial \lambda} \mathrm{d}\lambda$$

$$Q(\lambda) = \mathcal{N} \int \cdots \int \mathrm{d}\boldsymbol{p}\mathrm{d}\boldsymbol{r} \mathrm{e}^{-\beta \mathcal{H}(\boldsymbol{p},\boldsymbol{r},\lambda)}$$

$$\frac{\partial \ln Q(\lambda)}{\partial \lambda} = \mathcal{N} \int \cdots \int \mathrm{d}\boldsymbol{p}\mathrm{d}\boldsymbol{r} (-\beta) \frac{\mathcal{H}(\boldsymbol{p},\boldsymbol{r},\lambda)}{\partial \lambda} \mathrm{e}^{-\beta \mathcal{H}(\boldsymbol{p},\boldsymbol{r},\lambda)}$$

$$\frac{\partial A(\lambda)}{\partial \lambda} = -\frac{1}{\beta Q} \frac{\partial Q}{\partial \lambda} = \mathcal{N} \int \cdots \int \mathrm{d}\boldsymbol{p}\mathrm{d}\boldsymbol{r} \frac{\partial \mathcal{H}}{\partial \lambda} \mathrm{e}^{-\beta \mathcal{H}(\boldsymbol{p},\boldsymbol{r},\lambda)}$$

$$= \mathcal{N} \int \cdots \int \mathrm{d}\boldsymbol{p}\mathrm{d}\boldsymbol{r} \frac{\partial \mathcal{H}}{\partial \lambda} \left(\frac{\mathrm{e}^{-\beta \mathcal{H}(\boldsymbol{p},\boldsymbol{r},\lambda)}}{Q}\right) = \left\langle \frac{\partial \mathcal{H}}{\partial \lambda} \right\rangle_\lambda$$

Final result

$$\boxed{\Delta A = \int_0^1 \left\langle \frac{\partial \mathcal{H}}{\partial \lambda} \right\rangle_\lambda \mathrm{d}\lambda}$$

Implementation:

$$\Delta A \approx \sum_i \left\langle \frac{\partial \mathcal{H}}{\partial \lambda} \right\rangle_{\lambda_i}$$

Numerical integration of integral over $\lambda$. For each integration point $\lambda_i$ do a simulation and calculate the Boltzmann averaged value of $\frac{\partial \mathcal{H}}{\partial \lambda}\big|_{\lambda_i}$.

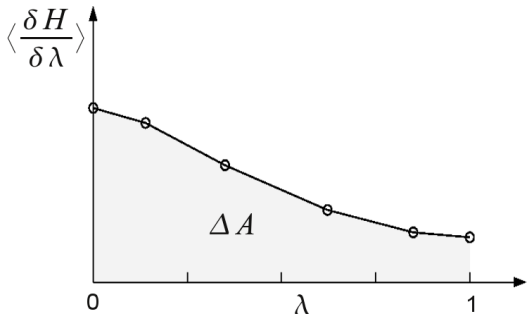


scheme 072

### 4.6.4 Umbrella sampling

Allows sampling in otherwise seldom visited regions of phase space using a bias potential $W(\boldsymbol{r})$.

Define a new total potential function

$$V'(\boldsymbol{r}) = V(\boldsymbol{r}) + W(\boldsymbol{r})$$

Choose $W(\boldsymbol{r})$ in such a way, that you get good sampling close to $\boldsymbol{r}_0$, e.g.

$$W(\boldsymbol{r}) = k_W(\boldsymbol{r} - \boldsymbol{r}_0)^2$$

The sampling with $V'(\boldsymbol{r})$ will result in a non-Boltzmann distribution (w.r.t. $V(\boldsymbol{r})$.

Correction of biased sampling:
We are looking for

$$\langle A \rangle = \frac{\int \cdots \int \mathrm{d}\boldsymbol{p}\mathrm{d}\boldsymbol{r} A \mathrm{e}^{-\beta\mathcal{H}(\boldsymbol{p},\boldsymbol{r})}}{\int \cdots \int \mathrm{d}\boldsymbol{p}\mathrm{d}\boldsymbol{r} \mathrm{e}^{-\beta\mathcal{H}(\boldsymbol{p},\boldsymbol{r})}}$$

The biased average of an observable $A$ calcuated is

$$\langle A \rangle_{\text{bias}} = \frac{\int \cdots \int \mathrm{d}\boldsymbol{p}\mathrm{d}\boldsymbol{r} A \mathrm{e}^{-\beta\mathcal{H}'(\boldsymbol{p},\boldsymbol{r})}}{\int \cdots \int \mathrm{d}\boldsymbol{p}\mathrm{d}\boldsymbol{r} \mathrm{e}^{-\beta\mathcal{H}'(\boldsymbol{p},\boldsymbol{r})}}$$

The biased average for a function $A\mathrm{e}^{\beta W}$ is

$$\langle A\mathrm{e}^{\beta W} \rangle_{\text{bias}} = \frac{\int \cdots \int \mathrm{d}\boldsymbol{p}\mathrm{d}\boldsymbol{r} A \mathrm{e}^{-\beta(\mathcal{H}' - W}}{\int \cdots \int \mathrm{d}\boldsymbol{p}\mathrm{d}\boldsymbol{r} \mathrm{e}^{-\beta\mathcal{H}'}} = \frac{\int \cdots \int \mathrm{d}\boldsymbol{p}\mathrm{d}\boldsymbol{r} A \mathrm{e}^{-\beta\mathcal{H}}}{\int \cdots \int \mathrm{d}\boldsymbol{p}\mathrm{d}\boldsymbol{r} \mathrm{e}^{-\beta\mathcal{H}'}}$$

The biased average for a function $\mathrm{e}^{\beta W}$ is

$$\langle \mathrm{e}^{\beta W} \rangle_{\text{bias}} = \frac{\int \cdots \int \mathrm{d}\boldsymbol{p}\mathrm{d}\boldsymbol{r} \mathrm{e}^{-\beta(\mathcal{H}' - W}}{\int \cdots \int \mathrm{d}\boldsymbol{p}\mathrm{d}\boldsymbol{r} \mathrm{e}^{-\beta\mathcal{H}'}} = \frac{\int \cdots \int \mathrm{d}\boldsymbol{p}\mathrm{d}\boldsymbol{r} \mathrm{e}^{-\beta\mathcal{H}}}{\int \cdots \int \mathrm{d}\boldsymbol{p}\mathrm{d}\boldsymbol{r} \mathrm{e}^{-\beta\mathcal{H}'}}$$

Using the two biased averages we can calculate the unbiased average of the original function $A$

$$\langle A \rangle = \frac{\langle A\mathrm{e}^{\beta W} \rangle_{\text{bias}}}{\langle \mathrm{e}^{\beta W} \rangle_{\text{bias}}}$$

Reconstruction of the free energy surface

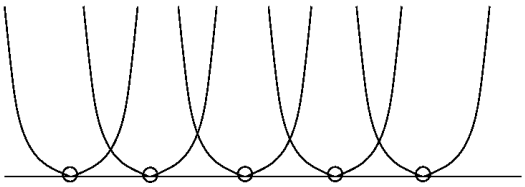

scheme 073

Matching of individual calculations.

# A Two-Dimensional Energy Surface for a Type II $S_N2$ Reaction in Aqueous Solution†

**Jiali Gao* and Xinfu Xia**

*Contribution from the Department of Chemistry, State University of New York at Buffalo, Buffalo, New York 14214*

*Received May 19, 1993**

**Abstract:** The role of aqueous solvation on the potential surface of the $S_N2$ Menshutkin reaction between ammonia and methyl chloride has been examined by using a combined quantum mechanical and statistical mechanical method. In the present simulation approach, the reactant molecules are treated by the semiempirical AM1 theory, while the solvent is represented by the empirical TIP3P model. Solute–solvent interactions are evaluated through Hartree–Fock molecular orbital calculations throughout the fluid simulation. In this paper, it is first demonstrated, by comparison with high-level ab initio results, that this hybrid quantum mechanical and molecular mechanical (QM/MM-AM1/TIP3P) model can provide an adequate description of intermolecular interactions between the solute and solvent for the Menshutkin reaction. The free energy surface in aqueous solution is then determined via statistical perturbation theory with a grid search algorithm. The results suggest that the solvent effects strongly stabilize the transition state and products. The computed free energy of activation (26 kcal/mol) is in good agreement with previous theoretical and experimental estimates. The most striking finding is that the transition state is shifted significantly toward the reactants, with a lengthening of the C–N bond by 0.30 Å and a shortening of the C–Cl bond by 0.15 Å. This is in accord with the Hammond postulate and consistent with previous theoretical studies. Analyses of the simulation results indicate that the charge separation during the present Type II $S_N2$ reaction is promoted by the solvent effect, with a charge transfer of about 65% complete at the transition state. Detailed insights into the structural and energetic nature of the differential solvation of the reactants and transition state are provided.

## Introduction

The bimolecular nucleophilic substitution reaction is one of the most fundamental processes in organic chemistry and has attracted numerous experimental and theoretical investigations.[1-3] In his classic work, Ingold classified nucleophilic substitutions into four categories according to the charge type of the nucleophile, being negative or neutral, and of the substrate, being neutral or positive.[1] This classification has helped qualitatively to explain the dramatic solvent effect on the rate of $S_N2$ reactions observed experimentally on the basis of charge distributions of the reactant and the transition state.[1-4] Quantitative characterization of the solute–solvent interaction at the molecular level, however, was only recently made possible, thanks to advances in computer technology and accurate free energy computational techniques. In particular, much attention has been paid to the prototypical Type I $S_N2$ reaction of $Cl^- + CH_3Cl \rightarrow ClCH_3 + Cl^-$, involving an anion and a neutral substrate in aqueous and organic solvents.[5-9] To further our understanding of the solvation effect on $S_N2$ reactions, extension of theory to other charge types is warranted.

Much progress has been made in elucidating the intrinsic properties of gas-phase $S_N2$ reactions through quantum mechanical ab initio calculations. The double-well potential energy surface for the Type I reaction[9] predicted by early theoretical studies was confirmed by the extensive experimental work of Brauman and co-workers.[10,11] In addition, ab initio calculations provide valuable information on the transition-state (TS) structure and charge distributions along the whole reaction coordinate. Recently, these computations have been extended to condensed-phase simulations using statistical mechanical Monte Carlo and molecular dynamics techniques.[5-8] This was led by the calculation of the reaction profile involving chloride and methyl chloride in aqueous and DMF solutions.[5a] The striking solvent effect observed

† Taken in part from the Ph.D. dissertation of X.X., SUNY, Buffalo, 1993.

* Abstract published in *Advance ACS Abstracts,* October 1, 1993.

(1) (a) Ingold, C. K. *Structure and Mechanism in Organic Chemistry*, 2nd ed.; Cornell University Press: Ithaca, NY, 1969. (b) Hughes, E. D.; Ingold, C. K. *J. Chem. Soc.* **1935**, 244.

(2) (a) Harris, J. M.; McManus, S. P., Eds.; *Nucleophilicity*; American Chemical Society: Washington, DC, 1987; Series 215. (b) Hartshorn, S. R. *Aliphatic Nucleophilic Substitution*; Cambridge University Press: London, 1973. (c) Hines, J. *Physical Organic Chemistry*; McGraw-Hill: New York, 1962. (d) Ritchie, C. D. In *Solute-Solvent Interactions*; Goetzee, J. F., Ritchie, C. D., Eds.; Marcel Dekker: New York, 1969; p 284.

(3) Dewar, M. J. S.; Dougherty, R. C. *The PMO Theory of Organic Chemistry*; Plenum Press: New York, 1975.

(4) (a) Menshutkin, N. *Z. Phys. Chem.* **1890**, *5*, 589. (b) Parker, A. J. *Chem. Rev.* **1969**, *69*, 1. (c) Abraham, M. H.; Greillier, P. L.; Abboud, J. M.; Doherty, R. M.; Taft, R. W. *Can. J. Chem.* **1988**, *66*, 2673. (d) Abboud, J. M.; Notario, R.; Bertran, J.; Solà, M. *Prog. Phys. Org. Chem.* **1993**, *19*, 1.

(5) (a) Chandrasekhar, J.; Smith, S. F.; Jorgensen, W. L. *J. Am. Chem. Soc.* **1984**, *106*, 3049; **1985**, *107*, 154. (b) Chandrasekhar, J.; Jorgensen, W. L. *J. Am. Chem. Soc.* **1985**, *107*, 2974. (c) Jorgensen, W. L.; Buckner, J. K. *J. Phys. Chem.* **1986**, *90*, 4651.

(6) (a) Chiles, R. A.; Rossky, P. J. *J. Am. Chem. Soc.* **1984**, *106*, 6867. (b) Huston, S. E.; Rossky, P. J.; Zichi, D. A. *J. Am. Chem. Soc.* **1989**, *111*, 5680. (c) Bash, P. A.; Field, M. J.; Karplus, M. *J. Am. Chem. Soc.* **1987**, *109*, 8092. (d) Hwang, J.; King, G.; Creighton, S.; Warshel, A. *J. Am. Chem. Soc.* **1988**, *110*, 5297.

(7) (a) Bergsma, J. P.; Gertner, B. J.; Wilson, K. R.; Hynes, J. T. *J. Chem. Phys.* **1987**, *86*, 1356. (b) Gertner, B. J.; Whitnell, R. M.; Wilson, K. R.; Hynes, J. T. *J. Am. Chem. Soc.* **1991**, *113*, 74. (c) Gertner, B. J.; Wilson, K. R.; Hynes, J. T. *J. Chem. Phys.* **1989**, *90*, 3537. (d) Kozaki, T.; Morihashi, K.; Kikuchi, O. *J. Am. Chem. Soc.* **1989**, *111*, 1547. (e) Basilevsky, M. V.; Chudinov, G. E.; Napolov, D. V. *J. Phys. Chem.* **1993**, *97*, 3270.

(8) (a) Tucker, S. C.; Truhlar, D. G. *J. Phys. Chem.* **1989**, *93*, 8138. (b) Tucker, S. C.; Truhlar, D. G. *J. Am. Chem. Soc.* **1990**, *112*, 3347.

(9) (a) Wolfe, S.; Mitchell, D. J.; Schlegel, H. B. *J. Am. Chem. Soc.* **1981**, *103*, 7602, 7694. (b) Dedieu, A.; Veillar, G. A. *J. Am. Chem. Soc.* **1972**, *94*, 6730. (c) Bader, R. F. W.; Duke, A. J.; Messer, P. R. *J. Am. Chem. Soc.* **1973**, *95*, 7715. (d) Carrion, F.; Dewar, M. J. S. *J. Am. Chem. Soc.* **1984**, *106*, 3531. (e) Vande Linde, S. G.; Hase, W. L. *J. Phys. Chem.* **1990**, *94*, 2778. (f) Shi, Z.; Boyd, R. J. *J. Am. Chem. Soc.* **1990**, *112*, 6789. (g) Shaik, S. S.; Schlegel, H. B.; Wolfe, S. *Theoretical Aspects of Physical Organic Chemistry. The $S_N2$ Mechanism*; Wiley: New York, 1992.

(10) (a) Olmstead, W. N.; Brauman, J. I. *J. Am. Chem. Soc.* **1977**, *99*, 4019. (b) Pellerite, M. J.; Brauman, J. I. *J. Am. Chem. Soc.* **1980**, *102*, 5993. (c) Bohme, D. K.; Young, L. B. *J. Am. Chem. Soc.* **1974**, *96*, 4027. (d) Gronert, S.; DePuy, C. H.; Bierbaum, V. M. *J. Am. Chem. Soc.* **1991**, *113*, 4009.

(11) (a) Graul, S. T.; Bowers, M. T. *J. Am. Chem. Soc.* **1991**, *113*, 9696. (b) Cyr, D. M.; Posey, L. A.; Bishea, G. A.; Han, C.-C.; Johnson, M. A. *J. Am. Chem. Soc.* **1991**, *113*, 9697. (c) Wilbur, J. L.; Brauman, J. I. *J. Am. Chem. Soc.* **1991**, *113*, 9699.

0002-7863/93/1515-9667$04.00/0 

experimentally was demonstrated by a predicted increase of 15 kcal/mol in activation free energy over its intrinsic (*in vacuo*) barrier.[5]

In the present study, we report the results of a theoretical examination of a Type II $S_N2$ reaction, the Menshutkin reaction in aqueous solution,[1,4a]

$$H_3N + CH_3Cl \rightarrow H_3NCH_3^+ + Cl^-$$

using the combined quantum mechanical and molecular mechanical (QM/MM) Monte Carlo simulation method described previously.[12] Several issues are of interest in this reaction. First, TS structures are generally expected to be different in the gas phase and in solution. This is not a serious problem for symmetric reactions because the solvent effects are the same on both sides of the TS along the reaction coordinate. Thus, the structural change is not expected to be considerably large and has been confirmed by Jorgensen and Buckner for the Type I reaction in water.[5c] However, switching to a system consisting of a neutral nucleophile and substrate (Type II), in which large charge separation occurs during the reaction, should yield an "uneven" solvation effect that is accompanied by a reduction of the reaction barrier and a shift in the TS structure according to the Hammond postulate.[13] In a recent communication, we reported the results of a study of the Menshutkin reaction using empirical potential functions.[14] That work, along with the study of Solà et al.,[15] confirmed the empirical expectation and demonstrated that the solvent effect can, indeed, significantly modify the position of the transition state. Consequently, the solvent effect should be included in the electronic structure calculations to determine the reaction path in solution. Second, the solvent effect on the polarization of the reactants is expected to enhance the charge separation of the Menshutkin reaction over that of the reaction in the gas phase.[14,15] Although this would be very difficult to investigate using empirical potential functions, the problem is naturally solved by the QM/MM method because the solvent effect is coupled into the electronic structure calculation in fluid simulations.[13,16] Therefore, additional insights into the solvent effect may be inferred from the QM/MM simulation. Finally, it is desirable to locate the minimum free energy path for the Menshutkin reaction in solution rather than to follow the reaction path of the gas-phase process.[5-9,14]

In this report, we have extended our study to cover the free energy surface of the Menshutkin reaction by mapping out the bond formation and breaking process independently. The results provide new insights into the structure and energetics for the understanding of $S_N2$ reactions in solution. In the following, computational details are given first, followed by results and discussion.

## Computational Details

**(a) Intermolecular Potential Functions.** In the present study, we adopt a combined QM/MM approach in statistical mechanical Monte Carlo simulations. The method has been reviewed recently by several authors; additional details are in ref 12. Here, the fluid system is partitioned into a quantum mechanical region consisting of the solute molecule, $H_3N$–$CH_3$–Cl, and a molecular mechanical region containing solvent monomers which are approximated by the three-site TIP3P model for water.[16,19]

**Table I.** Lennard-Jones Parameters Used in the AM1/TIP3P Model

| atom | $\sigma$, Å | $\epsilon$, kcal/mol |
|---|---|---|
| | $H_3N$-$CH_3$-Cl | |
| C | 3.4000 | 0.1000 |
| N | 3.0875 | 0.1615 |
| Cl | 4.1964 | 0.1119 |
| $H_C$ | 2.0000 | 0.0700 |
| $H_N$ | 0.0 | 0.0 |
| | Water | |
| O | 3.1506 | 0.1521 |
| H | 0.0 | 0.0 |

Clearly, to compute the energies of the QM solute molecule throughout the condensed-phase simulation, a computationally efficient method must be used. Therefore, the semiempirical Austin Model 1 (AM1) theory developed by Dewar and co-workers[17] is employed to form the AM1/TIP3P force field in this study.[12a,c] Warshel and co-workers have used the empirical valence bond (EVB) theory in their study of the Type I $S_N2$ reaction and enzymatic processes.[6d,12b]

For the QM region, the solute is represented by valence electrons and nuclei. The restricted Hartree–Fock wave function, $\Phi$, is used with a single Slater determinant of all doubly occupied molecular orbitals (MOs), which are linear combinations of a minimum basis set.[17,18] The total effective Hamiltonian of the system is given by[12]

$$\hat{H}_{eff} = \hat{H}^{\circ} + \hat{H}_{QM/MM} + \hat{H}_{MM} \quad (1)$$

where $\hat{H}^{\circ}$ is the AM1 Hamiltonian for the solute molecule, $\hat{H}_{MM}$ is the molecular mechanical solvent energy, and $\hat{H}_{QM/MM}$ is the solute–solvent interaction Hamiltonian (eq 2),

$$\hat{H}_{QM/MM} = \hat{H}^{el}_{QM/MM} + \hat{H}^{vdW}_{QM/MM} = \left(-\sum_{s=1}^{S}\sum_{i=1}^{2N}\frac{eq_s}{r_{si}} + \sum_{s=1}^{S}\sum_{m=1}^{M}\frac{q_s Z_m}{R_{sm}}\right) + \sum_{s=1}^{S}\sum_{m=1}^{M} 4\epsilon_{sm}\left[\left(\frac{\sigma_{sm}}{R_{sm}}\right)^{12} - \left(\frac{\sigma_{sm}}{R_{sm}}\right)^{6}\right] \quad (2)$$

where $e$ is the charge of electrons, $q_s$ and $Z_m$ are charges on the solvent and solute nuclei, $S$ and $M$ are the corresponding total numbers of interaction sites, and $r_{si}$ and $R_{sm}$ are the distances of the solute electrons and nuclei from the solvent sites, respectively. The Lennard-Jones term in eq 2 accounts for the dispersion interaction between the QM and MM regions, which are omitted in the hybrid QM/MM approximation;[16] it contains the only adjustable parameters for the solute ($\sigma_m$ and $\epsilon_m$) in the present approach. These parameters are listed in Table I. The combining rules used for the solute–solvent interaction are $\sigma_{sm} = (\sigma_s\sigma_m)^{1/2}$ and $\epsilon_{sm} = (\epsilon_s\epsilon_m)^{1/2}$.

The total potential energy in the combined QM/MM force field is computed using eq 3,

$$E_{tot} = \langle\Phi|\hat{H}_{eff}|\Phi\rangle = E_{QM} + E^{el}_{QM/MM} + E^{vdW}_{QM/MM} + E_{MM} \quad (3)$$

Here, $\Phi$ is the wave function of the solute in aqueous solution, $E_{MM}$ is the MM pair interaction energy for the solvent molecules enumerated with the empirical TIP3P potential, and ($E_{QM} + E^{el}_{QM/MM}$) is determined through Hartree–Fock self-consistent-field (SCF) MO calculations.

As usual, the intermolecular interaction energy for a water dimer in the MM region is given as the sum of Coulombic interactions between all atomic pairs plus a Lennard-Jones term between the two oxygen atoms (eq 4). The three-site TIP3P model is employed for water, with experimental geometry held fixed throughout the simulations.[19]

$$\Delta E_{ab} = \sum_{i}^{\text{on } a}\sum_{j}^{\text{on } b}(q_i q_j/r_{ij}) + 4\epsilon_{00}[(\sigma_{00}/r_{00})^{12} - (\sigma_{00}/r_{00})^{6}] \quad (4)$$

**(b) Geometrical Constraints.** Due to the symmetry of the Menshutkin reaction of $H_3N + CH_3Cl$, the three non-hydrogen atoms, N, C, and Cl,

(12) For reviews, see: (a) Field, M. J.; Bash, P. A.; Karplus, M. *J. Comput. Chem.* **1990**, *11*, 700. (b) Luzhkov, V.; Warshel, A. *J. Comput. Chem.* **1992**, *13*, 199. (c) Gao, J. *J. Phys. Chem.* **1992**, *96*, 537. Methods using continuum models such as the self-consistent reaction field theory are also relevant but are not specifically discussed. For recent applications and leading references, see: (d) Cramer, C. J.; Truhlar, D. G. *J. Am. Chem. Soc.* **1991**, *113*, 8305. (e) Karelson, M. M.; Zerner, M. C. *J. Phys. Chem.* **1992**, *96*, 6949.

(13) See, for example: (a) Issacs, N. S. *Physical Organic Chemistry*; John Wiley & Sons, Inc.: New York, 1987. (b) Connors, K. A. *Chemical Kinetics: the Study of Reaction Rates in Solution*; VCH: New York, 1990.

(14) Gao, J. *J. Am. Chem. Soc.* **1991**, *113*, 7796.

(15) Solà, M.; Lledos, A.; Duran, M.; Bertran, J.; Abboud, J. M. *J. Am. Chem. Soc.* **1991**, *113*, 2873.

(16) Gao, J.; Xia, X. *Science* **1992**, *258*, 631.

(17) Dewar, M. J. S.; Zoebisch, E. G.; Healy, E. F.; Stewart, J. J. P. *J. Am. Chem. Soc.* **1985**, *107*, 3902.

(18) Hehre, W. J.; Radom, L.; Schleyer, P. v. R.; Pople, J. A. *Ab Initio Molecular Orbital Theory*; Wiley; New York, 1986.

(19) Jorgensen, W. L.; Chandrasekhar, J.; Madura, J. D.; Impey, R. W.; Klein, M. L. *J. Chem. Phys.* **1983**, *79*, 926.

are constrained to be collinear along the $C_3$ symmetry axis. Dihedral variations of $H_3N$ and $CH_3$ groups about the C–N bond are allowed during the Monte Carlo simulation.[20b] The bond length and bond angles associated with the hydrogen atoms are optimized at a fixed H–N–C–H dihedral angle sampled in the calculation.

**(c) Monte Carlo Simulations.** Statistical mechanical Monte Carlo calculations were carried out in the isothermal–isobaric (NPT) ensemble at 25 °C and 1 atm.[20] A cubic box containing 265 water molecules (ca. 20 × 20 × 20 Å$^3$) was used in the free energy surface calculation, whereas a rectangular box consisting of 321 water molecules (ca. 19 × 19 × 28 Å$^3$) was employed for computing the reaction profile (see below) to allow adequate sampling at large separation distances along the reaction coordinate (RC). In the latter simulation, the $C_3$ symmetry axis is oriented to coincide with the $z$-axis of the water box. Standard Metropolis sampling procedures were adopted along with the Owicki–Scheraga preferential sampling technique using $1/(r^2 + c)$ weighting, where $c$ = 150 Å$^2$, to facilitate the statistics near the solute molecule.[21] At least 5 × $10^5$ configurations were taken in the equilibration stage for each point on the free energy surface, while $10^6$ configurations were collected to compute the statistical averages. The solute–solvent interaction energy was evaluated by single-point Hartree–Fock SCF calculations using the effective Hamiltonian of eq 1. The intermolecular interactions are feathered to zero between spherical cutoff distances of 9.0 and 9.5 Å for water–water and solute–water interactions, based roughly on the center-of-mass separation. New configurations were generated by randomly selecting a molecule, translating it in all three Cartesian directions, rotating it along a randomly chosen axis, and varying the internal rotation. An acceptance rate of about 40% was maintained by using ranges of ±0.11 Å and 10° for molecular motions. Volume changes were restricted to within ±100 Å$^3$ at every 1625 configurations. Standard deviations are estimated from averages of blocks $10^5$ configurations.

**(d) Free Energy Surface.** In order to assess the solvent effects on the TS structure of the prototypical Menshutkin reaction, $H_3N + CH_3Cl \rightarrow CH_3NH_3^+ + Cl^-$, in aqueous solution, a two-dimensional free energy surface was constructed through a grid search method. The two independent coordinates of the map are C–N distance $R_{CN}$ and C–Cl distance $R_{CCl}$. The grid searching was carried out in a rectangular region of 1.406 Å ≤ $R_{CN}$ ≤ 2.406 Å and 1.744 Å ≤ $R_{CCl}$ ≤ 2.444 Å, while statistical perturbation theory was used to compute free energy differences between neighboring grid points.[22] Specifically, at a given value of $R_{CCl}$, a series of perturbation calculations with $\Delta R_{CN}$ = ±0.05 Å were carried out to yield a free energy profile as a function of $R_{CN}$. The relative heights of two such neighboring profiles (parallel to each other) at an interval of 0.10 Å were determined by another perturbation calculation with respect to $R_{CCl}$ at a fixed $R_{CN}$ value. Finally, the potential surface was anchored relative to the free energy at an RC of –2.0 Å (see below). Hence, the whole free energy surface was constructed (Figure 1) through a total of 87 simulations. The numerical results are summarized in the supplementary material.

We note that Warshel and co-workers introduced an elaborate method that employs a mapping function to drive the reactant state to the product state.[6d,12b,23] The free energy of activation for the reaction is then recovered by an umbrella-sampling-type treatment,[24] making use of the energy gap, $\Delta\epsilon$, between the products and reactants on the mapping function potential surface as the reaction coordinate.[6d,23b] The method is particularly advantageous for use with the EVB approach, which has been applied to many chemical and biological systems by these authors.[23] The method, of course, can be used with the MO approach as described in ref 12b. Effectively, the method gives the probability of reaching the transition state from the reactant state, while the energy of the transition state (which is defined by $\Delta\epsilon$) results from a distribution of solute geometries in solution. Thus, structural constraints are not involved in these calculations, though the mapping function provides an energetic restriction. On the other hand, the present grid approach, as in many applications reported in the literature,[5,6] yields the potential of mean force for the reaction if a one-dimensional reaction coordinate is used or the solvent-averaged free energy surface with a multiple-dimensional reaction coordinate.

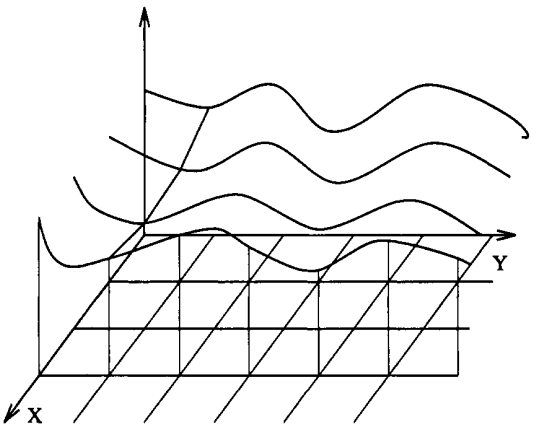


**Figure 1.** Schematic representation of the algorithm used in calculating the free energy map. X represents the C–Cl distance, and Y is the C–N separation in the Menshutkin reaction. In the first step, free energy profiles in the Y direction are constructed by perturbing Y with fixed X values. These profiles are then connected by perturbations with respect to X.

Recently, Pearlman and Kollman proposed a method for establishing the free energy surface using statistical perturbation theory.[25] They suggested perturbing the two independent variables, the dihedral angles in their study, in multiple directions. Consequently, several free energy changes can be obtained from a single fluid simulation. This would, indeed, be computationally efficient if empirical potentials are used because the time-limiting step is the configurational sampling in those simulations. However, the major cost in the hybrid QM/MM method is the quantum mechanical MO calculations. Furthermore, multiple-direction mutations over the present double-wide sampling[26] will also significantly increase the memory requirement in the combined QM/MM method. Thus, the grid search in the present study is limited to double-wide sampling.[26]

## Gas-Phase Reaction

**(a) Potential Surface in the Gas Phase.** In our previous study,[14] the transition-state structure for the Menshutkin reaction of $H_3N + CH_3Cl \rightarrow CH_3NH_3^+ + Cl^-$ was located through ab initio molecular orbital calculations at the 6-31 + G(d) level using GAUSSIAN 90.[27] A minimum energy path (MEP) was then determined by energy minimizations at different values of the reaction coordinate (RC) defined by[14]

$$RC = R_{CCl} - R_{CN} - RC_0 \qquad (5)$$

where $R_{CCl}$ and $R_{CN}$ are respectively the distances of Cl and N from C, and $RC_0$ is the difference between the C–Cl and C–N separations at the saddle point. A $C_{3v}$ symmetry was maintained during the minimizations. Correlation energies were obtained by single-point energy computations at the MP4SDTQ/6-31 + G(d) level for all structures considered. The gas-phase free energy profile was constructed using standard procedures by including zero-point energy and entropy corrections based on the 6-31 + G(d) vibrational frequencies.[14] In these calculations, ab initio vibrational frequencies were scaled by a factor of 0.89, and the

(20) All simulations were performed using (a) MCQUB (Monte Carlo QM/MM at University at Buffalo, Gao, J., SUNY at Buffalo, 1992) and (b) BOSS (Version 2.9; Jorgensen, W. L., Yale University, 1990) programs. (c) The quantum mechanical energy was evalulated with MOPAC (Stewart, J. J. P. *MOPAC*, Version 5; Quantum Chemistry Program Exchange 455, 1986, Vol. 6, No. 391.

(21) (a) Owicki, J. C.; Sheraga, H. A. *Chem. Phys. Lett.* **1977**, *47*, 600. (b) Owicki, J. C. *ACS Symp. Ser.* **1978**, *86*, 159. (c) Jorgensen, W. L.; Bigot, B.; Chandrasekhar, J. *J. Am. Chem. Soc.* **1982**, *104*, 4584.

(22) Zwanzig, R. W. *J. Chem. Phys.* **1954**, *22*, 1420.

(23) (a) Warshel, A. *J. Phys. Chem.* **1979**, *83*, 1640. (b) Hwang, J.-K.; Warshel, A. *J. Am. Chem. Soc.* **1987**, *109*, 715. (c) Warshel, A.; Sussman, F.; Hwang, J.-K. *J. Mol. Biol.* **1988**, *201*, 139. (d) Warshel, A.; Aqvist, J. *Annu. Rev. Biophys. Biophys. Chem.* **1991**, *20*, 267. (e) Warshel, A. *Curr. Opinion Struct. Biol.* **1992**, *2*, 230. (f) Warshel, A. *Computer Modeling of Chemical Reactions in Enzymes and Solutions*; Wiley: New York, 1991.

(24) (a) Patey, G. N.; Valleau, J. P. *J. Chem. Phys.* **1975**, *63*, 2334. (b) Valleau, J. P.; Torrie, G. M. In *Statistical Mechanics, Part A: Equilibrium Techniques*; Berne, B. J., Ed.; Plenum: New York, 1977; p 169.

(25) Pearlman, D. A.; Kollman, P. A. *J. Am. Chem. Soc.* **1991**, *113*, 7167.

(26) Jorgensen, W. L.; Ravimohan, C. *J. Chem. Phys.* **1985**, *83*, 3050.

(27) Frisch, M. J.; Head-Gordon, M.; Trucks, G. W.; Foreman, J. B.; Schlegel, H. B.; Raghavachari, K.; Robb, M.; Binkley, J. S.; Gonzalez, C.; Defrees, D. J.; Fox, D. J.; Whiteside, R. A.; Seeger, R.; Melius, C. F.; Baker, J.; Martin, R. L.; Kahn, L. R.; Stewart, J. J. P.; Topiol, S.; Pople, J. A. *GAUSSIAN 90*; Gaussian Inc.: Pittsburgh, PA, 1990.

**Table II.** Computed and Experimental Energies for the Menshutkin Reaction in the Gas Phase at 25 °C (kcal/mol)

| species | $\Delta H$ (AM1) | $\Delta G$ (MP4/6-31+G*)[a] | $\Delta G$ (expt)[a] |
|---|---|---|---|
| $H_3N + CH_3Cl$ | 0 | 0 | 0 |
| $[H_3N{-}CH_3{-}Cl]^*$ | 50.0 | 46.7 | |
| $CH_3NH_3^+ + Cl^-$ | 137 | 119 | 110 |

[a] Reference 14.

resulting vibrations that are lower than 500 $cm^{-1}$ were treated as rotations. In addition, the normal mode along the reaction coordinate, which becomes imaginary at the TS, was ignored. The computed free energy of reaction is in good agreement with the experimental data (Table II).[14,28] It should be pointed out that the reaction path calculated this way is not necessarily the steepest descent path (SDP) due to the restriction of eq 5. The SDP or the intrinsic reaction coordinate (IRC) may be obtained through the reaction-path-following procedure incorporated in GAUSSIAN 90.

The ab initio free energy profile described above has been used to compute the potential of mean force (pmf) for the Menshutkin reaction in aqueous solution through Monte Carlo simulations with fitted empirical potential functions.[14] Although the computed energetic results are in good agreement with the available experimental data, there is concern with the predicted transition-state structure in water because of the dramatic solvent effect.[14,15] In the previous empirical approach, it was not possible to determine a priori the solvent effect on the change of the reaction profile in solution. The solvation free energy has to be evaluated separately and added to the free energy profile in the gas phase. Consequently, the maximum point on the free energy profile in solution will always be along the gas-phase MEP. Hence, the "TS" structure obtained this way is not necessarily the true saddle point on the *free energy surface* in solution. A proper treatment of the solvent effects on the TS structure should couple the solute–solvent interaction and the chemical process simultaneously and consider a two-dimensional free energy surface by treating both bond formation and breaking processes.

Fortunately, the combined QM/MM-AM1/TIP3P Monte Carlo simulation method provides a viable solution, and it is adopted in this study. To ensure that the AM1 method is appropriate to describe the Menshutkin reaction of $H_3N + CH_3Cl$, structural and energetic results are compared with the ab initio 6-31 + G(d) findings (Table II and Figure 2).[14] Geometric variables for the reactant and product molecules predicted by the AM1 model are in excellent agreement with predictions by ab initio calculations at the 6-31 + G(d) level. The largest deviations are only 0.04 Å for the bond lengths and 1.3° for the bond angles. On the other hand, the AM1 model yields a much tighter TS structure than the ab initio approach. At the transition state, the C–N and C–Cl distances are 1.899 and 2.474 Å at the 6-31 + G(d) level, which are 0.24 and 0.23 Å longer than the AM1 values. In addition, the Walden inversion at the methyl group is about 3.8° more advanced in the AM1 structure. However, the ab initio geometric parameters appear to be somewhat overestimated for the Menshutkin reaction in view of the results for the $S_N2$ reaction of $Cl^- + CH_3Cl$, where the two C–Cl distances are 2.383 Å at the TS.[5] In any event, since the primary interest of the present study is the solvent effect on the change in TS structure, it seems to be reasonable to use the AM1 geometry in fluid simulations. An alternative approach would be to use the ab initio potential surface for the Menshutkin reaction in the gas phase, supplementing solvation free energies evaluated with the AM1/TIP3P model.

(28) Computed from standard free energies of formation: −3.91 ($NH_3$), −14.38 ($CH_3Cl$), −57.40 ($Cl^-$), and 149.2 ($CH_3NH_3^+$). *JANAF Thermochemical Tables*, 3rd ed.; U.S. Government Printing Office; Washington D.C., 1971. *J. Phys. Chem. Ref. Data Suppl.* 1982; Vol. 11, 1985; Vol. 14. The value for $CH_3NH_3^+$ was calculated from the process $CH_3NH_2 + H^+ \rightarrow CH_3NH_3^+$: Aue, D. H.; Webb, H. M.; Bowers, M. T. *J. Am. Chem. Soc.* **1976**, *98*, 311. Lias, S. G.; Liebman, J. F.; Levin, R. D. *J. Phys. Chem. Ref. Data* **1984**, *13*, 695.

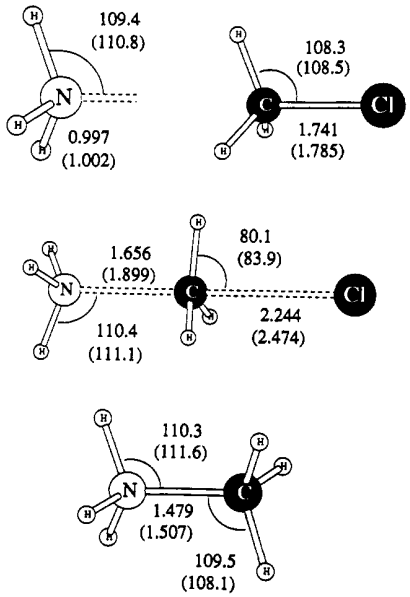


**Figure 2.** Optimized AM1 and 6-31 + G(d) (in parentheses) geometries: bond lengths in angstroms and angles in degrees.

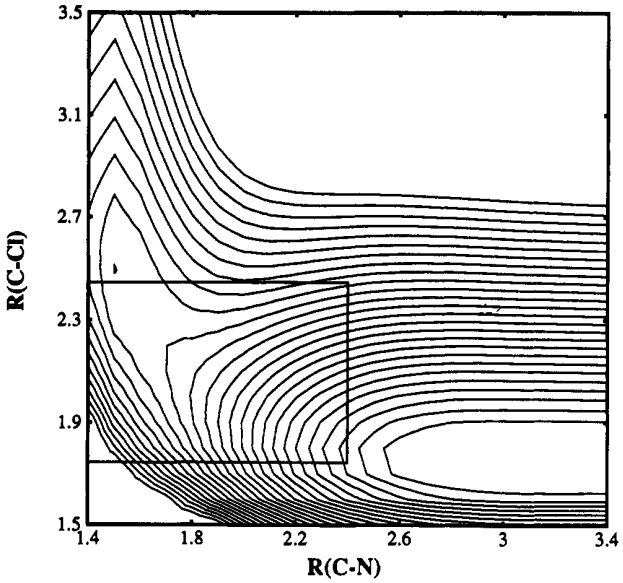


**Figure 3.** Contour of the heat of formation for the Menshutkin reaction, $H_3N + CH_3Cl \rightarrow CH_3NH_3^+ + Cl^-$, in the gas phase determined by AM1 calculations. The contour level is 2 kcal/mol. Values higher than 60 or less than −25 kcal/mol are not shown. Monte Carlo simulations are carried out within the rectangular region.

The AM1 energy contour for the reaction $H_3N + CH_3Cl \rightarrow CH_3NH_3^+ + Cl^-$ in the gas phase is shown in Figure 3. The feature of a shallow minimum for the product ion pair predicted by ab initio calculations is also revealed by the AM1 results.[14,15] Note that although standard enthalpies are computed in the AM1 geometry optimization, the numerical results are actually in good agreement with free energy changes predicted at the MP4SDTQ/6-31 + G(d) level with 6-31 + G(d) vibrational frequencies (Table II). It appears that the AM1 results without entropic corrections provide a reasonable approximation to the ab initio free energy profile and thus will be used in the present study (see below).

**(b) Bimolecular Interactions.** The most crucial element in the simulation of chemical reactions in solute is the reliability of the method for computing intermolecular interaction energies at

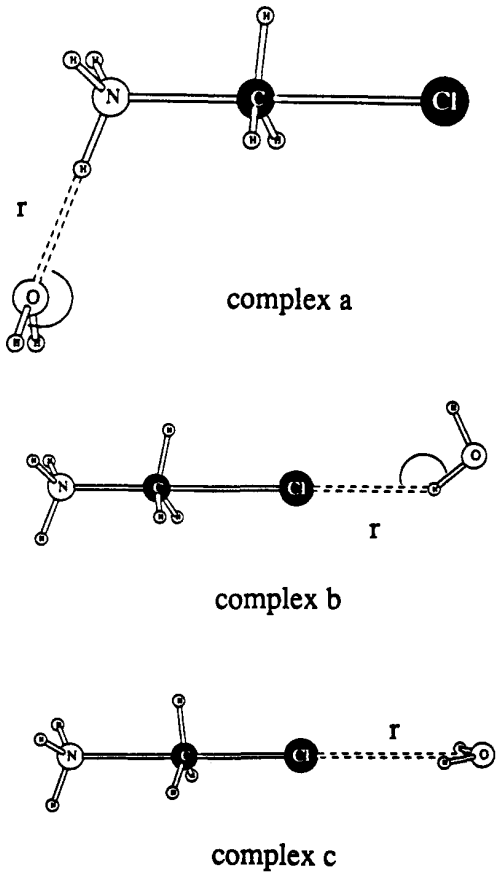


**Figure 4.** Structural arrangements of monohydrated clusters of [$H_3$–$CH_3$–Cl].

different stages of the reaction; of course, it is, too, important for the solvent effects and associated boundary conditions to be correctly incorporated into the quantum Hamiltonian.[12] Consequently, geometries and interaction energies for solute–water complexes at different values of $R_{CN}$ and $R_{CCl}$ are computed at the ab initio 6-31 + G(d) level and are compared with predictions from the QM/MM model, through which the Lennard-Jones parameters (eq 2) are determined. Values of $R_{CN}$ and $R_{CCl}$ are chosen along the 6-31 + G(d) MEP corresponding to RCs of −1.5, −1.0, −0.5, −0.25, −0.1, 0.0, 0.1, 0.25, 0.5, and 0.75. The ab initio results for these bimolecular complexes with water have been used to derive the empirical potential function employed in our previous study of the Menshutkin reaction in water.[14] At each of the selected points, two or three configurations of the solute–water complex are considered. Figure 4 depicts the structural arrangement of these bimolecular complexes. Structure a specifies the hydrogen-bonding interaction between the ammonium hydrogen and the oxygen of water, while complexes b and c denote the open and bifurcated forms between water and Cl. In all geometry optimizations (ab initio, QM/MM, and empirical), monomer geometries are fixed at the 6-31 + G(d) and experimental values for the reactants and water, respectively, while hydrogen-bonding parameters that are optimized are indicated in Figure 4. At the 6-31 + G(d) level, complex a has the strongest binding energy along the whole RC, whereas complex c forms the weakest complex of the three structures considered.

The ab initio interaction energies are first compared in Figure 5 (top) with those predicted by the empirical potential function used in ref 14. As expected, hydrogen-bonding interactions exhibit a gradual increase along the reaction coordinate. Excellent agreement is obtained with a root-mean-square (RMS) deviation of 0.4 kcal/mol between the two methods; however, the parametrization procedure was laborious and required a cubic spline

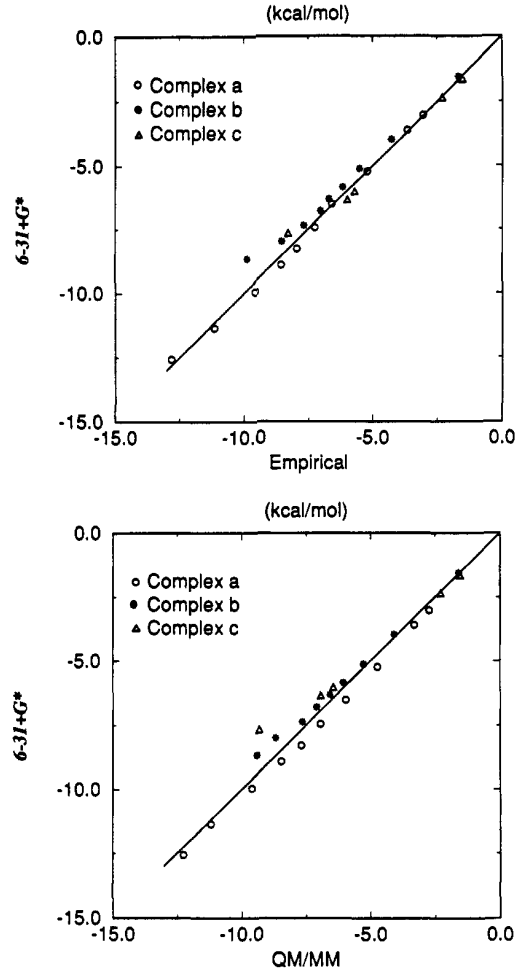


**Figure 5.** Comparison of the solute–solvent interaction energies predicted by the potential functions (top) and by the AM1/TIP3P model (bottom) vs the 6-31 + G(d) values. A line of slope = 1.0, indicating perfect agreement, is shown. All energies are in kilocalories per mole.

technique to specify the changes of the potential function parameters along the RC.[14] It is perhaps not even practical to derive such empirical potentials for the reaction surface considered here because the empirical parameter fitting would require consideration of bimolecular interactions spreading over the entire potential surface.[8] In contrast, the solute–solvent interaction is naturally determined in the combined QM/MM treatment.[12,16] Figure 5 (bottom) correlates the QM/MM prediction and the ab initio 6-31 + G(d) results. In these calculations, the solute, [$H_3$N–$CH_3$–Cl], is treated quantum-mechanically, while water is represented by the TIP3P model. The accord is good for an energy range of −1 to −12 kcal/mol; the overall RMS deviation is 0.5 kcal/mol. Large deviations between the QM/MM and 6-31 + G(d) results are mainly from complex c, without which the RMS deviation would be 0.4 kcal/mol. The agreement demonstrated here provides strong support for the use of the QM/MM method to study the Menshutkin reaction in aqueous solution.

### Free Energy Surface in Aqueous Solution

The principal goal of the present study is to determine the solvent effect on the potential surface of the Menshutkin reaction in water. This can be achieved by using statistical perturbation theory in Monte Carlo or molecular dynamics simulations. It is, of course, straightforward to compute the potential of mean force for the reaction along a predefined one-dimensional reaction path;[5,14] however, the construction of the potential surface requires

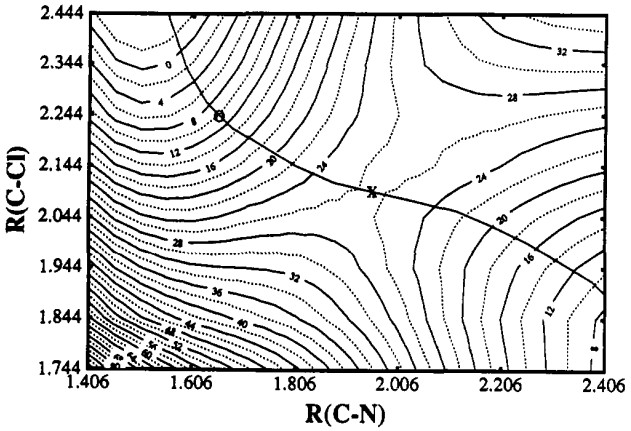


**Figure 6.** Computed free energy surface for the Type II $S_N2$ reaction [$H_3N$–$CH_3$–Cl] in aqueous solution as a function of C–N and C–Cl separations. The transition state is marked by an X, while the minimum energy path defined by eq 5 is indicated by the curve across the diagram. Energies are given in kilocalories per mole, and distances are in angstroms.

knowledge of relative free energies of all grid points (Figure 1) on the two-dimensional map.[25] This is a substantial undertaking in computational effort, especially with the use of the combined QM/MM potential. Consequently, emphasis is centered on the region indicated in Figure 3, where bond forming and breaking in the Menshutkin reaction take place. The results are shown in Figure 6, in which the saddle point at $R_{CN}$ = 1.96 Å and $R_{CCl}$ = 2.09 Å is marked by an X, while that in the gas phase is indicated by an O.

Several technical points should be addressed before the results are discussed further. First, in the present QM/MM approach, it is possible to decompose the computed total free energy change between two adjacent grid points into the intrinsic (gas-phase) contribution and the free energy of hydration.[29] This is accomplished by writing the quantum mechanical energy of given C–N and C–Cl distances $E_{QM}(R_{CN},R_{CCl})$ (eq 3) in terms of the gas-phase energy and an energy penalty required to polarized the electron distribution in solution:[16,29]

$$E_{QM}(R_{CN},R_{CCl}) = E^{\circ}_{gas}(R_{CN},R_{CCl}) + \Delta E_{dist}(R_{CN},R_{CCl}) \quad (6)$$

Here, $E^{\circ}_{gas}(R_{CN},R_{CCl}) = \langle\Phi^{\circ}|H^{\circ}_{QM}(R_{CN},R_{CCl})|\Phi^{\circ}\rangle$, and $E_{QM}(R_{CN},R_{CCl}) = \langle\Phi|H^{\circ}_{QM}(R_{CN},R_{CCl})|\Phi\rangle$, which are the electronic energies of the reactants in the gas phase and in water. $\Delta E_{dist}$ is the electron distortion energy due to solute–solvent interactions,[16,29] and $\Phi^{\circ}$ and $\Phi$ are the wave functions of the solute in the gas phase and in water, respectively. Thus, the solvation free energy for the Menshutkin reaction can be determined by subtracting the gas-phase potential (Figure 3) from the aqueous free energy surface (Figure 6) obtained via the QM/MM simulations. It should be emphasized that the combined QM/MM approach has the advantage of taking into account of the solvent polarization effects that are partially reflected by the $\Delta E_{dist}$ term.[16] Generally, this is of great concern if pairwise, empirical potential functions are used.

Second, the enthalpy change computed with the AM1 method is used here to *approximate* the free energy surface for the reaction of $H_3N$ + $CH_3Cl$ in the gas phase. Table II shows that the approximation is quite reasonable since the estimated enthalpy of activation (50 kcal/mol) is in reasonable accord with the free energy predicted at the MP4SDTQ/6-31 + G(d) level (47 kcal/mol). However, the AM1 method overestimates the energy of reaction for the Menshutkin reaction by 18 (27) kcal/mol compared with the ab initio (experimental) data.[28] The discrepancy is largely due to the poor performance of the AM1 theory for the chloride ion, whose heat of formation is predicted to be 18.2 kcal/mol higher than the experimental number.[17] This difference is expected to be fully transferred into the results from the QM/MM Monte Carlo simulation; however, it is not expected to affect the energetics in the region before/near the transition state.

(29) Gao, J. *J. Phys. Chem.* **1992**, *96*, 6432.

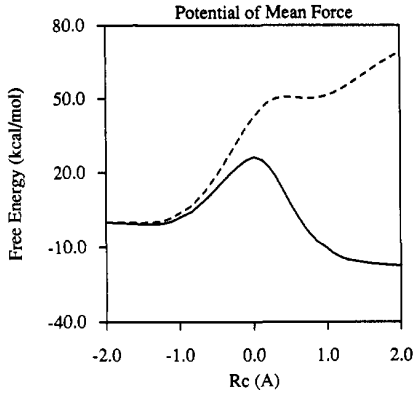


**Figure 7.** Potential of mean force for the Menshutkin reaction in water (solid curve) and in the gas phase (dashed curve). The reaction coordinate is the minimum energy path shown in Figure 6.

Finally, a major concern in the present study is the choice of the independent variables for the reaction surface. A linear approach of the nucleophile to $CH_3Cl$ is assumed, which appears to be reasonable; however, a full description of the reaction surface should also include the angular averaging of the nucleophilic attack. Extension beyond the present two-dimensional surface that treats the C–Cl and C–N variations independently is unfortunately beyond our current computational capability. Note that classical trajectory studies of the Type I $S_N2$ reactions with a box of solvent molecules have been carried out by Gertner et al.[7b] and by Hwang et al.,[6d] while Tucker et al.[8] used a multidimensional transition-state theory, but included only a few solvent molecules. It is of interest to perform similar calculations using the present QM/MM approach.

The most striking finding in Figure 6 is the shift of the TS structure that accompanies a dramatic solvent stabilization of the products. This finding is in good agreement with the prediction based on the Hammond postulate.[13] The structural change features a lengthening of the C–N distance of 0.30 Å from its gas-phase value of 1.66 Å and a decrease in the C–Cl bond length by 0.15 Å (2.09 Å in water). Therefore, the TS of the Menshutkin reaction occurs much earlier in aqueous solution than in the gas phase. For comparison, structural changes predicted in our previous investigation using empirical potentials are +0.15 and –0.10 Å for $R_{CN}$ and $R_{CCl}$, respectively.[14] However, that work differs from the present investigation in two ways: (1) there is no relaxation of the electronic structure allowed during the simulation and (2) the gas-phase MEP is held fixed without consideration of the symmetric stretch along the reaction path.[5c] The structural change is entirely due to solvation without consideration of electronic structure relaxation.[14] The present QM/MM method, on the other hand, allows electronic relaxation of the reactants on a two-dimensional free energy surface in aqueous solution through the quantum Hamiltonian.[16] Consequently, a much more dramatic solvent effect is observed. Note that a similar Menshutkin reaction involving $H_3N$ and $CH_3Br$ has been studied by Solà et al., using a continuum self-consistent reaction field method in ab initio molecular orbital calculations.[15] They found similar qualitative features for the TS structure when a dielectric constant of 78 was used to represent the aqueous solution.

Figure 7 illustrates the pmf along the reaction path shown in Figure 6 for the Menshutkin reaction, which has been extended by additional calculations along the path leading to the reactants

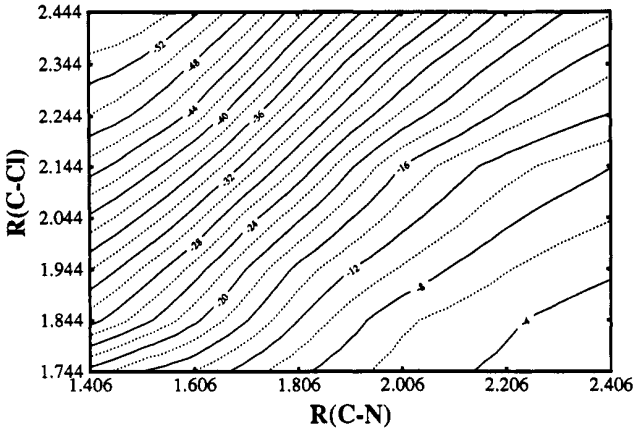


**Figure 8.** Free energy of hydration for the Menshutkin reaction in water. Energies are given in kilocalories per mole relative to the reactants at an RC = −2 Å.

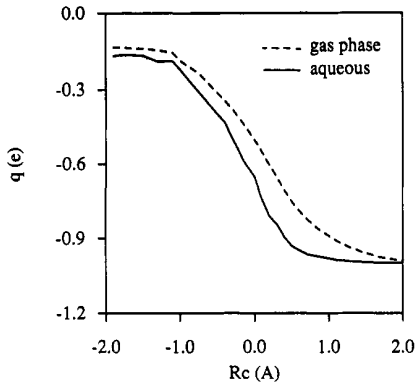


**Figure 9.** Comparison of the average charge transfer in aqueous solution (solid curve) and in the gas phase (dashed curve) along the reaction coordinate for $H_3N + CH_3Cl$. Partial charges for the leaving group (Cl) are given in electrons. Standard errors for the computed atomic charge in water are about 0.005 e.

and products. The RC of Figure 7 is defined by eq 5, but the TS structure in aqueous solution (Figure 6) is used to specify the reference state for $RC_0$. In Figure 7, the pmf is zeroed at RC = −2.0 Å, which is virtually flat for $|RC| \geq 1.0$ Å, suggesting that the SCF-type calculation can provide reasonable estimates for the energetics for the entire Menshutkin reaction, including the entrance and exit channels. It should be mentioned that the potential surface shown in Figure 6 is also anchored relative to this point (RC = −2.0 Å). The calculated free energy of activation is 26.3 ± 0.3 kcal/mol in water. Experimental data do not appear to be available for this particular system, perhaps due to practical difficulties in using gaseous $CH_3Cl$ to carry out these experiments; however, the result is in accord with the experimental activation *energy* (23.5 kcal/mol) for a similar reaction between $H_3N + CH_3I$ in water[30] and the previously computed value of 25.6 kcal/mol.[14] The agreement further supports the utilization of the combined QM/MM-AM1/TIP3P potential in the present study. For comparison, an activation energy of 8.3 kcal/mol was predicted by Solà et al. for $H_3N + CH_3Br$, which appears to be too small,[15] indicating that specific consideration of solute–solvent interactions is important for the present type II $S_N2$ reaction.

Figure 7 also gives the free energy of reaction, $\Delta G_{rxn}$, in water (−18 ± kcal/mol), which represents a solvent stabilization of about 155 kcal/mol relative to the gaseous process. The latter value is in exact agreement with the prediction of ref 14. The experimental estimate of $\Delta G_{rxn}$ from a thermodynamic cycle, using free energies of hydration and standard free energies of formation, is about −34 ± 10 kcal/mol.[14] As mentioned above, the AM1 model overestimates the heat of formation of $Cl^-$ by 18 kcal/mol.[17] If the experimental value were used, the computed reaction free energy would be −36 kcal/mol. The calculations by Solà et al. yield values of −27 to −44 kcal/mol with different basis sets.[15]

A detailed consideration of the free energy surface sheds light on the nature of the Menshutkin reaction in water. The attack of $H_3N$ toward the substrate leads to a charge separation to yield methylammonium and chloride ions. The process is extremely unfavorable in the gas phase due to Coulombic interactions. Indeed, Menshutkin reactions have never been reported in the gas phase.[31] However, in aqueous solution, the reactants become better and better solvated as the reaction proceeds, eventually leading to an exothermic process.[1,4a] The contour of the free energy of hydration is depicted in Figure 8, which shows a continuous enhancement of the reaction toward products. Therefore, the balance between the increase in energy due to charge separation during the reaction and the favorable solvation effects result in a shift in the position of the transition state and a reduction of the free energy of activation. Analogously Solà et al. used a Shaik-type state correlation diagram to rationalize the solvent effects on the change of the TS structure.[15,32] It is also interesting to notice that the pmf in Figure 7 corresponds to a unimodal energy profile in aqueous solution, which is consistent with the traditional notion of $S_N2$ reactions and with the prediction from the empirical approach.[1,14,15]

### Differential Solvation on the Reactants and the Transition State

**(a) Atomic Charges.** Additional insight into the solvent effect can be obtained by analyzing the extent of charge transfer during the reaction in the gas phase and in aqueous solution. The computed Mulliken population charges for the leaving group (Cl) along the reaction path of Figure 7 for both the gas-phase and the aqueous processes are shown in Figure 9, since it gives a good indication of the charge development during the reaction. Charge-population analyses have been performed by Bash et al.[6c] and by Hwang et al.[6d] in their molecular dynamics calculation of the reaction, $Cl^- + CH_3Cl \rightarrow CH_3Cl + Cl^-$, using the combined AM1/TIP3P potential and an EVB approach.[6c] Similar calculations have been performed for other systems.[7,12b,14,33] In contrast to the findings by Bash et al. for the Type I process, where charge transfer in water lags behind the process in the gas phase,[6c] the Type II reaction exhibits a solvent-promoted charge separation due to stabilization by interacting with the solvent molecules. This is, of course, consistent with the observed solvent effect on the activation energies for these reactions. For the Menshutkin reaction, a charge separation of more than 65% at the transition state in water is predicted from the QM/MM-AM1/TIP3P simulation, whereas it is only about 50% in the gas phase. It should be pointed out that although the Mulliken population analysis only gives a "rough" estimate of the charge distributions, the qualitative trends are still informative. Interestingly, the partial charge used in the empirical potential is about 0.7 e on the chlorine atom at the TS.[14]

**(b) Energy Distributions.** Details of the solute–solvent interaction are provided in Figure 10, which shows the distribution of pair interaction energies between the solute and water molecules. Three distributions, corresponding to the reactants (RC = −2 Å), TS (RC = 0 Å), and products (RC = 2 Å), are shown. As expected, the neutral reactant molecules interact weakly with the solvent without any specific structural features, while the

(30) (a) Okamoto, K.; Fukui, S.; Shingu, H. *Bull. Chem. Soc. Jpn.* **1967**, *40*, 1920. (b) Okamoto, K.; Fukui, S.; Nitta, I.; Shingu, H. *Bull. Chem. Soc. Jpn.* **1967**, *40*, 2354.

(31) Abraham, M. H. *Prog. Phys. Org. Chem.* **1974**, *11*, 1.

(32) Shaik, S. S. *Prog. Phys. Org. Chem.* **1985**, *15*, 197.

(33) (a) Cramer, C. J.; Truhlar, D. G. *Science*, **1992**, *256*, 213. (b) Tapia, O.; Colonna, F.; Angyan, J. G. *J. Chim. Phys.* **1990**, *87*, 875.

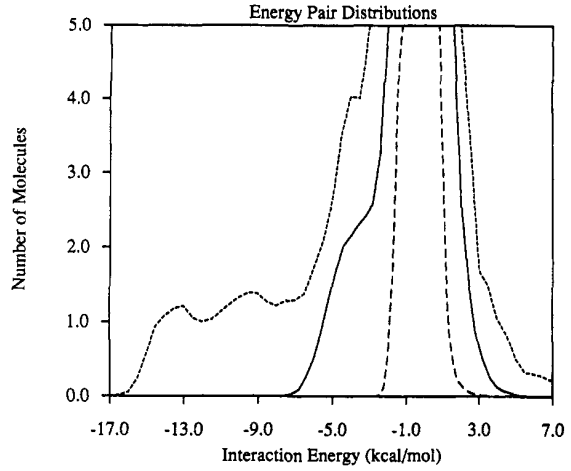


**Figure 10.** Computed solute–solvent energy pair distributions for the reactant (dashed curve), transition state (solid curve), and product (dotted curve). The ordinate gives the number of water molecules bound by the solute, with the energy shown on the abscissa. Units for the ordinate are molecules per kilocalories/mole.

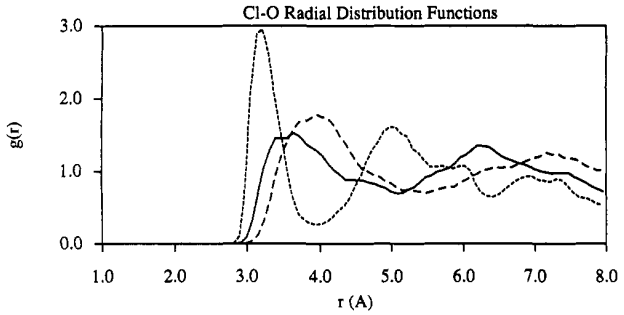


**Figure 11.** Computed Cl–O radial distribution functions. Dashed curves are for the reactant, solid curves are for the transition state, and dotted curves are for the product. This convention is used throughout.

striking pike centered at $E_{int}$ = 0 kcal/mol is due to interactions with distant water molecules. Although ammonia is a good hydrogen bond acceptor, the close proximity of the substrate prevents water from forming a hydrogen bond to the lone pair of electrons on the nitrogen atom. On the other hand, it is well known, both from gas-phase microwave experiments and theoretical investigations, that ammonia is a poor hydrogen bond donor.[34] The pair energy distribution is thus consistent with bimolecular interactions shown in Figure 6. At RC = –2 Å ($R_{CN}$ = 3.5 Å), the best reactant–water interaction energy is –2.6 kcal/mol. For the transition state, a hydrogen-bonding band begins to develop (solid curve in Figure 10). The best interaction energy from Figure 10 for the TS is –7.6 kcal/mol. Finally, two low-energy bands are clearly seen for the product ion pair (dotted curve). The lowest energy band can be assigned to water molecule solvating the ammonium ion, while the second peak is for the chloride ion–water complex. In fact, the low-energy bands can nearly be superimposed with pair energy distributions for $CH_3$-$NH_3^+$ and $Cl^-$ obtained from separate simulations.

Integration of the dotted curve to –12.0 kcal/mol yields about 3.7 water molecules, whereas integration of the second band from –12.0 to –8.0 kcal/mol reveals another 5 water molecules. The total number of the water molecules resulting from the first and second peaks is 8.7, which consists of approximately three $CH_3$-$NH_3^+$–water pairs and six $Cl^-$–water pairs. An important observation is that the number of strong hydrogen-bonding

(34) (a) Nelson, D. D., Jr.; Fraser, G. T.; Klemperer, W. *Science* **1987**, *238*, 1670. (b) Del Bene, J. E. *J. Phys. Chem.* **1988**, *92*, 2874. (c) Frisch, M. J.; Del Bene, J. E.; Binkley, J. S.; Schaefer, H. F., III *J. Chem. Phys.* **1986**, *84*, 2279.

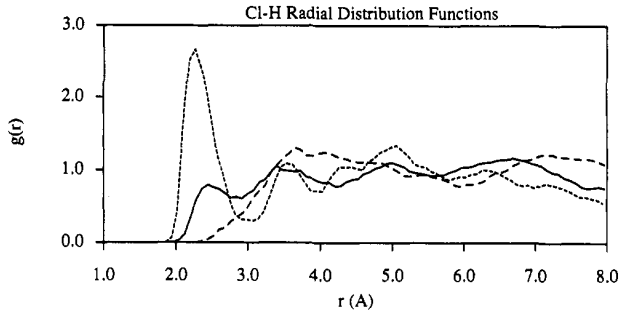


**Figure 12.** Computed Cl–H rdfs.

interactions increases from 0 for the reactants at RC = –2 Å to about 9 for the product ion pair. It is noteworthy to recall findings for the Type I reaction of $Cl^- + CH_3Cl$ in water, where the number of hydrogen bonds is roughly constant along the whole reaction path.[5a] The differential solvation for the reactants and the transition state in that study is due to variations in the strength of the hydrogen bonds.[5a] In contrast, increases both in the total number of hydrogen bonds and the strength of interaction energies are critical to the stabilization of the TS and products for this Type II $S_N2$ reaction in aqueous solution.

**(c) Radial Distribution Functions.** The solute–solvent structure can be further characterized by the radial distribution functions (rdfs) shown in Figures 11–15. In these figures, the first atom for an xy distribution, $g_{xy}(r)$, refers to a solute atom, and the second atom is either the hydrogen or the oxygen of water. The rdf $g_{xy}(r)$ gives the probability of finding an atom y at a distance r from atom x. Here, the dashed, solid, and dotted curves correspond respectively to the reactants (RC = –2 Å), TS (RC = 0 Å), and the products (RC = 2 Å) in aqueous solution.

The Cl–O and Cl–H distributions in Figures 11 and 12 reveal the progress of hydrogen-bonding interactions between chlorine and water during the reaction. The positions of the first peaks in the Cl–O rdfs (Figure 11), are 4.0, 3.6, and 3.2 Å for the reactant, TS, and product, respectively, indicating strengthened interactions with the solvent in the series. The trend is unambiguously demonstrated by the Cl–H rdfs in Figure 12 by the appearance of the hydrogen bond peak at 2.4 Å for the transition state and the striking first peak at 2.3 Å for the product chloride ion. The reactant methyl chloride shows no hydrogen-bonding interactions between Cl and water, consistent with previous findings by Chandrasekhar et al. using empirical potential functions.[5a] Note that for the product ion-pair structure, there is also a well-defined second solvation shell centered at 3.5 Å in the Cl–H rdf, while the third peak near 5 Å can be assigned to water molecules forming hydrogen bonds with the ammonium ion. Integration of the first peaks for the product and TS to their minima at 3 Å reveals 6.6 and 3.1 nearest neighbors forming hydrogen bonds with the chlorine atom. This is in accord with the prediction based on the integration of the pair energy distributions, where the number of hydrogen bonds to the chlorine atom is estimated to be about 6 for the product.

Similar trends exist for hydrogen-bonding interactions between the nucleophile $H_3N$ and water. In the ammonia $H_N$–O rdfs (Figure 13), there is no strong interaction between the ammonia hydrogen and the oxygen of water (dashed line), while a shoulder in the distribution at the hydrogen-bonding range occurs for the transition state (solid curve). Integration of the sharp first peak centered at 1.8 Å for the product gives 1.0 hydrogen bonds. Thus, there are a total of 3 water molecules hydrogen-bound to the ammonium ion. The progression of hydrogen bonding with the ammonia group is also indicated by the N–O rdfs given in Figure 14. Note that the location of the sharp first peak for the product ion pair (2.8 Å) is about 1 Å (N–H bond length) longer than the first peak in the $H_N$–O rdf.

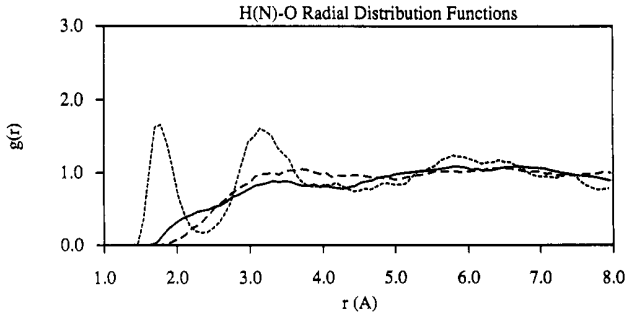


**Figure 13.** Computed ammonium hydrogen–water oxygen rdfs.

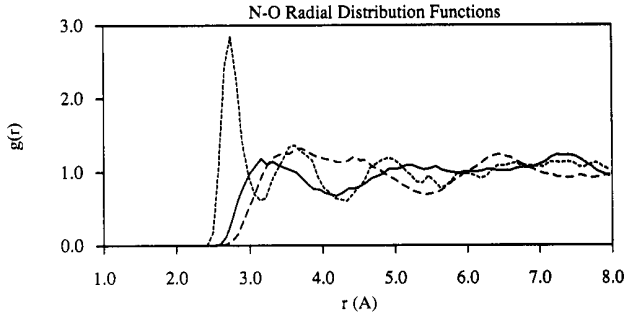


**Figure 14.** Computed N–O rdfs.

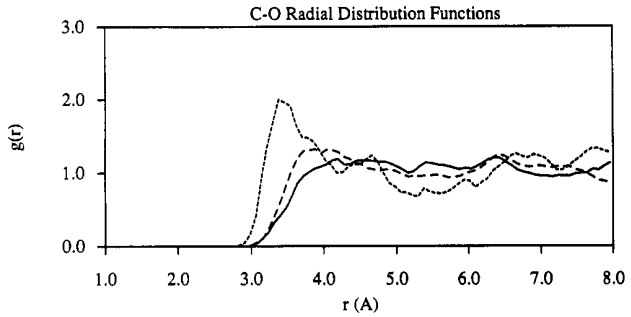


**Figure 15.** Computed C–O rdfs.

The C–O (Figure 15) rdfs may give some indication of the change in solvation at the methyl group that is being attacked by the nucleophile. However, no special features exist in these plots, especially for the reactant and transition state. Note that a strong first peak is shown in the C–O rdf for the product. This is perhaps due to electrostatic interaction between the ammonium ion and water, which have been observed for hydrophobic cations in water.[35] Comparing $g_{NO}$ (Figure 14) with $g_{CO}$ (Figure 15), two differences are apparent: (1) the distances in the carbon–water oxygen rdfs are much longer than those in the nitrogen–water oxygen rdfs and (2) the change in the rdf on going from the reactant to the product is less dramatic for $g_{CO}$ than for $g_{NO}$. Both observations suggest that the interaction between the methyl group and water is weak throughout the reaction.

## Conclusions

A comprehensive study of the Type II $S_N2$ reaction between $H_3N$ and $CH_3Cl$ in aqueous solution has been carried out through statistical mechanical Monte Carlo simulations using the combined quantum mechanical and molecular mechanical AM1/TIP3P potential. The endothermic Menshutkin reaction in the gas phase is strongly enhanced by the influence of aqueous solvation. This stems from the fact that a charge separation is developed in the course of the reaction, giving rise to favorable solvent stabilizations. The reaction becomes exothermic in water. The computed free energy of activation and free energy of reaction are in good agreement with experiment.

A major thrust of the present study is to characterize the solvent effect on the potential surface and the transition-state structure for the Menshutkin reaction. Thus, a two-dimensional free energy surface has been determined. The present study has the advantage of taking into account the effect of solute electronic structural relaxations, while the symmetric stretch along the reaction path is being considered through the grid search. In accord with previous theoretical studies and the empirical expectation according to the Hammond postulate, an early transition state is predicted in aqueous solution for the type II $S_N2$ reaction, with a dramatic increase in the C–N distance by 0.30 Å and a decrease in the C–Cl separation by 0.15 Å at the transition state. When the gas-phase minimum energy path was used to approximate the reaction path in water, the change for C–N and C–Cl was predicted to be +0.15 and –0.10 Å, respectively.[14] Clearly, solvent effects should be included in electronic structure calculations for asymmetric reactions in condensed phases. The combined QM/MM simulation method as demonstrated here and in other works provides a viable approach.

The present calculations also illustrate the power of the combined QM/MM Monte Carlo simulation method in providing both qualitative and quantitative insights into the solvent effects on chemical reactions. In the past decade, computer simulations have greatly enhanced our understanding of chemical processes and intermolecular interactions in solution. These techniques have been extended to enzymatic reactions. In the past, these calculations were performed primarily with the use of effective pairwise potential functions. Although the classical approximation is quite reasonable and can provide valuable information on solute–solvent interactions, the coupling between the solvent charge distribution and the solute electronic polarization, which is of central importance for reactions involving heterolytic bond cleavage,[6d,12] is not specifically considered. Further, it is generally not practical to fit parameters for a potential surface such as the one studied here. Using the combined QM/MM approach, we anticipate that a variety of chemical processes, both in solution and in enzymes, will be investigated with ease.

**Acknowledgment.** Gratitude is expressed to the National Science Foundation Supercomputing Center and the Pittsburgh Superconducting Center for computational support. X.X. thanks Professor T. George for encouragement. We thank Professor W. L. Jorgensen and Dr. J. J. P. Stewart for making their programs available, each of which forms an integral part of the procedure described here. Both referees provided valuable comments.

**Supplementary Material Available:** Computed free energy changes from the QM/MM simulations and geometrical and energetic results for the solute–water complexes determined with the 6-31 + G(d) basis set, the empirical potential function, and the combined AM1/TIP3P method (7 pages). Ordering information is given on any current masthead page.

(35) Jorgensen, W. L.; Gao, J. *J. Phys. Chem.* **1986**, *90*, 2174.

## 4.7 Chemical equilibrium in a solvent

Application of the reversible work principle to isomerization

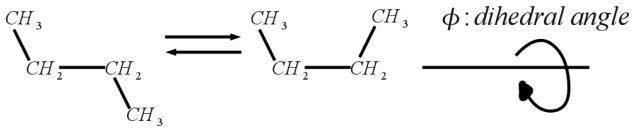


scheme 074

Potential energy function

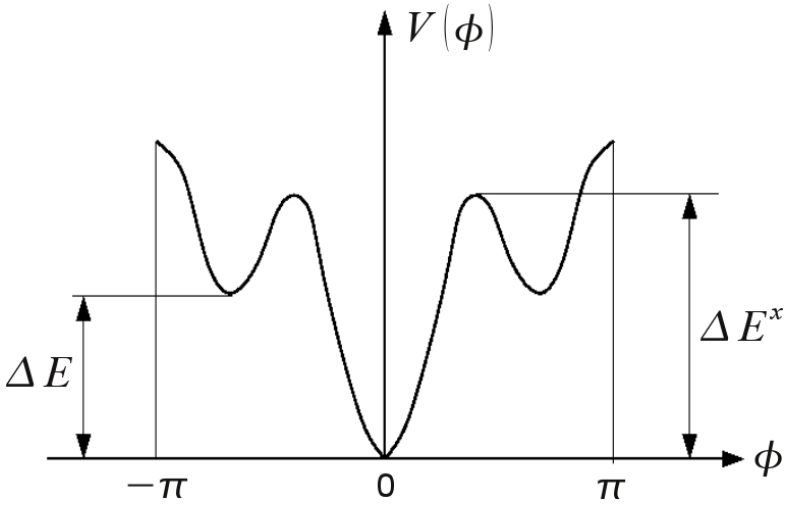


scheme 075

$V(\Phi)$ = reversible work surface for nuclei when molecule is in *vacuum*. It is the Born–Oppenheimer surface obtained by averaging over electronic fluctutaions, i.e. solving the Schrödinger equation.

In a solvent, the reversible work surface for $\Phi$ is $V(\Phi) + \Delta W(\Phi)$, where $\Delta W(\Phi)$ = solvent contribution to free energy, i.e.

$\Delta W(\Phi) + \Delta W(\Phi')$ reversible work or free energy change
at constant $N$, $V$, $T$
for solvent to accomodate a change of solute
conformation from $\Phi'$ to $\Phi$.

Accordingly the distribution function for $\Phi$ is

$$P(\Phi) \propto \mathrm{e}^{-\beta W(\Phi)} = \mathrm{e}^{-\beta V(\Phi)}\mathrm{e}^{-\beta \Delta W(\Phi)}$$
$$\propto P(\Phi)_{\mathrm{gas}}\mathrm{e}^{-\beta \Delta W(\Phi)}$$

with the gas phase distribution $P(\Phi)_{\mathrm{gas}} \propto \mathrm{e}^{-\beta V(\Phi)}$.

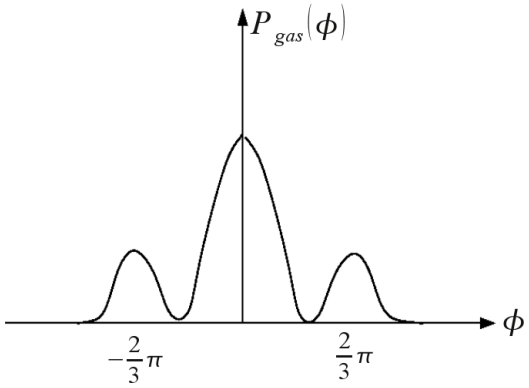


scheme 076

Thus, the equilibrium constant $K_X = \frac{X_{\mathrm{g}}}{X_{\mathrm{t}}}$ is given by

$$\frac{X_{\mathrm{g}}}{X_{\mathrm{t}}} = 2 \underbrace{\int_{\mathrm{g}^+} \mathrm{d}\phi P(\Phi)_{\mathrm{gas}}\mathrm{e}^{-\beta \Delta W(\Phi)}}_{\text{integration over gauch+ region}} / \underbrace{\int_{\mathrm{t}} \mathrm{d}\phi P(\Phi)_{\mathrm{gas}}\mathrm{e}^{-\beta \Delta W(\Phi)}}_{\text{integration over trans region}}$$

assume $P(\Phi)_{\mathrm{gas}}$ is highly localized near the maximums

$$\approx \left(\frac{X_{\mathrm{g}}}{X_{\mathrm{t}}}\right)_{\mathrm{gas}} \underbrace{\mathrm{e}^{-\beta[\Delta W(2/3\pi) - \Delta W(0)]}}_{\text{this factor is the solvent shift of } K_X}$$

Another application – Cundall's experiment (1895) dimerization of $NO_2$.

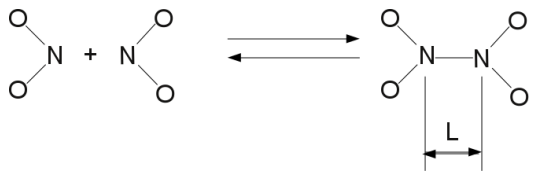


scheme 077

The condition of chemical equilibrium (constancy of chemical potentials) in this case is (since there are 2 $NO_2$ groups)

$$2\mu_{NO_2} = \mu_{N_2O_4}$$

Therefore,

$$\mathrm{e}^{-2\beta\mu_{NO_2}} = \frac{\begin{pmatrix}\text{Boltzmann weighted sum over all}\\ \text{fluctuations with 2 } NO_2 \text{ groups}\end{pmatrix}^{\star}}{\begin{pmatrix}\text{Boltzmann weighted sum over all}\\ \text{fluctuations with } no\ NO_2 \text{ groups}\end{pmatrix}} = \frac{Q(2NO_2 + \text{solvent})}{Q(\text{pure solvent})}$$

$\star$ The overwelming majority of these fluctuations are those with the 2 $NO_2$ groups far apart. This is why $\mu$ for 2 $NO_2$'s is twice $\mu$ for one $NO_2$.

and similarly

$$\mathrm{e}^{-\beta\mu_{N_2O_4}} = \frac{Q(N_2O_4 + \text{solvent})}{Q(\text{pure solvent})}$$

The chemical potential for the two species is

$$\beta\mu_{NO_2} = \beta\Delta\mu_{NO_2} + \ln\rho_{NO_2}$$
$$\beta\mu_{N_2O_4} = \beta\Delta\mu_{N_2O_4} + \ln\rho_{N_2O_4}$$

The $\Delta\mu$'s are independent of the concentrations of tagged molecules ($NO_2$ and $N_2O_4$). Therefore,

$$2\beta\Delta\mu_{NO_2} + \ln\rho^2_{NO_2} = \beta\Delta\mu_{N_2O_4} + \ln\rho_{N_2O_4}$$

or equivalently

$$K \equiv \frac{[\rho_{N_2O_4}]}{[\rho_{NO_2}]} = \exp\{-\beta[\Delta\mu_{N_2O_4} - \Delta\mu_{NO_2}]\}$$

We see that $K$ is a *constant* in the sense that it is independent of the concentrations of the tagged species.

This is the *Law of Mass Action*.

Now, what can we say about solvent effects?

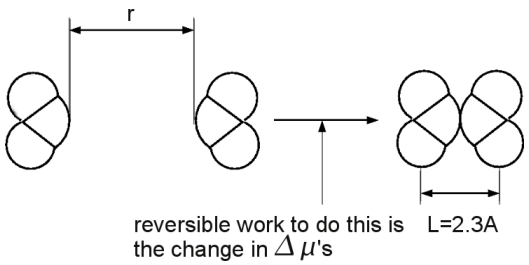


scheme 078

Assume the chemical bond is very localized and that the $NO_2$ groups do not change significantly during association. The reversible work principle then gives

$$K \approx K_{\text{gas}} \exp\{-\beta[\Delta W(L) - \Delta W(\infty)]\}$$

To compute solvent effects, we need to compute $\Delta W$'s.

## 4.8 Models for solvent contributions to reversible work surfaces

### 4.8.1 Packing effects, excluded volume

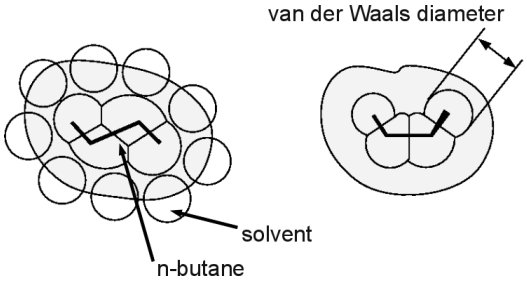


scheme 079

Volume excluded to solvent depends upon conformation of solute, and also the size and shape of the solvent molecules.

Space filling models: cloud shell species cannot overlap without high energy cost (due to Puli's exclusion principle) – high energy compared to $k_B T$. The radius of closest approach is the van der Waals radius or 1/2 the van der Waals diameter.

For a solvent of diameter $\sigma_s = 3$Å, the trans conformer picture above excludes a volume of about 315Å$^3$; and the gauche excludes a volume of roughly 302Å$^3$. The excluded volume of gauche is thus about

$$10\text{Å}^3/\text{molecule} \approx 0.06\text{l/mol}$$

smaller than that of trans when $\sigma_s = 3$Å.

To estimate the free energies associated with changes in excluded volume, consider packing and fluctuations of hard spheres, the simplest model of excluded volume effects – sufficient if excluded volume is most important, and shape effects are not so significant.

Let (HS: hard sphere),

| | |
|---|---|
| $\sigma$ | diamter of solute |
| $\sigma_s$ | diameter of solvent |
| $\rho_s$ | $\langle N\rangle/V$ = density of solvent |
| $\sigma = \sigma_s = 0$ | no interactions |

$$\begin{aligned}\beta\Delta\mu_{\mathrm{HS}}(\sigma,\sigma_s;\rho_s\sigma_s^3) &= \beta[\mu_{\mathrm{HS}}(\sigma,\sigma_s;\rho_s\sigma_s^3) - \mu_{\mathrm{HS}}(\text{no interactions})] \\ &= \textit{excess chemical potential} \text{ (over that of the ideal gas)} \\ &\quad \text{for a hard sphere solute of infinite solution}\end{aligned}$$

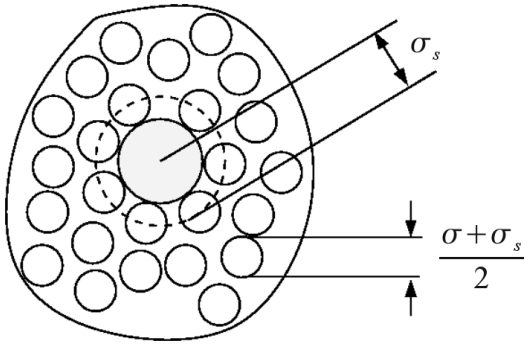


scheme 080

A region of the hard sphere solute-solvent mixture in an allowed configuration. What would be an example for a forbidden configuration?

$$\begin{aligned}\mathrm{e}^{-\beta\Delta\mu_{\mathrm{HS}}} &= \frac{\sum_j \mathrm{e}^{-\beta(E_j+\Delta E_j)}}{\sum_j \mathrm{e}^{-\beta E_j}} \\ &= \frac{\text{number of allowed configurations with solute inserted}}{\text{number of allowed configurations without solute}}\end{aligned}$$

with sums over all configurations of solvent, $E_j$ energy of solvent in configuration $j$ with no solute presence, and $\Delta E_j$ is the energy of solvent in configuration $j$ due to presence of solute.

The last equation is true, because for hard spheres, Boltzmann factors are 1 or 0 only, and independent of temperature.

$1 \rightarrow$ energy is 0 (no overlap)

$0 \rightarrow$ energy is $\infty$ (overlap)

Hey, this is an entropy calculation! There is actually no energy effect in the hard sphere model!

The ratio givin $e^{-\beta\Delta\mu_{\rm HS}}$ has been studied numerically with computers which perform explicitely the Boltzmann weighted sums over fluctuations. Th resulting $\beta\Delta\mu_{\rm HS}$ has been fit empirically to the following formula:

$$\begin{aligned}
\beta\Delta\mu_{\rm HS} &= (1-\eta)^{-3}(s_1\eta + s_2\eta^2 + s_3\eta^3) + s_4\ln(1-\eta) \\
\eta &= (\pi/6)\rho_s\sigma_s^3\ , \quad s_i = s_i(\sigma,\sigma_s) \\
s_1 &= 3\gamma + 6\gamma^2 - \gamma^3 \\
s_2 &= 3(-2\gamma - 3\gamma^2 + 2\gamma^3) \\
s_3 &= 3(\gamma + \gamma^2 - \gamma^3) \\
s_4 &= 3\gamma^2 - 2\gamma^3 - 1 \\
\gamma &= \sigma/\sigma_s
\end{aligned}$$

One way to use this information:

- sphere of diameter $\sigma$ excludes volume $\pi/6[\sigma+\sigma_s]^3$
- estimate $V(\Phi)$ = volume excluded by solute in conformation $\Phi$.
- let $\sigma(\Phi)$ be the diameter satisfying $V(\Phi) = \pi/6[\sigma+\sigma_s]^3$
- use $\beta\mu(\Phi) \approx \beta\Delta\mu_{\rm HS}(\sigma(\Phi), \sigma_s, \rho_s\sigma_s^3)$

Applied to disubstitued ethane

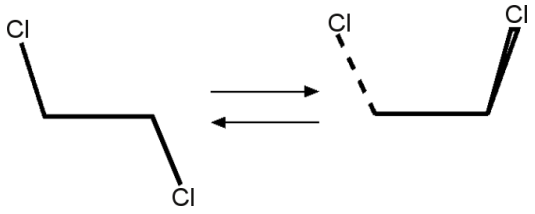

scheme 063

This procedure predicts (precise number depends upon system under investigation)

$$\beta\Delta\mu(\text{trans}) - \beta\Delta\mu(\text{gauche}) \approx 0.5 - -1$$

$$K_X = \frac{X_\text{g}}{X_\text{t}} = K_{X,\text{gas}} \cdot \text{e}^{05to1}$$

These results often agree well with experiment. But there is something else going on too!

### 4.8.2 Electrostatic effects

**Solvation of charge distributions** Here, we think about the energetics of charges coupled to a neutral fluid with charge density fluctuations – a polarizable system, a dielectric.

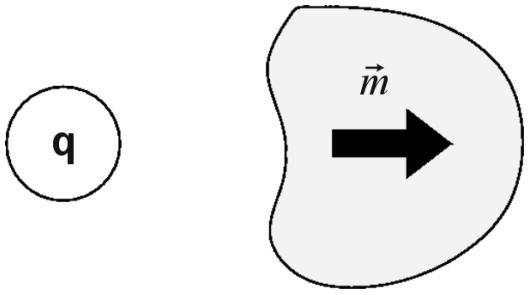


scheme 081

The charge $q$ exerts an electric field, $\vec{\varepsilon}$, on the material that solvates it.

$\vec{m}$ = dipole of the polarizable system.
The coupling of a dipole to an electric field gives an energy $E = -\vec{m} \cdot \vec{\varepsilon}$.

A polarizable system or a dielectric is a material for which an applied electric field induces a change in polarization, i.e., a change in dipole moment.

**Drude model** A simple harmonic model.

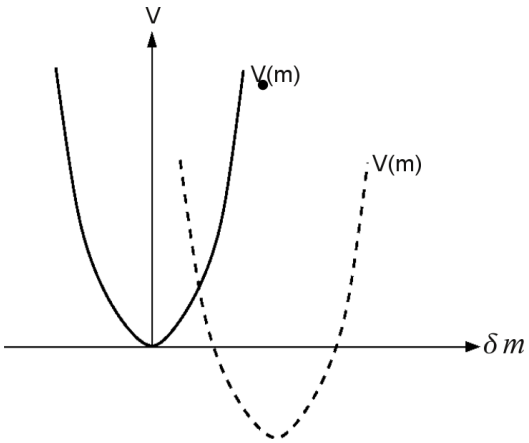


scheme 082

$\delta m$ is the deviation of dipole from its average value in uperturbed system.

$$V_0(m) \approx \frac{1}{2}k(\delta m)^2$$
$$V(m) \approx \frac{1}{2}k(\delta m)^2 - \varepsilon\delta m - \varepsilon\langle m\rangle_0$$

The last term $\varepsilon\langle m\rangle_0$ is constant and we need not think about it further.

We see that the induced dipole in Drude model is

$$\langle\delta m\rangle_\varepsilon \equiv \alpha\varepsilon = \frac{1}{k}\varepsilon$$

This is the definition of polarizability $\alpha$. The result for the Drude model we get from the equilibrium condition for the perturbed system $\mathrm{d}V(m)/\mathrm{d}\delta m = 0$.

**Another way to look at it: Boltzmann averageof $\delta m$** This is thermodynamic perturbation theory.

$$\langle \delta m \rangle_\varepsilon = \frac{\int \mathrm{d}(\delta m) \mathrm{e}^{-\beta V_0(m) + \beta\varepsilon\delta m} \delta m}{\int \mathrm{d}(\delta m) \mathrm{e}^{-\beta V_0(m) + \beta\varepsilon\delta m}}$$

series expansion of $\mathrm{e}^{\beta\varepsilon\delta m}$

$$\langle \delta m \rangle_\varepsilon = \frac{\int \mathrm{d}(\delta m) \mathrm{e}^{-\beta V_0(m)} (1 + \beta\varepsilon\delta m + \cdots)\delta m}{\int \mathrm{d}(\delta m) \mathrm{e}^{-\beta V_0(m)} (1 + \beta\varepsilon\delta m + \cdots)}$$

$$\int \mathrm{d}(\delta m) \mathrm{e}^{-\beta V_0(m)} \delta m \propto \langle \delta m \rangle_0 = \langle m - \langle m \rangle \rangle_0 = 0$$

$$\langle \delta m \rangle_\varepsilon = \varepsilon\beta \langle (\delta m)^2 \rangle_0 + \mathcal{O}(\varepsilon^2)$$

There, independent of the precise form of $V_0(m)$, we have

$$\boxed{\alpha = \beta \langle (\delta m)^2 \rangle_0}$$

This is another fluctuation response formula. It says

$$\langle (\delta m)^2 \rangle_0 = \left( \frac{\partial \langle m \rangle}{\partial \varepsilon} \right) \Bigg|_{\varepsilon = 0}$$

which is analogous to

$$\langle (\delta N)^2 \rangle = \frac{\partial \langle N \rangle}{\partial \beta\mu}$$

Actually, in 3 dimensions, the answer is

$$\alpha = \beta \langle (\delta m_z)^2 \rangle_0 = \beta \frac{1}{3} \langle \|\delta m\|^2 \rangle_0$$

where $\delta m_z$ is $\delta m$ in direction of the field and we assume that without field on, the system is isotropic (factor of 1/3).

For the harmonic Drude model, $\langle (\delta m)^2 \rangle_0 = \frac{1}{\beta k}$, which you can easily check.

The average energy due to coupling between a charge and a polarizable system is $(-\langle \varepsilon_q \delta m \rangle)$, where $\varepsilon_q$ is the electric field which charge $q$ exerts on polarizable system.

$$-\langle \varepsilon_q \delta m \rangle = -\varepsilon_q \langle \delta m \rangle_{\varepsilon_q} = -\beta \varepsilon_q^2 \langle (\delta m)^2 \rangle_0$$

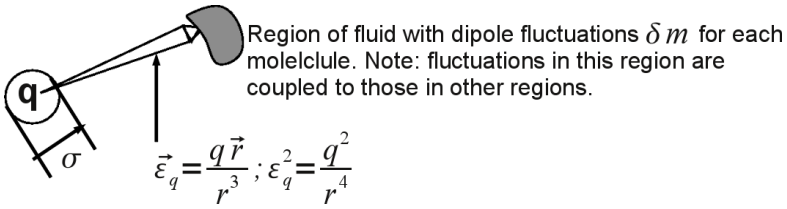


scheme 083

$$\begin{aligned}\Delta\mu &= \text{energy change due to adding the charge } q \text{ to the system} \\ &\approx -\beta\langle(\delta m)^2\rangle_0\rho\int_\sigma^\infty \frac{4\pi q^2 r^2 \mathrm{d}r}{r^4}\end{aligned}$$

This is $-\beta\varepsilon_q^2\langle(\delta m)^2\rangle_0$ with $\varepsilon_q = \frac{q^2}{r^4}$ replaced and integrated over all space outside charge with $\sigma$ the size of charge. The result of integration is

$$\Delta\mu = -4\pi\beta\rho\langle(\delta m)^2\rangle_0\frac{q^2}{\sigma}$$

- The energy to solvate a charge is favorable (see minus sign!).
- Solvation energy becomes more favorable as $q$ goes up and $\sigma$ goes down (= high charge in small volume)
- $4\pi\beta\rho\langle(\delta m)^2\rangle_0$ is a property of the solvent. This property of the solvent is $1 - 1/\epsilon$, where $\epsilon$ is the dielectric constant.

**Dielectric constant** $\epsilon$ The relation between electric displacement field $\vec{D}$, electric field $\vec{\varepsilon}$ and polarization density $\vec{P}$

$$\vec{\varepsilon} = \vec{D} - 4\pi\vec{P} = \epsilon\vec{\varepsilon} - 4\pi\vec{P}$$

or

$$\begin{aligned}\vec{P} &= \textit{polarization density} \text{ or dipole per unit volume} \\ &= [(\epsilon - 1)/4\pi]\vec{\varepsilon}\end{aligned}$$

In a dilute gas (uncorrelated molecules), just add up separately the induced dipoles of each molecule per unit volume.

In that case

$$\epsilon - 1 = 4\pi \frac{\langle N \rangle}{V} \alpha = 4\pi\beta\rho\langle(\delta m)^2\rangle_0$$

These observations suggest

$$\Delta\mu \approx -(\epsilon - 1)\frac{q^2}{\sigma} \ ,$$

which is correct for solvation of a charge by a gas. For a dense fluid, however, we must account for dipolar coupling between different regions; this leads to the *Debye–Langevin equation*:

$$\frac{\epsilon - 1}{4\pi\epsilon} \approx \beta\rho\langle(\delta m)^2\rangle_0$$

Thus

$$\boxed{\Delta\mu \approx -\left(1 - \frac{1}{\epsilon}\right)\frac{q^2}{\sigma}}$$

*Born's charging formula* for the solvation energy of a charge in a dielectric fluid.

The general idea we have illustrated here is the idea of a reaction field.

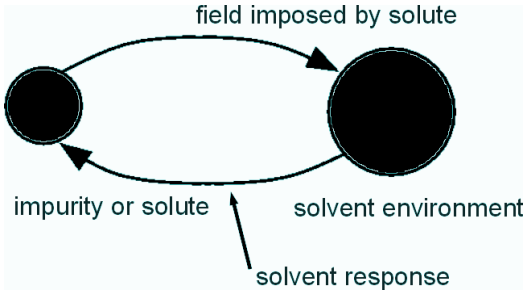


scheme 084

The solvent responds or reacts to the imposed field thus creating a reaction field that interacts back with solute.

Consider now a dipolar solute

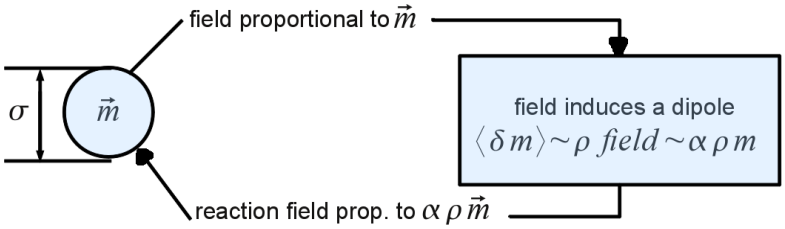


scheme 085

energy of $\vec{m}$ in the reaction field $= -\vec{m} \cdot [\text{reaction field}] \approx -\vec{m} \cdot [\alpha\rho\vec{m}]/\sigma^3$

Distance dependence of dipole field $\propto 1/r^3$.

The detailed reaction field calculation in this case yields

$$\boxed{\Delta\mu = -\frac{8(\epsilon-1)}{2\epsilon+1}\frac{m^2}{\sigma^3}}$$

Debye's formula for the solvation energy of a dipole in a dielectric fluid.

These formulas for solvation of charge distributions treat the solvent as a dielectric continuum (neglecting molecular structure of solvent) which reacts linearly to applied electric field. A nonlinear theory would have to use

$$\langle \delta m \rangle_\varepsilon = \alpha\varepsilon + \frac{1}{2}\chi\varepsilon^2 + \cdots$$

**Another view of the Born solvation formula** Consider two ions far apart

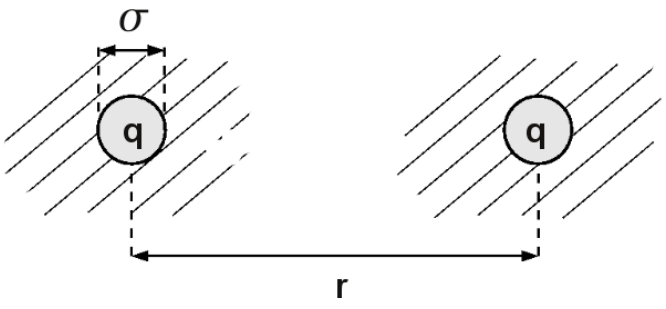

Reversible work surface is (Coulomb's law in a dielectric)

$$w(r) = \frac{q^2}{\epsilon r} + \text{constant}$$

We can write this as a direct interaction term plus the solvation contribution with dielectric screening

$$w(r) = \frac{q^2}{r} - q^2(1 - \frac{1}{\epsilon}\frac{1}{r} + w(\infty) \qquad ((a))$$

Consider just the solvation part, as if direct interaction did not exist

$$\begin{aligned} \Delta\mu(r) &= \text{solvation energy for two ions fixed in solution a distance r apart} \\ &= 2\Delta\mu_q + [w(r) - w(\infty)] \end{aligned} \qquad ((b))$$

where $\Delta\mu_q$ is the solvation energy of an independent ion.

Assuming linear response of solvent

$$\Delta\mu_q = -q^2 f \ , \qquad f = \text{factor independent of } q \qquad ((c))$$

Further

$$\Delta\mu_q \approx \Delta\mu(\sigma) \qquad ((d))$$

Combine (a), (b), (c), and (d) to get

$$\boxed{f \approx (1 - 1/\epsilon)\frac{1}{\sigma}}$$

**Test of Born theory** What can be measured? Enthalpy changes, $\Delta H$, can be determined – relative to a standard or reference state – through caolorimetry.

Hess' Law; enthalpy is a state function.

$$H_2 + Cl_2 \longrightarrow 2HCl \qquad \Delta H_0 = \underbrace{H(2HCl)}_{\text{enthalpy per mole}} \quad \underbrace{-H(H_2) - H(Cl_2)}_{= 0\text{standard states of the elements}}$$

$$HCl \xrightarrow{H_2O} H^+ + Cl^- \ (aq.); \qquad \Delta H_1 = H(H^+; aq) + H(Cl^-; aq) - H(HCl)$$

$$\frac{\Delta H_0}{2} + \Delta H_1 = \text{enthalpy per mole of } Cl^- \text{ relative to enthalpy of } H^+$$

Partial molar enthalpies are related to $\mu$'s

$$G = H - TS \quad \Rightarrow \quad \mu_i = h_i - Ts_i$$

$h_i, s_i$ : partial molar enthalpy, entropy for species i

$$\left(\frac{\partial \mu_i}{\partial T}\right)_{p,N's} = -s_i$$

Thus,

$$\frac{\partial(\mu_i/T)}{\partial T} = -\frac{1}{T^2}\mu_i + \frac{1}{T}s_i = -\frac{h_i}{T^2}$$

$$h_i = T^2 \frac{\partial(\mu_i/T)}{\partial T}$$

According to Born

$$\frac{\partial(\mu_{\text{Born}}/T)}{\partial T} = \frac{\partial}{\partial T}\left[-\frac{1}{T}\frac{e^2}{\sigma}(1 - 1/\epsilon)\right]$$

$$\Delta H(Cl^-) = -\frac{e^2}{\sigma_{Cl^-}}\left[1 - \frac{1}{\epsilon} - \frac{T}{\epsilon^2}\frac{\partial \epsilon}{\partial T}\right]$$

Estimate ionic radii from colvalent radii of cations and bond length of the salts

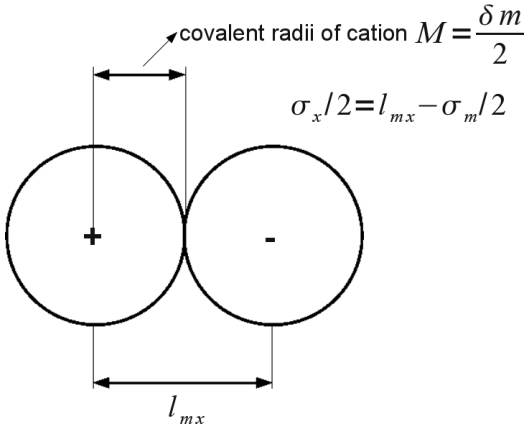


scheme 087

Enthalpies of hydration for ions relative to that of $H^+$, choosing $\Delta H(H^+; aq) = -260$ kcal/mol. (Alexander A. Rashin and Barry Honig, J. Phys. Chem **89**, 5588 (1985))

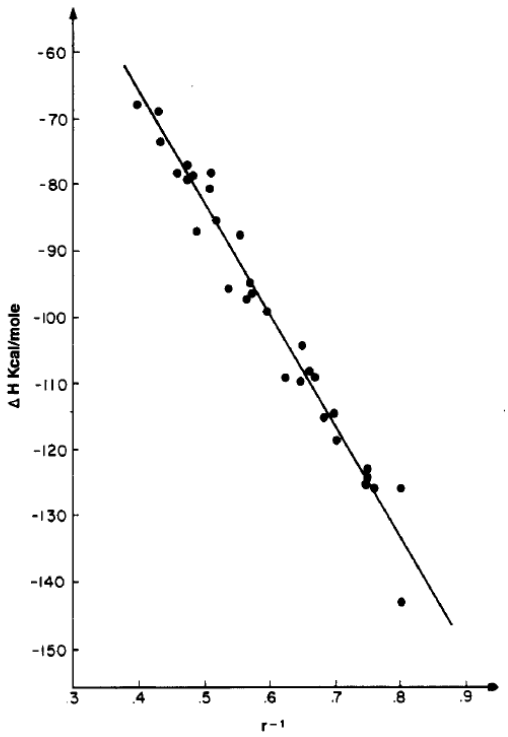

Look at the size of those enthalpies. Do you remember that the $NaCl$ bond strength was about 80 kcal/mol. No wonder $NaCl$ disolves in water.

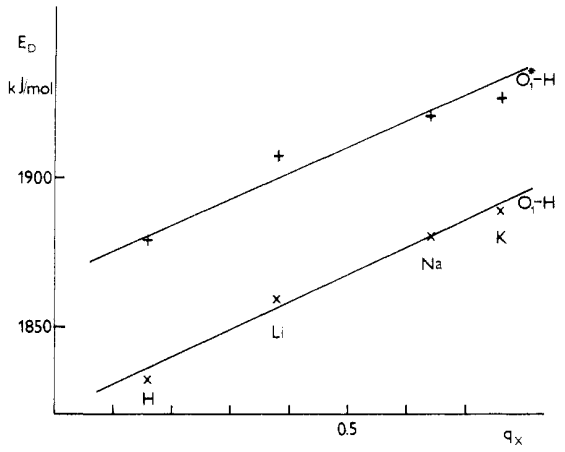


**Figure 2.** Correlation between the dissociation energies of the $O_1$–H and $O_1$*–H groups and the charges located on the ion bonded to the $O_3$ oxygen calculated for clusters $O_3Al_3oO_6(OH)_{10}H_2X$ (where X stands for H, Li, Na, and K atoms).

acidity of the skeletal $O_1$–H groups decreases in the order H > Li > Na > K.

These results thus indicate that the acidity of the skeletal hydroxyl groups is determined by the actual charge localized on the zeolite skeleton, in addition to a number of other factors (Si:Al ratio, structural characteristics, etc.); thus, this acidity depends on the amount of electron density transferred from the skeleton to the ions compensating its negative charge. It follows from the calculation that this transfer is smaller for the cations than for H ions forming the hydroxyl groups (in fact, ab initio calculations predict very small transfer of electron density to the cation[6]). Together with the fact that the acidity of the skeletal hydroxyl groups decreases with increasingly negative charge on the zeolite skeleton, this fact leads to the following general conclusions: (i) the acidity of the skeletal hydroxyl groups of the purely H form of the zeolite is always higher that that of these OH groups in the indentical (structurally and with the same Si:Al ratio) zeolites containing both the OH groups and cations compensating the negative skeletal charge; (ii) for various types of cations localized to the same degree (the same degree of decationization) in the same zeolite, the acidity of the skeletal OH groups decreases with decreasing electronegativity of the cation.

The same conclusions may be drawn by using Sanderson's model of electronegativity.[27-31] If the acidity of OH groups is characterized by the charge located on their H atoms (acidity increases with increasing charge), then for zeolites with the overall formula $H_nX_{1-n}Si_{96}Al_{96}O_{384}$ (where X is a monovalent cation and $0 < n < 96$) the average partial charge on the H atoms is given[27] as

$$q_H = \frac{(S_O^4 S_{Al} S_{Si} S_H^x S_X^{1-x})^{1/7} - S_H}{2.08 S_H^{1/2}}$$

where $S$ is the atomic electronegativity of individual atoms and $x = n/96$ is the degree of decationization. As for the cations studied the electronegativities decrease[27] in the following order: $S_H$ (3.55) > $S_{Li}$ (0.74) > $S_{Na}$ (0.70) > $S_K$ (0.56), it is apparent that this approach results in the same conclusions as mentioned above.

Finally, it should be noted that the terminal OH groups of the clusters with individual cations exhibit similar behavior as the skeletal OH groups. For the ions studied, the acidity of these terminal OH groups increases in the order K < Na < Li < H, as indicated by the charges calculated on their H atoms (which increase), as well as by the values of the O–H bond orders (which decrease).

(27) Sanderson, R. T. "Chemical Bonds and Bond Energy", 2nd ed.; Academic Press: New York, 1976.
(28) Jacobs, P. A.; Mortier, W. J.; Uytterhoeven, J. B. *J. Inorg. Nucl. Chem.* **1978**, *40*, 1919.
(29) Jacobs, P. A.; Mortier, W. J. *Zeolites* **1984**, *2*, 227.
(30) Mortier, W. J. *J. Catal.* **1978**, *55*, 138.
(31) Hočevar, S.; Držaj, B. *J. Mol. Catal.* **1982**, *73*, 205.

# Reevaluation of the Born Model of Ion Hydration

**Alexander A. Rashin† and Barry Honig***

*Department of Biochemistry and Molecular Biophysics, Columbia University, New York, New York 10032*
*(Received: June 5, 1985; In Final Form: August 23, 1985)*

In this paper we demonstrate that the Born theory provides an accurate means of calculating the solvation energies of ions in water. The well-known equation $\Delta G_s^\circ = -(q^2/2r)(1 - 1/D)$ is rederived in a somewhat modified form ($r$ is a radius and $D$ is the dielectric constant), and it is found that the value of $r$ most consistent with the model is the radius of the cavity formed by the ion in a particular solvent. The failures of the Born theory are attributed to the use of ionic radii rather than cavity radii. The ionic radii of anions are shown to be a reasonable measure of the cavity size, but for cations we argue, based on electron density profiles in ionic crystals, that covalent radii rather than ionic radii must be used. When these measures of cavity size are introduced into the Born equation, experimental solvation energies are fairly well reproduced. Moreover, the addition of a single correction factor into the model, an increase of 7% in all radii, leads to excellent agreement with experiment for over 30 ions ranging in charge from 1- to 4+. This need for corrected radii may be due in part to an increase in cavity size resulting from packing defects and to our neglect of dielectric saturation effects. However, it appears that dielectric saturation is not a dominant factor since the model works quite well for polyvalent ions where saturation effects should be strongest. Applications of the Born method to the transfer of ions between different solvents are discussed, and the relation of our results to detailed simulations of ion–solvent interactions is considered.

## Introduction

The Born theory,[1] proposed over 60 years ago, has provided a useful and intuitively simple method of estimating the solvation energy of ions. Interactions between the ion and solvent are assumed to be electrostatic in origin with the ion viewed as a charged sphere of radius $r$ and the solvent as a dielectric continuum of dielectric constant $D$. The electrostatic work associated with charging the ion immersed in the dielectric continuum is then given by

† Present address: Department of Physiology and Biophysics, Mount Sinai School of Medicine, One Gustave L. Levy Place, New York, NY 10029.

(1) Born, M. *Z. Phys.* **1920**, *1*, 45.

0022-3654/85/2089-5588$01.50/0 

$$W = q^2/2Dr \quad (1)$$

where $q$ is the net charge of the ion. The free energy of transferring the ion from vacuum to a medium of dielectric constant $D$ is just the difference in the charging energies, i.e.

$$\Delta G_s^\circ = -\frac{q^2}{2r}\left(1 - \frac{1}{D}\right) \quad (2)$$

It has been traditional to use ionic radii derived from crystal structures to evaluate eq 2 (i.e., to set $r = r_{ionic}$), and under this assumption qualitatively reasonable results can be obtained.[2] For example, as predicted by eq 2, the solvation energies of halide anions and alkali cations are inversely related to the ionic radius. However, Latimer et al.[3] found that it is necessary to add 0.1 Å to the ionic radii of anions and 0.85 Å to the ionic radii of cations to make the Born equation fit experimental data on a series of alkali halide salts. They provided a qualitative justification for these corrections in terms of the distance from the center of the ion to the center of the nearest water dipole. While this "adjusting" of parameters may be viewed as evidence for the failure of the theory, it is rather remarkable that such a crude electrostatic model works at all and yields rather good agreement with experiment. Furthermore, the correction required for halide ions is small enough to suggest that the theory has the potential to yield reasonably accurate results.

With this possibility in mind, we have in this paper reevaluated the assumptions implicit in the Born model. We find (in agreement with standard practice) that the use of ionic radii for anions is consistent with the model but that it is inappropriate to use the ionic radii of cations in eq 2. Rather, we demonstrate that covalent radii provide a logically consistent choice of $r$ for cations. Since the covalent radii of cations are on the order of 0.6–0.8 Å larger than the corresponding ionic radii, our results provide a straightforward quantitative explanation for the correction applied to cations by Latimer et al.[3] Moreover, we demonstrate that the Born theory in its simplest form provides an accurate means of estimating solvation energies in water.

Detailed descriptions of various attempts to improve the Born model appear in a number of excellent reviews (see e.g. ref 2 and 4–7). In the following we briefly discuss the physical basis of the various corrections that have been introduced. As pointed out by Born,[1] the free energy, $\Delta G_s^\circ$, of bringing a charged sphere from vacuum to a dielectric continuum is equal to the sum of the free energies of the following three processes: (1) stripping the sphere of its charge in vacuum, $\Delta G_1^\circ$; (2) transferring the uncharged sphere from vacuum into the solvent, $\Delta G_2^\circ$; and (3) recharging the sphere in the solvent, $\Delta G_3^\circ$. In the original Born theory, $\Delta G_2^\circ$ was assumed to be zero, and thus, only the charging and discharging terms contribute to the solvation energy. These lead directly to eq 2.

Equation 2 has only one parameter, the radius $r$, which is generally set equal to the ionic radius. As pointed out above, the use of ionic radii leads to an overestimate of experimental solvation energy of anions, and in particular, the calculated solvation energy of cations can be almost 100 kcal/mol greater than the experimental values.[2] If the Born model is to be retained, there are, in principle, three ways to reduce the calculated solvation energies: (1) Increase the effective radius used in eq 2. (2) Decrease the effective dielectric constant of water. (3) Add a correction term to account for $\Delta G_2^\circ$, the energy of transferring the neutral sphere from vacuum to water.

Latimer et al.[3] were able to fit experimental solvation energies to the Born equation by increasing the effective radius of the ions. Stokes[8] suggested the use of van der Waals radii for calculating the charging energy in vacuum while retaining ionic radii for the ions in water. Since it is the vacuum term that makes the largest contribution to the solvation energy (due to the $1/D$ term in eq 2), the use of van der Waals radii which are larger than ionic radii, particularly for cations, produced improved agreement with experiment. While Stokes was the first to question the use of ionic radii in the Born expression, we will demonstrate below that the same radius should be used in vacuum and in water and that van der Waals radii are not the optimal choice.

Most attempts to improve the Born model have been based on a reduction of the effective dielectric constant of the solvent.[9-13] The justification for this procedure, suggested by Noyes,[9] is that dielectric saturation occurs in the vicinity of the solvated ion, and thus, the effective dielectric constant in this region is less than 80. However, we will demonstrate that the Born model produces satisfactory agreement with experiment even if the effects of dielectric saturation are ignored. In fact, our results suggest that the effects of dielectric saturation are relatively small, even for multivalent ions.

The third approach that has been used to refine the Born model is to explicitly account for $\Delta G_2^\circ$, the energy of transferring the discharged ion from vacuum to water.[5,8-10,13] While this term is likely to make some contribution, the magnitude of the effect is small,[5,9] and it cannot by itself account for the large discrepancies between predicted and experimental solvation energies.

It should be pointed out that there has been considerable progress in the explicit simulation of ion–water interactions.[14-17] However, there still remain significant discrepancies between theoretical and experimental solvation energies, due in part to the various approximations (e.g., cutoffs, periodic boundary conditions, potential functions) that are used in the simulations. Thus, continuum models retain their value both as a simple means of calculating solvation energies and as a source of insight into the results of detailed simulations.

## A Revised Born Model

*Rederivation of the Born Equation.* In this section we reconsider the Born cycle by breaking up the discharging and charging processes into a number of discrete steps. This will allow us to arrive at an unambiguous definition of the radius to be used in eq 2. We will carry through the derivation for the case of a cation; the derivation for anions is completely analogous. It should first be pointed out that since discharging a cation involves adding an electron to the ion, the total electrostatic energy actually involves a nuclear–electronic attraction term in addition to the positive self-energy of the electronic shell itself. However, the spherical symmetry of the ion makes it possible to describe the situation in terms of discharging a shell of positive charge so that the nuclear attraction term need not be treated explicitly.

The classical expression for the electrostatic work involved in discharging a cation in vacuum[1] is just

$$\Delta G_1^\circ = -q^2/2R_{ao} \quad (3)$$

where $R_{ao}$ is the orbital radius of the neutral atom. (Note that

(2) Bockris, J. O'M.; Reddy, A. K. N. "Modern Electrochemistry"; Plenum Press: New York, 1977; Vol. 1.
(3) Latimer, W. M.; Pitzer, K. S.; Slansky, C. M. *J. Chem. Phys.* **1939**, *7*, 108.
(4) Conway, B. E.; Bockris, J. O'M. In "Modern Aspects of Electrochemistry"; Tompkins, F. C., Ed.; Academic Press: New York, 1954; Vol. 1, p 47.
(5) Rosseinsky, D. R. *Chem. Rev.* **1965**, *65*, 467.
(6) Conway, B. E. "Ionic Hydration in Chemistry and Biophysics"; Elsevier: Amsterdam, 1981.
(7) Desnoyers, J. E.; Jolicoeur, C. In "Comprehensive Treatise of Electrochemistry"; Conway, E. B., Bockris, J. O'M., Yeager, E., Eds.; Plenum Press: New York; 1983; Vol. 5.
(8) Stokes, R. H. *J. Am. Chem. Soc.* **1964**, *86*, 979.
(9) Noyes, R. M. *J. Am. Chem. Soc.* **1962**, *84*, 513.
(10) Millen, W. A.; Watts, D. W. *J. Am. Chem. Soc.* **1967**, *89*, 6051.
(11) Padova, J. *J. Chem. Phys.* **1972**, *56*, 1606.
(12) Beveridge, D. L.; Schnuelle, G. W. *J. Phys. Chem.* **1975**, *79*, 2562.
(13) Abraham, M. H.; Liszy, J. *J. Chem. Soc., Faraday Trans. 1*, **1978**, *74*, 1604.
(14) Mezei, M.; Beveridge, D. L. *J. Chem. Phys.* **1981**, *74*, 6902.
(15) Szasz, I.; Heinzinger, K. *Z. Naturforsch. A: Phys., Phys. Chem., Kosmophys.* **1982**, *38A*, 214.
(16) Chandrasekhar, J.; Spellmeyer, D. C.; Jorgensen, W. L. *J. Am. Chem. Soc.* **1984**, *106*, 910.
(17) Clementi, E.; Barsotti, R. *Chem. Phys. Lett.* **1980**, *59*, 21.

it is the orbital radius rather than the ionic radius that enters into the expression because the electron is added to this orbit during this discharging process.)

Transferring the neutral atom into the solvent produces a cavity of radius $R_{ac}$ (ac denotes atomic cavity). $R_{ac}$ will in general be larger than $R_{ao}$. The energy of recharging the cation in the solvent, $\Delta G_3°$, may be divided into three separate contributions: (a) $\Delta G_{3a}°$, the energy of dispersing the electron from $R_{ao}$ to $R_{ac}$ in vacuum; (b) $\Delta G_{3b}°$, the energy of dispersing the electron from $R_{ac}$ to infinity in water; (c) $\Delta G_{3c}°$, the work associated with the shrinking of the cavity around the ion to the ionic cavity radius, $R_{ic}$ ($R_{ic} < R_{ac}$). Thus

$$\Delta G_{3a}° + \Delta G_{3b}° = q^2/2R_{ao} - q^2/2R_{ac} + q^2/2DR_{ac} \quad (4)$$

$\Delta G_{3c}°$ is just the difference in the electrostatic energy of a spherical shell of charge between $R_{ac}$ and $R_{ic}$ when filled with vacuum or with the dielectric medium. This can easily be shown to be

$$\Delta G_{3c}° = q^2/2R_{ac} - q^2/2R_{ic} + q^2/2DR_{ic} - q^2/2DR_{ac} \quad (5)$$

Thus

$$\Delta G_3° = q^2/2R_{ao} - q^2/2R_{ic} + q^2/2DR_{ic} \quad (6)$$

and

$$\Delta G_1° + \Delta G_3° = (q^2/2R_{ic})(1/D - 1) \quad (7)$$

Equation 7 is just the Born expression with the ionic cavity radius appearing explicitly in the denominator. It should be pointed out that due to a cancellation of terms *only the cavity radius in the solvent appears in the final expression* (*eq 8*). Note that this radius would in general be expected to change in different solvents.

*The Ionic Cavity Radius.* Equation 7 states that the appropriate radius to be used in the Born expression is the radius of the cavity formed by an ion in a particular solvent. This is also quite reasonable on intuitive grounds since it is at this distance from the ion that the dielectric constant becomes different than that of vacuum and the medium actually begins. We are left then with the problem of arriving at appropriate values of the cavity radius for both cations and anions.

It seems plausible to define the ionic cavity as a sphere which contains a negligible electron density contribution from the surrounding solvent. Analysis of electron density distributions in ionic crystals[18] (see e.g. Figure 1) reveals that the electron density due to positive ions begins to become significant at a distance of about the ionic radius from the center of the anion. It thus provides a reasonable measure of the cavity radius formed by an anion. The situation is quite different for cations. The ionic radius of the cation does not extend out to the high electron density region of the bound anion. In fact, due to quantum effects,[19,20] the electron cloud of the anion is unable to significantly penetrate the empty valence orbital of the cation. As a result, the electron density of the anion begins to become significant at a distance from the nucleus of the cation corresponding approximately to the orbital radius of its valence electron. This radius provides a far more accurate measure of the cavity size formed by a cation than does the ionic radius. Since orbital radii correspond closely to covalent radii, which are experimentally determined quantities, we propose the use of covalent radii as a reasonable and convenient estimate of the radius to be used in the Born equation as applied to solvated cations. As discussed above, the ionic radius constitutes a good estimate for the cavity radius formed by solvated anions.

Analysis of electron density maps demonstrates that the covalent radii of cations and the ionic radii of anions are closely related and provide a useful first approximation of the cavity radius

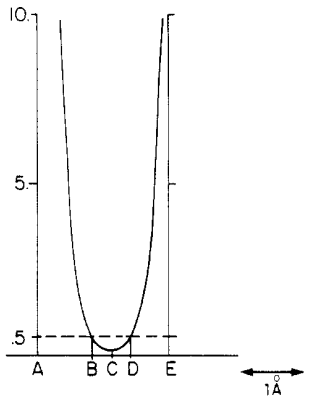


**Figure 1.** Electron density distribution in LiF crystal along the line connecting the centers of the fluoride ion (point A) and lithium ion (point E).[18] Segments AD and DE correspond to ionic radii of F and Li. CD = 0.32 Å,[18] BD = 2CD, AE = 1.96 Å, and DE = 0.6 Å.[21]

**TABLE I: Internuclear Distances in Alkali Fluorides, the Radii of Cavities Formed by Alkali Ions, and Their Covalent Radii**

| | $Li^+$ | $Na^+$ | $K^+$ | $Rb^+$ | $Cs^+$ |
|---|---|---|---|---|---|
| internuclear distance[21] | 1.96 | 2.31 | 2.69 | 2.84 | 3.05 |
| cavity radii[a] | 1.24 | 1.59 | 1.97 | 2.12 | 2.33 |
| covalent radii[21] | 1.23 | 1.57 | 2.03 | 2.16 | 2.35 |

[a] Calculated by setting the hard-core radius of $F^-$ equal to 0.72 Å (see text).

formed by the respective ions in salt crystals. Figure 1 plots the electron density distribution in LiF[18] which is clearly quite symmetric about the minimum, defined by point C. The ionic radius of $F^-$ corresponds to the segment AD. The electron density due to $Li^+$ begins to rise steeply at point D, which as discussed above is the justification for using ionic radii to define the cavities formed by anions. In order to obtain an internally consistent definition of the cavity formed by cations, we use the electron density at point D, which corresponds to the ionic radius of $F^-$, to define the electron density at the boundary of any ionic cavity. Point B has the same electron density as point D, and thus, the segment EB defines the cavity formed by the $Li^+$ ion. This is found to be 1.24 Å which is close to the covalent radius of Li of 1.23 Å. The segment AB, equal to 0.72 Å, may be viewed as defining a "hard core" of the $F^-$ ion beyond which the cavity formed by the cation begins. If we use this value in all alkali fluoride salts, it is possible to obtain a consistent measure of the cationic cavity radii by subtracting 0.72 Å from the internuclear distance.

In Table I, the cavity radii obtained in this way are compared to covalent radii. The remarkable correspondence between the two values strongly supports our suggestion that covalent radii be used to define the cavity radius of cations. Moreover, it demonstrates that the ionic radii of anions and the covalent radii of cations measure the same property, i.e., the distance from the nucleus at which the electron density of the surrounding medium begins to become significant. This then provides the underlying justification for the use of these values in the Born equation.

It should be pointed out that previous attempts have been made to use electron density maps as a basis for defining ionic radii. In particular, Gourary and Adrian[18] equated ionic radii to the distance between the point of minimum electron density (point C in Figure 1) and the center of either ion. The radii so defined removed the asymmetry in the solvation energies of positive and negative ions but did not produce accurate agreement with experimental values.[22] In contrast to the radii of Gourary and Adrian,[18] *the sum of the radii used in this work is not equal to the internuclear distance.* This is reasonable since we are interested in obtaining cavity radii and both the anion and cation

(18) Gourary, B. S.; Adrian, F. J. *Solid State Phys.* **1960**, *10*, 127.
(19) Slater, J. C. *J. Chem. Phys.* **1964**, *41*, 3199.
(20) Vainshtein, B. K.; Fridkin, V. M.; Indenbom, V. L. "Modern Crystallography"; Vainshtein, B. K., Ed.; Nauka: Moscow, 1979; Vol. 2.
(21) "Lang's Handbook of Chemistry", 11th ed.; Dean, J. A., Ed.; McGraw-Hill: New York, 1973.
(22) Blandamer, M. J.; Symons, M. C. R. *J. Phys. Chem.* **1963**, *67*, 1304.
(23) Gold, E. S. "Inorganic Reactions and Structure"; Holt, Reinhart and Winston: New York, 1960.

**TABLE II: Experimental and Theoretical Values of the Heats of Solvation of Salts (in kcal/mol)[a]**

| salt | $\Delta H_{exptl}$ | $\Delta H_{calcd}$ | % error | $\Delta H_{calcd}(cor)$ | % error |
|---|---|---|---|---|---|
| LiF | −245.2 | −261.0 | 6.4 | −243.9 | 0.5 |
| Cl | −211.2 | −227.7 | 7.8 | −212.8 | −0.8 |
| Br | −204.7 | −221.1 | 8.0 | −206.6 | −0.9 |
| I | −194.9 | −211.7 | 8.6 | −197.9 | −1.5 |
| NaF | −217.8 | −231.6 | 6.3 | −216.4 | 0.6 |
| Cl | −183.8 | −198.3 | 7.9 | −185.4 | −0.9 |
| Br | −177.3 | −191.7 | 8.1 | −179.2 | −1.1 |
| I | −197.5 | −182.3 | 8.8 | −170.4 | −1.7 |
| KF | −197.8 | −207.5 | 4.9 | −194.0 | 1.9 |
| Cl | −163.8 | −174.2 | 6.4 | −162.9 | 0.5 |
| Br | −157.3 | −167.6 | 6.5 | −156.7 | 0.4 |
| I | −147.5 | −158.2 | 7.2 | −147.9 | −0.3 |
| RbF | −192.7 | −202.6 | 5.1 | −189.3 | 1.8 |
| Cl | −158.7 | −169.3 | 6.7 | −158.3 | 0.2 |
| Br | −152.2 | −162.7 | 6.9 | −152.4 | −0.1 |
| I | −142.4 | −153.3 | 7.6 | −143.3 | −0.6 |
| CsF | −186.9 | −196.4 | 5.1 | −183.5 | 1.8 |
| Cl | −152.9 | −163.1 | 6.7 | −152.4 | 0.3 |
| Br | −146.4 | −156.5 | 6.9 | −146.2 | 0.1 |
| I | −136.6 | −147.1 | 7.7 | −137.5 | −0.7 |

[a] The experimental values are from ref 2. The enthalpies of the salts are sums of the solvation enthalpies of the individual ions calculated according to eq 8 with radii taken from ref 21 and 23 (for halogens).

share a common low electron density region (segment B–D) as part of their cavities. Thus, cavity radii will always sum to values larger than the internuclear distance.

## Results and Discussion

*Solvation Enthalpies of Ions in Water.* Since the free energies of solvation of individual ions cannot be measured directly, eq 2 cannot be tested for individual ions. However, the enthalpies of solvation of various salts are known and can be compared to theoretical values obtained from the Born expression for the enthalpy[2]

$$\Delta H_s = \frac{-q^2}{2r}\left[1 - \frac{1}{D} - \frac{T}{D^2}\frac{\partial D}{\partial T}\right] \qquad (8)$$

where $T(\partial D/\partial T)/D = -1.357$ for water at 298 K.[9] Table II compares calculated and experimental values of the enthalpies of solvation of alkali halide salts. As can be seen by comparing columns two and three, the agreement between theory and experiment, even with uncorrected radii, is quite good. This level of accuracy has not been obtained previously from the uncorrected Born expression. It appears then that the Born expression works quite well, even if dielectric saturation is ignored.

As can be seen from Table II, the calculated results are consistently larger than the experimental ones by about 10–15 kcal/mol. This error might be attributed to the inherent limitations of the theory, but the fact that it is so systematic suggests that it is due to an identifiable factor. One possibility, the neglect of dielectric saturation, will be discussed below. However, perhaps the most straightforward explanation is that anionic radii and covalent radii for cations underestimate the cavity size. Indeed, as is evident from Figure 1, the electron density of the atoms surrounding the central ion continues to increase at distances from the nucleus that are greater than these radii. Moreover, the problem of packing bound solvent molecules would be expected to expand the cavity somewhat. Thus, it seems quite reasonable to expect that the cavity radii that best fit the Born model be somewhat larger than those defined above. In order to obtain an optimal fit to the experimental results of Table II, we have defined corrected Born radii by increasing each ionic and covalent radius by 7%. The corrected enthalpies of solvation obtained from these radii deviate from the experimental values by a maximum of only 4 kcal/mol.

In order to test the reliability of our modified Born model, it is necessary to compare calculated and experimental solvation energies for ions not included in our original sample (Table II). Since experimental values for isolated ions cannot be determined directly, we base our comparison on the relative heats of solvation, $\Delta H_{rel}$ (relative to $H^+$ ions).

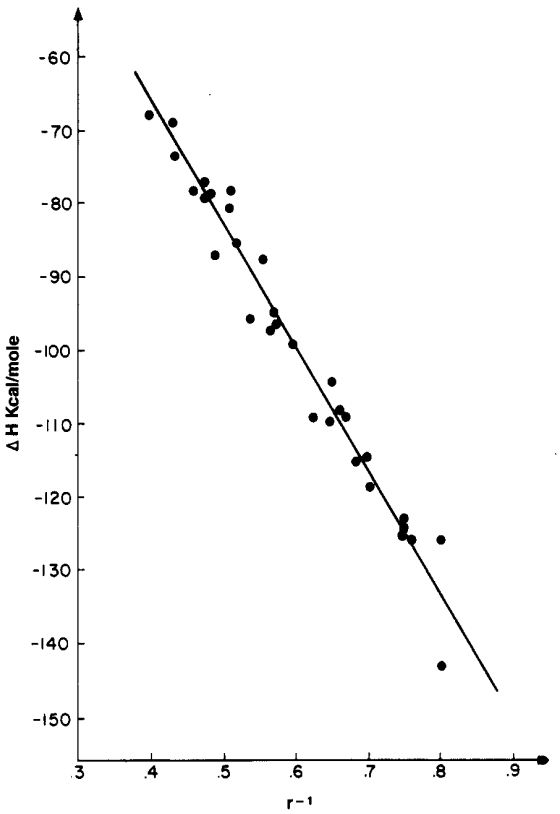


**Figure 2.** Comparison of experimental (dots) and predicted (solid line) enthalpies of ion hydration. The enthalpies are given per unit charge.

These are defined by[2]

$$\Delta H_{rel}(X^-) = \Delta H_{abs}(X^-) + \Delta H_{abs}(H^+) \qquad (9)$$

$$\Delta H_{rel}(M^+) = \Delta H_{abs}(M^+) - \Delta H_{abs}(H^+) \qquad (10)$$

where $X^-$ and $M^+$ denote respectively anions and cations and $\Delta H_{abs}$ denotes absolute heats of hydration.

The fourth column in Table III contains experimentally determined relative heats of hydration for 31 ions. By calculating the absolute heat of solvation for each ion from the Born expression, we can obtain from eq 9 and 10 a value of $\Delta H_{abs}(H^+)$ which is appropriate for each ion. Since the heat of solvation of a proton must be a constant, the variation in the calculated values for $\Delta H_{abs}(H^+)$ is a test of the internal consistency of the model. We find for alkali and halide ions that $\Delta H_{abs}(H^+)$ varies between −260.00 and −264.3 kcal/mol with a mean value of −262.18 kcal/mol. Thus, to within 1%, $\Delta H_{abs}(H^+)$ is constant.

As another test of the model we use the value of −262.18 kcal/mol for the solvation energy of a proton and the experimentally determined values for relative solvation energies to obtain a series of solvation enthalpies of the individual ions. These are listed in Table III and plotted as a function of the corrected radius in Figure 2. There appears to be excellent agreement between the experimental values and the straight line derived from eq 8. Thus by introducing only one adjustable parameter into the Born model, we have successfully reproduced experimental results for 31 ions. Previous attempts to improve the theory have involved the use of more parameters and have not in general considered as large a number of ions.[24]

Some of the ions for which the relative heats of hydration are

(24) Since the "covalent radius" of ammonium is not a well-defined quantity, we have obtained a measure of the cavity radius from the following procedure. The $Na^+$–oxygen internuclear separation in water is approximately 2.35 Å.[5] Since the $Na^+$ cavity radius is 1.68 Å, the "hard-core" radius of the oxygen is approximately 0.67 Å. Since a typical $NH_4^+$···O hydrogen bond has a length of 2.8 Å, the cavity size of ammonium is 2.13 Å as listed in Table IV.

**TABLE III: Cavity Radii and Hydration Enthalpies**

| ion | corrected radius,[a] Å | $\Delta H_{calcd}$,[b] kcal/mol | $\Delta H_{rel}$,[c] kcal/mol | $\Delta H_{abs}$,[e] kcal/mol | % error[f] | $\Delta H_{abs}(H^+)$,[d] kcal/mol |
|---|---|---|---|---|---|---|
| $Li^+$ | 1.316 | −126.7 | 136.34 | −125.8 | −0.7 | −263.0 |
| $Na^+$ | 1.680 | −99.3 | 163.68 | −98.5 | −0.8 | −263.0 |
| $K^+$ | 2.172 | −76.8 | 183.74 | −78.4 | 2.1 | −260.5 |
| $Rb^+$ | 2.311 | −72.2 | 188.8 | −73.4 | 1.7 | −261.0 |
| $Cs^+$ | 2.514 | −66.3 | 194.6 | −67.6 | 1.9 | −260.9 |
| $F^-$ | 1.423 | −117.2 | −381.5 | −119.3 | 1.8 | −264.3 |
| $Cl^-$ | 1.937 | −86.1 | −347.5 | −85.3 | −0.9 | −261.4 |
| $Br^-$ | 2.087 | −79.9 | −341.0 | −78.8 | −1.4 | −261.1 |
| $I^-$ | 2.343 | −71.2 | −331.2 | −69.0 | −3.1 | −260.0 |
| $Cu^+$ | 1.252 | −133.2 | 118.7 | −143.5 | 7.2 | |
| $Ag^+$ | 1.434 | −116.3 | 147.1 | −115.1 | −1.1 | |
| $Cu^{2+}$ | 1.252 | −532.8 | 19.9 | −504.5 | −5.6 | |
| $Mg^{2+}$ | 1.455 | −458.4 | 62.0 | −462.4 | 0.9 | |
| $Ca^{2+}$ | 1.862 | −358.3 | 140.8 | −383.6 | 6.6 | |
| $Sr^{2+}$ | 2.054 | −324.7 | 176.1 | −348.3 | 6.8 | |
| $Ba^{2+}$ | 2.119 | −314.8 | 210.1 | −314.3 | −0.2 | |
| $Zn^{2+}$ | 1.338 | −498.7 | 32.8 | −491.6 | −1.5 | |
| $Cd^{2+}$ | 1.509 | −442.1 | 89.8 | −434.6 | −1.7 | |
| $Hg^{2+}$ | 1.541 | −432.9 | 85.0 | −439.4 | 1.5 | |
| $Al^{3+}$ | 1.338 | −1122.7 | −331.6 | −1118.1 | −0.4 | |
| $Sc^{3+}$ | 1.541 | −974.1 | −153.3 | −939.8 | −3.6 | |
| $Y^{3+}$ | 1.733 | −865.8 | −82.1 | −868.6 | 0.3 | |
| $La^{3+}$ | 1.808 | −830.0 | −2.5 | −789.0 | −5.2 | |
| $Ce^{4+}$ | 1.761 | −1515.0 | −508.0 | −1556.7 | 2.7 | |
| $Ce^{3+}$ | 1.761 | −852.2 | −67.0 | −853.5 | 0.2 | |
| $Ga^{3+}$ | 1.338 | −1122.1 | −337.6 | −1124.1 | 0.2 | |
| $In^{3+}$ | 1.605 | −935.1 | −199.9 | −986.4 | 5.2 | |
| $NH^{4+}$ [g] | 2.130 | −77.9 | 185.0 | −77.2 | −1.0 | |
| $OH^-$ | 1.498 | −111.3 | −371.0 | −108.8 | −2.3 | |
| $S^{2-}$ | 1.969 | −338.8 | −849.4 | −325.0 | −4.2 | |
| $SH^-$ | 1.969 | −84.7 | −341.0 | −78.8 | −7.5 | |

[a] The radii are taken from ref 21 and 23 (for halogens) increased by 7% (see text). [b] The enthalpies of solvation are calculated from eq 8 with the radii from column two. [c] The relative enthalpies of solvation are from ref 5, except for the first nine which are from ref 2. [d] The absolute heats of solvation of hydrogen ion are calculated from eq 9 and 10. [e] The absolute enthalpies of solvation are calculated from eq 9 and 10 and the calculated mean value of the absolute heat of solvation of the hydrogen ion, $\Delta H_{abs}(H^+)$, of 262.18 kcal/mol (see text). [f] The errors are in calculated values from column three compared to the $\Delta H_{abs}$ in the fifth column. [g] See ref 24.

available[5] are not listed in Table II. These include $Tl^+$, $Tl^{3+}$, $Pb^{2+}$, $Co^{2+}$, $Ni^{2+}$, $Mn^{2+}$, $Cr^{2+}$, $Cr^{3+}$, $Fe^{2+}$, and $Fe^{3+}$. For these ions the differences between the calculated and experimental enthalpies exceed 10%. However, these ions form coordination complexes with water (ref 6, p 335) and, therefore, it would not be expected that the cavity size for these ions follows the same rules that hold for other ions. Finally, we have also excluded $Be^{2+}$ from the table. For $Be^{2+}$, the difference between the experimental and calculated value is 17%, a discrepancy which may be due to large saturation effects resulting from the fact that $Be^{2+}$ is a particularly small ion.

The success of a continuum dielectric model in reproducing experimental results even for multivalent ions demonstrates that corrections due to the effects of dielectric saturation are not large in the calculation of solvation enthalpies (a point first made by Latimer et al.[3]). This may not be the case in the calculation of other thermodynamic quantities.[5,6] Although conflicting estimates of saturation effects have been reported in the literature,[6,10,13,25] it is interesting to note that the saturation effects obtained by Millen and Watts[10] are on the order of the 7% correction factor in the cavity radius that we have introduced.

*Solvation in Nonaqueous Media.* It is of interest to consider how the Born model might be applied to solvents other than water. This question is of particular importance for biological systems where problems concerning the free energies of transfer of ions from water to proteins and membranes arise in a variety of contexts.[26,27]

The Born equation as developed above can in principle be used to calculate the energies of transfer of ions from vacuum to any solvent. However, since the cavity size produced by a particular ion will vary in different solvents, a general expression for transfer energies must take this into account. We obtain an expression for the free energy of transfer of an ion between two solvents by considering the process in which the ion is first transferred from one solvent to vacuum and then from vacuum into the second solvent. The energies associated with each of these processes are given by eq 7, but different cavity radii must be used. Thus

$$\Delta G_{1\to 2}^{\circ} = (q^2/2R_{c_1})(1 - 1/D_1) - (q^2/2R_{c_2})(1 - 1/D_2) = q^2/2\{(1/R_{c_2}D_2 - 1/R_{c_1}D_1) + (1/R_{c_1} - 1/R_{c_2})\} \quad (11)$$

where $R_{c_1}$ and $R_{c_2}$ are the two cavity radii. When $R_{c_1}$ is equal to $R_{c_2}$, the standard Born expression is recovered.

The correction to the standard expression can in principle be quite large. Consider for example the transfer of a $Cl^-$ ion from water to hexane ($D_1 = 80$, $D_2 = 2$). If we use the corrected radius of 1.937 Å (Table III) for the $Cl^-$ ion in water and assume that the cavity radius in hexane is equal to the van der Waals radius of the $Cl^-$ ion ($R_{c_2} = 2.252$ Å), the total transfer energy is calculated to be 47.8 kcal/mol or 6 kcal/mol larger than if $R_{c_1} = R_{c_2} = 1.937$ Å. While it is not clear that the value we have assumed for the cavity radius in hexane is the correct one, the magnitude of the effect emphasizes the need to account for variations in cavity radii in estimating transfer free energies.

It should be pointed out that the cavity radii we have used should constitute a good first approximation for any hydrogen-bonding solvents. This implies that the correction term will be small in going, say, from water to ethanol. Since the $1/D$ terms are small in both solvents, the free energies of transfer should also be small, as is observed experimentally.[13] Similarly, the Born expression using the corrected radii of Table III should be appropriate for many applications to proteins where ions and ionizable groups appear to always be hydrogen bonded.[28]

(25) Schellman, J. A. *J. Chem. Phys.* **1957**, *26*, 1225.
(26) Parsegian, A. *Nature (London)* **1969**, *221*, 884.
(27) Honig, B. H.; Hubbell, W. *Proc. Natl. Acad. Sci. U.S.A.* **1984**, *81*, 5412.

*Relation to Simulations.* The success of the Born model in reproducing the observed solvation energies suggests that it may be capable of providing useful insights regarding molecular dynamics and Monte Carlo simulations of ions in water. One striking prediction of the Born model is that the transfer energy of an ion to a particular solvent is essentially independent of the dielectric constant, once the dielectric constant is high, say above 30. This follows from the $1 - 1/D$ dependence of the transfer energy. For example, the Born model predicts about a 3 kcal/mol difference in transfer energies between water and methanol for a univalent ion, a value which is in good agreement with experimental results.[13] It would appear then that any model for water which produces a high bulk dielectric constant should be successful in reproducing solvation energies, even if the calculated dielectric constant is incorrect.

On the other hand, the Born energy is highly sensitive to the choice of the cavity radius. When translated into the parameters used in detailed simulations, this implies that it is necessary to have accurate potential functions which successfully reproduce short-range interactions and can account, for example, for binding energies in the gas phase.[29] Finally, since the Born theory predicts that ion–solvent interactions at fairly long distances are still substantial (i.e., 10 kcal/mol for interactions above 10 Å), it would appear necessary to determine whether the use of periodic boundary conditions is capable of accounting for this contribution to the total solvation energy. In any case, the apparent success of the Born model in treating the solvation energies of ions suggests that the continuum model will continue to be useful in a variety of applications.

*Acknowledgment.* We thank Michael Gilson and Bruce Berne for useful and stimulating discussions. This work was supported by Grants GM-30518 (NIH) and PCM82-07145 (NSF).

(28) Rashin, A. A.; Honig, B. *J. Mol. Biol.* **1984**, *173*, 515.

(29) Arshadi, M.; Yamdagui, R.; Kebarle, P. *J. Phys. Chem.* **1970**, *74*, 1475.

# Laser Multiphoton Dissociation of Alkyl Cations: 1. Fragmentation Mechanism of Homologous Alkyl Cations Produced from Their Iodides

**H. Kühlewind, H. J. Neusser,* and E. W. Schlag**

*Institut für Physikalische und Theoretische Chemie der Technischen Universität München, D-8046 Garching, West Germany (Received: June 24, 1985)*

A homologous series of alkyl cations and their corresponding multiphoton mass spectra are produced from alkyl iodides to test the degree of fragmentation pattern transferability from one ion $C_nH_{2n+1}^+$ to the next larger one, etc., in multiphoton mass spectrometry. In electron impact ionization all ions in the same mass range, even when produced from different parentages, produce similar fragmentation. In direct contrast to this multiphoton mass spectra of homologous alkyl compounds display strong differences. The wavelength of the exciting light influences the fragmentation pattern in a direct way, thus leading to two-dimensional control of the fragmentation pattern. These features can be exploited for mixture analysis using mass spectrometry. Mechanistically this can be understood as being due to the ladder switching mechanism leading to optical selective photon absorption by fragment ions. Results are also presented that a classification in terms of a single average energy for decomposing ions is not adequate. A parametrization in terms of differing internal energies for differing ions is required.

## I. Introduction

Multiphoton ionization (MPI) is known to be an unique method providing additional variables for the production of polyatomic molecular ions in a mass spectrometer.[1-7] One such possibility is the use of high light intensities in excess of $10^7$ W/cm$^2$ to lead to fragmentation of organic ions with a large amount of small fragments, even $C^+$ cations,[2] these being energetically very high lying.

In order to exploit this new technique there is considerable interest in the clarification of the complex mechanism of the multiphoton fragmentation processes of polyatomic molecular ions. Photon absorption exclusively within the molecular parent ion,[8,9] competing light absorption and dissociation in the neutral manifold[10] and in the ionic manifold in a so-called "ladder switching" mechanism,[11,12] as well as ionization and dissociation of superexcited neutrals[5] have been discussed. Two-laser experiments of our group[12,13] and more recently photoelectron kinetic energy measurements from other laboratories have shown that for aromatic hydrocarbons, e.g., benzene, toluene, and chlorobenzene,[14-16] as well as for a series of small molecules[17,18] the "ladder switching"

(1) Boesl, U.; Neusser, H. J.; Schlag, E. W. *Z. Naturforsch., A* **1978**, *33A*, 1546.
(2) Zandee, L.; Bernstein, R. B.; Lichtin, D. A. *J. Chem. Phys.* **1978**, *69*, 3427.
(3) Antonov, V. S.; Knyazev, I. N.; Letokhov, V. S.; Matiuk, V. M.; Morshev, V. G.; Potapov, V. K. *Opt. Lett.* **1978**, *3*, 37.
(4) Rockwood, S.; Reilly, J. P.; Hohla, K.; Kompa, K. L. *Opt. Commun.* **1979**, *28*, 175.
(5) Lubman, D. M.; Naaman, R.; Zare, R. N. *J. Chem. Phys.* **1980**, *72*, 3034.
(6) Fisanick, G. J.; Eichelberger IV, T. S.; Heath, B. A.; Robin, M. B. *J. Chem. Phys.* **1980**, *72*, 5571.
(7) Cooper, C. D.; Williamson, A. D.; Miller, J. C.; Compton, R. N. *J. Chem. Phys.* **1980**, *73*, 1527.
(8) Rebentrost, F.; Kompa, K. L.; Ben-Shaul, A. *Chem. Phys. Lett.* **1981**, *77*, 394.
(9) Rebentrost, F.; Ben-Shaul, A. *J. Chem. Phys.* **1981**, *74*, 3255.
(10) Yang, J. J.; Gobell, D. A.; Pandolfi, R. S.; El-Sayed, M. A. *J. Phys. Chem.* **1983**, *87*, 2255.
(11) Dietz, W.; Neusser, H. J.; Boesl, U.; Schlag, E. W.; Lin, S. H. *Chem. Phys.* **1982**, *66*, 105.
(12) Boesl, U.; Neusser, H. J.; Schlag, E. W. *J. Chem. Phys.* **1980**, *72*, 4327.
(13) Boesl, U.; Neusser, H. J.; Schlag, E. W. *Chem. Phys. Lett.* **1982**, *87*, 1.
(14) Long, S. R.; Meek, J. T.; Reilly, J. P. *J. Chem. Phys.* **1983**, *79*, 3206.
(15) Long, S. R.; Meek, J. T.; Reilly, J. P. *J. Phys. Chem.* **1982**, *86*, 2809.
(16) Anderson, S. L.; Rider, D. M.; Zare, R. N. *Chem. Phys. Lett.* **1982**, *93*, 11.
(17) Achiba, Y.; Sato, K.; Shobatake, K.; Kimura, K. *J. Chem. Phys.* **1982**, *77*, 2709.
(18) Glownia, Y. H.; Riley, S. J.; Colson, S. D.; Miller, J. C.; Compton, R. N. *J. Chem. Phys.* **1982**, *77*, 68.

0022-3654/85/2089-5593$01.50/0 

## 4.9 Osmotic pressure

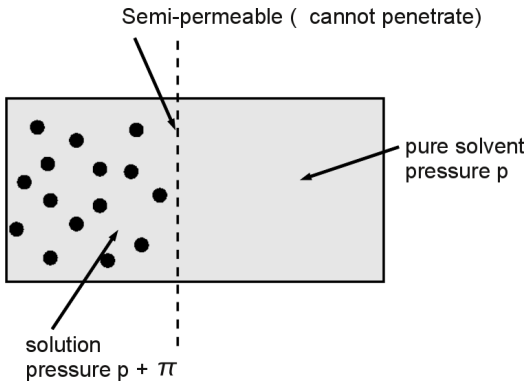


scheme 089

We assume an ideal solution.

Conditions of equilibrium:

$$\mu_1(\text{left side}) = \mu_1(\text{right side})$$
$$T(\text{left side}) = T(\text{right side})$$

$\mu_2$ cannot equilibrate

$$\pi = p(\text{left side}) - p(\text{right side})$$

Ideal solution

$$\beta\mu_2 = \beta\Delta\mu_2 + \ln \rho_2$$

$\Delta\mu_2$ is independent of $\rho_2$, but depends on the solvent.

$\pi$ is a state function and depends on $\rho_2$, $\mu_1$, and $T$. The total differential is

$$\mathrm{d}\pi = \left(\frac{\partial\pi}{\partial\rho_2}\right)_{T,\mu_1} \mathrm{d}\rho_2 + \left(\frac{\partial\pi}{\partial T}\right)_{\rho_2,\mu_1} \mathrm{d}T + \left(\frac{\partial\pi}{\partial\mu_1}\right)_{T,\rho_2} \mathrm{d}\mu_1$$

Holding $T$, $\mu_1$ constant and changing $\rho_2'$ from 0 to $\rho_2$ gives

$$\pi(\rho_2) - \pi(0) = \int_{\pi(0)}^{\pi(\rho_2)} \mathrm{d}\pi = \int_0^{\rho_2} \mathrm{d}\rho_2' \left(\frac{\partial \pi}{\partial \rho_2'}\right)_{T,\mu_1}$$

$\pi(0) = 0$ if there is no solute, the solvent pressure is equilibrated

$$\pi = \int_0^{\rho_2} \mathrm{d}\rho_2' \left(\frac{\partial p_{\text{left}}}{\partial \rho_2'}\right)_{T,\mu_1}$$

Define an auxiliary function

$$F = E - TS - \mu_1 N_1$$

with

$$\begin{aligned}
\mathrm{d}F &= \mathrm{d}E - \mathrm{d}(TS) - \mathrm{d}(\mu_1 N_1) \\
&= T\mathrm{d}S - p\mathrm{d}V + \mu_1 \mathrm{d}N_1 + \mu_2 \mathrm{d}N_2 - T\mathrm{d}S - S\mathrm{d}T - \mu_1 \mathrm{d}N_1 - N_1 \mathrm{d}\mu_1 \\
&= -S\mathrm{d}T - p\mathrm{d}V - N_1 \mathrm{d}\mu_1 + \mu_2 \mathrm{d}N_2
\end{aligned}$$

Therefore $F$ is a natural function of $T$, $V$, $\mu_1$, and $N_2$.

$$F = F(T, V, \mu_1, N_2)$$

The density is a simple function of natural variables of $F$

$$\rho_2 = \frac{N_2}{V}$$

Let's choose

$$\left(\frac{\partial p}{\partial \rho_2}\right)_{T,\mu_1,V} = \left(\frac{\partial p}{\partial (N_2/V)}\right)_{T,\mu_1,V} = V \left(\frac{\partial p}{\partial N_2}\right)_{T,\mu_1,V}$$

Maxwell relation from $F$

$$\left(\frac{\partial (-p)}{\partial N_2}\right)_{T,\mu_1,V} = \left(\frac{\partial \mu_2}{\partial V}\right)_{T,\mu_1,N_2}$$

So, we get

$$\begin{aligned}\left(\frac{\partial p}{\partial \rho_2}\right)_{T,\mu_1,V} &= -V\left(\frac{\partial \mu_2}{\partial V}\right)_{T,\mu_1,N_2} \\ &= -V\left(\frac{\partial \mu_2}{\partial (1/V)}\right)_{T,\mu_1,N_2}\left(\frac{\partial (1/V)}{\partial V}\right)_{T,\mu_1,N_2} \\ &= -VN_2\left(\frac{\partial \mu_2}{\partial (N_2/V)}\right)_{T,\mu_1,N_2}\left(\frac{-1}{V^2}\right) \\ &= \rho_2\left(\frac{\partial \mu_2}{\partial \rho_2}\right)_{T,\mu_1,N_2}\end{aligned}$$

Back to the osmotic pressure

$$\pi = \int_0^{\rho_2} \mathrm{d}\rho_2' \left(\frac{\partial p}{\partial \rho_2'}\right)_{T,\mu_1,V} = \int_0^{\rho_2} \mathrm{d}\rho_2' \rho_2' \left(\frac{\partial \mu_2}{\partial \rho_2'}\right)_{T,\mu_1,N_2}$$

From the ideal system assumption

$$\begin{aligned}\beta\mu_2 &= \beta\Delta\mu_2 + \ln\rho_2 \\ \beta\frac{\partial \mu_2}{\partial \rho_2'} = \beta\frac{\partial \Delta\mu_2}{\partial \rho_2'} + \frac{\partial \ln \rho_2'}{\partial \rho_2'} &= \frac{1}{\rho_2'} \\ \pi &= \int_0^{\rho_2} \mathrm{d}\rho_2' \rho_2' \frac{1}{\beta\rho_2'} = \beta^{-1}\rho_2\end{aligned}$$

$$\boxed{\beta\pi = \rho_2}$$

or in general

$$\beta\pi = \sum_i \rho_i$$

**Example** Osmotic pressure of 0.1 moles $NaCl$ in 1 l water at normal conditions.

$$\begin{aligned}\pi &= \mathrm{k_B}T(\rho_{Na^+} + \rho_{Cl^-}) \\ &= 1.3810^{-23}\ \mathrm{JK^{-1}} \cdot 300\ \mathrm{K} \cdot (0.1 + 0.1)\ \mathrm{mol} \cdot 6.02210^{23}\ \mathrm{mol^{-1}} \cdot 10^{-3}\ \mathrm{m^{-3}} \\ &= 4.9910^5\ \mathrm{J/m^3} = 4.9910^5\ \frac{\mathrm{N}}{\mathrm{m^2}} \approx 510^5\ \mathrm{Pa} \approx 5\ \mathrm{atm}\end{aligned}$$

## 4.10 To be ideal or not

For an ideal solution or gas

$$\mu_i = \Delta\mu_i + \mathrm{k_B}T \ln \rho_i$$

and $\Delta\mu_i$ is independent of $\rho_i$.

If the solution were not ideal

$$\begin{aligned}
\Delta\mu_i &= \Delta\mu_i(T, \rho_{\text{solvent}}; \rho_i) \\
&\qquad \text{Taylor expansion in powers of } \rho_i \\
&= \Delta\mu_i(T, \rho_{\text{solvent}}; 0) + \left(\frac{\partial \Delta\mu_i}{\partial \rho_i}\right)_{T,\rho_{\text{solvent}}}\Bigg|_{\rho_i=0} \rho_i + \cdots \\
&= \Delta\mu_i(T, \rho_{\text{solvent}}; 0) + 2\mathrm{k_B}TB_i\rho_i + \cdots
\end{aligned}$$

Now, recall that

$$\mu_i = \left(\frac{\partial A}{\partial N_i}\right)_{T,V,N_{i\neq j}} \quad \text{and} \quad \beta p = \left(\frac{\partial(-\beta A)}{\partial V}\right)_{T,N}$$

Using $\mu_i = \mu_i^{(\text{ideal})} + 2\mathrm{k_B}TB_i\rho_i + \cdots$, we have

$$\beta A = \beta A^{(\text{ideal})} - VB_i\rho_i^2 + \cdots$$

For several components of solutes

$$-\beta[A - A^{(\text{ideal})}] = \sum_{i,j} VB_{ij}\rho_i\rho_j + \cdots$$

where the sums are over all solute species.

Thus,

$$\beta\pi = \beta\pi^{(\text{ideal})} + B\rho_i^2$$

or for a simple one component gas

$$\beta p = \rho + B\rho^2 + \mathcal{O}(\rho^3)$$

In this case the constant $B$ is called the second virial coefficient of the gas.

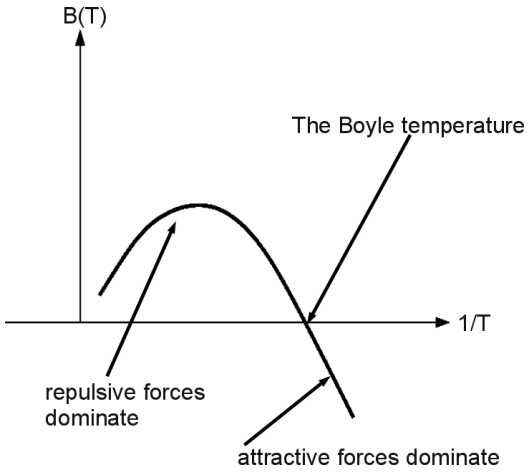


scheme 090

Pressure of low density real gas.

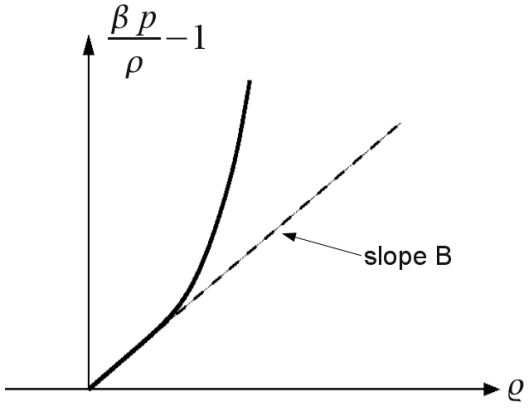


scheme 091

**Example** van der Waals gas

$$\beta p_{\mathrm{vdW}} = \frac{\rho}{1 - b\rho} - a\frac{\rho^2}{\mathrm{k_B}T}$$

$\frac{\rho}{1-b\rho}$ accounts for finite size of molecules

excluded volume

$\rho = \frac{N}{V} \to \frac{N}{V^\star} = \frac{N}{V(1-bN/V)}$

$a\frac{\rho^2}{\mathrm{k_B}T}$ accounts for attractive forces between molecules

Notice: excluded volume part is independent of $T$, but the attractive force part decreases in size with $T$ increasing.

The parameter $b$ is roughly the volume of one molecule. Low density is therefore $b\rho \ll 1$. In that region

$$\beta p_{\mathrm{vdW}} = \rho + b\rho^2 + \cdots - a\frac{\rho^2}{\mathrm{k_B}T}$$

Hence

$$B_{\mathrm{vdW}}(T) = b - \frac{a}{\mathrm{k_B}T}$$

The Boyle temperature for this equation of state is

$$\frac{1}{\mathrm{k_B}T_{\mathrm{Boyle}}} = \frac{b}{a}$$

Osmotic pressure of aqueous $Na^+\ Cl^-$ solution at concentration $c$

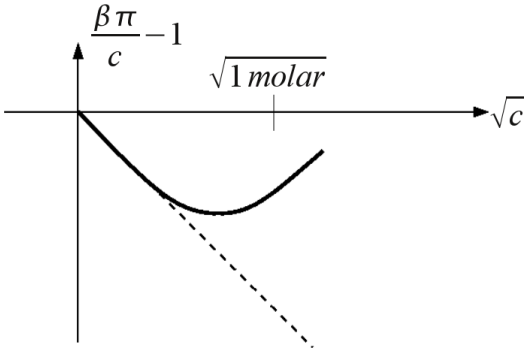


scheme 092

What is going on here? Experimental osmotic pressure of $Na^+\ Cl^-$ solution doesn't look like $\beta\pi = \rho_{Na^+} + \rho_{Cl^-} + \cdots$. Also the corrections from ideality cannot be expressed as interger powers of density.

What we see in the case of strong electrolytes is the result of

1. Fluctuations in density must preserve macroscopic charge neutrality

2. screening

Peter Debye figured all this out in his famous Bebye–Hückel theory of ionic solutions. To discuss this theory, consider first

$$\begin{bmatrix}\text{average energy of interaction}\\ \text{for an ion } q\text{, coupled to other}\\ \text{ions, } q'\text{, at average density } \rho.\end{bmatrix} \approx 4\pi\rho \underbrace{\int_R^\infty r^2 \mathrm{d}r \frac{qq'}{\epsilon r}}_{This integral diverges!}$$

The Coulomb potential has infinite range. It seems as if you can never separate charges enough to make their interactions negligible. This is not what we have in a van der Waals gas where the volume b is finite.

To analyze carefully, consider a charge $q$ at the origin in an electrolyte solution with charges $z_i$ of densities $\rho_i$.

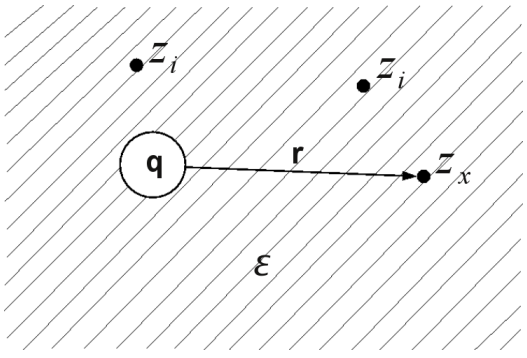


scheme 093

Charge neutrality requires $\sum_i z_i \rho_i = 0$.

$$\begin{aligned}
\langle \rho_x(\boldsymbol{r}) \rangle_q &= \text{average density of charge species } x \text{ at position } \boldsymbol{r} \\
&= \rho_x \mathrm{e}^{-\beta W_x(\boldsymbol{r})} \\
\rho_2 &: \text{bulk uniform density} \\
W_x(\boldsymbol{r}) &: \text{reversible work to bring ion } x \text{ from } \infty \text{ to a distance} \\
&\quad \boldsymbol{r} \text{ from the origin}
\end{aligned}$$

Think about reaction fields. $W_x(\boldsymbol{r})$ should have at least two contributions. The direct Coulomb interaction between $q$ and $z_x$, and then another part from the non-uniform charge densities induced by $q$.

Specifically,

$$W_i(\boldsymbol{r}) \approx \frac{q z_i}{\epsilon r} + \sum_j \int \mathrm{d}\boldsymbol{r}' \frac{q z_j}{\epsilon \| \boldsymbol{r} - \boldsymbol{r}' \|} \langle \delta \rho_j(\boldsymbol{r}') \rangle_q$$

where the deviation from the uniform desnity induced by $q$ has been introduced.

$$\langle \delta \rho_j(\boldsymbol{r}') \rangle_q = \rho_j \left( \mathrm{e}^{-\beta W_j(\boldsymbol{r})} - 1 \right)$$

Recall from your knowledge of electrostatics

$$\nabla^2 \frac{1}{\|1\|} = -4\pi \delta(\boldsymbol{r})$$

with $\delta(\boldsymbol{r})$ Dirac's delta function, zero everywhere except at $\boldsymbol{r} = 0$ and net volume equal to 1.

Use this relationship and operate left and right with $\nabla^2$. You get

$$\nabla^2 W_i(\boldsymbol{r}) \approx -\frac{q z_i}{\epsilon} 4\pi \delta(\boldsymbol{r}) - \frac{4\pi}{\epsilon} q \sum_j z_j \rho_j \left( \mathrm{e}^{-\beta W_j(\boldsymbol{r})} - 1 \right)$$

For large $r$ (this should be the relevant region if concentration of ions is very low), expand the exponential since $W_j(\boldsymbol{r})$ will be small. This gives

$$\nabla^2 W_i(\boldsymbol{r}) \approx -\frac{q z_i}{\epsilon} 4\pi \delta(\boldsymbol{r}) + \frac{4\pi}{\epsilon} q \beta \sum_j z_j \rho_j W_j(\boldsymbol{r})$$

This is a linear differential equation for $W_i(\boldsymbol{r})$. You can verify that the solution is

$$\boxed{W_i(\boldsymbol{r}) = \frac{qz_i}{\epsilon r}\mathrm{e}^{-\kappa r}}$$

where

$$\kappa = \sqrt{\frac{4\pi\beta}{\epsilon}\sum_i \rho_i z_i^2}$$

$$\kappa^{-1} = \text{Debye screening length}$$

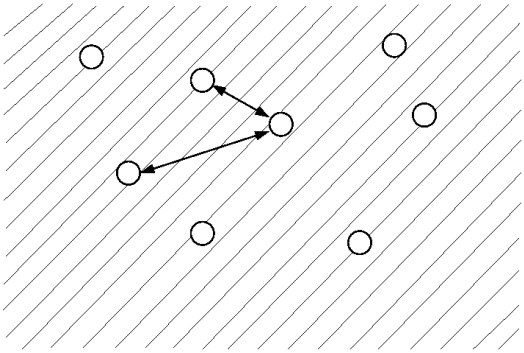

scheme 094

Effect of one ion on another – the pair correlations – decay as $\mathrm{e}^{-\kappa r}$. Screening of ions by ionic atmosphere. The effective radius of an ion is ($c$ ion concentration)

$$\frac{1}{\kappa} = \text{Debye length} \approx \frac{1}{\sqrt{c}}$$

Now we do the correct calculation of

$$\begin{aligned}\langle U\rangle &= \text{average energy of interaction for a tagged} \\ &\qquad \text{ion coupled to all other ions} \\ &= \sum_i \int \mathrm{d}\boldsymbol{r}\frac{qz_i}{\epsilon r} \qquad \underbrace{\rho_i \mathrm{e}^{-\beta W_i(\boldsymbol{r})}}_{\substack{\text{density of ions} \\ \text{surrounding ion } q}}\end{aligned}$$

The interaction energy of ion $q$ with ions of type $i$ is $\frac{qz_i}{\epsilon r}$. The exponential in the density of ions can be expanded and only the first two terms are kept, the other terms can be neglected at very low $\rho_i$ because the ions are generally very far apart.

$$\rho_i \mathrm{e}^{-\beta W_i(\boldsymbol{r})} \approx \rho_i - \beta\rho_i W_i(\boldsymbol{r}) + \cdots$$

$$\begin{aligned}\langle U\rangle &= \int \mathrm{d}\boldsymbol{r} \left\{ \sum_i \frac{qz_i}{\epsilon r}\rho_i - \frac{q}{\epsilon r}\sum_i \frac{\beta\rho_i q z_i^2}{\epsilon r}\mathrm{e}^{-\kappa r} + \cdots \right\} \\ &= -\frac{q^2}{\epsilon}\int_0^\infty \mathrm{d}r r^2 4\pi \sum_i \frac{\beta\rho_i z_i^2}{\epsilon}\frac{\mathrm{e}^{-\kappa r}}{r^2} + \cdots \\ &= -\frac{q^2}{\epsilon}\kappa = -\frac{q^2}{\epsilon\text{Debye length}} \propto (\text{concentration})^{1/2}\end{aligned}$$

Analysis of the osmotic pressure can also be done (tedious). The result is

$$\beta\pi = \sum_i \rho_i - \frac{\kappa^3}{24\pi} \qquad \text{Debye–Hückel limiting law}$$

With salt $M_{\nu_+}X_{\nu_-} \longrightarrow \nu_+ M_+ + \nu_- X_-$ (e.g. $NaCl, \nu_+ = \nu_- = 1$) we have

$$\mu_{M_{\nu_+}X_{\nu_-}} = \nu_+\Delta\mu_+ + \nu_-\Delta\mu_- + \mathrm{k_B}T\ln\rho_+^{\nu_+}\rho_-^{\nu_-} + \mathrm{k_B}T\ln\gamma_\pm^\nu \qquad \nu = \nu_+ + \nu_-$$

where $\gamma_\pm$ is the mean activity coefficient

$$\gamma_\pm = -\frac{1}{\nu}(\nu_+ z_+^2 + \nu_- z_-^2)\frac{\kappa}{2\epsilon\mathrm{k_B}T}$$

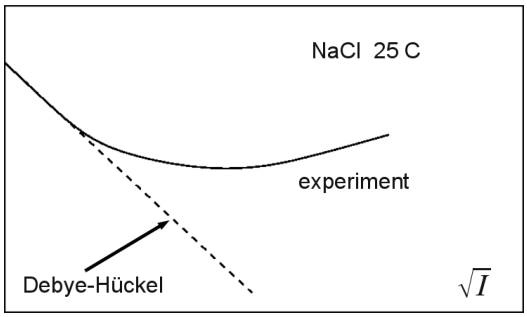


scheme 095

# Chapter 5

# Chemical Kinetics

## 5.1 General considerations and formal development

First recall some old ideas:

**Two state system** (e.g. spin up and spin down)

State 2 ——— $E_2$

State 1 ——— $E_1$

} Relative populations of equilibrium determined by $\Delta E = E_2 - E_1$

$K \equiv \frac{\rho_2}{\rho_1} = \frac{P_2}{P_1} = \mathrm{e}^{-\beta \Delta E}$

How do these two states equilibrate? And how much time does it take to equilibrate?

- How $\longrightarrow$ Mechanism
- Time $\longrightarrow$ Kinetics

**Trans/gauche conformations**

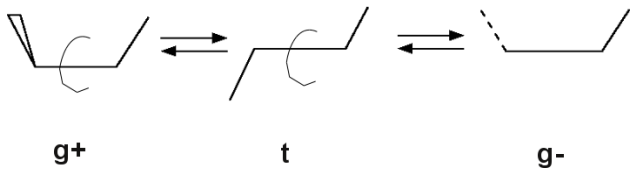


scheme 100

State $g^+$ ——— ——— $E_g$

State $t$ ——— $E_t$

$$K \equiv \frac{\rho_g}{\rho_t} = 2\mathrm{e}^{-\beta(E_g - E_t)}$$

This looks like a 3–state system! Is it? If we say the energy of intermediate conformations is very high compared to $\mathrm{k_B}T$, then those states have *no population* and are unimportant *at equilibrium*!

But, if we want to know *how fast* a $g^+ \rightarrow t$ occurs, for example, we must consider all the intermediate states! This is the central idea of chemical kinetics.

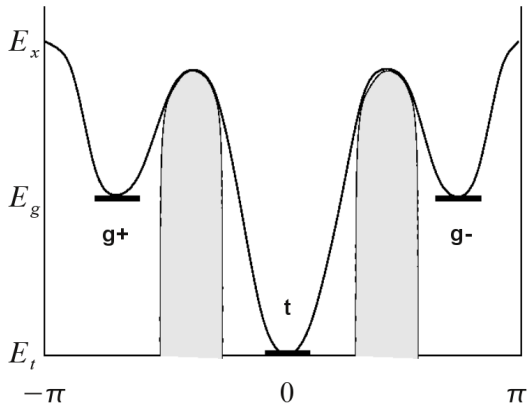


scheme 101

Not really a 3–state system! To know exactly how fast a conversion from $t \to g^-$ is, for example, we would have to know the energy of all the intermediate angles. But as a first guess to the rate, we only have to know $E^\star$!

**Conclusion**

1. Thermodynamic popoulations $\longrightarrow$ energy of stable states

2. Kinetic rates $\longrightarrow$ energy between stable states

Most fundamental distinction in physical chemistry

| **Thermodynamics** | **Kinetics** |
|---|---|
| $\Downarrow$ | $\Downarrow$ |
| Assuming an equilibrium system at $t = \infty$, allowing all fluctuations | Non-equilibrium system at $t < \infty$, so all fluctuations not yet achieved. |

Think of tedious chore to illustrate difference!

**Formal development** Consider the reaction $A \longrightarrow B$.

Want a notion of *rate* of reaction.

$$\begin{aligned} \text{Rate} &= \text{number of } B \text{ molecules appearing per time.} \\ &= \text{number of } A \text{ molecules disappearing per time.} \end{aligned}$$

If constant volume reaction, can use concentrations to count molecules of species $A$ and $B$.

Let $c_A = [A], c_B = [B]$, both $c_A$ and $c_B$ depend on time.

$$\left.\begin{array}{lll} \text{Rate} & = \dot{c}_B(t) & = \frac{\mathrm{d}}{\mathrm{d}t}c_B(t) \\ & = -\dot{c}_A(t) & = -\frac{\mathrm{d}}{\mathrm{d}t}c_A(t) \end{array}\right\} \quad \begin{array}{l} \text{Note } \dot{c}_B(t) = -\dot{c}_A(t) \Rightarrow \frac{\mathrm{d}}{\mathrm{d}t}(c_A + c_B) = 0 \\ c_A + c_B \text{constant in time} \\ \rightarrow \text{conservation of mass} \end{array}$$

Now we need equations for the rate. The rate equaions are determined by the *Reaction Mechanism.*

- Elementary Reactions (easy)
- Complex Reactions (tough)

Let's do easy first: $A \longrightarrow B$

Assume: Rate $\propto c_A$ (This is a big intelectual jump!?)
Then, (Rate equation)

$$\text{Rate} = \dot{c}_B(t) = \boxed{-\dot{c}_A(t) = kc_A(t)}$$

where $k$ is the Rate constant.

Easily solved to give

$$\begin{aligned} c_A(t) &= c_A(0)\mathrm{e}^{-kt} \\ c_B(t) &= c_B(0) + c_A(0)\left(1 - \mathrm{e}^{-kt}\right) \end{aligned}$$

This is called a first order rate equation.

$$A \xrightarrow{k} B$$

$B$ could go backwards to make $A$. Let the rate constant for that inverse process be $k_{-1}$

$$A \underset{k_{-1}}{\overset{k}{\rightleftarrows}} B$$

$$\begin{aligned} \dot{c}_A(t) &= -kc_A(t) + k_{-1}c_B(t) \\ \dot{c}_B(t) &= kc_A(t) - k_{-1}c_B(t) \end{aligned}$$

At equilibrium,

$$\dot{c}_A = 0 = \dot{c}_B \Rightarrow 0 = -kc_A + k_{-1}c_B$$

and we get

$$\underbrace{K}_{\text{thermodynamics}} \equiv \frac{c_B}{c_A} = \underbrace{\frac{k}{k_{-1}}}_{\text{kinetics}} \quad \Longleftarrow \boxed{\text{Detailed Balance}}$$

## 5.2 Arrhenius law

Temperature of a chemical reaction.

- not clearly defined, as temperature as a statistical quantity only applies to equilibrium
- for most systems in good approximation on can use the statistical temperature
- be careful with special systems, like flames.

Arrhenius plot

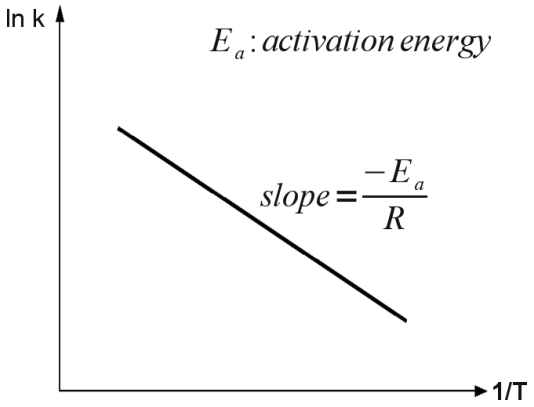


scheme 102

$$\frac{\mathrm{d}\ln k}{\mathrm{d}(1/T)} = -\frac{E_a}{R} \quad \Rightarrow \quad \frac{\mathrm{d}\ln k}{\mathrm{d}T} = \frac{E_a}{RT^2}$$

For the back reaction we get

$$\frac{\mathrm{d}\ln k'}{\mathrm{d}T} = \frac{E_a'}{RT^2}$$

These are empirical laws!

From, $K = \frac{k}{k'}$, we get

$$\ln K = \ln k - \ln k'$$

$$\underbrace{\frac{\mathrm{d}\ln K}{\mathrm{d}T}}_{\text{ideal gas}} = \frac{\mathrm{d}\ln k}{\mathrm{d}T} - \frac{\mathrm{d}\ln k'}{\mathrm{d}T}$$

$$\frac{\Delta H}{RT^2} = \frac{E_a}{RT^2} - \frac{E_a'}{RT^2}$$

$$\underbrace{\Delta H}_{\substack{\text{thermodynamic quantity; change in enthalpy for the reaction}}} = \underbrace{E_a - E_a'}_{\text{kinetic quantity}}$$

## 5.3 Transition state theory

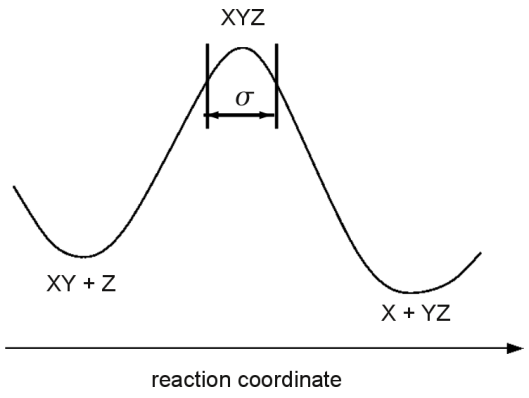

Let's consider a bi–molecular reaction in the gas phase

$$A + B \longleftrightarrow X + Y$$

$\overrightarrow{[C]}$ : concentration of activated complex for forward reaction

$\overleftarrow{[C]}$ : concentration of activated complex for backward reaction

Assumption Equilibrium of activated complexes for backward/forward reaction

$$A + B \longleftrightarrow \overrightarrow{C}$$
$$\overleftarrow{C} \longleftrightarrow X + Y$$

We get the equlibrium constants

$$\overrightarrow{K_c} = \frac{\overrightarrow{[C]}}{[A][B]}$$
$$\overleftarrow{K_c} = \frac{\overleftarrow{[C]}}{[X][Y]}$$

Write $\overrightarrow{K_c}$ with partition sums

$$\overrightarrow{[C]} = \frac{Q_c}{Q_a Q_b} \mathrm{e}^{-\frac{E_0}{\mathrm{k_B} T}} [A][B]$$

$E_0$ is the energy difference of the ground states of $A + B$ and $C$ (zero of energy definitions).

$$Q_c = Q(\mathrm{trans})Q(\mathrm{rot})Q(\mathrm{vib}) \cdots$$

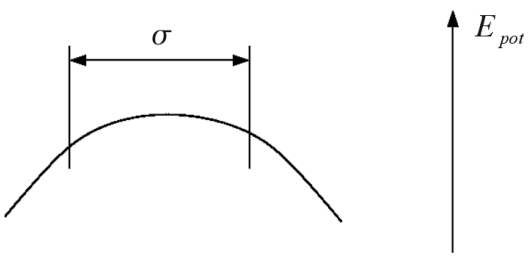

For the translational partition sum at the transition state all molecules move along $\delta$ (reaction path) and $E_{\text{pot}} \approx$ const. and we have free translation with

$$q_\delta = \frac{\delta}{h}\sqrt{2\pi m \mathrm{k_B} T} \cdot \frac{1}{2}$$

where $m$ is the mass of the complex and the factor $1/2$ is due to the fact that we only have to consider the forward movement.

$$\overrightarrow{[C]} = \frac{\delta}{2h}\sqrt{2\pi m \mathrm{k_B} T}\frac{Q^\sharp}{Q_a Q_b}\mathrm{e}^{-\frac{E_0}{\mathrm{k_B}T}}[A][B]$$

$\bar{v}$: average velocity of complexes at the transition state
$\tau = \frac{\delta}{\bar{v}}$: average time at the transition state

Velocity of reaction

$$\overrightarrow{[C]}\frac{\bar{v}}{\delta} = \frac{\bar{v}}{2h}\sqrt{2\pi m \mathrm{k_B} T}\frac{Q^\sharp}{Q_a Q_b}\mathrm{e}^{-\frac{E_0}{\mathrm{k_B}T}}[A][B]$$

We need an estimate for $\bar{v}$: Maxwell distribution

$$P(v, v+\mathrm{d}v) = \sqrt{\frac{m}{2\pi \mathrm{k_B} T}}\mathrm{e}^{-\frac{mv^2}{2\mathrm{k_B}T}}\mathrm{d}v \cdot N$$

where $N$ is a normalization constant

$$\bar{v} = \int_0^\infty P \cdot v \mathrm{d}v = \int_0^\infty v\mathrm{e}^{-\frac{mv^2}{2\mathrm{k_B}T}}\mathrm{d}v \Big/ \int_0^\infty \mathrm{e}^{-\frac{mv^2}{2\mathrm{k_B}T}}\mathrm{d}v$$

and we get

$$\bar{v} = \sqrt{\frac{2\mathrm{k_B}T}{\pi m}}$$

$$\underbrace{\overrightarrow{[C]}\frac{\bar{v}}{\delta}}_{\frac{\mathrm{d}\overrightarrow{[C]}}{\mathrm{d}t}} = \underbrace{\frac{\mathrm{k_B}T}{h}\frac{Q^\sharp}{Q_a Q_b}\mathrm{e}^{-\frac{E_0}{\mathrm{k_B}T}}}_{k}[A][B]$$

This looks exactly like the empirical equations of kinetics

$$\frac{\mathrm{d}\overrightarrow{[C]}}{\mathrm{d}t} = k[A][B]$$

with

$$\begin{aligned} k &= \frac{\mathrm{k_B}T}{h}\frac{Q^\sharp}{Q_a Q_b}\mathrm{e}^{-\frac{E_0}{\mathrm{k_B}T}} \\ &= \frac{\mathrm{k_B}T}{h}K^\sharp \\ \overrightarrow{K_c} &= K^\sharp\left(\frac{\pi m \mathrm{k_B}T}{2}\right)^{1/2}\frac{\delta}{h} \end{aligned}$$

$K^\sharp$ is an artificial equilibrium constant.

Comparision with Arrhenius:

$$\left.\begin{array}{ll} \frac{\mathrm{d}\ln k}{\mathrm{d}T} & = \frac{1}{T} + \frac{\mathrm{d}\ln K^\sharp}{\mathrm{d}T} \\ \frac{\mathrm{d}\ln \overrightarrow{K_c}}{\mathrm{d}T} & = \frac{\mathrm{d}\ln K^\sharp}{\mathrm{d}T} + \frac{1}{2T} \end{array}\right\}\text{eliminate}K^\sharp$$

$$\left.\begin{array}{l} \underbrace{\frac{\mathrm{d}\ln k}{\mathrm{d}T}}_{\frac{E_a}{RT^2}} = \underbrace{\frac{\mathrm{d}\ln \overrightarrow{K_c}}{\mathrm{d}T}}_{\frac{\Delta H}{RT^2}} + \frac{1}{2T} \\ \\ E_a = \Delta H + \frac{RT}{2} \end{array}\right.$$

From the interpretation of $K^\sharp$ as an equilibrium constant

$$\Delta G^\sharp = -RT\ln K^\sharp$$

and

$$k = \frac{\mathrm{k_B}T}{h}\mathrm{e}^{-\Delta G^\sharp/\mathrm{k_B}T}$$

or

$$\begin{aligned} \Delta G^\sharp &= \Delta H^\sharp - T\Delta S^\sharp \\ k &= \frac{\mathrm{k_B}T}{h}\mathrm{e}^{-\Delta H^\sharp/\mathrm{k_B}T}\mathrm{e}^{-\Delta S^\sharp/\mathrm{k_B}} \end{aligned}$$

Compare to Arrhenius $k = A\mathrm{e}^{-\Delta E_a/RT}$ to get

$$\begin{aligned} E_a &= \Delta H^\sharp && \text{activation energy} \\ A &= \frac{\mathrm{k_B}T}{h}\mathrm{e}^{-\Delta S^\sharp/R} && \text{frequency factor} \end{aligned}$$

**Relation to experiment** In experiment we measure $k(T)$

- Eyring plot: $\ln\left(\frac{k}{T}\right)$ vs. $1/T$
  - slope: $-\frac{\Delta H^\ddagger}{R}$
  - intercept: $\frac{\Delta S^\ddagger}{R}$
- Arrhenius plot: $\ln k$ vs. $1/T$
  - slope: $-\frac{E_a}{R}$
  - intercept: $A$ (assuming no temperature dependence of $A$)

## 5.4 Kinetic isotope effect (KIE)

Dependence on the rate of chemical reaction on the isotopes in the reactants

$$\text{KIE} = \frac{k(\text{isotope 1}}{k(\text{isotope 2}} = \frac{k_H}{k_D}$$

**Primary Isotope Effect** rate change due to isotopic substitution at a site of bond breaking or bond making in the rate determining step of a mechanism.

**Secondary Isotope Effect** all other

Typical primary KIE values.

| | $k_{\text{light}}/k_{\text{heavy}}$ [25 deg. C] |
|---|---|
| $C-H/C-D$ | 6–8 |
| $C-H/C-T$ | 15–16 |
| ${}^{12}C/{}^{13}C$ | 1.04 |
| ${}^{12}C/{}^{14}C$ | 1.07 |
| ${}^{14}N/{}^{15}N$ | 1.03 |
| ${}^{16}O/{}^{18}O$ | 1.02 |
| ${}^{32}S/{}^{34}S$ | 1.01 |
| ${}^{35}Cl/{}^{37}Cl$ | 1.01 |

From transition state theory

$$\begin{aligned}\text{KIE} = \frac{k_{\text{light}}}{k_{\text{heavy}}} &= \frac{\frac{\mathrm{k_B}T}{h}\frac{Q_l^\sharp}{Q_{R,l}}\mathrm{e}^{-E_0^l/\mathrm{k_B}T}}{\frac{\mathrm{k_B}T}{h}\frac{Q_h^\sharp}{Q_{R,h}}\mathrm{e}^{-E_0^h/\mathrm{k_B}T}} \\ &= \frac{Q_l^\sharp}{Q_h^\sharp}\frac{Q_{R,h}}{Q_{R,l}}\mathrm{e}^{-(E_0^l-E_0^h)/\mathrm{k_B}T}\end{aligned}$$

Molecular partition sum

$$Q = \underbrace{Q_{\text{trans}} \cdot Q_{\text{rot}} \cdot Q_{\text{vib}}}_{\text{mass dependent}} \cdot Q_E$$

In the Born–Oppenheimer approximation $Q_E$ is independent of mass. The most important contribution to the KIE is from $Q_{\text{vib}}$.

$$Q_{\text{vib}} \longrightarrow \frac{1}{2}\hbar\omega \qquad \text{zero point contribution}$$

$$\omega = \sqrt{\frac{f}{\mu}} \qquad f\text{: force constant; } \mu\text{: reduce mass}$$

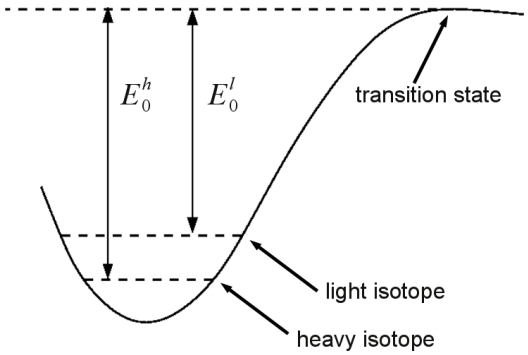


scheme 105

Under the assumption that at the transition state the bond is broken, there is no specific contribution to $Q^{\sharp}_{\text{vib}}$.

$$\begin{aligned}\Delta E_0 &\approx \Delta E(\text{zero point energy}) \\ &= \frac{1}{2}\hbar(\omega_{\text{light}} - \omega_{\text{heavy}}) \\ \text{KIE} = \frac{k_{\text{light}}}{k_{\text{heavy}}} &\approx \mathrm{e}^{-\frac{1}{2}\hbar\Delta\omega/\mathrm{k_B}T}\end{aligned}$$

estimate for primery isotope effect

**Example** $C-H$ vs. $C-D$

$$\left.\begin{aligned}\mu_H &= \tfrac{12\cdot 1}{12+1} \approx 1 \\ \mu_D &= \tfrac{12\cdot 2}{12+2} \approx 2\end{aligned}\right\} \quad \frac{\omega_H}{\omega_D} \approx \sqrt{2} \approx 1.4 \rightarrow \text{KIE} \approx 5$$

**Examples of KIE** Dehydrohalogenation reactions

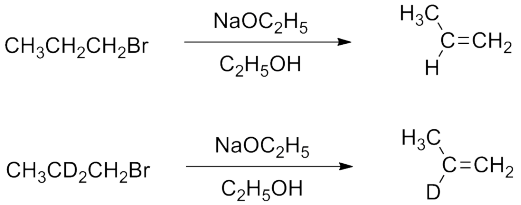

scheme 106

$$\frac{k_H}{k_D} = 6.7 \rightarrow \text{primary KIE for } C-H/C-D$$

Transition state

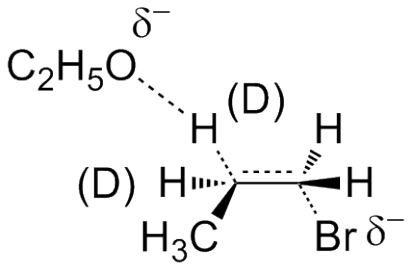


scheme 107

Rate limiting step involves $H(D)$ abstraction.

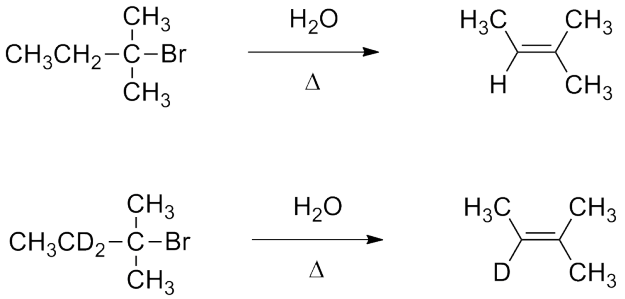


scheme 108

$$\frac{k_H}{k_D} = 1.4 \rightarrow \text{secondary KIE for } C-H/C-D$$

Transition state (rational)

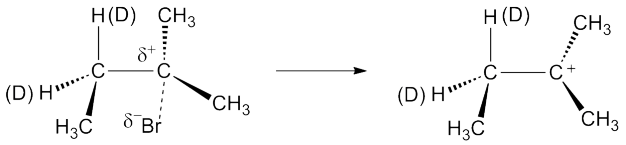


scheme 109

Rate limiting step is $Br^-$ elimination.

Decomposition of azo compound

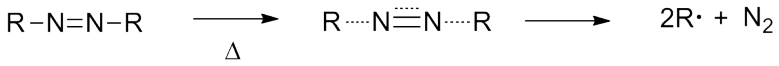


scheme 110

$$\frac{k_{14_N}}{k_{15_N}} = 1.02 \rightarrow \text{primary KIE}$$

KIE can be used to elucidate reaction mechanisms.

Origins of secondary KIE

- Differences in steric demand

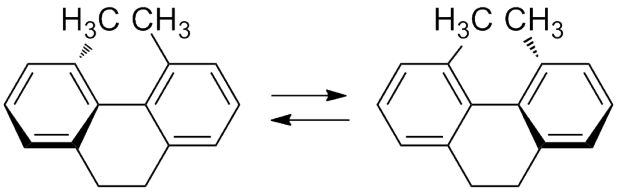


scheme 111

$$\frac{k_D}{k_H} = 1.15$$

$C - D$ has smaller vibrational amplitude.

- Hyperconjugative effects
- Differences in inductive effect, e.g. $H$ is mor electronegative than $D$.

**Tunneling** Quantum mechanical effect: transfering through instead over a barrier.

Basic exercise in QM

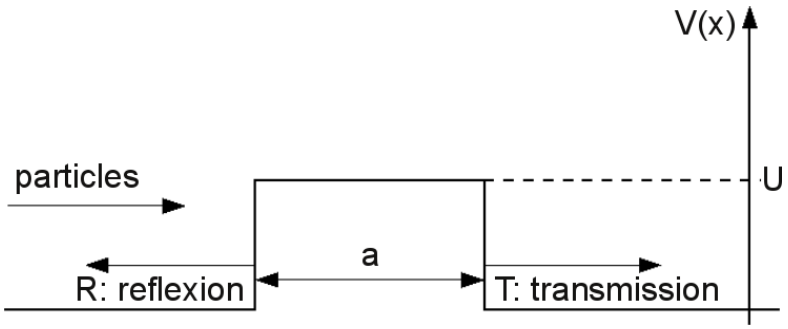


scheme 112

| | | | | |
|---|---|---|---|---|
| Classical physics | $E > U$ | $R$ | $= 0$ | $T = 1$ |
| | $E < U$ | $R$ | $= 1$ | $T = 0$ |

Quantum mechanics

$$E < U \qquad R = \frac{(\lambda^2+1)^2 \sinh^2 \kappa a}{4\lambda^2 + (\lambda^2+1)^2 \sinh^2 \kappa a}$$
$$T = \frac{4\lambda^2}{4\lambda^2 + (\lambda^2+1)^2 \sinh^2 \kappa a}$$

with

$$\kappa^2 = \frac{2m}{\hbar^2}(U - E) \qquad \text{mass dependence}$$

$$k^2 = \frac{2m}{\hbar^2}E$$

$$\lambda = \frac{\kappa}{k}$$

Example: $U = 2E; \quad \kappa = k \quad \lambda = 1$

$$T = \frac{4}{4 + 4\sinh^2 \kappa a} = \frac{1}{1 + \sinh^2 \kappa a} \qquad x = \kappa a$$

$$\approx 1 - x^2 + 2/3x^4 + \cdots$$

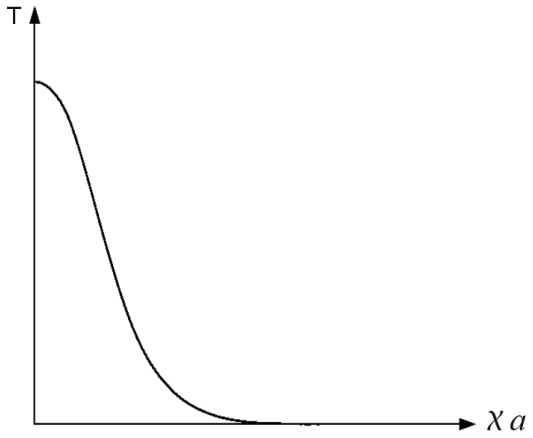


scheme 113

Importance in chemical reactions

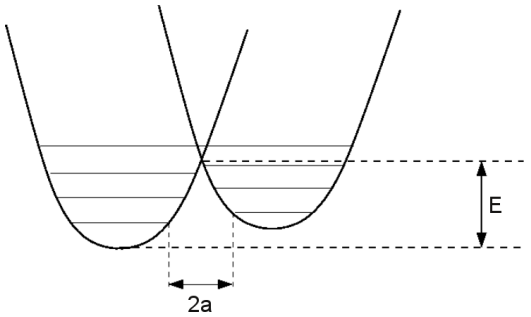


scheme 114

**Bell's modification**

$$k = Q \cdot A\mathrm{e}^{-E_a/\mathrm{k_B}T} \qquad Q : \text{tunneling factor}$$

$$Q = \frac{\mathrm{e}^{\alpha}}{\beta - \alpha}\left(\beta \mathrm{e}^{-\alpha} - \alpha \mathrm{e}^{-\beta}\right)$$

where

$$\alpha = \frac{E}{\mathrm{k_B}T} \qquad \beta = \frac{2a\pi^2\sqrt{2mE}}{h}$$

$\beta$ depends on mass ($\sqrt{m}$) and barrier width ($a$). Largest effects for small $m$ and small $a$.

Example: proton transfer

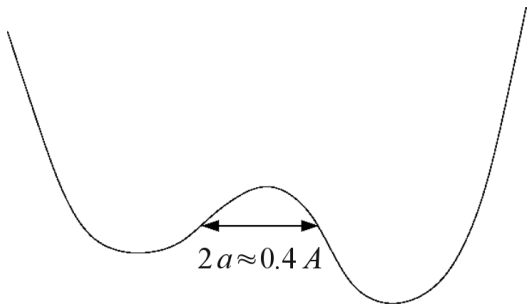


scheme 115

Can be important in proton transfer in enzymatic reactions, e.g., dehydrogenases.

## 5.5 Electron transfer reactions: Marcus theory

**Electron transfer:** the simplest chemical process

- molecular structures are preserved

- no bonds are broken or formed
- bond adjustments
- solvent repolarization

**Electron transfer:** plays a central role in

- inorganic redox chemistry
- organic chemistry
- electrochemistry (fueld cells, batteries)
- solid state and surface physics
- biology

**Examples**

$$[Fe(phen)_3]^{3+} + [Fe(CN)_6]^{4-} \longrightarrow [Fe(phen)_3]^{2+} + [Fe(CN)_6]^{3-}$$
$$[Co(NH_3)_6]^{3+} + [Co(NH_3)_6]^{2+} \longrightarrow [Co(NH_3)_6]^{2+} + [Co(NH_3)_6]^{3+}$$
$$[Co(NH_3)_6]^{3+} + [Ru(NH_3)_6]^{2+} \longrightarrow [Co(NH_3)_6]^{2+} + [Ru(NH_3)_6]^{3+}$$

where $phen = 1,10 - phenanthroline$.

In all these reaction is a single electron exchanged

$$\begin{aligned} \text{rates} \qquad & \approx 10^{9}\ \mathrm{M^{-1}s^{-1}} \\ & \approx 10^{-7}\ \mathrm{M^{-1}s^{-1}} \\ & \approx 10^{-2}\ \mathrm{M^{-1}s^{-1}} \end{aligned}$$

There are 16 orders of magnitude difference in the rates of these simple reactions!

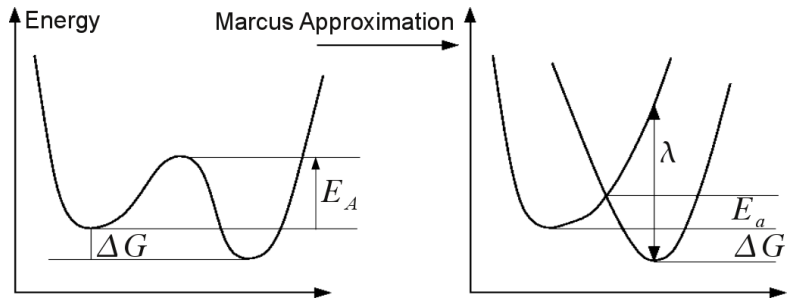


scheme 120

$\lambda$: solvent reorganization energy.

**Derivation of the Marcus formula** (Nobel prize in chemistry 1992)

| | |
|---|---|
| Reactants | $y_1 = x^2$ |
| Products | $(y_2 - b) = (x - a)^2$ |
| | $y_2 = x^2 - 2ax + a^2 + b$ |

Calculation of intersection point coordinates $(x_s, y_s)$ .

$$\begin{aligned} y_1(x_s) &= y_2(x_s) \\ x_s^2 &= x_s^2 - 2ax_s + a^2 + b \\ 0 &= -2ax_s + a^2 + b \\ 2ax_s &= b + a^2 \\ x_s &= \frac{b + a^2}{2a} \end{aligned}$$

Interpretation of parameters:

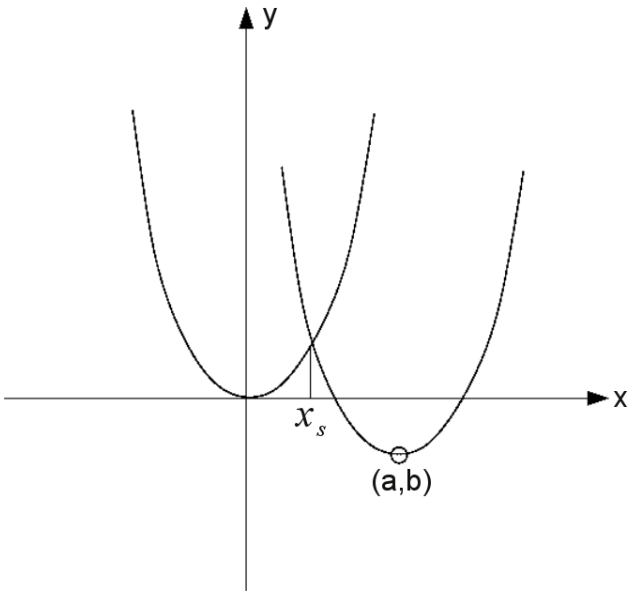


scheme 121

$$b = \Delta G$$
$$y_s = x_s^2 = E_a$$
$$a^2 = \lambda$$

With this we get

$$E_a = \frac{(b + a^2)^2}{4a^2} = \frac{(\Delta G + \lambda)^2}{4\lambda}$$

Rate constant

$$k = A\mathrm{e}^{-\frac{(\Delta G+\lambda)^2}{4\lambda \mathrm{k_B} T}}$$

Formula for prefactor

$$A = \frac{2\pi}{\hbar}\|H_{AB}\|^2 \frac{1}{\sqrt{4\pi\lambda \mathrm{k_B} T}}$$

$H_{AB}$ : electronic coupling element
how easy is it for an electron
to go from state $A$ to $B$

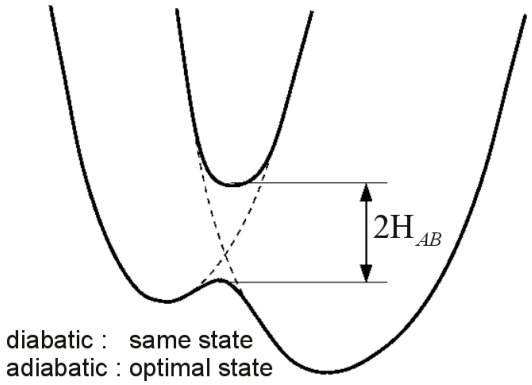


scheme 122

What is the physical meaning of the reorganization energy $\lambda$?

Amount of energy required to distort the nuclear configurations of the reactants (inclusive solvent) into the nuclear configuration of the products without electron tarnsfer occuring.

What is the relationship between the free energy change and the reorganziation energy when the rate constant is maximal?

$$\begin{gathered}\text{Max.}k \rightarrow E_a = 0 \quad (\text{as} E_a \geq 0) \\ (\delta G + \lambda)^2 = 0 \\ -\delta G = \lambda\end{gathered}$$

Does the rate always increase as the free energy change becomes more negative?

No, gecreases as soon as $\delta G > \lambda$. This is called the *inverted region.*

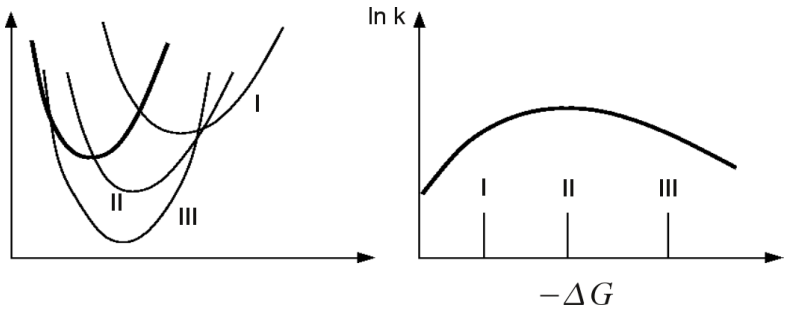


scheme 123

**Electron transfer in biological systems** Charge transfer, i.e. electron transfer, proton transfer and coupled ET/PT are essential steps in biological systems.

Overall equation of aerobic metabolism

$$\text{Photosynthesis (light)}$$
$$\longrightarrow$$
$$6CO2 + 6H_2O \leftrightarrow C_6H_{12}O_6 + 6O_2$$
$$\longleftarrow$$
$$\text{Respiratory system}$$

Bacterial metabolism

$$4H_2 + SO_4^{2-} \leftrightarrow S^{2-} + 4H_2O$$
$$\text{acetat} + SO_4^{2-} \leftrightarrow H_2O + CO_2 + HCO_3^- + S^{2-} + \cdots$$

Photosynthesis

- **Step 1:** light absorption
- **Steps 2–12:** all electron and proton transfer

Schematic view of aerobic biological metabolism

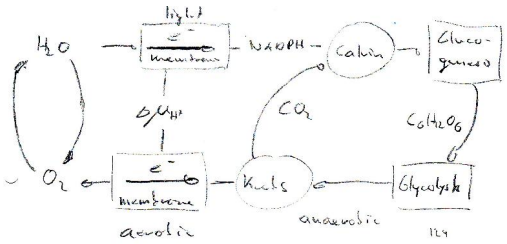


scheme 124

Photosynthetic reaction center

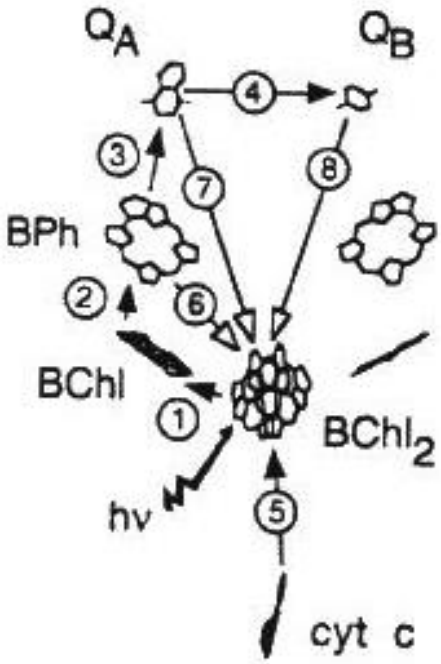


scheme 125

Steps 1–8 are electron transfer processes.

Modifying aminoacids changes $\Delta G^0$

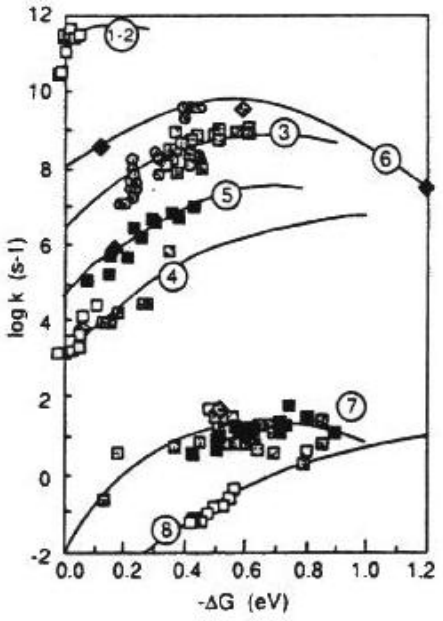


scheme 126

From this data an empirical rule for the relationship $k$, $\Delta G^0$, $\lambda$ and the distance between donor and acceptor can be derived.

Dutton's rule

$$\log_1 0k = 13 - 0.6(R - 3.6) - 3.1(\Delta G^0 + \lambda)^2/\lambda$$

**Application of Marcus theory** Computer simulation of redox potentials (J. VandeVondele et al. Chimia, **61** 155 (2007))

$$A + D \leftrightarrow A^- + D^+$$

Calculate half cell redox potentials

$$\begin{aligned} A + e^- &\leftrightarrow A^- && \Delta A_1 \\ D^+ + e^- &\leftrightarrow D && \Delta A_2 \\ A + D &\leftrightarrow A^- + D^+ \Delta A = \Delta A_1 + \Delta A_2 \end{aligned}$$

Assume no direct interaction of $A$ and $D$ – rather long range electron transfer.

$\Delta A$ is free energy difference between different redox states – we use thermodynamic integration

$$\Delta A = \int_0^1 \left\langle \frac{\partial \mathcal{H}(\alpha)}{\partial \alpha} \right\rangle \mathrm{d}\alpha$$

where $\alpha$ is the coupling parameter between the two states

$$\begin{aligned} \mathcal{H}(\alpha) &= \alpha \mathcal{H}_{\mathrm{re}} + (1-\alpha)\mathcal{H}_{\mathrm{ox}} \\ \frac{\partial \mathcal{H}(\alpha)}{\partial \alpha} &= \mathcal{H}_{\mathrm{re}} - \mathcal{H}_{\mathrm{ox}} = \Delta E \end{aligned}$$

$\Delta E$ is the total energy difference between reduced and oxidized form at given atomic positions.

$$\Delta A = \int_0^1 \langle \Delta E \rangle_\alpha \, \mathrm{d}\alpha$$

$\langle \cdot \rangle_\alpha$ indicates a Boltzmann sampling for ensemble generated by $\mathcal{H}(\alpha)$.

Marcus theory:

$$\begin{aligned} \Delta E &= y_1 - y_2 && \text{with} && y_1 = x^2 \\ &= 2xa - a^2 - b && && y_2 = x^2 - 2xa + a^2 + b \end{aligned}$$

Therefore

$$\begin{aligned} \langle \Delta E \rangle_\alpha &= \int_{-\infty}^{\infty} (2xa - a^2 - b) \mathrm{e}^{-\beta \mathcal{H}(\alpha)} \mathrm{d}x \Big/ \int_{-\infty}^{\infty} \mathrm{e}^{-\beta \mathcal{H}(\alpha)} \mathrm{d}x \\ &= 2\alpha a^2 - a^2 + b \qquad \text{linear in } \alpha! \end{aligned}$$

and we get

$$\Delta A = \int_0^1 \langle \Delta E \rangle_\alpha \, \mathrm{d}\alpha = \alpha^2 a^2 - \alpha a^2 + ab \Big|_0^1 = b$$

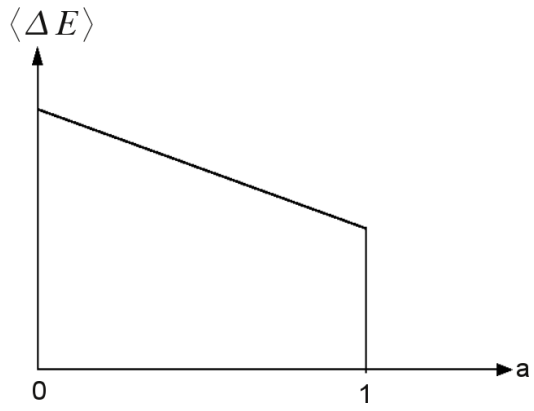


scheme 127

$$\Delta A = \frac{1}{2}\left(\langle \Delta E \rangle_0 + \langle \Delta E \rangle_1\right)$$

or

$$\begin{aligned}\Delta A &= \langle \Delta E \rangle_0 + \frac{1}{2} q \\ &= \langle \Delta E \rangle_0 + \frac{1}{2} q\end{aligned}$$

where $q$ is the slope

$$\begin{aligned} q &= \frac{\mathrm{d}}{\mathrm{d}\alpha} \langle \Delta E \rangle_\alpha = 2a^2 = 2\lambda \\ \lambda &= \frac{1}{2} q = \frac{1}{2}\left(\langle \Delta E \rangle_0 - \langle \Delta E \rangle_1\right) \end{aligned}$$

and

$$\begin{aligned}
\frac{\mathrm{d}}{\mathrm{d}\alpha}\left\langle \Delta E\right\rangle_{\alpha} &= \frac{\mathrm{d}}{\mathrm{d}\alpha}\left(\frac{\int \frac{\partial \mathcal{H}(\alpha)}{\partial \alpha}\mathrm{e}^{-\beta\mathcal{H}(\alpha)}\mathrm{d}x}{\int \mathrm{e}^{-\beta\mathcal{H}(\alpha)}\mathrm{d}x}\right) \\
&= \frac{\int \frac{\partial^2 \mathcal{H}(\alpha)}{\partial \alpha^2}\mathrm{e}^{-\beta\mathcal{H}(\alpha)}\mathrm{d}x}{\int \mathrm{e}^{-\beta\mathcal{H}(\alpha)}\mathrm{d}x} - \beta\frac{\int \left(\frac{\partial \mathcal{H}(\alpha)}{\partial \alpha}\right)^2 \mathrm{e}^{-\beta\mathcal{H}(\alpha)}\mathrm{d}x}{\int \mathrm{e}^{-\beta\mathcal{H}(\alpha)}\mathrm{d}x} \\
&\quad + \beta\frac{\left(\int \frac{\partial^2 \mathcal{H}(\alpha)}{\partial \alpha^2}\mathrm{e}^{-\beta\mathcal{H}(\alpha)}\mathrm{d}x\right)^2}{\left(\int \mathrm{e}^{-\beta\mathcal{H}(\alpha)}\mathrm{d}x\right)^2} \\
&\quad \text{as } \mathcal{H}(\alpha) \text{ is linear in } \alpha : \frac{\partial^2 \mathcal{H}(\alpha)}{\partial \alpha^2} = 0 \\
&= -\beta\left(\left\langle \Delta E^2\right\rangle_{\alpha} - \left\langle \Delta E\right\rangle_{\alpha}^2\right) \\
&= -\beta\sigma_{\alpha}^2 \qquad \text{fluctuations of energy difference}
\end{aligned}$$

The solvent reorganization energy $\lambda$ can therefore be calculated as

$$\lambda = \frac{\sigma_0^2}{2\mathrm{k_B}T} = \frac{\sigma_1^2}{2\mathrm{k_B}T}$$

Simulation protocol

1. Generate an ensemble of configurations by molecular dynamics in the reduced ($\alpha = 0$) or oxidized state ($\alpha = 1$).

2. For each configuration calculate the vertical energy ($\Delta E$) as difference in total energy between oxidized and reduced state.

3. Compute average and variance of $\Delta E$ to obtain $\Delta A$ and $\lambda$.

doi:10.2533/chimia.2007.155 CHIMIA **2007**, *61*, No. 4

Chimia 61 (2007) 155–158

ISSN 0009–4293

# Electron Transfer Properties from Atomistic Simulations and Density Functional Theory

Joost VandeVondele[§*a], Marialore Sulpizi[b], and Michiel Sprik[b]
[§]METTLER TOLEDO Award Winner (Oral Presentation)

*Abstract:* Marcus theory of electron transfer is the quintessential example of a successful theory in physical chemistry. In this paper, we describe the theoretical approach we have adopted to compute key parameters in Marcus theory. In our method, based on molecular dynamics simulations and density functional theory, the redox center and its environment are treated at the same level of theory. Such a detailed atomistic model describes specific solvent–solute interactions, such as hydrogen bonding, explicitly. The quantum chemical nature of our computations enables us to study the effect of chemical modifications of the redox centers and deals accurately with the electronic polarization of the environment. Based on results of previous work, we will illustrate that quantitative agreement with experiment can be obtained for differences in redox potentials and solvent reorganization energies for systems ranging from small organic compounds to proteins in solution.

**Keywords:** Density functional theory · Electron transfer · Marcus theory · Molecular dynamics

## 1. Introduction

Electron transfer (ET) reactions play a crucial role in a number of processes of biological and technological importance. Well-known examples include cell respiration, photosynthesis, fuel cell catalysis and photovoltaics.[1,2] The efficiency of these processes can be optimized by tuning the ET properties of electron-donor and -acceptor or the pathway between them. The relative stability of the electron at these sites (*i.e.* differences in redox potentials), and the rate of electron transfer between them are of particular interest, as they reflect directly what is thermodynamically and kinetically feasible. In this paper, we will summarize some of our previous work[3–15] aimed at computing these quantities directly from atomistic models using density functional Theory (DFT). The quantum chemical nature of DFT allows the effects of chemical modifications of the redox centers to be studied without a need for prior knowledge or empirical parameterization. This can thus make our method truly predictive.

A key feature of ET reactions, or redox reactions in general, is the crucial role played by the environment. Indeed, oxidation (reduction) potentials are the condensed phase equivalents of ionization potentials (electron affinities) in the gas phase, and these quantities can differ significantly. Our atomistic models explicitly include the environment (*e.g.* solvent and/or protein) so that not only dielectric properties but also specific interactions, such as hydrogen bonding or conformational changes are taken explicitly into account. Furthermore, the environment is far from being a static spectator. Its fluctuations bring donor and acceptor sites in an energy resonant state, triggering ET, and its ability to relax after ET influences significantly the energetics. In order to probe these fluctuations and relaxations in our computational setup, molecular dynamics is employed to generate a sufficiently large number of representative configurations of solute and solvent.

A major step in the understanding of ET reactions was the formulation by Marcus[16,17] of the rate of electron transfer ($k_{ET}$) as a simple function of the reaction free energy ($\Delta G$), the solvent reorganization energy ($\lambda$) and a proportionality constant ($\kappa$) depending on the quantum coupling between donor and acceptor states.

$$k_{ET} = \kappa \exp\left(\frac{-(\lambda + \Delta G)^2}{4\lambda kT}\right) \qquad (1)$$

The fruitful concept that underlies this formula is the assumed harmonic nature of the free energy surface with respect to the reaction coordinate of electron transfer. This restricts the validity of this formula to the range of systems that fall in the linear response regime, which might thus exclude systems that undergo significant changes in conformation or solvation upon electron transfer. Ultimately, the success of this theory is based on its capability to predict and explain experimental results. As will be illustrated in Section 2, our and other groups[18–22] have adopted the central concept of this theory to simplify and guide calculations.

So far we have focused on computing two of the three central parameters in Marcus theory: $\Delta G$, the driving force of the ET reaction, and $\lambda$, the solvent reorganization energy. Anticipating our results in Section 3, we find good agreement with experiment for systems ranging from small organic

*Correspondence: Dr. J. VandeVondele[a]
Tel.: + 41 44 635 4421
Fax: + 41 44 635 6838
E-Mail: vondele@pci.unizh.ch
[a]Institute of Physical Chemistry
University of Zurich
Winterthurerstrasse 190
CH-8057 Zürich
[b]Department of Chemistry
University of Cambridge
Lensfield Road
CB2 1EW, Cambridge, UK

CHIMIA **2007**, *61*, No. 4

compounds to proteins in solution. Whereas our DFT calculations typically involve a few hundred atoms, the latter system was modeled using a DFT description for over 2800 atoms.[15]

## 2. Atomistic Theory of Electron Transfer

A central element of our approach to ET so far, is the observation that ΔG and λ can be obtained from standard electronic ground state calculations, thus avoiding the complexity of excited state calculations, if one focuses on electrochemical half reactions. In this case, a single redox active center is explicitly present in the simulation cell, either in reduced or oxidized form. Such a setup only makes sense if there is no strong coupling between the donor and acceptor site, and is thus most easily applied in the case of long-range electron transfer. The free energy difference between the reduced and oxidized redox state, which we will denote by ΔA, to indicate that our simulations are at constant volume, can be computed in a number of ways. In the present work, we derive expressions for ΔA based on thermodynamic integration, *i.e.* integrating the reversible work needed to change the system's Hamiltonian linearly from the reduced $[H_{re}(\{R_i\})]$ to the oxidized $[H_{ox}(\{R_i\})]$ one. We write

$$\Delta A = \int_0^1 \left\langle \frac{\partial H_\alpha(\{R_i\})}{\partial \alpha} \right\rangle_\alpha d\alpha = \int_0^1 \langle \Delta E(\{R_i\}) \rangle_\alpha d\alpha$$
$$H_\alpha(\{R_i\}) = \alpha H_{ox}(\{R_i\}) + (1-\alpha) H_{re}(\{R_i\})$$
$$\frac{\partial H_\alpha(\{R_i\})}{\partial \alpha} = \Delta E(\{R_i\}) = H_{ox}(\{R_i\}) - H_{re}(\{R_i\}) \qquad (2)$$

where $H_\alpha$ is a Hamiltonian, formed as a linear combination of the two physical Hamiltonians $H_{ox}$ and $H_{re}$. Its derivate with respect to α is the vertical energy gap ΔE, a central quantity in the following. The integrand $\langle \Delta E(\{R_i\}) \rangle_\alpha$ is the canonical average of the vertical energy as obtained from a sampling based on the Hamiltonian $H_\alpha$, for which we will introduce the short hand notation $\Delta E_\alpha$. The above expression for ΔA is exact, and practical for actual *ab initio* calculations.[11]

Nevertheless, let us assume that the system is in the Marcus regime, or equivalently in the linear response regime. In this case, the integrand $\Delta E_\alpha$ varies linearly between the integration limits α = 0 and α = 1, and a number of simple expressions for ΔA can be derived. We illustrate in the Fig. that the assumption of linearity can be valid with remarkable accuracy, but see *e.g.* ref.[11] for a counterexample. Three expressions that are exact in the linear regime, and that have been used in our previous work are:

$$\Delta A = \frac{1}{2}(\Delta E_0 + \Delta E_1)$$
$$= \Delta E_0 - \frac{\sigma_0^2}{2kT}$$
$$= \Delta E_1 + \frac{\sigma_1^2}{2kT} \qquad (3)$$

where the first expression is a two-point estimate of the integral, and the latter two expressions are obtained from integrating the surface under a straight line through either the initial or the final point, with a slope given by the first derivative of the integrand in that point:

$$\frac{d}{d\alpha}\left[\langle \Delta E(\{R_i\}) \rangle_\alpha\right]$$
$$= -\frac{1}{kT}\left[\langle \Delta E(\{R_i\})^2 \rangle_\alpha - \langle \Delta E(\{R_i\}) \rangle_\alpha^2\right]$$
$$= -\frac{1}{kT}\sigma_\alpha^2 \qquad (4)$$

The latter expression shows that the slope of the integrand is proportional to the variance (fluctuations) of the vertical energy. The assumed linear behavior of $\Delta E_\alpha$ implies that the first derivative is constant, and that all higher derivatives vanish. While this leads trivially to the property that $\sigma_0^2$ equals $\sigma_1^2$, it is a lengthier derivation, beyond the scope of this paper, to show that this leads to a Gaussian probability distribution of ΔE. The corresponding free energy profile, given by –kT times the logarithm of this probability distribution, is parabolic, and the solvent reorganization energy (λ) can directly be associated with the fluctuations as

$$\lambda = \frac{\sigma_0^2}{2kT} = \frac{\sigma_1^2}{2kT} = \frac{1}{2}(\Delta E_0 - \Delta E_1) \qquad (5)$$

where the last equality is obtained by subtracting the last two equations for ΔA.

In the remainder of this paper, we will use the above equations in a simple three-step recipe to compute ΔA and λ:

i) Generate an ensemble of atomistic configurations by running molecular dynamics simulations in the reduced (α = 0) and/or the oxidized state (α = 1).
ii) For each of these configurations, compute the vertical energy (ΔE) as the difference in total energy between the oxidized and the reduced state.
iii) Compute the average ($\Delta E_\alpha$) and variance ($\sigma_\alpha^2$) of the set of values of ΔE to obtain ΔA and λ.

Additionally, based on careful considerations of the system's complexity, we will choose which formula for ΔA and λ we employ, and how we generate the ensemble. For example, the expressions depending on the variance of ΔE converge significantly slower than those depending only on the average of ΔE, but have nevertheless the advantage that they can be evaluated with just one simulation in an oxidation state of choice. The expression based on the average of the vertical energy at both end points is likely to be more reliable if some deviation from linearity is to be expected.

Finally, we conclude this section with a brief discussion of our computational setup, referring to ref.[23] for a complete technical review of the method, and refs.[10,12,15] for specific computational details for each of the selected applications. The unifying theme for the simulations that we have selected for this paper is that all DFT calculations have been performed using the freely available simulation package CP2K/Quickstep.[23,24] Based on the hybrid Gaussians and plane waves (GPW) scheme,[25] excellent efficiency and accuracy is obtained for systems containing up to a few thousand atoms.[26,15] The efficiency is obtained by exploiting the locality and compactness of a Gaussian basis, and the linear scaling cost of evaluating the Coulomb (Hartree) energy in a plane wave basis. Furthermore, Born-Oppenheimer molecular dynamics simulations can be performed using a robust wavefunction optimization technique[26] and a density matrix extrapolation scheme.[23]

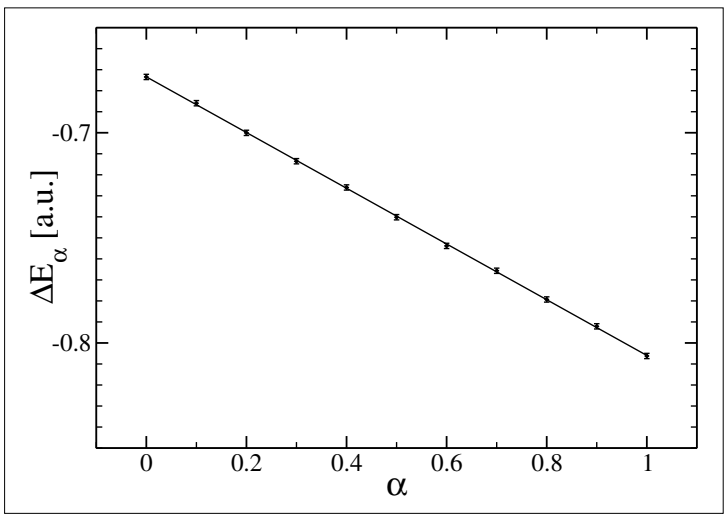


Fig. Computed values of the integrand $\Delta E_\alpha$ for a classical model of the $Fe^{2+}/Fe^{3+}$ redox pair in aqueous solution are shown with error bars indicating the statistical uncertainty. The line represents a linear fit to the data. The high quality of this fit convincingly demonstrates, for this system, the validity of a key assumption underlying Marcus theory and our computational approach.

The value of this approach can be best appreciated for 'electronically difficult' systems such as radicals and transition metal compounds, typically encountered in ET systems, where these methods bring enhanced stability.

Nevertheless, these simulations remain challenging and a number of issues that might affect their accuracy have been discussed in more detail in ref.[14] Errors arise from the approximate nature of DFT and from the limited length and timescales that can be assessed by *ab initio* techniques. The most serious DFT error is likely to come from the self-interaction error, despite the fact that our half-cell approach avoids the difficulties associated with a computational setup where both donor and acceptor are present in the same simulation cell. The latter setup can lead to an unphysical delocalization of the electron and requires proper treatment. However, even with the half cell approach, the self-interaction error is a major concern for systems containing an unpaired electron in an electronic state that is (nearly) degenerate with the band of occupied solvent state. In this case, an unphysical delocalization of the spin over the solvent might be observed.[27] System size effects can be expected for quantities, such as λ, that are sensitive to the long-range nature of the electrostatics, since charged solutes are treated in relatively small simulation cells. However, when investigating differences between systems that have a similar spatial distribution of the charge, the same unit cell, and a similar environment, these errors are expected to cancel. Finally, in assuming a linear response regime for our calculations, we have introduced a systematic error. This is error must be balanced to the statistical uncertainty in the results, since only a relatively small number of configurations (100–1000 s) can be computed using methods based on DFT.

## 3. Results and Discussion

In the following, we present three applications that have been used to explore the capabilities and limits of our methodology within the framework of CP2K. These are:

i) the organosulphur compounds tetrathiafulvalenene (TTF) and thianthrene (TH) in acetonitrile (ACN) solution,[10]
ii) model quinones, benzoquinone (BQ) and duroquinone (DQ) in two different solvents, ACN and methanol (MeOH),[12]
iii) two natural varieties of the iron–sulfur protein rubredoxin in aqueous solution.[15]

Three variants of the same three-step recipe have been employed. For the organosulphur compounds, we have employed *ab initio* molecular dynamics simulations to generate the configurations, leading to parameter-free estimates of the reaction free energies shown in the Table, which agree with experiment to within our estimated statistical uncertainty (60 meV). For the other two applications, configurations have been generated using classical molecular dynamics, and DFT has only been employed to compute the vertical energies. These results are thus not truly parameter-free, since a classical force field must be available to describe the geometries. However, this approach allows much longer timescales to be explored, and both systems have been simulated for several nanoseconds, retaining a few hundred to thousands of configurations for DFT-based analysis. The simulations of the quinones exhibit similar agreement with experiment for the reaction free energies (hence validating our mixed classical/quantum approach), but more interestingly allow the effect of hydrogen bonding on the solvent reorganization free energy to be illustrated, and hence the rate of electron transfer. Indeed, we have selected two solvents (ACN and MeOH) with very similar dielectric properties. In particular, their Pekar factors, which in a continuum description are proportional to the solvent reorganization energy, differ only by about 5%. However, we find that the solvent reorganization energies of both solutes are larger by approximately 230 meV in the hydrogen bonding solvent, consistent with experiment.[28] This illustrates the limits of a continuum theory approach, which predicts a much smaller difference. Our third application is also based on classical sampling with DFT calculations of the vertical energies, but applies this technique to a significantly larger system, the mesophilic *Clostridium pasteurianum* (Cp) and the hyperthermophilic *Pyrococcus furiosus* (Pf) variants of the iron–sulphur protein rubredoxin. We consider it a significant break-through that we are now able to obtain redox potentials differences in agreement with experiment (see the Table) for a system of this size (2800 atoms). Furthermore, we also obtain solvent reorganization energies (0.5–0.7 eV) that are in good agreement with the estimates employed in kinetic models of the self-exchange reaction.[29] This is significant, since simulations based on standard force fields yield results that are much larger. This overestimate is consistent with the continuum dielectric expression of the solvent reorganization energy, and underlines the importance of the high frequency dielectric response. The latter term is absent in non-polarizable force fields, but included in our DFT description.

Finally, we note that atomistic and electronic information is available in these simulations as well. For example, the response of the solvent to the ionization of the solute can be analyzed,[10] the contribution of particular residues to the solvent reorganization energy estimated,[15,30] or the correlation between one-electron energies levels and redox potentials obtained.[14] In this paper, we focused on the computation of key parameters in Marcus theory and compared these results with experiment where available. The results presented here are a good indication that the method is quantitative and predictive, and that our approach can thus be applied in cases where experiments might be difficult or more approximate theories inappropriate.

Table. Computed reaction free energies in eV for the full reactions discussed in the text. The statistical uncertainty on the computed results is about 60 meV for the first four and about 30 meV for the last reaction.

| Redox reaction | | solvent | Ref. | Computed [eV] | Experiment [eV] |
|---|---|---|---|---|---|
| $TH+TTF^{+}$ | -> $TH^{+}$ + TTF | ACN | [10] | 0.96 | 0.93 |
| $TH^{+}+TTF^{2+}$ | -> $TH^{2+}+TTF^{+}$ | ACN | [10] | 1.09 | 1.08 |
| $BQ^{-}+DQ$ | -> $BQ+DQ^{-}$ | ACN | [12] | 0.42 | 0.35 |
| $BQ^{-}+DQ$ | -> $BQ+DQ^{-}$ | MeOH | [12] | 0.43 | 0.42 |
| CpFe(III)+PfFe(II) | -> CpFe(II)+PfFe(III) | Water | [15] | 0.04 | 0.06 |

Received: December 18, 2006

[1] R. A. Marcus, N. Sutin, *Biochim. Biophys. Acta* **1985**, *811*, 265.
[2] M. Graetzel. *Nature* **2001**, *414*, 338.
[3] I. Tavernelli, R. Vuilleumier, M. Sprik, *Phys. Rev. Lett.* **2002**, *88*, 213002.
[4] J. Blumberger, M. Sprik, *J. Phys. Chem. B* **2004**, *107*, 6529.
[5] J. Blumberger, L. Bernasconi I. Tavernelli, R. Vuilleumier, M. Sprik, *J. Am. Chem. Soc*. **2004**, *126*, 3928.

[6] J. Blumberger, M. Sprik, *J. Phys. Chem. B* **2005**, *109*, 6793.
[7] Y. Tateyama, J. Blumberger, M. Sprik, I. Tavernelli, *J. Chem. Phys.* **2005**, *122*, 234505.
[8] J. Blumberger, Y. Tateyama, M. Sprik, *Comp. Phys. Comm.* **2005**, *169*, 256.
[9] J. Blumberger, M. Sprik, *Theor. Chem. Acc*. **2006**, *115*, 113.
[10] J. VandeVondele, R. Lynden-Bell, E. J. Meijer, M. Sprik, *J. Phys. Chem. B* **2006**, *110*, 3614.
[11] J. Blumberger, I. Tavernelli, M. L. Klein, M. Sprik, *J. Chem. Phys.* **2006**, *124*, 064507.
[12] J. VandeVondele, M. Sulpizi, M. Sprik, *Angew. Chem. Int. Ed*. **2006**, *45*, 1936.
[13] R. Ayala, M. Sprik, *J. Chem. Theory Comp.* **2006**, *2*, 1403.
[14] J. VandeVondele, R. Ayala, M. Sulpizi, M. Sprik, *J. Electroanalytical Chem*., doi: 1016/J.Jelechem.2007.01.009.
[15] M. Sulpizi, S. Raugei, J. VandeVondele, P. Carloni, M. Sprik. *J. Chem. Phys. B*, accepted.
[16] R. A. Marcus, *J. Chem. Phys.* **1956**, *24*, 966.
[17] R. A. Marcus, *Rev. Mod. Phys.* **1993**, *65*, 599.
[18] A. Warshel, *J. Phys. Chem.* **1982**, *86*, 2218.
[19] G. King, A. Warshel, *J. Chem. Phys*. **1990**, *93*, 8682.
[20] M. Tachiya, *J. Phys. Chem*. **1993**, *97*, 5911.
[21] D. W. Small, D. V. Matyushov, G. A. Voth, *J. Am. Chem. Soc.* **2003**, *125*, 7470.
[22] M. H. M. Olsson, G. Hong, A. Warshel, *J. Am. Chem. Soc.* **2003**, *125*, 5025.
[23] J. VandeVondele, M. Krack, F. Mohamed, M. Parrinello, T. Chassaing, J. Hutter, *Comp. Phys. Comm*. **2005**, *167*, 103.
[24] CP2K can be obtained free of charge from *http://cp2k.berlios.de/*
[25] G. Lippert, J. Hutter, M. Parrinello, *Mol. Phys.* **1997**, *92*, 477.
[26] J. VandeVondele, J. Hutter, *J. Chem. Phys.* **2003**, *118*, 4365.
[27] J. VandeVondele, M. Sprik, *Phys. Chem. Chem. Phys*. **2005**, *7*, 1363.
[28] T. Yago, Y. Kobori, K. Akiyama, S. Tero-Kubota, *Chem. Phys. Lett.* **2003**, *369*, 49.
[29] P. Kennepohl, E. I. Solomon, *Inorg. Chem.* **2003**, *42*, 696.
[30] J. Blumberger, M. L. Klein, *J. Am. Chem. Soc.* **2006**, *128*, 1854.

# Chapter 6

# Summary

### Mass equilibrium

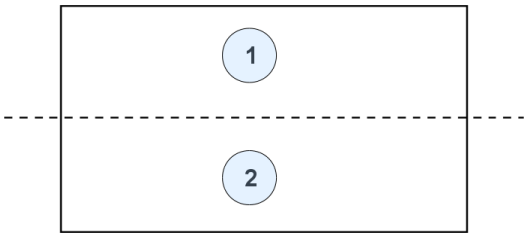


scheme 150

The boundary can be a hypothetical or real physical boundary (liquid/vapor, liquid/liquid).

Condition for equilibrium:

$$\mu^{(1)} = \mu^{(2)}$$

This is equivalent to conditions for equilibrium for $p$ and $T$!

For multiple components we have

$$\mu_i^{(1)} = \mu_i^{(2)}$$

Compare this again to conditions for $p$ and $T$.

Condition for equilibria in chemical reactions

$$aA + bB + \cdots \leftrightarrow cC + dD + \cdots$$
$$a\mu_A + b\mu_B + cdots = c\mu_C + d\mu_D + \cdots$$

From the fact that $G(T, p, N_1, N_2, \ldots)$ is an extensive function, we get

$$G = \mu_1 N_1 + \mu_2 N_2 + \cdots$$

with $\mu_i = \mu_i(T, P)$ and dependent on other components.

Using $\mathrm{d}G(T, p, N_1, N_2, \ldots) = \mathrm{d}G(\mu_1, \mu_2, \ldots, N_1, N_2, \ldots)$, we get the *Gibbs–Duhem equation*

$$S\mathrm{d}T - V\mathrm{d}p + \sum_i N_i \mathrm{d}\mu_i = 0$$

For a one component system, we can derive

$$N\left(\frac{\partial \mu}{\partial p}\right)_T = V \qquad \text{and} \qquad N\left(\frac{\partial \mu}{\partial T}\right)_p = -S$$

**Chemical potential for an ideal solution** Configurational contribution

$$\beta\mu_{\mathrm{conf}} = \ln X_{\mathrm{sol}}$$

where $X_{\mathrm{sol}}$ is the mole fraction.

Reversible work to create a solute molecule in solution $\Delta\mu$. The sum of these two contributions is the total chemical potential of an ideal solution (Raoult's Law).

$$\beta\mu = \beta\Delta\mu + \ln X_{\mathrm{sol}}$$

**Reversible work surface** Hold specific coordinates fixed
→ partition function $\tilde{Q}(x_1, \ldots, x_N; \beta, N, V)$

$$\frac{\partial \ln \tilde{Q}}{\partial x_1} = \beta\langle f_{x_1}\rangle$$

$\langle f_{x_1} \rangle$ is the average force on coordiante $x_1$, with $x_1, \ldots, x_N$ hold fix.

$$\ln \tilde{Q} = -\beta \underbrace{W(x_1, \ldots, x_N; \beta, N, V)}$$

reversible work surface
potential of mean force
free energy surface

$\exp[-\beta(\text{reversible work surface for } x_1, \ldots, x_N)]$
$= \text{Boltzmann weighted sum over all fluctuations with } x_1, \ldots, x_N \text{ fixed}$
$\propto \text{probability for observing system with } x_1, \ldots, x_N$

**Free energy calculations and measurements** We go for $\begin{matrix} \Delta A & \text{free energy difference} \\ \frac{\partial A}{\partial \lambda} & \text{free energy derivatives} \end{matrix}$

Expectation value in canonical ensemble

$$\langle f(\mathcal{H}) \rangle = \frac{\int_\Gamma f(\mathcal{H}) \mathrm{e}^{-\beta \mathcal{H}} \mathrm{d}\Gamma}{\int_\Gamma \mathrm{e}^{-\beta \mathcal{H}} \mathrm{d}\Gamma}$$

where $\mathcal{H}(\boldsymbol{p}, \boldsymbol{q})$ is the Hamilton function (= total energy function = kinetic + potential energy) of the full system. $\Gamma$ is short for all phase space variables $(r_1, r_2, \ldots, r_N, p_1, p_2, \ldots, p_N) = 6N$ variables, $N$= number of particles in the system.

$$\text{Partition function} \qquad Q = \int_\Gamma \mathrm{e}^{-\beta \mathcal{H}} \mathrm{d}\Gamma$$

Helmholtz free energy: $A = -\mathrm{k_B} T \ln Q$.

$$\begin{aligned} \Delta A = A_Y - A_X &= -\mathrm{k_B} T \ln \frac{Q_Y}{Q_X} \\ &= -\mathrm{k_B} T \ln \left\langle \mathrm{e}^{-\beta(\mathcal{H}_Y - \mathcal{H}_X)} \right\rangle_X \end{aligned}$$

where the sampling is over distribution of system $X$.

Multiple configurations $\mathcal{H}_1 \to \mathcal{H}_2 \to \mathcal{H}_3 \cdots$.

$\to$ overlapping distributions

$\to$ better convergence of simulations

Thermodynamic integration

$$A(\lambda) = -kbT \ln Q(\lambda)$$
$$\Delta A = A(\lambda = 1) - A(\lambda = 0) = \int_0^1 \frac{\partial A(\lambda)}{\partial \lambda} \mathrm{d}\lambda$$
$$= \int_0^1 \left\langle \frac{\partial \mathcal{H}}{\partial \lambda} \right\rangle_\lambda \mathrm{d}\lambda \approx \sum_i \left\langle \frac{\partial \mathcal{H}}{\partial \lambda} \right\rangle_{\lambda_i}$$

Umbrella sampling

Make use of a bias potential $W(\boldsymbol{r})$. This enhances sampling of some configurations, but has to be corrected in averaging.

$$\langle A \rangle = \frac{\left\langle A \mathrm{e}^{\beta W} \right\rangle_B}{\left\langle \mathrm{e}^{\beta W} \right\rangle_B}$$

The sampling (B) is over the biased potential $\mathcal{H} + W$.

**Chemical equilibrium in a solvent**

$$A \leftrightarrow B$$

Chemical potentials have to be the same

$$\mu_A = \mu_B$$

Thus, (ideal gas formula)

$$\beta \Delta \mu_A + \ln \rho_A = \beta \Delta \mu_B + \ln \rho_B$$

and, we get

$$K = \frac{\rho_A}{\rho_B} = \underbrace{\mathrm{e}^{-\beta(\Delta\mu_A - \Delta\mu_B)}}_{\substack{\text{no concentration} \\ \text{dependent terms!}}}$$

Approximation:

$$K \approx K_{\text{gas}} \mathrm{e}^{-\beta \Delta W}$$

$\Delta W$ free energies of solvation differences.
Sources for $\Delta W$

- packing effect, excluded volume
- electrostatic effects
  Born model
  $$\Delta\mu \approx -(1-1/\epsilon)\frac{q^2}{\sigma}$$
  Debye formula
  $$\Delta\mu \approx -\frac{8(\epsilon-1)}{2\epsilon+1}\frac{m^2}{\sigma^3}$$
  where $q, m$: charge and dipole of solute, $\sigma$: size of solute, $\epsilon$: dielectric constant of solvent.

Another application of $\beta\mu = \beta\Delta\mu + \ln\rho$:

$$\text{Osmotic pressure} \qquad \beta\pi = \sum_i \rho_i$$

Beyond ideal solutions

$$\beta\mu = \beta\Delta\mu + \ln\rho$$

but now make $\Delta\mu$ concentration dependent.

$$\begin{aligned} \Delta\mu &= \Delta\mu^0 + \frac{\partial\Delta\mu}{\partial\rho}\rho + \cdots && \text{Taylor expansion} \\ &= \Delta\mu^0 + 2\mathrm{k_B}TB\rho + \cdots && B\text{: 2nd virial coefficient} \end{aligned}$$

Equation of state of real gas

$$\beta p = \rho + B\rho^2 + \cdots$$

**Chemical kinetics** Thermodynamics: energy of stable states
Kinetics: energy between stable states

$$K = \frac{k}{k_{-1}} \qquad \text{detailed balance}$$

| thermodynamics | kinetics |
|---|---|
| equilibrium constant | rates of reactions |

Arrhenius (empirical formula)

$$k = A\mathrm{e}^{-\frac{\Delta E_a}{\mathrm{k_B}T}}$$

$A$: frequency factor; $\Delta E_a$: activation energy

Eyring (from transition state theory)

$$k = \frac{\mathrm{k_B}T}{h}\mathrm{e}^{\frac{\Delta S^\sharp}{\mathrm{k_B}}}\mathrm{e}^{-\frac{\Delta H^\sharp}{\mathrm{k_B}T}}$$

Eyring plot: $\ln(k/T)$ vs. $1/T$
slope: $-\Delta H^\sharp/\mathrm{k_B}$
intercept: $\Delta S^\sharp/\mathrm{k_B}$

Transition state theory:

$$[\dot{C}] = \underbrace{\frac{\mathrm{k_B}T}{h}\frac{Q^\sharp}{Q_A Q_B}\mathrm{e}^{-E_0/\mathrm{k_B}T}}_{k(Eyring)}[A][B]$$

From equilibrium assumption
$[A] + [B] \leftrightarrow [C] \leftrightarrow$ products

Kinetic isotope effects

$$\mathrm{KIE} = \frac{k(\text{isotope 1})}{k(\text{isotope 2})}$$

| | |
|---|---|
| primary KIE | isotope involved in bond breaking or forming |
| secondary KIE | all other |

Typical size of primary KIE:

| | |
|---|---|
| $C-H/C-D$ | $6-8$ |
| all other isotopes | $< 1.1$ |

From transition state theory

$$\mathrm{KIE} = \frac{Q_l^\sharp}{Q_h^\sharp}\frac{Q_{R,h}}{Q_{R,l}}\mathrm{e}^{-(E_0^l - E_0^h)/\mathrm{k_B}T}$$

Molecular partition functions; $Q_{\text{vib}}$ has largest mass dependence
$\Delta E_0 \approx \Delta E$(xero point energy)

$$\text{KIE} \approx \text{e}^{1/2\hbar\Delta\omega/\text{k}_\text{B}T}$$

where $\Delta\omega$ is change in frequency due to isotope substitution, assumes $\omega^\sharp = 0$.

Tunneling: other source for KIE
Important mainly for protons or at low temperatures, e.g., enzymatic reactions.

**Marcus theory of electron transfer** Based on transition state theory
Assumes free energy curves along reaction coordinates (reversible work surface) are parabola (diabatic states).

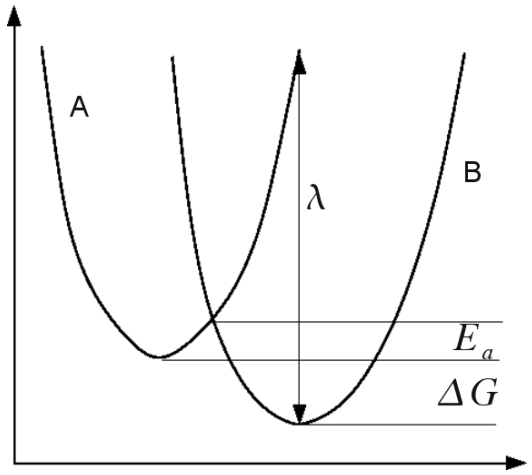


scheme 151

$\lambda$: reoranization energy = excess energy of state $A$ at equilibrium position of state $B$.

$$k = A\text{e}^{-\frac{(\Delta G+\lambda)^2}{4\lambda\text{k}_\text{B}T}}$$

Regions of electron transfer

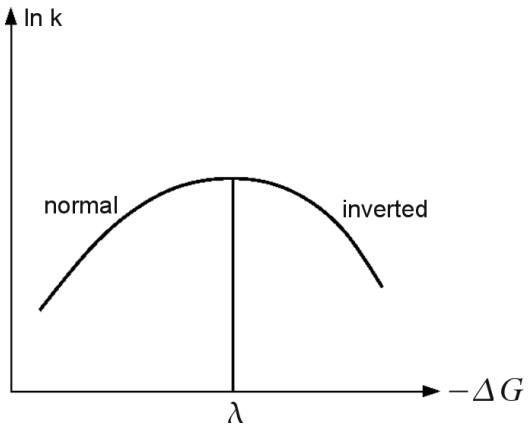


scheme 152

## Literature


- [**MDF**] Ken A. Dill and Sarina Bromberg, *Molecular Driving Forces*, Garland Science, 2nd Edition, 2011.
- David Chandler, *Introduction to Modern Statistical Mechanics*, Oxford University Press, 1987.
- T. L. Hill, *An Introduction to Statistical Thermodynamics*, Dover, 1986.
- K. Denbigh, *Prinzipien des chemischen Gleichgewichts*, Steinkopf Darmstadt, 1974.
- P. Atkins, J. de Paula, *Physical Chemistry*, Chapters 19 and 20 (7th edition), Oxford, 2002.
- T. Engel, P. Reid, *Physikalische Chemie*, Kapitel 30-35, Pearson, 2006.
- D. A. McQuarrie, J. D. Simon, *Physical Chemistry*, Chapters 17-28, University Science Books, 1997.

## Molecular Driving Forces (MDF)

### Principles of Macroscopic Systems

| | |
|---|---|
| Probabilities and correlation | **MDF** Chapter 1 p1–28 |
| Fluctuations | **MDF** Chapter 1 p18–21 |
| Extensive and intensive properties | **MDF** Chapter 6 p93–94 |
| Principle of equal weight | **MDF** Chapter 5 p81–92 |
| Definition of entropy | **MDF** Chapter 5 p81–92 |
| The Second Law and the meaning of temperature | |
| Partitionfunction | **MDF** Chapter 5 p81–92 |
| Second Law | **MDF** Chapter 3 p39–57 |
| Entropy as a function of $E$, $N$ and $V$ | **MDF** Chapter 6 p93–107 |
| Definition of temperature, pressure and chemical potential | **MDF** Chapter 6 p93–107 |
| Microcanonical ensemble | **MDF** Chapter 10 p188–189 |
| Ideal gas law | **MDF** Chapter 6 p97–99; Chapter 11 p207–211 |
| Canonical ensemble | **MDF** Chapter 10 p169–189 |
| Temperature and energy fluctuations | **MDF** Chapter 12 p230–232 |
| Canonical partition function | **MDF** Chapter 10 p169–189 |
| Low temperature and the Third Law | **MDF** Chapter 8 p141–143 |

Partition function of molecular gases **MDF** Chapter 11 p193–210

Partition function and free energy **MDF** Chapter 8 p131–143

Thermodynamic functions of the monoatomic ideal gas **MDF** Chapter 11 p193–210

Einstein and Debye's model of a crystal **MDF** Chapter 11 p193–210

**Summary and Mathematical Properties**

Microcanonical and canonical ensemble **MDF** Chapter 10 p169–189

Mathematical properties of state functions **MDF** Chapter 4 p54–79

Heat capacity **MDF** Chapter 12 p221–234

Free energies **MDF** Chapter 8 p131–143

Thermodynamics of rubber bands **MDF** Chapter 9 p158–159

**Chemical Potential and Mass Equilibrium**

Conditions for equilibrium **MDF** Chapter 13 p235–251

Gibbs–Duhem equation **MDF** Chapter 14 p253–268

Partial molar quantities **MDF** Chapter 9 p160–165

Ideal solution chemical potential **MDF** Chapter 15 p269–276

Chemical potential and reversible work

Free energy calculations; Helmholtz free energy from computer simulations

Chemical equilibrium in a solvent **MDF** Chapter 15 p269–276

Models for solvent contributions to reversible work surfaces

Born and Debye formula for charge and dipole in a dielectric fluid
**MDF** Chapter 22 p444–453

Osmotic pressure **MDF** Chapter 16 p293–299

Non ideal solutions

Electrolytes, Debye–Hückel theory **MDF** Chapter 23 p455–462

**Chemical Kinetics**

Arrhenius law **MDF** Chapter 19 p360–362

Transition state theory **MDF** Chapter 19 p363–370

Kinetic isotope effect (KIE) **MDF** Chapter 19 p370–371

Electron transfer reactions: Marcus theory **MDF** Chapter 19 p377–379